OIL SHALE RD&D PROGRAM OVERVIEW

A.M. Hartstein and B.M. Harney, U.S. Dept. of Energy, Washington, D.C. 20545

The largest untapped fossil fuel resource in the United States is the oil bearing shales in the western part of the country and the black, gas bearing shales in the east. The oil shale resource concentrated in three western states is estimated to be equivalent to more than two trillion barrels of crude oil. Associated with the western oil shales of Colorado are huge amounts of saline minerals capable of providing a major domestic source of commercial alumina and supplies of other commercial saline minerals which may be produced with shale oil. Due to the critical shortage of new energy supplies, particularly liquid fuels, it appears that development of shale oil and other synthetic fuels will become a necessary reality.

Since the earliest commercial interest more than 100 years ago, the history of oil shale has been one of ups-and-downs. In almost cyclical fashion, the shale industry has appeared to be on the verge of expanding rapidly, economics have appeared potentially viable, and the problems have seemed minimal. But then, a combination of factors, such as jumps in construction costs, the requirement for new environmental data, or the discovery of new conventional oil resources, have led to delays and in some cases, to pullouts by companies.

The Department of Energy (DOE) has established a research, development, and demonstration (R,D&D) program for encouraging the development of the country's oil shale resource at a commercial scale to help in the mitigation of the present and future energy demands. The aim of the Oil Shale Program is to stimulate the commercial production of shale oil by eliminating technical and environmental barriers. This paper provides an overview of the DOE Oil Shale R,D&D Program, addressing its essential elements.

Program Goal and Objectives

The Department of Energy's primary oil shale goal, as indicated below, is to foster the development of a commercial oil shale industry. In concert with this goal, the objectives of the DOE Oil Shale Program are to assist in the development of this industry through R,D&D, financial incentives, and the mitigation of institutional barriers, but not to mandate the choice of technology or markets to be served.

Program Goal

- To foster the development of a commercial oil shale industry.

Program Objectives

- To provide financial incentives to the private sector to encourage the construction of pioneer demonstration plants.

- To mitigate institutional barriers to commercial oil shale development.

- To provide, through an integrated technology base program, technical, economic, and environmental information to the private sector which will enhance its capability to build a shale oil industry.

- To optimize oil shale processes or develop new oil shale concepts to ensure the most efficient and cost effective utilization of the nation's oil shale resource.

- To obtain environmental data and develop environmental protection systems to ensure that the oil shale resource is developed in the most environmentally acceptable manner.

The analysis of commercialization incentives and mitigation of institutional barriers is the responsibility of the Assistant Secretary for Resource Applications. R,D&D activities are the responsibility of the Assistant Secretary for Fossil Energy, although the lead for environmental planning rests with the Assistant Secretary for Environment.

PROGRAM STRATEGY

In essence, the DOE program goal is to develop the technology necessary for the production of oil shale on a commercial basis and in an environmentally acceptable manner. The DOE strategy to accomplish this end is comprised of two major activity elements:

- Research and Development

- Commercial Development and Demonstration Support

Through the existence of these parallel activities, the DOE Oil Shale R,D&D Program focuses near term research and development (R&D) on supporting indusrial development while maintaining an adequate level of more advanced R&D attuned to future needs. The technology developments that will result by achieving the program's objectives will be made available to the oil shale industrial community. Their participation in DOE sponsored demonstrations is encouraged as means of maintaining the technological alignment of the R,D&D Program with the needs of industry. These demonstration activities and direct financial incentives involve the DOE Program in the industrial decision process and facilitate oil shale industry growth. Information and experience gained through the construction and operation of any facilities resulting from these industry supportive activities will be used in assisting to define future R&D requirements which may be satisfied directly by the private sector through the program.

The Program's R&D activity elements are structured to parallel and complement activities that industrial developers would need to perform when establishing a commercial oil shale operation. The initial activities of a developer

include tasks to characterize the resource under consideration and site planning for resource development. Following this, the developer needs to consider the potential physical environment and socioeconomic impacts before committing to a proposed project. Oil shale resource development and extraction entail site preparation, mining (except for true in situ technologies), and rubbling the in situ retort in preparation for in place combustion or transporting the mined oil shale to a surface retort. Retorting would then be undertaken, after which the shale oil would be upgraded and refined. At each point in this sequence, the Oil Shale Program will develop enhanced technology to establish a potential developer's effectiveness.

KEY TECHNICAL AND ENVIRONMENTAL NEEDS IN R,D&D

Technical

The Oil Shale R,D&D Program is directed toward developing a greater understanding of the oil shale resource and perfecting effective means for the recovery of shale oil and associated mineral products. Program activities are directed toward the solution of key technical and environmental needs representing significant barriers to commercial oil shale development. Based on a review of technology required for oil shale development, the following Key Technical Needs have been identified as those that should receive the highest priority in the R,D&D Program:

- Efficient Oil Shale Rock Breakage and Retort Bed Preparation Techniques,
- Surface Retort Scaleup and Development,
- Development of Retort Diagnostics and Instrumentation,
- Development of Retort Control Procedures,
- Systems Engineering Methods for Total Oil Shale Process Development,
- Efficient and Effective Oil Shale Mining Systems,
- Advanced Shaft Sinking Technology,
- Shale Oil Upgrading Technology,
- Chemical Kinetics of the Total Pyrolysis Process,
- Understanding Retorting Mechanisms and Developing a Prediction Capability, and
- Development of Alternative Retorting Procedures.

Rock Breakage and Retort Bed Preparation. Efficient recovery of oil from shale depends critically upon having a bed of oil shale rubble that is relatively uniform, both in particle size and void fraction. Mining and rubbling methods must be developed to assure optimal uniformity. Otherwise sweep efficiency will be poor, and significant amounts of oil shale rubble will not be retorted.

It is expected that the R,D&D effort will result in the development of technology for breaking oil shale for mining and preparing rubble beds such that efficient and productive shale extraction and modified in situ retorting can be accomplished. Retorts will be designed and constructed which meet the processing requirements for particle size distribution, uniform permeability, uniform void distribution, and bounding of the fractured region.

Surface Retort Scaleup and Development. Currently, the most practical method of recovering shale oil is to mine the shale, crush it, and then retort it on the surface. Even with the employment of modified in situ technologies, some combination of in situ processing with surface retorting of the mined fraction is expected to be utilized. Surface retorting is the most proven technology for extraction of shale oil. However, the technology has been demonstrated only at pilot scale. Therefore, an increasing government effort is needed to advance surface retorting to a commercial scale. The DOE now is working toward the cooperative development of a full scale, surface module demonstration plant. The objective of this program is to stimulate the development of an oil shale industry by demonstrating the engineering, economic, and environmental feasibility of a surface retorting process at a unit scale considered necessary to provide commercial feasibility.

Retort Diagnosis and Instrumentation. The development of control instrumentation and methods for in situ retorting is important for determining retort performance and yield efficiency. The effort of the RD&D program will result in the design of thermal sensors, gas sampling devices, pressure probes, remote sensing devices, strain and displacement gauges, and health and safety monitoring equipment. This equipment will be designed and then tested and modified through use in several field tests.

Retort Control Procedures. The development of retort control and operating procedures is crucial to the success of both in situ and modified in situ retorting of oil shale. The R,D&D effort will establish a set of baseline operating plans from data collected from laboratory experiments, field tests and the outputs of predictive models. From the data collected, an evaluation will be made on the effects of intermittent air flows, liquid water additions, and other control parameters. The result of this effort will be a retort operating plan that maximizes retorting rate and yield while controlling temperature and burn front symmetry.

Systems Engineering. A systematic procedure for resource identification and characterization and for determination of appropriate recovery processes is needed to assure efficient and effective use of all domestic oil shale resources. The need related objectives of the R,D&D program are: (1) to develop and utilize methods for the planning of oil shale development by matching oil shale resources with appropriate recovery processes; (2) to develop planning tools (e.g., equipment selection criteria, production models, economic models) which will aid in the design and analysis of efficient shale oil production facilities; and (3) to determine the overall economics for the recovery of energy products from oil shale by the alternative processes.

Oil Shale Mining Systems. Equipment and methods now used for coal and hard rock mining are well developed but are not always applicable to the demands of oil shale mining. Research and development is needed to meet the particular requirements of the oil shale industry. The objective of the R,D&D program is to develop technology and equipment for high volume, cost effective, underground and surface mining methods for extracting oil shale for subsequent surface and modified in situ processing.

Shaft Sinking Technology. The development of shaft sinking systems is crucial for the large scale commercial utilization of oil shale. The R,D&D effort will carefully examine the current state of the art in shaft/slope development. A comprehensive research and development plan will be established that attacks all the major deficiencies in the current state of the art for accessing oil shale resources. Access development system concepts will be defined after a series of tasks which examine cutting and drilling methods, water/ground control, and large scale drilling. The expected result of this effort will be the development of techniques for efficient, safe, and environmentally acceptable shaft sinking.

Shale Oil Upgrading Technology. Crude shale oils generally contain greater amounts of certain elements and compounds that are not characteristic of conventional crude oils. These elements and compounds cause shale oils to exhibit properties that cause problems in storage, transportation and refining. The technology exists to convert and upgrade shale oils to products which can be processed in conventional ways, but it is necessary to determine which process schemes are most effective and economical. The R,D&D program will examine the production parameters of beneficiation, stabilization and preparation, denitrification, and alternative end-use options for liquid fuel products and heavy liquid fractions as they relate to the various retorting processes.

Chemical Kinetics. Several models have been developed which simulate the physical properties of oil shale retorting (e.g., shale composition, retorting rates, particle sizes, porosity distribution, etc.). For the models to accurately simulate retorting, they should include the details of the major chemical reactions in the system. The R,D&D program will develop the basic data on chemical kinetics needed to model the complex reactions taking place in retorting. Among these reactions are mineral decomposition, especially that of carbonates, which are large consumers of energy; reactions of char with steam and carbonate to produce valuable CO and hydrogen; degradation (loss) reactions of oil; gas phase reactions producing hydrogen and CO_2; gaseous sulfur evolution; etc. More work is needed on gas phase reactions, especially on water gas and water gas shift reactions, oil cracking stoichiometry of hydrocarbon combustion, and sulfur reactions in shale.

Retorting Mechanisms. Retorting technology is only crudely understood in lab and field retorts. Important operational problems include control of burn front, startup and sweep efficiency, effect of particle size distribution, inlet gas composition, especially steam and air mixtures, bed irregularities, flow rate, permeability changes during retorting, and temperature control. Program research will address key questions in the area of retorting mechanisms. A knowledge of the mechanisms taking place during retorting is

required to interpret results of experiments in pilot and field retorts to develop predictive models, and finally to suggest process modifications in order to optimize retort performance, expecially oil yields, and production rates. The development of retorting models will also be pursued as a means of understanding and predicting retort behavior.

Alternative Retorting Procedures. Oil shale retorting is approaching commercially viable levels of development. However, the technology is not sufficiently advanced to assure that optimally efficient and cost effective retorting methods are employed. The R,D&D program will examine alternative retorting processes with the objective of improving extraction efficiency and economics. Studies will include: (1) the use of oxygen (instead of air) plus steam to obtain high BTU outlet gas and reduce exit gas handling and cleanup; (2) the substitution of water mist for steam to improve heat balance; (3) determining retorting conditions to produce various optimum product mixes, e.g., maximum naphtha, minimum residuals, etc.; and (4) determining retorting conditions to produce minimum environmental effects (e.g., lowest sulfur in outlet gas, least soluble spent shale, etc.); (5) use of fluid beds to increase throughput, improve yield and lead to more favorable economics.

Environmental

The environmental research in the R,D&D Program represents a significant portion of the DOE's Environmental Development Plan. The overall objective of the Program's Environment Activity is to develop solutions to environmental problems associated with the process technologies involved in oil shale production. To achieve this objective, a series of Key Environmental Needs have also been established:

- Development of Environmentally Acceptable Retort Abandonment Strategy,
- Guidelines to Ensure Health and Safety of Workers and General Public,
- Development of Solid Waste Management Systems,
- Development of Water Treatment Systems,
- Development of an Emission Control Strategy,
- Mitigation of Ecological Impacts,
- Mitigation of Social and Economic Impacts,
- Development of Compliance Plans, and
- Development of Subsidence Control Procedures.

Development of Environmentally Acceptable Retort Abandonment Strategy. The spent shale remaining in underground retorts after product recovery contains salts and carbonaceous residues that can be leached by groundwater and thereby contaminate aquifers. In addition, some caving in from the weight of the overburden may occur resulting in subsidence at the surface.

The research related to this need will determine (1) the potential for groundwater intrusion, what materials are likely to be dissolved in groundwater, the permeability of the geologic media to the soluble components, the toxic properties of these components, and the persistence of any toxic components; and (2) the effectiveness of alternative measures for control of leaching and subsidence. The more general problem of subsidence in underground mines, the safety and ecological aspects, are dealt with in a separate area.

Guidelines to Ensure Health and Safety of Workers and General Public. Operations of an oil shale industry will introduce a new set of industrial working conditions and possible public health risks as a result of plant operations or product distribution. The research directed toward this need will examine the potential health and safety risks to workers and the general public. All aspects of the fuel cycle will be examined from the mine and retort to the refinery and end use of the shale oil products. Protective measures, whether they be through controls, process modification, or isolation of high risk areas, will be evaluated and effective measures will be applied.

Development of Solid Waste Management Systems. Surface processes produce extremely high volumes of solid waste in the form of spent shale. This research will evaluate methods of compacting and stabilizing spent shale and other solid wastes such as sludges and spent catalysts. The research will lead to the evaluation of alternatives for stabilizing and achieving self-sustaining ecosystems on the solid waste piles with minimum potential for water and wind erosion of toxic materials.

Development of Water Treatment Systems. In situ processes produce approximately one barrel of retort water contaminated with carbonaceous residues for each barrel of shale oil recovered. Surface processes also produce retort water but in lower quantities. Although current plans do not call for discharge of wastewater, it must be cleaned for reuse in the process and other uses, such as dust control and solid waste management. An objective of this research is to identify components in the wastewater that present either a health or environmental hazard with respect to the intended use of the water and to develop systems to remove these components. Another objective is to determine the consumptive water requirements of different oil shale processes.

Development of an Emissions Control Strategy. There are two major components to the emissions control need. One is directed toward determination of the emission control requirements based on the projected emission rates and composition of the emission streams. In the case of criteria or regulated pollutants, systems must be engineered to maintain ambient air quality within the region. In addition, modification of available technology and development of new systems may be required if risk analysis indicates that unique substances in the emission stream require removal.

The other component is directed toward estimation of the capacity of the region to accept industrial development--the regional carrying capacity--based on the meteorological characteristics of the region. More specific needs are (1) more accurate atmospheric models to predict the transport and dispersion of atmospheric pollutants, (2) determining rates at which pollutants are removed from the atmosphere, and (3) quantitative information on the effects of air pollutants on critical atmospheric processes related to undesirable effects, e.g., precipitation quality, decreased visibility, and local climate modification.

The research tasks that compose this segment of the plan will lead to the development of workable emission controls and estimates of effects of industrialization on regional air quality.

Mitigation of Ecological Impacts. Oil shale operations will cause much disruption of the surface environment through normal construction and operation activities--large amounts of solid waste stockpiles on the surface, water treatment operations, steam generation, mining, material handling, etc. The objectives of the ecological research, in addition to that which is an integral part of other activities such as the solid waste management system, will be to (1) evaluate overall effects of the operation on the ecological communities (plants, wildlife, fish) and (2) develop ecological test procedures that will be used by other parts of the program to evaluate systems performance with respect to ecological criteria. This work will be geared to the environmental impact approach described above.

Mitigation of Social and Community Economic Impacts. The social and community economic aspects of technological developments are among the most difficult to deal with. To a large extent, this is due to the fact that solutions involve institutional arrangements and legislative initiatives beyond the scope of most R&D operations. The problems do not lend themselves to controlled experiments that can be carried out in the field or laboratory. Installation of mitigating measures such as front-end financial support to communities for planning and development will be dealt with in DOE's industrialization plant. This R,D&D plan will focus on the social and economic issues for which solutions are not known and which therefore require additional research.

Methods for Controlling or Preventing Subsidence. Underground mines are always susceptible to subsidence, which presents a concern for safety and environmental disturbance, including aquifer disruption and changes in the surface land form. Some of the retort abandonment control measures will also act to prevent subsidence. The R&D conducted to satisfy this need will focus on general underground mining whether related to underground processes or surface retorting processes. It will be closely tied to the mining tasks and include analyses of safety, hydrological disruption, and changes in surface features. The research will focus primarily on prevention or planned, controlled subsidence.

Development of Compliance Plans. The R,D&D tasks, for environmental as well as the other three activities included in the Management Plan are carried out in conjunction with, or as part of, major field projects. These projects, which involve engineering and construction activities, must comply with Federal, state, and local standards, and in particular, with provisions of the National Environmental Policy Act (NEPA).

DOE prepares Environmental Assessments, and Environmental Impact Statements when appropriate, for those major field projects. Air, water, and other environmental monitoring, as required to demonstrate compliance with NEPA and applicable permits, is conducted as part of this need; that data is made available to other tasks for various analyses and decisions.

PROCESS SPECIFIC R,D&D

In addition to satisfying key needs which presently impede oil shale commercialization the Oil Shale R,D&D Program will simultaneously address the following processes.

Surface Processing. The DOE is pursuing a surface module demonstration program as described in PL 95-238. This program will result in both design and business proposals for the construction of a surface retort module. A decision to proceed with construction of designed modules on a cost shared basis will be made in late FY1980. Other research and development supporting surface retorting is mainly focused on mining and environmental effects with long term R&D directed to improving surface retorting processes.

In Situ Processing. The current near term emphasis of the Program's research activities is on developing and expanding in situ retorting process technology, with particular emphasis on modified in situ methods. This programmatic direction is based on the fact that in situ oil shale technology has not advanced to the point where it has been proven to be technically or economically feasible. Engineering analyses indicate that in situ processes have the potential to be more cost effective and less disruptive to the environment than surface retorting. Therefore, the program is focused on developing the necessary technical and environmental information from which an economic and environmentally acceptable in situ technology can be engineered.

In addition to this technology base program, the DOE is also sponsoring several major in situ oil shale field demonstration tests. The field demonstration test program and the technology based R&D programs are integrally related, in that field demonstration sites are often used as sites for R,D&D program efforts and information gained from the field tests is used to guide the

overall R,D&D program. Each of these projects has been evaluated to determine the program technology requirements that can be met by ongoing industry contracts and the other technology requirements that can be achieved through modification of the ongoing effort. In addition to providing valuable technology base information, it is anticipated that one or more of these projects could provide technical evidence of process feasibility. Use of existing projects to accomplish planned tasks will be maximized to reduce total program costs.

Novel Processing Techniques. In addition to the developmentally more advanced aboveground and in situ methods, research is being conducted into new and novel technologies for extraction and processing of oil shale products. Although not currently competitive for near term commercial development, these efforts are indicators of likely second generation advances in oil shale technology.

The novel technologies being developed are in two general categories.

- Radio Frequency Heating
- Hydrogen Retorting

PROGRAM OPERATING PLANS

The Oil Shale R,D&D Program is defined in two program plans presently in draft status: a Management and Strategic Plan which describes the R,D&D program management structure and the long term strategic aspects of the Department of Energy's program for achieving its technology objectives, and an Implementation Plan which details oil shale R,D&D activities over the next several years to the subactivity task level. In contrast to the Implementation Plan, the Management and Strategic Plan describes the Program's objectives as they will be attained by satisfying a series of technological needs, each of which may require the successful performance of one or more sets of tasks sometime in the future. Described are oil shale R,D&D activities for a multiyear period in terms of needs, with emphasis placed upon solving key technical and environmental needs inhibiting oil shale commercialization and developing an activity baseline for each of several candidate technologies to establish program direction, resource requirements, and expected accomplishment. Both plans serve as a basis for developing and justifying future budget requests over their respective periods.

Strategic Plan. The policy, management, organization, and long term aspects of the Oil Shale R,D&D Program, as directed toward satisfying its goal and objectives, are described in the Management and Strategic Plan. The discussion is in three parts, addressing planned program efforts concerned with:

- Key Technical Need R,D&D
- Key Environmental Need R,D&D
- Process Specific R,D&D

These efforts are defined at the fundamental needs level, each R,D&D objective (a key need being one such objective) requiring the fulfillment of one or more of these fundamental needs before it is obtained. This is in contrast to the manner in which the Implementation Plan is defined, wherein needs are specified in terms of the detailed tasks required to satisfy them. Strategic plans are outlined in a plane higher than that used in the Implementation Plan. Another distinction between the two is in their planning time horizon. Strategic plans are defined over a long term period, generally about ten years, whereas the Implementation Plan concentrates on the near term period not exceeding five years. To show continuity between the two plans, the time span addressed in the Implementation Plan is also defined with the strategic plans and need identifiers uniquely assigned in the Implementation Plan are referenced in the strategic plans.

Implementation Plan. Short term plans are defined in the Implementation Plan in terms of the activities and tasks to be performed. Outlined within the Plan are the research tasks that will be performed during the next five year period to enhance and encourage commercial oil shale development. The R,D&D tasks are described with respect to major activity areas (resource characterization, environment, development and extraction, and processing and instrumentation). Component subactivities within each of these activities provides a framework for organizing tasks around specified technology areas. For each program task the performance periods are specified in conjunction with task deliverables and participating organizations. The Plan, conceived as a working document which is annually updated, thus serves as a basis for implementing the R,D&D Program by the various research and industry participants.

The Commercial Scale Refining of Paraho Crude Shale Oil Into Military Specification Fuels

N. J. Wasilk

The Standard Oil Company (Ohio)
P.O. Box 696
Toledo, Ohio 43694

E. T. Robinson

The Standard Oil Company (Ohio)
4440 Warrensville Center Road
Warrensville Heights, Ohio 44146

Introduction

In September, 1977 The Standard Oil Company (Ohio) was contracted by the U.S. Navy to refine up to 100,000 barrels of crude Paraho shale oil into military transportation fuels. The objective of the program was to demonstrate that shale oil could be converted into stable, specification military fuels utilizing conventional refining technology and in sufficient volumes to support an extensive engine testing program. Yields of JP-5 and DFM were to be maximized while minimizing the yield of residual fuel.

The crude shale was produced by Paraho Development Corp. over the three year period from 1976 to 1978. Paraho's Anvil Point, Colorado works utilizes a vertical direct heat retort to recover the oil from crushed shale[1].

For contractual reasons the program was divided into three phases. During Phase I, the proposed shale oil processing scheme was tested and developed in appropriate pilot plants. Phase II constituted engineering preparation and the actual refinery run. Post run analysis and report writing were completed in Phase III.

Paraho Shale Oil

The unique nature of crude shale oil requires special consideration in handling and processing. Table I summarizes some typical inspections of raw shale oil and a West Texas crude. In comparison to conventional petroleum, shale oil has several deleterious characteristics:

[1] High nitrogen and oxygen content.
[2] Low hydrogen/carbon ratio.
[3] Low yield of 650° minus material (<30 vol.%).
[4] Moderate arsenic and iron content.
[5] Suspended ash and water.

The high nitrogen content is probably the largest area of concern, as it is an order of magnitude higher than that found in petroleum. The technology for processing high nitrogen crudes is not nearly as advanced as comparable technologies for desulfurization or cracking (increasing yield of lower boiling hydrocarbons).

Nitrogen compounds are known poisons for many petroleum processing catalysts such as fluid bed catalytic cracking, naphtha reforming and hydrocracking catalysts. In addition, nitrogen compounds have been found to create stability problems in gasoline, jet and diesel fuels. Fuel bound nitrogen will also increase the NO_x emissions from practically any type of combustor. Finally, nitrogen compounds quite often have a peculiar and offensive odor which is uncommonly difficult to remove[2].

Shale Oil Refining Process

A schematic of the process developed for this program is shown in Figure 1. The crude shale oil is initially allowed to settle batchwise at above ambient temperature. This has been found to be effective in breaking the water/oil emulsion, thereby precipitating suspended water and ash to the bottom of the tank. The shale oil is also pumped through a 20 micron filter enroute to the hydrotreater to remove any entrained debris left in the tank.

After settling, the shale oil is mixed with hydrogen, preheated and passed through a guard bed. The purpose of the guard bed is to remove the organic Fe and As as well as any ash and solids which survived the settling and filtering procedure.

Following the shale oil pretreatment steps (settling and guard bed demetallization) the whole shale oil is catalytically hydrotreated at elevated temperature and hydrogen partial pressure. Hydrotreating, the most important processing step, is the catalytic reaction of hydrogen with sulfur, oxygen and nitrogen compounds to form H_2S, H_2O and NH_3, respectively, plus heteroatom-free hydrocarbons. In addition, aromatic saturation and cracking occur to some extent -- thereby increasing the hydrogen/carbon ratio and increasing the yield of military fuel feedstock (650°F minus material).

The hydrotreated shale oil is fractionated by distillation methods into gasoline, jet, diesel, and 650°F bottoms (residua). The jet and diesel fuel boiling ranges were determined experimentally to meet flash and freeze or pour requirements while maximizing yields. The residua or bottoms material could not be utilized in the diesel or lighter cuts due to pour point requirements. Some of the residua was recycled back to the hydrotreater to increase jet and diesel fuel yields.

A final finishing step, acid and clay treating, was included to meet military specification gum and stability requirements.

Refinery Modifications

Prior to the shale oil operation, facilities modifications at the Toledo refinery were required to be able to receive, store and process the shale oil and its products without contamination from normal refinery stocks.

Raw shale oil was shipped from the Paraho facilities to Toledo by railroad tank car. An underutilized railcar rack was revamped to provide a new unloading as well as a product loading system. A new steam heated tank was built in which to store the shale oil as it was received over a 3 month period.

A hydrocracker which normally processes distillate fuels into gasoline products was modified to process the shale oil. New catalyst (Shell 324) was charged to the first stage reactor. A guard bed packed with alumina extrudate was placed in the feed preheat train. A 20 micron filter was installed on the inlet line from the shale oil storage tank. A new stripper tower was installed on the distillation tower to strip the DFM product. Numerous instrumentation and piping modifications were made to allow for a single stage hydrotreater operation.

For acid treating of the DFM and JP products a "new" acid treater was designed and built, the major vessels of which were refinery surplus equipment. These vessels included a settler, clay contactor and sludge storage tank.

To provide product storage for JP-5 and DFM, two tanks were removed from refinery service and cleaned prior to processing.

All lines used for shale oil material which interconnected with lines containing normal refinery stocks were either blanked or had the isolating valves chained and locked.

Refinery Logistics and Process Flow

When all the shale oil had been received, the storage tank was heated to 185°F, and an attempt was made to drawoff any free water. No free water was found. The shale oil received at Toledo measured only ~0.06 vol.% sediment and water,(BS&W)whereas earlier pilot plant samples contained ~0.8 vol.% B.S. and W. The shale oil was pumped continuously from the tank through the 20 micron feed filter into the hydrotreater surge drum. From here it was pumped through the feed preheat section and guard bed together with hydrogen gas and into the reactor. Reactor effluent was cooled, water washed and recycle hydrogen and light ends removed, prior to entering a multidraw distillation column. Here four products were recovered from the effluent: an overhead gasoline stock, a jet fuel cut (JP-5 or JP-8), a marine diesel fraction (DFM) and a bottoms residual fuel fraction. The gasoline stock was sampled, but not recovered in bulk, instead it was used as feed to another hydrocracker. The JP-8 was acid treated on rundown to a railcar, while JP-5 and DFM were run down to storage for later acid treating. Any off spec JP-5, JP-8 or DFM were returned to the shale oil storage tank. Part of the bottoms residua were recycled through the hydrotreater to increase conversion, while the remainder was used as cat cracker feed with a small

amount rundown directly to railcars for recovery as heavy fuel oil.

Refinery Run

The hydrotreating run began on November 4, 1978 and ended on December 4, 1978. In that time 73,100 barrels of the 88,225 barrels of shale oil received were hydrotreated. However some of the products from this volume were returned to the shale oil storage tank as off specification product. An excessively high pressure drop across the Guard Bed caused the run to be terminated before all the shale oil was processed. The hydrocracker was first shutdown on day 25 of the run because of a high guard bed pressure drop. The top 25% of the Guard Bed packing was removed because a black viscous sludge was present on the top of the bed. When returned to operation, the Guard Bed soon redeveloped a high pressure drop and the run was terminated due to contractual time limitations.

Original plans called for the JP products to be acid treated on rundown to tankage or railcar. This plan was modified after acid treater start-up problems resulted in poor denitrification. The JP-5 was rundown to tankage without acid treating, as was the DFM, and both were treated after the hydrotreating run was complete. Fortunately, the acid treating problems were resolved in time to treat the JP-8 on rundown to a railcar.

The residual hydrotreated shale oil was mixed with regular refinery cat cracker feed at a rate of 3%, with no detectable shifts in yields or other adverse consequences. Similarly, the gasoline range cut had no detectable effect on hydrocracker operations at 1.5% of feed.

The shale oil which remained after the processing run was burned as boiler fuel. No problems developed over the 1 month combustion period.

Following conclusion of the run, an examination of the Guard Bed contents revealed two separate problems, the sludge at the top of the bed and FeS_x fines throughout the bed. The sludge was theorized to have been formed by a reaction between shale oil, iron, and sulfuric acid. The acid had been unwittingly introduced into the shale oil feed tank by recycling off-spec JP-5 from the acid treater during startup. A large quantity of fines containing a high concentration of FeS_x was found throughout the bed. Apparently FeS_x had been depositing throughout the run and filled the interstitial spaces among the extrudate, thus causing a high pressure drop.

Material Balances

Essentially all of the conversion of 650°F plus bottom material to transportation fuel occurs in the hydrotreating step. Table II summarizes the overall material balance and yield structure from our hydrotreating section. Table II also compares the actual yields and nitrogen levels obtained at Toledo with original pilot plant results. These data indicate that the denitrification activity of the catalyst was consistent with prior results, however the apparent yield structure was different. The differences in yields are attributed to two factors: [1] poorer distillation efficiency in the refinery operation and [2] lower DFM pour point and flash point targets during the refinery run. The actual conversion of 650°F plus bottoms material attained in the refinery run is very similar to the pilot plant results. The distillation curve of whole hydrotreated products (minus recycle) shown in Figure 2, illustrates this observation.

Net hydrogen consumption metered in the refinery run was significantly less than pilot plant results [~1500 versus ~1050 SCFB]. Chemical analyses of the various hydrotreated products indicate that the level of aromatic saturation, cracking and heteroatom removal for both refinery and pilot plant were nearly the same. The difference in measured hydrogen consumption is most probably a result of scale-up and pilot plant error. Needless to say, hydrogen consumption is a very important parameter in determining overall shale oil economics.

The total amount of each finished fuel produced is shown in Table III. In acid treating the yield losses were found to be proportional to nitrogen content and molecular weight of the fuel. For a 3300 ppm nitrogen JP-5 stock, yield loss was 4 wt.% and on a 3300 ppm nitrogen DFM the loss was 5.4 wt.%. Other losses incurred in the system were start-up and line-out slop, heel left in feed tanks and treating vessels and losses during the clay column changes.

Product Analyses

Gasoline Stock

Analyses of the refinery and pilot plant gasoline stocks are shown in Table IV. Both materials are very similar in aromatic content, nitrogen level and octane. Neither is usable as a direct gasoline blending stock or as reformer feed. Additional hydrotreating is required to reduce the nitrogen content to levels acceptable to catalytic reforming, which is required to boost the octane of this material.

Jet Fuels

Product JP-5, before and after acid treating is compared to pilot plant prepared material in Table V. Again both stocks have similar nitrogen, hydrogen and aromatic content. Note that the thermal stability of the untreated fuel is poor. However, once the nitrogen compounds are selectively removed by acid treating, the fuels' stability as determined by gum and JFTOT (ASTM D-3241) measurements is very good. In addition, storage stability characteristics of the fuels were tested by aging the material for 1 month at 140°F and then repeating the JFTOT and gum tests. The aging test results, shown in Table VI for a composite sample of all treated JP-5 produced at the refinery, indicate that this fuel has very good storage stability properties.

Diesel Fuel Marine

Physical inspections of pilot plant and refinery DFM are compared in Table VII. As previously mentioned, the distillation (hence nearly everything else) are different due to refinery fractionation practices and altered target specs. Again, acid treating is required to meet fuel stability specifications, i.e. ASTM 2274 - (accelerated oxidation gum test). These fuels have good combustion properties, as shown by the cetane number (>50) and hydrogen contents (>13 wt.% hydrogen).

Residual Fuel

The residual fuel produced by both the pilot and refinery meets all government specifications for low sulfur, high pour #6 fuel oil. The residual fuels are in fact very "clean" as shown in Table VIII by the high hydrogen and low sulfur, metals, carbon and asphaltenes content. This stock is better utilized as cat cracker feed than residual fuel, since higher value gasoline and kerosine fuel can be easily produced via catalytic processing.

Product Fuels Distribution

All 6165 bbls of the treated JP-5 produced at the Toledo refinery was shipped to Rickenbacher Air Force Base in Lockbourne, Ohio. The treated DFM was shipped to four destinations: 3021 bbls went to General Motors Detroit Diesel, Allison Plant #5 in Indianapolis, Ind., 8334 bbls were shipped to Philadelphia Naval Base in Philadelphia, Pa., 235 bbls were sent to Wright Patterson Air Force Base, Fairborn, Ohio and 4785 bbls went to the Defense Fuel Support Point in Cincinnati, Ohio. Of the 4670 bbls of residual fuel reserved for shipment, 4345 bbls were sent to the U.S. Navy at Mechanicsburg, Pa., and the remaining 325 bbls were shipped to the E.P.A. at the Naval Ship Yard in Long Beach, California. These fuels are undergoing extensive engine testing and evaluation by the parties involved. In addition to the fuels produced, numerous samples of feed, intermediate and product streams were taken for health effect studies by the D.O.D. and D.O.E.

Conclusions

1) Fuels meeting military specifications and possessing good storage stability characteristics can be produced from crude shale oil, utilizing conventional refinery equipment.
2) The processing scheme utilized in this study requires:
   (a) Settling and a guard bed to protect the hydrotreating catalyst.
   (b) Hydrotreating to remove heteratoms, increase the hydrogen/carbon ratio and improve the 650°F minus liquid yield of shale oil.
   (c) Acid and clay treating to meet thermal and storage stability requirements of the jet and diesel fuel.

Acknowledgement

This program was administered by the U. S. Navy Energy and Natural Resources R&D offices under the direction of Lt. Commander Lawrence Lukens.

In addition, we wish to acknowledge the long hours and skillful assistance and operation provided by the Toledo Refinery Operations Staff and the Central Engineering Division.

References

1) Jones, J. B., Heistand, R.N., "Recent Paraho Operations", 12th Oil Shale Symposium Proceedings, Colo. School of Mines, April 18-20, 1979 pg. 184-194.
2) Robinson, E. T., "Refining of Paraho Shale Oil Into Military Specification Fuels", IBID, pg. 195-212.

Table I Properties of Paraho Shale Oil and West Texas Sour Crude

	Paraho Shale Oil	West Texas Sour
Gravity, °API	20.4	34.1
Specific Gravity @60°	0.9315	0.8545
Pour Point, °F	+85	Fluid @ -30
Viscosity, SSU		
@ 60°F	Too heavy	57.1
@ 100°F	213	43.1
@ 210°F	44.9	--
Viscosity-Gravity Constant	0.8899	0.722
RVP, lbs.	--	5.1
Total Acid No., mgKOH/g	1.988	0.265
Asphaltenes, wt.%	0.889	1.028
Ramsbottom Carbon, wt.%	2.977	2.65
BS&W, Vol. %	0.05 (0.06 unsettled)	0.30
Salt, lb./M Bbls.	4.9 (8.2 unsettled)	3.3
Elemental Analysis		
C, wt.%	83.68	--
H, wt.%	11.17	--
O, wt.%	1.38	--
N, wt.%	2.02	0.10
S, wt.%	0.70	1.40
Metals		
As, ppm	7.5	--
Na, ppm	<0.3	--
K, ppm	0.17	--
V, ppm	0.17	4.4
Ni, ppm	2.4	2.6
Fe, ppm	53	2.0
TBP 650°F Point, vol. %	28.24	58.64

Table II Shale Oil Hydrotreating Yields

	Toledo Refinery			Pilot Plant	
	Bbls.	Vol.%	Wt.% N	Vol. %	Wt.% N
Gasoline stock (including Butanes)	8743	11.96	0.067	11.00	0.050
JP-5	9546	13.73	0.220	25.30	0.250
JP-8	490				
DFM	18939	25.90	0.340	34.50	0.430
Residual Fuel	37220	50.91	0.380	35.20	0.220
	74938	102.50		106.00	
H_2 Cons. SCFB		1050		1500	

Table III Net Fuels Produced After Acid/Clay Treating

	Bbls.
Gasoline Stock	7,718
JP-5	6,615
JP-8	462
DFM	16,375
Residual Fuel	37,220

Table IV Gasoline Stocks Analyses

	Pilot Plant	Toledo
API Gravity	57.8	54.7
RVP, psi	1.3	5.6
Distillation	D-86	D-86
IBP, °F	190	200
10	226	249
50	258	283
90	288	317
EP	332	370
% Rec.	99.0	98.0
% Res.	1.0	1.0
Paraffins	58.87	49.95
Monocyclo. Par.	29.61	31.62
Dicyclo Par.	1.11	2.40
Alkylbenzenes	9.97	15.20
Indans + Tetralins	0.11	0.51
Naphthalenes	0.33	0.32
Carbon No. Par.	8.01	9.36
Carbon No. Alkybenzenes	7.81	7.85
Nitrogen, Wt. %	0.040	0.078
Research Octane, clear	47	Not run

Table V JP-5 Analyses

A - Untreated JP-5

	Pilot Plant	Toledo	Mil Spec
API Gravity	41.8	42.7	API < GR < 48
Flash, °F	157	158	140 Min.
Freeze, °F	-52	-57	-51 Max.
Existent gum (D-381) Mg/100 cc	12.2	Not run	7.0 Max.
Distillation	D-86	D-86	D-86
IBP, °F	356	370	R
10	380	384	401 Max.
50	415	400	R
90	456	436	R
EP	477	480	554 Max.
Nitrogen, Wt. %	0.32	0.29	--
Paraffins, Vol. %	43.9	42.5	--
Naphtenes, Vol.%	33.1	36.0	--
Aromatics, Vol. %	23.0	21.5	25% Max.
JFTOT Visual	4 (Fail)	--	<3

B - Treated JP-5

	Pilot Plant	Toledo	Mil Spec
API Gravity	43.0	43.6	36 < API Gr < 48
Nitrogen, PPM	8	0.5	--
TAN, mg KOH/gm	Nil	0.005	0.015 Max.
WSIM	86	95	85 Min.
Existent gum Mg/100 cc	0.6	1.4	
JFTOT @ 500°F			
Visual	2	1	< 3
Max Spun Rate	10	0	< 17
Max ΔP mm Hg	1.0	0.5	< 25
Paraffins Vol.%	46.0	43.7	
Naphtenes Vol. %	33.1	34.5	
Aromatics Vol. %	20.9	21.8	25% max.

Table VI Refinery JP-5 Stability Properties

	Unaged Fuel	Aged @ 140°F for 1 month
JFTOT Break Point, °F	625	> 500
Color	+ 30	+ 30
D-381 Existent Gum Mg/100 cc	1.4	1.6
JFTOT @ 500°F, visual	<2	< 2
JFTOT @ 500°F, Max Spun Tube	1.0	3.0
JFTOT @ 500°F, Max Spot Tube	2.0	2.0
JFTOT @ 500°F, ΣTDR	1.5	6.5
JFTOT @ 500°F, Δ P MM Hg	0.0	0.0

Table VII — Diesel Fuel Marine Analyses

A - Untreated DFM

	Pilot Plant	Toledo	Mil Spec
API Gravity	33.4	36.8	R
Pour, °F	15	0	20 Max
Flash, °F	290	162	140 Min
Distillation	D-86	D-86	D-86
IBP	507	396	--
10	529	456	--
50	553	512	R
90	595	562	675 Max
EP	628	582	725 Max
% Res	1.0	1.0	3 Max
Nitrogen, Wt.%	0.40	0.33	
Cetane Index	50.1	52.5	45 Min

B - Treated DFM

	Pilot Plant	Toledo	Mil Spec
API Gravity	34.8	38.1	R
Carbon, Wt. %	86.75	86.27	--
Hydrogen, Wt. %	13.02	13.28	--
Nitrogen, ppm	90	3.9	
Paraffins Vol. %	42.2	45.5	--
Naphthenes, Vol. %	25.8	25.5	--
Aromatics, Vol. %	32.0	29.0	--
TAN, Mg KOH/gm	0.029	0.010	0.30 Max
Cetane Number	55.3	50.1	45 Min
ASTM 2274 Mg/100 cc (acc. oxid. test)	0.37	0.51	2.5 Max

Table VIII — Residual Fuel Analyses

	Pilot Plant	Toledo
API Gravity	30.3	29.6
Pour Pt., °F	105	80
Rams Bottom Carbon, Wt. %	Not run	0.096
Asphaltenes, Wt. %	0.244	0.059
Vis. @ 210°F, CST	6.45	2.00
Distillation	D-2887	D-2887
IBP	689	331
10	739	582
50	830	732
90	958	900
EP	1000	1032
Carbon Wt. %	87.32	86.71
Hydrogen, Wt. %	12.59	12.75
Nitrogen, Wt. %	0.33	0.44
Oxygen, ppm	102	182
Sulfur, ppm	< 20	< 20

Table VIII, Continued

	Pilot Plant	Toledo
Saturates, Vol. %	57.1	Not run
Aromatics, Vol. %	42.9	Not run
Iron, ppm	0.93	0.10
Arsenic, ppm	0.13	0.4
Vanadium, ppm	0.36	0.02
Sodium, ppm	0.79	0.6
Potassium, ppm	< 0.10	0.6

FIGURE 1

Shale Oil Processing Block Flow Diagram

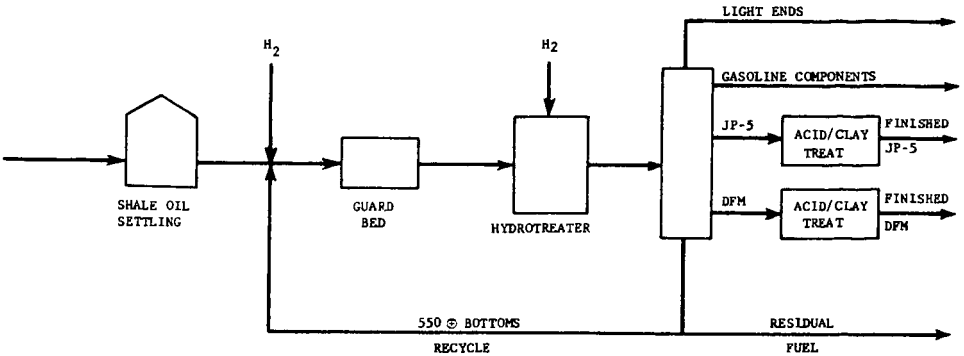

FIGURE 2
T.B.P. Distillation Comparison of Pilot Plant and Refinery Whole Hydrotreated Product

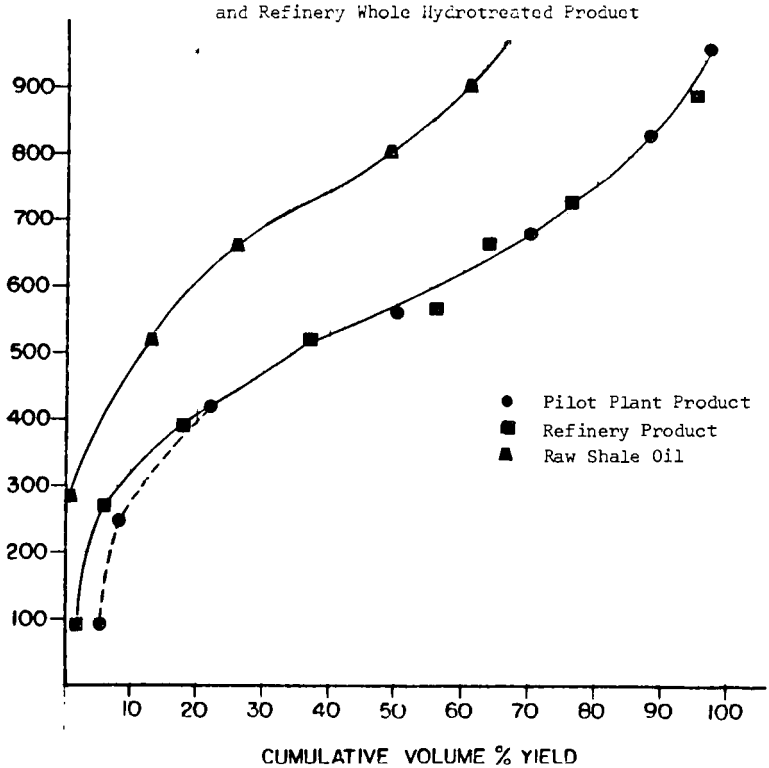

RELATION BETWEEN FUEL PROPERTIES AND CHEMICAL COMPOSITION. II. CHEMICAL CHARACTERIZATION OF U.S. NAVY SHALE-II FUELS

Jeffrey Solash, Robert N. Hazlett, Jack C. Burnett
Erna Beal and James M. Hall

Naval Research Laboratory
Code 6180
Washington, D.C. 20375

As domestic and imported petroleum supplies dwindle and petroleum increases dramatically in cost, it is imperative for the Navy to consider future liquid fuel options. The Navy has two thrusts in transportation fuels: (a) explore the relaxation of fuel specifications and (b) examine alternate sources of fuels. This paper deals with one of the alternate sources, shale oil.

The bulk of the Navy's vehicles utilize middle distillate fuels; a kerosene type jet fuel, JP-5, for aircraft and diesel fuel marine (DFM) for ships and boats. Reasonable yields of these fuels can be obtained from shale oil. Further, shale crude oil has a good hydrogen content which allows upgrading to finished fuel with modest additions of expensive hydrogen. Thus the interest in Navy fuels from shale oil.

The Navy has completed two crude production/refining exercises with shale. The first of these, a 10,000 barrel operation (Shale-I), is described in two reports (1,2). The second, a 73,000 barrel operation (Shale-II), was completed in 1979 at the Toledo refinery of Sohio (3). This paper describes the chemical characterization of the JP-5 and DFM from the Shale-II project.

EXPERIMENTAL

Samples - One gallon samples of the various refinery streams were obtained from Sohio throughout the approximately one month of production. Periodic samples of finished JP-5 and DFM were also obtained during the acid treatment process which was completed subsequent to the hydrocracking and fractionation steps. Drum samples of the finished homogeneous JP-5 and DFM products were also examined.

Total Nitrogen - The fuel samples were pyrolyzed/combusted at 1000°C in a flow of argon/oxygen and the chemiluminescence for the reaction of NO with ozone measured (4). Types of specific nitrogen compounds found will be discussed in another paper of this symposium.

GC Analyses - The n-alkanes in the fuel samples were determined with a 100 meter OV-101 wall coated glass capillary column. The inlet split ratio was 50:1, the column oven was temperature programmed from 80 to 240°C, and the inlet temperature was 310°C.

LC Separation - Preparative scale liquid chromatography was performed with Waters PrepPak radially compressed silica columns. Fuel charges of 6 to 10 ml were carried through the column with n-pentane at a flow of 200 ml/minute. Refractive index, 254 nm ultraviolet, and 313 nm ultraviolet detectors monitored the LC effluent and keyed the collection of fractions.

Mass Spectrometry - Electron impact mass spectrometry was done at NRL on the effluent from a 6 ft. OV-101 packed GC column programmed from 70 to 210°C. Field ionization mass spectrometry (FIMS) was performed by SRI International on contract to NRL. In this latter analysis, the fuel sample was frozen on a solids inlet probe prior to insertion into the mass spectrometer. The spectra accumulated for each mass during a temperature program were normally totaled for data presentation (5). Molecules boiling below 140°C are lost or depleted with this technique but such compounds comprise a very small fraction of JP-5 or DFM. Since the ionization efficiency for hydrocarbon classes is currently under study, the FIMS data is utilized primarily in a qualitative sense.

NMR Examination - Fuel samples and fractions were analyzed by proton and ^{13}C NMR at the Naval Biosciences Laboratory. The spectra were taken on a Varian FT-80A. Chromium acetonyl acetonate was added as a relaxation reagent.

RESULTS

Nitrogen Content - The bulk of the shale oil nitrogen was removed in the hydrocracking step. All four products from fractionation of the hydrocrackate--naphta, jet, diesel and heavy oil--contained substantial amounts of nitrogen, however. The data in Table I indicate that the lighter products had less total nitrogen.

All products increased in nitrogen content as the refining run progressed. For instance, the 25 day hydrocrackate contained 2 1/2 times the nitrogen found in the 12 day product. The jet and diesel fractions almost doubled in nitrogen over the same time span. The hydrocracking catalyst lost activity throughout the run.

The nitrogen content of the JP-5 and DFM fractions, the products important to the Navy, was too high to afford satisfactory stability. Extensive acid treatment with sulfuric acid reduced the nitrogen content in the finished fuels, however, to one ppm(w/v) for the JP-5 and 18 ppm (w/v) for DFM.

n-Alkane Content - Shale fuels exhibit higher freeze and pour points than similar fuels made from most petroleum crudes. This is related to the symmetrical n-alkane molecules which are major components of shale derived fuels (6). The content of these molecules in the Shale-II middle distillate fuels is listed in Table II. The relationship between freezing point and composition will be considered in another paper of this symposium.

FIMS Fingerprint - Field ionization mass spectrometry of a mixture affords a spectrum of the molecular ions since fragmentation is minimal. Thus a distribution of molecular sizes and hydrocarbon classes can be obtained from a single analysis. This is illustrated in Figures 1 and 2 which compare the FIMS fingerprints for JP-5 from Shale-I and Shale-II refining. Distinct differences can be noted. The preponderance of alkanes (C_nH_{2n+2}) is highlighted in Shale-I fuel which was produced by cracking the shale crude by delayed coking. Shale-II, a hydrocracking process, produced a product much lower in alkanes. Analysis for total n-alkane content agrees with this finding, 37% in Shale-I JP-5 (6) and 22% for Shale-II. Other significant differences between the two jet fuels can be noted in the much higher

peaks for substituted benzenes (C_nH_{2n-6}) and tetralins (C_nH_{2n-8}) in the Shale-II product.

Other differences can be noted in the FIMS data assembled in Table III. For instance, Shale-II also has higher peak sums for monocyclic alkanes (C_nH_{2n}) and dicyclic alkanes (C_nH_{2n-2}) than Shale-I (coking). Data for a third JP-5 sample, a ten gallon quantity produced by fractionation of Paraho shale crude followed by 1200 psi catalytic hydrogenation of the jet fuel cut (7), is also shown in Table III. Again this fuel has a distinctly different FIMS fingerprint in response to the refining process used.

Preparative Scale LC - Separation of JP-5 and DFM on the Waters radially compressed silica column gave many fractions. This is illustrated in Figure 3 for six ml of DFM. Fraction one, beginning at 3.2 min, is the saturate fraction which was detected with a refractive index detector. Fraction 2, indicated by slight absorption on the 254 nm uv detector, corresponds to the olefin fraction. The subsequent fractions, as indicated by the strong absorption on one or both of the uv detectors, are comprised of aromatic fractions. It is noteworthy that fractions 7,8 and 9 exhibit significant absorption at 254 nm but none at 313 nm. The JP-5 sample gave only five fractions in the same type of analysis.

Evaporation of the n-pentane solvent gave an estimate of the amount of the various fractions. The percentages normalized to total 100% are listed in Table IV. Recoveries of input sample amounted to 96 and 93% for the DFM and JP-5, respectively. The losses were due to evaporation of volatile components during the removal of the solvent. As expected, fractions 1 and 3 comprised the bulk of the fuel samples, 88.5% of the DFM and 95.3% of the JP-5.

Mass Spectrometry of LC Fractions - The fractions from the preparative scale LC were subjected to GC/MS analysis with electron impact ionization. The total fractions were also analyzed by field ionization mass spectrometry with a direct insertion probe. The FIMS m/e plot for DFM fraction five is depicted in Figure 4. The two major hydrocarbon series observed in this fraction are C_nH_{2n-12} and C_nH_{2n-14}, naphthalene and acenaphthenes. Trace amounts of the C_nH_{2n-10} and C_nH_{2n-8} series also appear in Figure 4.

A summary of the hydrocarbon series in the nine DFM and five JP-5 LC fractions are listed in Table V. The data are qualitative in nature and based on both MS techniques, EI and FI. The trends with fraction number are as expected, hydrocarbons with less hydrogen appear in the later fractions. Further, the trend in aromatic ring size was 1 ring (fraction 3), 2 rings (fraction 4), and 3 rings (fractions 5-9). The JP-5 has very little three ring material but the DFM exhibits evidence for considerable amounts of acenaphthenes, fluorenes, and phenanthrenes/anthracenes.

The LC separation did not give sharp separation by ring size, however. For instance, tetralins appeared in fractions 3-5 and naphthalens occurred in fractions 4-7. Larger molecules in a particular series eluted in later fractions.

Significant amounts of partially or fully saturated ring compounds were found in the jet and diesel products. Mono- and dicyclic

alkanes were a major portion of the saturate fraction and a fair amount of tricyclic alkanes were also found. Tetralins/indanes were also found in abundance. Some partially hydrogenated tricyclic aromatics -- C_nH_{2n-10} (tetrahydroacenapthene, hexahydrofluorene, and octahydrophenanthrene) -- were also observed. The presence of these types of compounds is evidence of the high pressure hydrocracking step in the refining process.

NMR analyses - Fraction 3 from the LC separation was subjected to proton nmr examination. The information from this examination was treated by the method of Clutter and co-workers (8) to describe the average molecule. The calculated parameters are summarized in Table VI. The values obtained are consistent with the other information in this paper and in the description of the Shale-I JP-5 reported in an earlier article (6).

CONCLUSIONS

The information presented in this paper shows that shale oil has an excellent potential as a source for high quality middle distillate fuels. The composition of such fuels may vary widely, however, depending on the overall refining process. Much work is needed to explore other refining options and to examine the effect of refining on finished fuel composition and properties.

ACKNOWLEDGEMENT

The authors thank Dr. S. E. Buttrill, Jr., of SRI International for performing the FIMS analyses and LCDR William Coleman of the Naval Biosciences Laboratory for conducting the nmr analyses.

REFERENCES

1. H. Bartick, et al, "The Production and Refining of Crude Shale Oil into Military Fuels," Applied Systems Corp., Vienna, Va., ONR Contract N00014-75-C-0055, Aug. 1975.

2. Applied Systems Corp., Vienna, Va., "Compilation of Oil Shale Test Results," ONR Contract N00014-76-C-0427, Apr. 1976.

3. ONR Contract N00014-79-C-0001, June 13, 1978.

4. H.F. Drushel, Anal. Chem., 49, 932 (1977).

5. G.A. St. John, S.E. Buttrill, Jr. and M. Anbar, Ch. 17, "Field Ionization and Field Desorption Mass Spectrometry Applied to Coal Research," in ACS Sym. Series No. 71, Organic Chemistry of Coal, ed. John Larson, 1978.

6. J. Solash, R. N. Hazlett, J.M. Hall and C.J. Nowack, FUEL, 57, 521 (1978).

7. AFAPL-TR-75-10, USAF Tech. Rpt. "Evaluation of Methods to Produce Aviation Turbine Fuels from Synthetic Crude Oils, Phase 2," Exxon R&E Co., Linden, N.J., May 1976.

8. D.R. Clutter, L. Petrakis, R.L. Stenger and R.K. Jensen, Anal. Chem., 44, 1395 (1972).

TABLE I. Shale-II Refining Nitrogen Content*

Days of Operation	Product: Hydro-crackate	Naphtha	Jet Pre-Acid	DFM Pre-Acid	Fractionation Residue
12	1400	---	1700	2500	1940
18	2000	---	2300	2900	2700
21	3000	640	2500	4000	----
25	3800	---	2900	4700	----

* - PPM (wt/vol).
Crude shale oil contained 2.1% nitrogen

TABLE II. n-Alkanes in Shale-II Fuels

n-Alkane	Weight Percent: JP-5	DFM
C_8	---	0.06
C_9	0.14	0.13
C_{10}	4.20	0.46
C_{11}	7.23	0.93
C_{12}	6.08	1.40
C_{13}	3.30	2.22
C_{14}	0.93	2.39
C_{15}	0.28	2.61
C_{16}	0.06	2.19
C_{17}	0.01	2.11
C_{18}	---	1.40
C_{19}	---	0.65
C_{20}	---	0.04
Total	22.23	16.59

TABLE III. Hydrocarbon Classes in JP-5 Samples by FIMS*

Hydrocarbon Series	Shale-I (Coking)	Shale-II (Hydrocracking)	Shale-I (Fractionation & Hydrogenation)
C_nH_{2n+2}	50.8	30.4	40.6
C_nH_{2n}	12.2	16.9	20.8
C_nH_{2n-2}	4.1	7.1	11.2
C_nH_{2n-4}	1.9	0.8	3.2
C_nH_{2n-6}	16.6	19.6	14.4
C_nH_{2n-8}	12.2	23.8	7.3
C_nH_{2n-10}	1.7	1.0	2.2

* Ion intensities (total = 100)

TABLE IV. Yields From LC Separation

	Percent Yield	
FRACTION	DFM	JP-5
1	68.9	73.6
2	0.8	2.9
3	19.6	21.7
4	7.1	1.6
5	1.2	0.3
6	0.6	---
7	0.7	---
8	0.5	---
9	0.7	---
% recovered	96	93

TABLE V. Hydrocarbon Series in Shale-II Fuels

MASS Series	LC Fraction* 1	2	3	4	5	6	7	8	9
2n + 2	J(M),D(M)	J(t),D	---------	--------	--------	------	-------	-------	-------
2n	J(M),D(M)	J ,D(M)	---------	--------	--------	------	-------	-------	--------
2n - 2	J(M),D(M)	J(M),D(M)	---------	--------	--------	------	-------	-------	--------
2n - 4	J ,D	J(M),D(M)	---------	--------	--------	------	-------	-------	--------
2n - 6	J(t),D(t)	J ,D(M)	J(M),D(M)	J ,D(t)	J(t)	------	-------	-------	--------
2n - 8	---------	J(t),D	J(M),D(M)	J(M),D(M)	J(t),D(t)	------	-------	-------	--------
2n - 10	---------	---- D(t)	J(t),D	J ,D(M)	J ,D(t)	D(t)	D(t)	-----	-------
2n - 12	---------	---------	J(t),D(t)	J(M),D(M)	J(M),D(M)	D(M)	D(t)	D(t)	D(t)
2n - 14	---------	----------	---------	J(t),D	J(M),D(M)	D(M)	D(M)	D(M)	D(M)
2n - 16	---------	----------	---------	---------	---- D(t)	D(t)	D(M)	D(M)	D(M)
2n - 18	---------	----------	---------	---------	---------	D	D(M)	D(t)	----

* J - present in JP-5 D - present in DFM
J(M) - major series in JP-5 D(M) - major series in DFM
J(t) - trace amount in JP-5 D(t) - trace amount in DFM

TABLE VI. Average Molecule in Fraction Three

Parameter	JP-5	DFM
Aromaticity	0.49	0.39
Aromatic Rings/ Molecule	1.0	1.0
Average Mol. Wt.	164	206
Average Mol. Formula	$C_{12.2}H_{16.8}$	$C_{15.2}H_{23.3}$
Alkyl Substituents/ Molecule	3.2	3.1
Carbons/Alkyl Substituent	2.0	3.0
Naphthene Rings/ Molecule	0.5	0.7

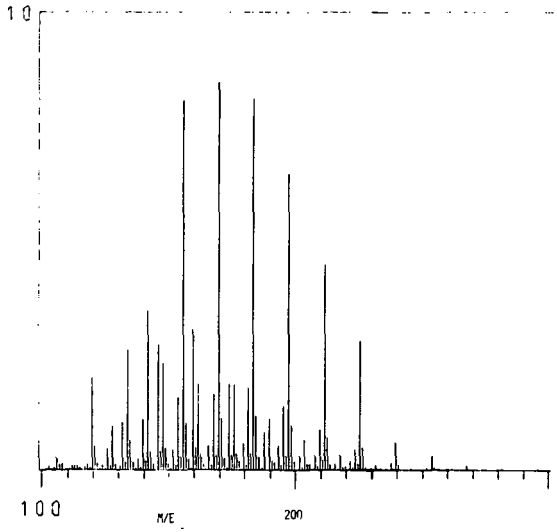

FIG. 1. FIELD IONIZATION MASS SPECTRUM OF SHALE-I JP-5.

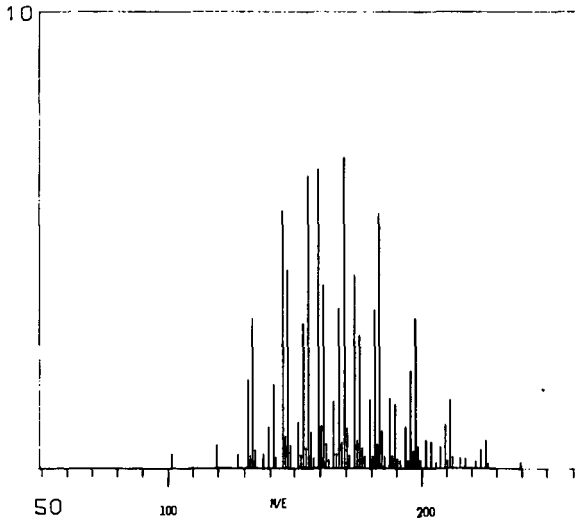

FIG. 2. FIELD IONIZATION MASS SPECTRUM OF SHALE-II JP-5.

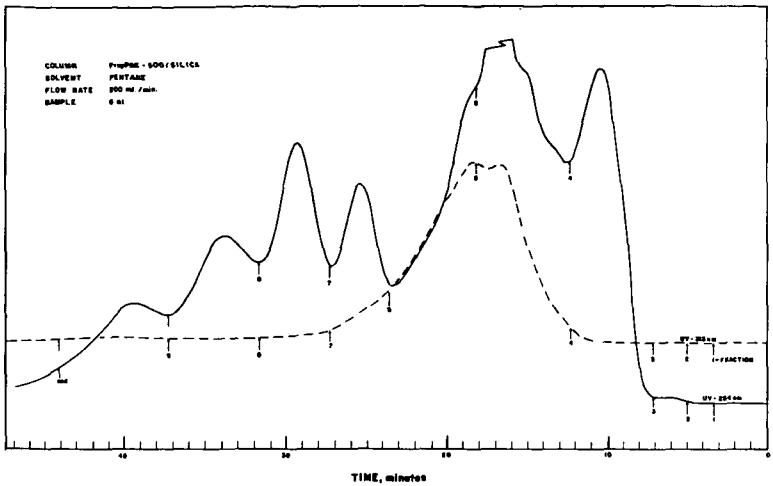

FIG. 3. PREPARATIVE SCALE LC SEPARATION OF SHALE DIESEL FUEL MARINE; SOLID LINE - 254 NM UV DECTECTOR, DOTTED LINE - 313 NM UV DETECTOR, RI DETECTOR TRACE NOT SHOWN; SMALL NUMBERS INDICATE TIMES WHEN FRACTION COLLECTION WAS BEGUN.

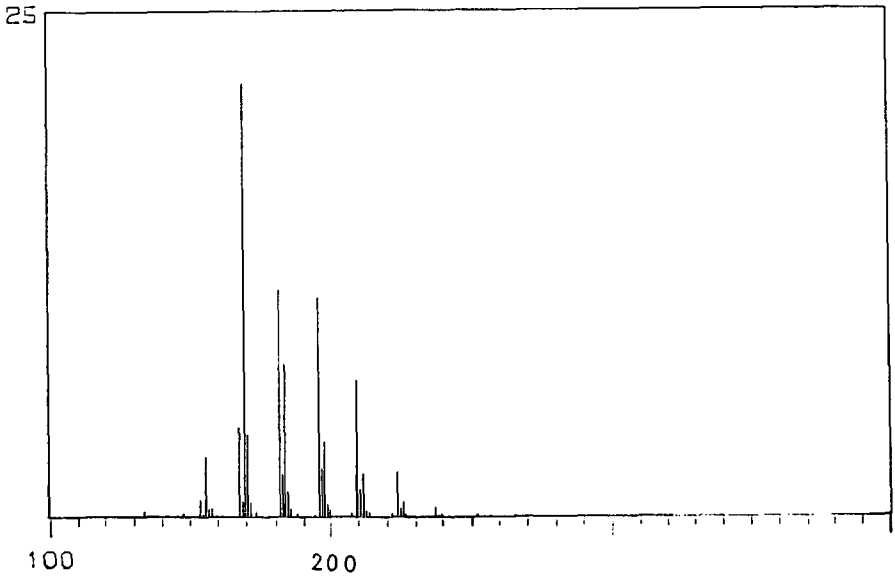

FIG. 4. FIELD IONIZATION MASS SPECTRUM OF DIESEL FUEL MARINE, FRACTION 5. MAJOR HYDROCARBON SERIES ARE C_NH_{2N-12} AND C_NH_{2N-14}.

Relationship Between Fuel Composition and Properties.

III - Physical Properties of U. S. Navy Shale-II Fuels

W. A. Affens, J. M. Hall, E. Beal, R. N. Hazlett
Naval Research Laboratory
Washington, D. C. 20375

C. J. Nowack, G. Speck
Naval Air Propulsion Center
Trenton, New Jersey 08628

INTRODUCTION

The U. S. Navy has been involved for some time in the development of Navy fuels from alternative sources (shale oil, tar sands and coal) and as a part of this effort, the Naval Research Laboratory and the Naval Air Propulsion Center have been studying the characteristics of these fuels (1,2). NRL and NAPC are currently participating in a program to characterize the products from the Shale-II refining process conducted by the Standard Oil Company of Ohio (SOHIO) at their refinery in Toledo, Ohio. This paper is concerned with a part of this program and is a summary of the work on the physical and related properties of three military type fuels derived from shale: JP-5 and JP-8 jet turbine fuels, and diesel fuel marine (DFM) (3-5). Another paper of this symposium (6) will discuss the chemical characterization of the fuels.

JP-5 (3) is a "high flash point" Navy fuel for carrier-based jet aircraft and helicopters and occasionally for shipboard power plants and propulsion. JP-8 (4), a U. S. Air Force jet fuel, is very similar to "Jet A" kerosene used by commercial jet aircraft in the United States and elsewhere.

The shale derived fuels which were used in these studies were derived from Paraho crude shale oil. The refining process which was used is described elsewhere (7).

A total of thirty-six Shale-II fuel samples have been examined including seventeen JP-5 samples, five JP-8 samples and fourteen DFM samples. Of the thirty-six samples, twenty-six were "finished" fuels in that they had been treated with sulfuric acid to remove organic bases, and ten were "pre-acid treatment" samples. Six of the finished samples did not contain additives but the remaining twenty samples did. The latter group included two pilot plant samples, one JP-5 ("J-PP") and one DFM ("D-PP").

GC SIMULATED DISTILLATION

The boiling range distribution of a representative sample of each of the three fuels was determined by gas chromatography (GC Simulated Distillation) using ASTM method D 2887 (8). Data are given in Table I and plots of the data for JP-5 and DFM are shown in Figure 1. JP-8 data have been omitted from the figure since the data for JP-5 and JP-8 are quite similar. The temperatures for the JP-8 averaged 4°C lower than for the JP-5 at the various percentages. The only exception was the 0.5% distilled point, for which JP-5 was

5°C lower. The JP-5 data are somewhat low compared to current JP-5 from petroleum (9). As a rule, data obtained by a GC simulated distillation do not agree with analogous data obtained by actual distillation. Temperatures by the simulated distillation are lower than that of simple ASTM pot distillations (10) at the initial temperatures, higher near the end point temperatures, and in close agreement near the midpoint temperatures (3,4). From the distillation data and other data which follow, the JP-8 Shale-II samples can be considered to be "JP-5" fuel for all practical purposes.

MISCELLANEOUS PHYSICAL PROPERTIES

Specific gravity, freezing point and pour point data are shown in Table II. For each fuel four kinds of data are given (where available): the range of the data (minimum and maximum values obtained), the average value for all the samples examined, the military specification requirement for that property, and an average value for a representative petroleum derived fuel. Also shown in the table are the number of fuel samples which were examined in each case. This format is also used for Table III which will follow.

Specific Gravity - The specific gravities of the Shale-II jet fuels (one sample of each type) were very similar to each other, met specification requirements, and were about the same as that of an average petroleum derived fuel. The two Shale-II DFM specific gravities were very similar but slightly lower than that of an average petroleum derived fuel.

Freezing Point - With the exception of one JP-8 sample (J-11), all the samples of the jet fuels froze below the specification maximum. The single exception froze less than 0.5°C above the allowed value for JP-8, -50°C. The similar freezing points for the JP-5 and JP-8 samples reinforce the conclusion from the distillation data that the two types of jet fuels made in the SOHIO process are very similar. The highest JP-5 freezing point was that of the pre-acid treatment sample (J-7) which froze at -46.8°C. The freezing point of jet fuels is greatly affected by the concentration of the higher n-alkanes, such as n-hexadecane (1). The relationship between freezing point and the concentration of n-hexadecane in the fuel appears to be consistent with that of the Shale-I studies. The amount of these alkanes in the Shale-II jet fuels is relatively low (6), a result of keeping the distillation end point lower than normal (3,4).

Pour Point - The pour points of each of two samples of DFM were -20.6°C. This value is well below the specification maximum of -6.7°C (4) and that of an average petroleum derived DFM (11,12).

FLAMMABILITY, IGNITION AND ELECTROSTATIC PROPERTIES

Flammability, ignition, and electrostatic properties are shown in Table III. As in the case of the miscellaneous physical properties (Table II), the range of the data, averages, specification requirements, and representative values for petroleum derived fuels are given in the table.

Flash Point - Flash points were determined by the Tag closed cup method (16) rather than by the Pensky-Martens method (20) as

called for in the specifications for JP-5 (3) and DFM (5). The Tag closed cup, however, is specified for JP-8 (4). The Tag method was chosen in order to have a basis of comparison for all three fuels and because it gives values which are closer to the lower flammability temperature limits which is important from the standpoint of safety. For fuels in the JP-5/DFM flash point range, the Tag method gives values which are 2-4°C lower than that of the Pensky-Martens (12). The JP-8 and the DFM flash points are seen to be well above the specification requirements of 38° and 60°C (4,5). In the case of the JP-5 samples, four of the six samples had Tag flash points which were below the required 60°C (3). However, if we assume that the Pensky-Martens flash points would average about 3°C higher, four of the six samples would then meet the 60°C minimum and the other two would be less than a degree low. The Shale-II JP-8 flash point data are somewhat higher than that of an average petroleum derived JP-8 and quite close to that of the Shale-II JP-5.

Autoignition Temperatures - The autoignition data (AIT) shown in Table III were determined by ASTM D 2155 (17). The Shale-II JP-8 and DFM AIT values (238°C) were identical and similar to that of their petroleum derived counterparts. The Shale-II JP-5 AIT (232°C), however, was slightly lower than that of the other two fuels as well as that of representative petroleum JP-5 (241°C), but was well within the 11°C reproducibility limit set by the method (17). There are no AIT requirements in the military specifications for JP-5, JP-8 and DFM (3-5).

Electrostatic Properties - Electrostatic data are shown in Table II. The electrical conductivity and charging tendency of jet fuels are important with respect to electrical charge buildup in flowing fuel equipment, particularly filter separators. Electrical charge buildup can result in a spark discharge capable of igniting flammable vapors if they are present. This is a frequent cause of accidental fires and explosions and is an important factor in safety. Therefore, these properties were measured on the Shale-II jet fuels to determine if these fuels posed a lesser or greater hazard than their petroleum-derived counterparts. The values which were found for the Shale-II jet fuels in Table III are in the normal ranges found for petroleum derived jet fuels. The response to the addition of a static dissipator additive, ASA-3, is also normal. These Shale-II jet fuels behaved significantly different than the Shale-I JP-5 which exhibited abnormally high electrical conductivity (215 pS/m) and charging tendency (7035 $\mu C/m^3$) without the addition of any additives (2).

COPPER CORROSION

Tests for corrosion are of a qualitative type and are made to determine whether the fuel is free of tendency to corrode copper bearing alloys in aircraft pumps. The results of the ASTM copper strip corrosion tests (22) are shown in Table IV. The samples in the table are grouped in accordance with their refining treatment and by the additives the fuels were reported to contain. The fuels fall into four groups as seen in Table IV: (a) nine samples taken in the refining process before the acid treatment; (b) six finished samples which contained no additives; (c) nine jet fuels containing fuel system icing inhibitor (FSII) and an anti-oxidant; and (d) finished fuels

containing only anti-oxidant. In the table a "+" or "-" sign is used in each column to show the applicability of the column headings. In the case of the FSII column, seven of the nine jet fuels which contained the icing inhibitor show actual data in place of the "+" symbol. In those cases, concentration was determined by analysis (23). The specification requirement (3,4) for both jet fuels is 0.10 - 0.15% FSII (ethylene glycol monomethyl ether).

The corrosion test results are shown in the last column. In order to meet the specification requirement (3,4), a maximum value of "1" is acceptable in a scale of one through four (22). For example, "1B" would pass, but "2A" would not. It is seen in the table that only one of the nine pre-acid treatment samples and one of the six additive free finished samples failed the test. But of the sixteen additive containing samples, only two (J-PP and D-PP) passed the test. These two samples were pilot plant samples which contained a different anti-oxidant, AO-29. Since almost all of the finished samples failed the test and since most of the pre-acid or non-additive samples passed the test, these results need to be related to the sequence of operations in the refinery process and to the nature of the additives which were used. It seems probable that either there was a problem with the acid treatment process by which a corrosive species was produced which ended up in the finished samples or that the additives used may have been contaminated. Both aspects may be involved.

Free sulfur (17 ppm) and mercaptans (10 ppm) have been detected in the Shale-II JP-5. Model studies found that the combined presence of these two species, each at about the 10 ppm level, can cause failure of the copper corrosion test. The anti-oxidant, AO-30, exhibited indications of reinforcing the effects of the sulfur species in the model studies. Fortunately, a concentration of 5 ppm of benzotriazole enables Shale-II JP-5 to pass the copper strip corrosion test.

CONCLUSIONS

The physical properties of the Shale-II fuels were similar to that of equivalent fuels derived from petroleum. The differences observed could be minimized by modest changes in refining steps.

ACKNOWLEDGMENT

The authors thank Mr. Charles Stansky of UOP, Inc. for determination of free sulfur in the JP-5 and for consultation on the copper corrosion problem.

The authors are also indebted to Mr. John De Guzman for assistance in obtaining the flash point and freezing point data.

REFERENCES

(1) J. Solash, R. N. Hazlett, J. M. Hall, C. J. Nowack, Fuel, 57, 521 (1978).

(2) W. A. Affens, J. T. Leonard, G. W. McLaren and R. N. Hazlett, Preprints, Symposium on Oil Shale, Tar Sands, and Related Materials, Division of Fuel Chemistry, Amer. Chem. Soc., 21, No. 6, 249 (Sept. 1976).

(3) Military Specification, Turbine Fuel, Aviation Grades, JP-4 and JP-5, MIL-T-5624L, 18 May 1979.

(4) Military Specification, Turbine Fuel, Aviation, Kerosene Type, Grade JP-8, MIL-T-83133A, 18 May 1979.

(5) Military Specification, Fuel Oil, Diesel Marine, MIL-F-16884G, 7 March 1973; Amend. 22 March 1978.

(6) J. Solash, R. N. Hazlett, J. C. Burnett, E. Beal, and J. M. Hall, "Relation Between Fuel Properties and Chemical Composition. II. Chemical Characterization of U. S. Navy Shale-II Fuels", This Symposium.

(7) L. W. Kruse and E. T. Robinson, "Shale Oil- II Pilot Plant Refining Studies", Naval Air Systems Command-Naval Research Laboratory Workshop on Basic Research Needs for Synthetic Hydrocarbon Jet Aircraft Fuels," 37-57, June 15-16, 1978.

(8) "Boiling Range Distribution of Petroleum Fractions by Gas Chromatography", Amer. Soc. for Test. and Mater., ASTM D2887, 1973.

(9) E. M. Shelton, "Aviation Turbine Fuels, 1978," Bur. of Mines, Petrol. Survey 109, May 1979.

(10) "Distillation of Petroleum Products," Amer. Soc. for Test. and Mater., ASTM D86 (1972).

(11) "Distillate Fuel Economic Study," Nav. Ship Engr. Center, May 1974.

(12) W. A. Affens, "Shipboard Safety - A Meaningful Flash Point Requirement for Navy Fuels," Naval Research Laboratory Report 7999, Oct. 28, 1976.

(13) "Density and Relative Density (Specific Gravity) of Liquids by Bingham Pycnometer," Amer. Soc. for Test. and Mater., ASTM D1217 (1976).

(14) "Freezing Point of Aviation Fuels," Amer. Soc. for Test. and Mater., ASTM D2386 (1972).

(15) "Pour Point of Petroleum Oils," Amer. Soc. for Test. and Mater., ASTM D97 (1971).

(16) "Flash Point by Tag Closed Tester," Amer. Soc. for Test and Mater., ASTM D56 (1975).

(17) "Autoignition Temperature of Liquid Petroleum Products," Amer. Soc. for Test. and Mater., ASTM D2155 (1976).

(18) "D-C Electrical Conductivity of Hydrocarbon Fuels," Amer. Soc. for Test. and Mater., ASTM D3114 (1972).

(19) D. A. Young, "Mini-Static Test Procedure", Exxon Research and Engineering Co., Linden, N. J., June 1972.

(20) "Flash Point by Pensky-Martens Closed Tester," Amer. Soc. for Test. and Mater., ASTM D93 (1974).

(21) Coordinating Research Council, "A Survey of Electrical Conductivity and Charging Tendency Characteristics of Aircraft Turbine Fuels," CRC Report 478, April 1975.

(22) "Detection of Copper Corrosion from Petroleum Products by the Copper Strip Tarnish Test," Amer. Soc. for Test. and Mater., D130 (1976).

(23) "Fuel System Icing Inhibitor in Hydrocarbon Fuels (Iodometric Method)," Fed. Test Method Std. 791B, Method 5327.3, Jan. 15, 1969.

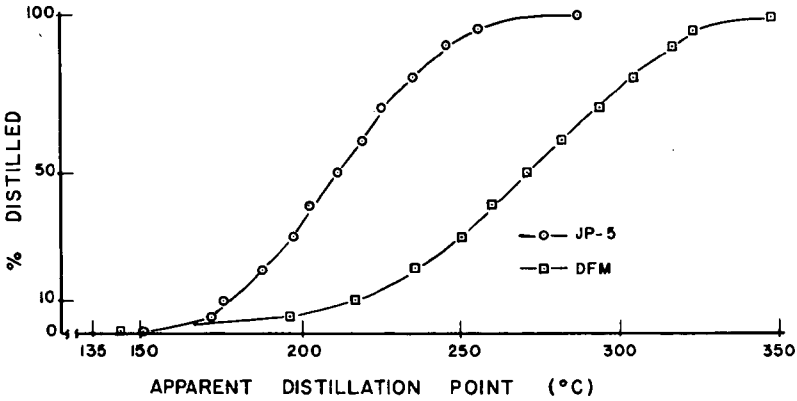

FIGURE 1 - GC SIMULATED DISTILLATION OF SHALE-II FUELS

TABLE I. GC Simulated Distillation*

Percent Distilled	Temperature (°C) JP-8 (J-11)	JP-5 (J-18)	DFM (D-1)
0.5	156	151	144
5.0	169	172	196
10.0	175	177	217
20.0	182	187	235
30.0	191	197	250
40.0	199	202	260
50.0	205	211	271
60.0	216	219	282
70.0	221	224	294
80.0	231	234	305
90.0	240	245	316
95.0	253	255	323
99.5	281	287	347

*ASTM D2887 (8)

TABLE II. Miscellaneous Physical Properties

	Specif. Grav. (25/25°C)[a]	Freezing Point (°C)[b]	Pour Point (°C)[c]
JP-5 (10 samples)			
Range	-	-46.8 - -51.7	-
Average	0.8122[d]	-49.7	-
Specification	0.788 - 0.845	-46 (max.)	-
Petroleum[e]	0.818	-49	-
JP-8 (2 samples)			
Range	-	-49.6 - -50.4	-
Average	0.8098[d]	-50.0	-
Specification	0.775 - 0.830	-50 (max.)	-
Petroleum[e]	0.810	-54	-
DFM (2 samples)			
Range	0.8390 - 0.8393	-	-20.6[f]
Average	0.8392	-	-20.6
Specification	-	-	-6.7 (max.)
Petroleum[e]	0.850	-	-14

a - ASTM D 1217 (13)
b - ASTM D 2386 (14)
c - ASTM D 97 (15)
d - One sample tested.
e - Data for representative petroleum derived fuel (9,11,12)
f - Same result for both samples.

TABLE III. Flammability, Ignition and Electrostatic Properties

	Flash Point (°C)[a]	AIT (°C)[b]	Conductivity (pS/m)[c]	Charging Tendency ($\mu C/m^3$)[d]
JP-5 (6 samples)				
Range	55.1 - 61.2	-	-	-
Average	58.0	232[e]	6.6[e] (228)[f]	2100[e] (16600)[f]
Specification	60 (min.)[g]	-	-	-
Petroleum[h]	64	241	0.8 - 15	1500 - 4000
JP-8 (2 samples)				
Range	53.4 - 58.7	-	-	-
Average	56.1	238[e]	5.3[e] (142)[f]	890[e] (12300)[f]
Specification	38 (min.)	-	200 (min.) - 600 (max.)	-
Petroleum[h]	53	238	-	-
DFM (2 samples)				
Range	71-75	238[e]	-	-
Average	73.4	238[e]	-	-
Specification	60 (min.)[g]	-	-	-
Petroleum[h]	79	240	-	-

a - ASTM D 56 (16)
b - ASTM D 2155 (17)
c - ASTM D 3114 (18)
d - Exxon Minitester (19) (Measured with Type 10 filter paper)
e - One sample tested
f - One ppm ASA-3 added; result with additive in parenthesis
g - ASTM D 93 (20)
h - Data for representative petroleum derived fuel (9, 11, 12, 21)

TABLE IV. Copper Strip Corrosion Tests

Sample	Fuel	Pre-Acid Treat.	Acid Treated Fuel Sample Additives[g] None	FSII (%v/v)[a]	Anti-Oxid.[b]	Test Result[c]
J-7	JP-5	+	-	-	-	1A
J-8	"	+	-	-	-	1A
J-9	"	+	-	-	-	1A
J-10	"	+	-	-	-	1A
J-13	JP-8	+	-	-	-	3B
J-14	"	+	-	-	-	1A
D-7	DFM	+	-	-	-	1A
D-8	"	+	-	-	-	1A
D-10	"	+	-	-	-	1B
J-1	JP-5	-	+	0[d]	-	1A
J-19	"	-	+	0[d]	-	1A
J-11	JP-8	-	+	0[d]	-	1A
J-12	"	-	+	0[d]	-	1A
J-17	"	-	+	0[d]	-	1A
D-1	DFM	-	+	-	-	2C
J-PP	JP-5	-	-	0.11[d]	+[f]	1A
J-2	"	-	-	0.21[d]	+	3B
J-3	"	-	-	+[e]	+	3B
J-4	"	-	-	0.20[d]	+	3B
J-5	"	-	-	+[e]	+	3B
J-6	"	-	-	0.19[d]	+	3B
J-16	"	-	-	0.18[d]	+	3B
J-18	"	-	-	0.09[d]	+	3B
J-22	"	-	-	0.10[d]	+	3B
D-PP	DFM	-	-	-	+[f]	1A
D-2	"	-	-	-	+	3B
D-3	"	-	-	-	+	3B
D-5	"	-	-	-	+	3B
D-6	"	-	-	-	+	3B
D-11	"	-	-	-	+	3B
D-12	"	-	-	-	+	3B

a - Ethylene glycol monomethyl ether fuel system icing inhibitor (3, 4)
b - Anti-oxidant "AO-30" (2,4-dimethyl-6-tertiary-butyl phenol).
c - ASTM D 130 (22). Specification (max.) = 1B (3-5)
d - By FSII determination (23)
e - FSII reported to be present (0.10 - 0.15%) (3,4)
f - Anti-oxidant "AO-29" (2,6-ditertiary-butyl-4-methyl-phenol) in pilot plant fuels.

Relation Between Fuel Properties and Chemical Composition. IV. Stability of Oil Shale Derived Jet Fuel

C. J. Nowack, R. J. Del Fosse and G. Speck
Naval Air Propulsion Center
Trenton, New Jersey 08628
and
J. Solash and R. N. Hazlett
Naval Research Laboratory
Washington, D. C. 20375

INTRODUCTION

The Navy has been interested in the utilization of alternate fossil fuels for sometime (1). Our interest is focused primarily in establishing the effects of chemical composition on fuel properties, since such relations will lead to production efficiency and better utilization of fuels. We recently reported some of our results on jet fuels derived from coal, tar sands and oil shale (1a). Earlier papers in this series report on other aspects of oil shale derived fuels obtained from a large production experiment performed by Paraho, Inc. (2). In this paper, we report on some aspects of stability of a jet fuel prepared from Paraho shale oil.

Previous work with shale oil derived middle distillates has noted the very high freezing point of these fuels (3, 4, 1a). In addition, shale oil fuels which were high in nitrogen gave as much as 45% conversion of fuel bound nitrogen to NO_x emmissions when burned under typical jet engine conditions (1d). The high nitrogen content shale oil jet fuels were also found to form particulates and gums upon standing at ambient temperatures in the absence of light (3).

Stablity of fuels concerns the tendency of fuels to form particulates and/or coatings or deposits on engine surfaces under two different sets of conditions. One set of conditions are those of storage: temperatures of ≤40°C, quiescent exposure to air, no light. The other set of conditions are those which the fuel is likely to encounter in a jet engine fuel system: temperatures in the range 150-250°C, agitation in the presence of air, no light. Shale oil derived fuels used in this work were significantly poorer than petroleum derived fuels under both stability regimes and a thorough study of the stability of these fuels was undertaken.

EXPERIMENTAL

The shale oil derived jet fuel (designated Shale-I) used in this work was produced from a crude shale oil (supplied by Paraho, Inc.) by hydrotreatment at the Gary-Western refinery. The entire production operation has been fully described elsewhere (1c). The physical properties of the jet fuel have been reported (1a).

High temperature stability of the fuels was measured using an Alcor, Inc. Jet Fuel Thermal Oxidation Tester (JFTOT) (5). Low temperature (storage) stability was determined by measurement of gums, contamination and peroxide concentration (all by ASTM standard methods) before and after exposure to temperatures of 60°C for four weeks. The

fuels were stored in 1ℓ low actinic, dark pyrex glass bottles and were loosely covered to prevent exposure to airborne particulates. Air could still diffuse into the vessel. The vessels with fuel and various additives were thermostated at 60°C for the specified length of time.

Isolation of shale oil jet fuel basic nitrogen compounds was accomplished by acid extraction followed by neutralization of the HCl adducts (3). The basic nitrogen compounds thus obtained were analyzed by gas chromatography using a Perkin-Elmer model 3920B gas chromatograph equipped with a 100m OV-101 glass WCOT column and nitrogen-specific detector. This column separated the nitrogen compounds into at least 70 incompletely resolved components. Tentative identification of some of the components was made by combined gas chromatography-mass spectrometry (gc-ms) using a Hewlett-Packard model 5982 gc-mass spectrometer with a Hewlett-Packard model 5933A dedicated data system. The mass spectrometer was equipped with a 33m SE-30 SCOT column and was operated in the EI mode at 70 eV. In addition, the extracted basic nitrogen compounds were subjected to field ionization mass spectroscopy (FIMS). Ions produced by field ionization tend not to fragment and an accurate MW profile of a mixture can be constructed (6).

RESULTS AND DISCUSSION

Oil shale, as well as crude shale oil, typically smell of nitrogenous compounds. Early work with refined shale oil clearly showed (3) that the shale oil jet fuels used (∿1000 ppm nitrogen) were unstable and rapidly plugged filters upon standing for several days. Removal of nitrogenous material by acid extraction or by passing the fuel over clay or silica gel resulted in improved storage properties. The chemical constitution of the nitrogen containing materials was sought in an effort to discover specific classes of compounds which could cause stability problems. It is well-known that pyrroles and indoles are quite reactive toward air and light (7) and if present in large quantities in these fuels might account for the observed instability.

The Shale-I jet fuel contained 976 ppm nitrogen, of which 860 ppm nitrogen was acid extractable. The neutralized extract was subjected to gas chromatrography using an all glass system with high efficiency capillary column. A chromatogram of the acid extract obtained using a nitrogen specific detector is shown in Figure 1. As shown, retention time matching implies that the majority of compounds are pyridine-type bases. The mixture was also subjected to gc-mass spectroscopy. The total ion chromatogram is shown in Figure 2. The lower resolution SCOT column used on the mass spectrometer did not permit unequivocal assignment of each peak. Tentative assignments of the numbered peaks are noted in Table I. In many cases, the electron impact mass spectrum clearly showed the presence of more than one compound. However, the main compound type observed was alkyl substituted pyridine with lesser quantities of quinolines. We used another mass spectral technique to help confirm our gc-ms assignments. The FIMS results are tabulated in Table II. Since molecules tend not to fragment when field ionized, the FIM spectrum can be scanned for parent masses and compound classes and higher alkyl substituted homologs readily recognized. The FIMS data confirms the presence of major amounts of pyridine compounds with lesser quantities of quinoline and tetrahydroquinoline types. Significantly, indoles and pyrroles are present only in very small amounts. While ionization efficiencies for various classes of compounds under

FI conditions are not known with certainty we do not expect them to be very different for the aromatic nitrogen types observed here. We have observed that FIMS data on basic nitrogen compounds results in a higher than expected intensity for parent +1 peaks. This was observed for our basic nitrogen extracts but not for n-alkane or neutral fuel samples. We attribute this phenomenon to the presence of water in the basic nitrogen extracts; the water rapidly protonates the radical cation generated by FI.

Extraction of the Shale-I jet fuel with HCl is approximately 90% efficient for removal of nitrogen containing material. Remaining in the fuel are 116 ppm of non-basic nitrogen compounds. Presumably, these compounds will be comprised primarily of pyrrole, indole and carbazole types. Only traces of substituted pyrroles and indoles were observed by FIMS in the basic nitrogen fraction (Table II). Shale oil nitrogen compounds have been characterized previously (8) and since carbazoles and pyrroles could not be titrated it is not surprising that they are also not efficiently extracted by 1N HCl.

High Temperature (Thermal) Stability - The high temperature stability of the Shale-I jet fuels was measured using the JFTOT technique (5). The thermal oxidative stability of the received fuel (976 ppm N) was measured. The fuel was then acid extracted, the isolated basic nitrogen compounds added back into the extracted shale fuel in varying quantity, and the thermal oxidative stability redetermined. A petroleum derived JP-5 was also subjected to JFTOT testing. The petroleum fuel had a breakpoint temperature of 275°C and at 260°C did not produce significant TDR readings or develop a significant pressure drop across the in-line JFTOT filter. A number of nitrogen compounds, typical of those found in this study, were then added to the petroleum derived JP-5 and the high temperature stability redetermined. The results with shale and petroleum fuels are displayed in Table III.

In previously reported stability work with shale oil derived jet fuels (9) it was shown that the JFTOT thermal stability of shale oil derived fuels increased with decreasing total nitrogen content of the fuels. In Table III, it is observed that the thermal stability of the Shale-I fuel increases as the concentration of basic nitrogen compounds decreases. In previous work (9) the lower nitrogen contents of the shale oil jet fuels were achieved by more severe hydrotreatment. It can also be observed that there apparently are two major modes of high temperature thermal instability and the effect of basic nitrogen is different in each. If thermal stability by JFTOT is measured only by tube deposits, then for the Shale-I fuel a slight rise in breakpoint temperature is observed as the basic nitrogen content is reduced (breakpoint by TDR from 244°C to 254° as basic N changes from 838 to 7 ppm). However, if the filter pressure drop is used for determining breakpoint then a much larger change, 227 to 279°C in breakpoint temperature, is observed as basic nitrogen content is reduced.

In order to confirm some of the effects of nitrogen compounds on high temperature stability, pure compounds which are similar to those found in the Shale-I basic nitrogen fractions (Tables I and II) were added to a petroleum based jet fuel of high stability (Table III). Most of the basic nitrogen compounds used resulted in negligible deposit (TDR) formation with the exception of 2-amino-3-methylpyridine. 4-t-Butylpyridine showed evidence of filter plugging but little TDR

deposits were formed. Pyrrole, however, was found to produce a very high deposit rating (TDR) and also plugged the in-line filter. Much more work with pure compounds in simple carrier vehicles is necessary before definitive mechanistic inferences can be drawn regarding the effects of the various classes of nitrogen compounds.

Storage Stability - The low temperature or storage stability of the Shale-I fuel was followed by determining changes in peroxide concentration, gum and contamination levels and changes in high temperature stability (JFTOT behavior). The latter method was employed since deposit precursors, which might form at low temperatures, could seriously degrade engine operation if present in sufficient concentration. The test fuel was placed in 1ℓ glass bottles which were loosely covered to permit air diffusion to the fuel. Ten ml of distilled water and 1 g of iron fillings were placed in each sample. These conditions simulated actual storage tank conditions since water is always present in fuel storage tanks and the fuel is in contact with usually uncoated metal surfaces of storage tanks. The samples were maintained at 60°C for four weeks. The results of the storage stability experiments are presented in Table IV.

Storage stability measurements have been performed on some shale derived fuel (10). In that study, a Paraho jet fuel (very similar to our Shale-I) was found to form some gums (increase in gums of about 2 mg/100 ml fuel after 32 weeks storage at 43°C) but there was only a small increase in acid number and no increase in viscosity. In our storage tests, we tried to determine the effects of basic nitrogen compounds on the storage stability of the Shale-I fuel. The combination of acid extraction followed by silica gel chromatography of the Shale-I fuel was found to be effective for removing all nitrogen containing compounds. The nitrogen free Shale-I showed some tendency to accumulate peroxides under our test conditions, but no appreciable gums were formed. In addition, the high temperature (JFTOT) stability of the aged nitrogen-free fuel was similarly acceptable (Table IV). Increasing quantities of basic nitrogen compounds, which were acid extracted from the fuel, were then reintroduced into the fuel and the storage stability redetermined. It will be noted that as the concentration of basic nitrogen compounds increases from 8.4 to 125 ppm N, both the gum content and peroxide concentration after storage rise to a maximum (25 ppm N) then fall back to lower levels (Table IV, expt. #2, 3, 4). However, the JFTOT deposit rating after storage was monotonically degraded by increasing nitrogen levels. The results imply a relationship between gum formation and peroxide concentration. It is possible that the relation between the gum and peroxide is of the form:

$$RH \xrightarrow[k_1]{O_2} [\text{peroxide}] \xrightarrow[k_2]{} \text{gum}$$

Fuel hydroperoxides are known to be stable to temperatures of approximately 250°C (11). However, hydroperoxides can react at mild conditions to attack some rubbers. We propose that some fuel components, particularly those containing sulfur, nitrogen, oxygen, and olefinic functional groups, also react under storage conditions with peroxides. Condensation or dimerization of the free radical intermediates formed in these

reactions can build the highly polar, medium molecular weight (400-500) gums observed in some studies (12). Antioxidants of either the phenylene diamine or hindered phenol type were effective for inhibiting both peroxide and gum formation in the current studies (Table IV, expts. #5, 6, 8).

A pyridine compound was found to storage degrade the Shale-I fuel faster than a pyrrole compound (Table IV, expt. #9,11). After storage the Shale-I fuel doped with 50 ppm 5-ethyl-2-methylpyridine had an order of magnitude more gums and 20 times the peroxide level compared to the same fuel containing 50 ppm 2,5-dimethylpyrrole after storage. Antioxidants were effective at inhibiting both gums and peroxides in the nitrogen doped fuels after storage (Table IV, expt. #10, 12). 5-Ethyl-2-methylpyridine caused a large decrease in JFTOT results after storage (TDR reading from four prior to storage to 35 after storage). In contrast, 2,5-dimethylpyrrole caused equally poor JFTOT performance before and after storage.

SUMMARY

High temperature thermal stability and storage stability experiments were conducted using Shale-I jet fuel. As basic nitrogen compounds are removed by acid extraction from the Shale-I fuel, JFTOT stability improves (especially filter pressure drop performance). After four weeks of accelerated storage, the Shale-I fuel containing basic nitrogen compounds formed more gums and peroxides, and exhibited degraded JFTOT performance. The basic nitrogen compounds extracted from the Shale-I fuel were characterized by way of various mass spectral methods. Compounds similar to those found in the basic nitrogen fraction were used as additives for JFTOT and storage tests on a petroleum fuel and nitrogen-free Shale-I fuels. Both pyridines and pyrroles evidence participation in unstable behavior. Much more work must be performed in order to establish clear trends and to deduce a detailed mechanism of fuel degradation.

REFERENCES

1. (a) J. Solash, R. N. Hazlett, J. M. Hall and C. J. Nowack, Fuel, 57, 521 (1978); (b) F. S. Eisen, Sun Oil Company Final Report on U.S. Navy Contract No. N-00140-74-C00568, Feb. 6, 1975; (c) H. Bartick, K. Kunchal, D. Switzer, R. Bowen and R. Edwards, Applied Systems Corp. Final Report on Office of Naval Research Contract No. N-00014-75-C-0055, Aug. 1975; (d) A. F. Klarman and A. J. Rollo, Naval Air Propulsion Center Report No. NAPC-PE-1, Nov. 1977.

2. See, W. A. Affens, et al, ACS Fuel Div., Preprints, this symposium; and J. Solash, et al, ACS Fuel Div., Preprints, this symposium.

3. J. Solash, C. J. Nowack and R. J. Del Fosse, Naval Air Propulsion Center Report No. NAPTC-PE-82, May 1976.

4. J. Solash and R. N. Hazlett, Presentation at 21st Rocky Mountain Conference, July 1979.

5. ASTM Method D-3241.

6. S. E. Buttrill, Jr., Analysis of Jet Fuels by Mass Spectrometry, in Naval Research Laboratory Workshop on Basic Research Needs for Synthetic Hydrocarbon Jet Aircraft Fuels, Naval Air Systems Command, June 15-16, 1978, and references therein.

7. (a) J. W. Frankenfeld and W. F. Taylor, Final Report under Naval Air Systems Command Contract No. N-0019-76-0675, Feb. 1979, and references therein; (b) B. Witkop, J. Amer. Chem. Soc., 72, 1428 (1950); (c) B. Witkop and J. B. Patrick, J. Amer. Chem. Soc., 73, 713 (1951); (d) I. Saito, T. Matsuura, M. Nakagawa and T. Hino, Accts. Chem. Res., 10, 346 (1977); (e) R. J. S. Beer, L. McGrath, and A. Robertson, J. Chem. Soc., 3283 (1950).

8. C. M. Frost and R. E. Poulson, Amer. Chem. Soc., Div. Petroleum Preprints, 20, 176 (1975).

9. T. W. Reynolds, National Aeronatics and Space Administration, Technical Memorandum No. TM-X-3551, June 1977.

10. D. W. Brinkman, M. L. Whisman and J. N. Bowden, Bartlesville Energy Technology Center, Report of Investigation No. 78/23, March 1979.

11. (a) R. N. Hazlett, J. M. Hall and M. Matson, Ind. Eng. Chem., Prod. Res. Dev., 16, 171 (1977); (b) D. M. Brown and A. Fish, Proc. Roy. Soc., A308, 547 (1969); (c) N. M. Emanuel, E. T. Denisov and Z. K. Maizus, The Liquid Phase Oxidation of Hydrocarbons, Plenum Press, New York, 1967.

12. C. C. Ward, F. G. Schwartz and M. L. Whisman, Technical Report #11 under Ordnance Project TB5-01-010, Bartlesville Energy Technology Center, July 1961.

TABLE I. Tentative Structural Assignments of GC-MS Peaks

Peak #[A]	Prominent Peaks m/e (Peak, Rel. Abundance)	Tentative Assignment
1	78 (M^+, Base), 77 (M^+-1, 20%), 52 (15%)	benzene
2	107 (M^+, Base), 106 (M^+-1, 50%), 92 (M^+-CH_3, 20%), 79 (M^+-HCN, 30%)	4-ethylpyridine
3	121 (M^+, 40%), 120 (M^+-1, Base), 107 (M^+-CH_2, 25), 93 (M^+-C_2H_4, 20%)	2-methyl-ethylpyridine
4	121 (M^+, Base), 120 (M^+-1, 30%), 106 (M^+-CH_3, 21%), 79 (M^+-C_3H_6, 35%)	4-i-propyl pyridine
5	121 (M^+, 85%), 120 (M^+-1, Base), 107 (M^+-CH_2, 25%), 93 (M^+-C_2H_4, 15%), 79 (M^+-C_3H_6, 35%)	2-propylpyridine
6	121 (M^+, Base), 120 (M^+-1, 55%), 106 (M^+-CH_3, 50%), 93 (M^+-C_2H_4, 15%)	3-ethyl-4-methylpyridine
7	135 (M^+, 45%), 134 (M^+-1, Base), 121 (M^+-CH_2, 45%), 107 (M^+-C_2H_4, 25%), 106 (M^+-C_2H_5, 30%)	2-propyl-methylpyridine
8	135 (M^+, Base), 134 (M^+-1, 55%), 121 (M^+-CH_2, 20%), 120 (M^+-CH_3, 50%)	3,4-diethylpyridine
9	135 (M^+, 45%), 134 (M^+-1, Base), 121 (M^+-CH_2, 30%), 120 (M^+-CH_3, 35%), 107 (M^+-C_2H_4, 65%)	2-propyl-methylpyridine
10	135 (M^+, Base), 134 (M^+-1, 75%), 121 (M^+-CH_2, 15%), 120 (M^+-CH_3, 30%), 107 (M^+-C_2H_4, 28%), 106 (M^+-C_2H_5, 30%)	4-butylpyridine
11	149 (M^+, 15%), 148 (M^+-1, 33%), 135 (M^+-CH_2, 33%), 134 (M^+-CH_3, 56%), 121 (M^+-C_2H_4, Base)	3-propyl-4-ethylpyridine
12	163 (M^+, 6%), 162 (M^+-1, 11%), 149 (M^+-CH_2, 53%), 148 (M^+-CH_3, 40%), 121 (M^+-C_3H_6, Base)	3-propyl-4-ethyl-5-methylpyridine
13	163 (M^+, 8%), 162 (M^+-1, 15%), 149 (M^+-CH_2, 60%), 148 (M^+-CH_3, Base), 134 (M^+-C_2H_5, 44%), 121 (M^+-C_3H_6, 30%)	3-ethyl-4-butylpyridine
14	163 (M^+, 25%), 162 (M^+-1, 55%), 149 (M^+-CH_2, 34%), 148 (M^+-CH_3, 55%), 135 (M^+-C_2H_4, Base)	2-propyl-3-methyl-4-ethylpyridine
15	163 (M^+, 9%), 162 (M^+-1, 25%), 148 (M^+-CH_3, 18%), 134 (M^+-C_2H_5, 30%), 121 (M^+-C_3H_6, Base)	2-butyl-4-ethylpyridine
16[B]	163 (M^+, 27%), 162 (M^+-1, 20%), 147 (45%), 121 (M^+-C_3H_6, Base)	3,4-dipropylpyridine + tetrahydromethyl quinoline
17[B]	176 (M^+-1, 11%), 163 (M^+-CH_2, 30%), 162 (M^+-CH_3, 37%), 147 (M^+, 80%), 146 (70%), 143 (M^+, Base)	C_7-pyridine + 3-methylquinoline + tetrahydromethyl quinoline

TABLE I - continued

Peak #[A]	Prominent Peaks m/e (Peak, Rel. Abundance)	Tentative Assignment
18[B]	Complex spectrum	probable species include C_6-pyridine, C_1-quinoline, methyl-tetrahydroquinoline, ethyl tetrahydroquinoline
19[B]	177(M^+,6%),176(M^+-1,10%),162(M^+-CH_2,18%),161(M^+,18%),135(M^+-C_3H_6,Base)	probable components: C_7-pyridine (one butyl group), ethyl-tetrahydroquinoline, methyl tetrahydroquinoline, methylquinoline
20[B]	177(M^+,8%),176(M^+-1,15%),160(M^+-1,15%),134(M^+-C_3H_7,26%),121(M^+ C_4H_8,Base)	major: C_7-pyridine (with 2-pentyl gp)
21[B]	Complex spectrum	probable major components: C_2-quinoline, C_2-tetrahydroquinoline; minor: C_7-pyridine
22[B]	Complex spectrum	probable major components: C_2-quinoline; minor components: C_2-tetrahydroquinoline, C_7-pyridine; trace: C_4-tetrahydroquinoline
23[B]	Complex spectrum	probable major component: C_8-pyridine; very minor components; C_2-quinoline, C_2-tetrahydroquinoline
24[B]	191(M^+,14%),190(M^+-1,5%),171(M^+,45%),170(M^+-1,25%),121(M^+-70,Base)	major: C_8-pyridine, C_3-quinoline; minor: C_2-quinoline, C_2-tetrahydroquinoline
25[B]	171(M^+,Base),170(M^+-1,30%),156(M^+-CH_3,25%),149(25%)	3-methyl-4-ethyl quinoline; minor: C_8-pyridine, other quinoline types
26[B]	Complex spectrum	probable major components: C_9-pyridine, C_3-quinoline
27[B]	Complex spectrum	probable major components: C_9-pyridine + C_3-quinoline

[A] Refer to Figure 2 for numbered peak position in total ion chromatogram of gc-mass spectrum. [B] EI spectra showed evidence of more than one compound.

TABLE II. Field Ionization Mass Spectrum Base Fraction from Shale-I JP-5

Series	Range of "n" Values*	Compounds	Relative Ion Count
$C_nH_{2n+1}N$	7 - 12 - 14	Piperidines	10
$C_nH_{2n-3}N$	7 - 9 - 15	Pyrroles	28
$C_nH_{2n-5}N$	7 - 9 - 16	Pyridines	1000
$C_nH_{2n-7}N$	9 - 11 - 16	Tetrahydro-quinolines	170
$C_nH_{2n-9}N$	8 - 13 - 15	Indoles	13
$C_nH_{2n-11}N$	9 - 11 - 14	Quinolines	157

* Underlined value of "n" indicates components in largest amount.

TABLE III. High Temperature Stability of Jet Fuels [A]

Fuel Type	Organic Nitrogen, ppm Acid Extractable	Organic Nitrogen, ppm Total	Breakpoint Temperature,[B] °C Heater Tube (TDR)	Breakpoint Temperature,[B] °C Filter
Shale Oil-Jet Fuel	860	976	-	232
	838[C]	954[C]	244	227
	97[C]	213[C]	243	232
	50[C]	166[C]	251	241
	7[C]	123[C]	254	279

Petroleum[D]	Additive Conc., ppm	260°C Max TDR	260°C ΔP, mm
	4-t-butylpyridine, 56	1	20
	2-t-butylpyridine, 49	10	1
	5-ethyl-2-methylpyridine, 107	11	3
	4-benzylpyridine, 56	7	2
	2-amino-3-methylpyridine, 134	45	14
	N,N-dimethylaniline, 82	6	5
	pyrrole, 100	32	Bypass[E]

[A] Measured using Alcor, Inc. JFTOT according to ASTM Standard Method D-3241. [B] Breakpoint is defined as the temperature of test at which a maximum TDR of >17 is observed or a pressure drop of >25 mm Hg is attained across the in-line JFTOT filter. [C] Shale Oil JP-5 extracted with HCl, washed, and the isolated basic nitrogen compounds reintroduced to the shale oil fuel. [D] The petroleum derived jet fuel had a breakpoint temperature of 275°C and had negligible TDR or filter pressure drop at 260°C. [E] Pressure drop of >25mm developed after which the test continued for standard 2.5 hr. period with the hot fuel bypassing the filter.

TABLE IV. Results of Storage Stability Tests of Treated Shale-I JP-5[A]

Sample (Expt.#)	N-Additive, ppm[C]	Inhibitor,[B] ppm	Storage Results: Existent Gums, mg/100 ml		Contamination, ppm		Peroxide, meg/kg		JFTOT 260°C Max TDR	
			Before	After	Before	After	Before	After	Before	After
Treated Shale-I (1)	0	0	0	0	0	0	0.14	60	1	10
" (2)	8.4	0	0	1.4	1.4	2.4	1.4	64.3	9	13
" (3)	25	0	0	5.4	0.9	1.7	1.0	96.8	4	27
" (4)	125	0	0	1.6	0.9	2.0	0.2	42.5	5	48
" (5)	0[D]	25-DA	0	0	0	0.8	0	1.0	0	2
" (6)	39[D]	25-DA	0	0	0	1.8	0	0.6	0	2
" (7)	123	25-DA	0	0	0.7	2.0	0.1	0.1	5	13
" (8)	0	24-HP	0	0	-	-	0.7	0.7	4	9
" (9)	5-ethyl-2-methylpyridine, 50	0	0	5	-	-	0.6	83	4	46
" (10)	"	24-HP	0	5	-	-	0.6	0.6	4	35
" (11)	2,5-dimethylpyrrole, 50	0	0	0.4	-	-	0.6	4.2	25	25
" (12)	"	24-HP	0	0.6	-	-	0.6	0.5	26	25

[A] Shale-I JP-5 containing 976 ppm nitrogen was first acid extracted then treated with silica gel to yield a nitrogen-free fuel. Conditions of storage test: temp=60°C; time=4 weeks; no agitation; air allowed to freely diffuse into fuel.
[B] Antioxidants used were commercial products qualified for Navy fuel use; DA=phenylene diamine (1,4-diamino benzene); HP=hindered phenol (2,6-di-tert-butyl-4-methylphenol). [C] Acid extracted nitrogen compounds added to nitrogen-free Shale-I JP-5 to bring nitrogen content to designated level. [D] Corrected for antioxidant nitrogen content.

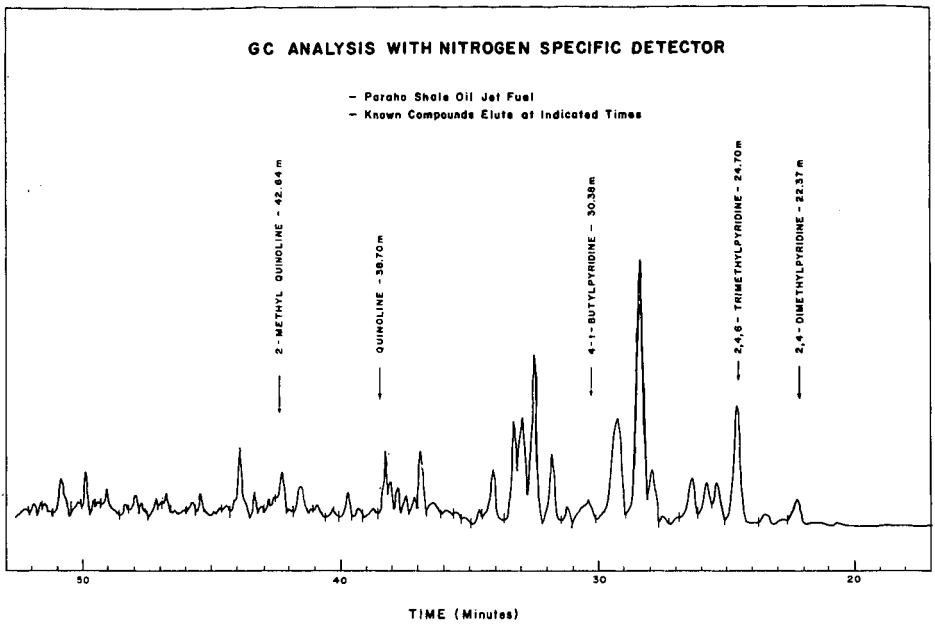

Fig. 1. Gas Chromatogram of Shale-I basic nitrogen compounds using a 100m OV-101 WCOT column.

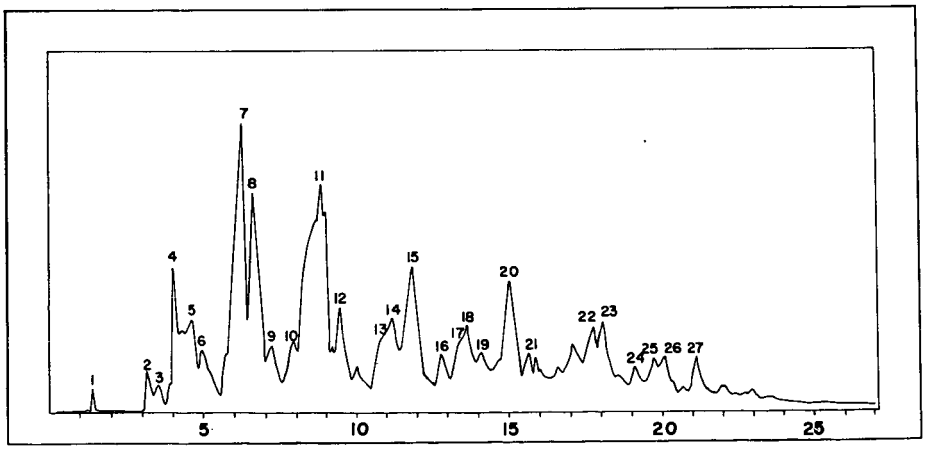

Fig. 2. Total Ion Chromatogram of Shale-I basic nitrogen fraction.

PYROLYSIS OF SHALE OIL RESIDUAL FRACTIONS

Robert N. Hazlett, Erna Beal, Thomas Vetter,
Richard Sonntag and William Moniz

Naval Research Laboratory
Washington, D. C. 20375

INTRODUCTION

JP-5, the Navy jet fuel, must meet many stringent requirements if satisfactory performance in aircraft and fuel handling and storage systems is to be attained (1). In considering JP-5 derived from alternate fossil fuels, several properties are affected more by the chemical characteristics of the fuel than by the physical properties. The important specification requirements may be primarily controlled by elemental composition, the amounts of each of the hydrocarbon classes - paraffin, naphthene, aromatic, olefin - or by specific chemical compounds. The three critical properties which are controlled by composition are (a) low temperature properties, (b) fuel stability, and (c) combustion behavior.

Low temperature properties of concern are fuel freezing point and viscosity. The freezing point is the property of concern in this paper. Jet aircraft are exposed to low temperatures and the fuels must not interfere with flying operations by freezing and plugging filters. It has not been practical to make JP-5 from some petroleum crudes because the freezing point cannot be met along with the required flash point. Dimitroff et al (2) examined the influence of composition on freezing point of several types of fuels. They found the saturate fraction of a fuel usually exerted the greatest effect on freezing point but the aromatic fraction seemed to be important in some cases.

NRL has related the freezing point of JP-5 type fuels to the n-alkane content, specifically n-hexadecane (1). This relationship applies to jet fuels derived from alternate fossil fuel resources, such as shale oil, coal, and tar sands, as well as those derived from alternate fossil energy sources such as shale oil, coal, and tar sands. In general, jet fuels from shale oil have the highest and those from coal the lowest n-alkane content. The origin of these n-alkanes in the amounts observed, especially in shale derived fuels, is not readily explained on the basis of literature information. Studies of the processes, particularly the ones involving thermal stress, used to produce these fuels are needed to define how the n-alkanes form from larger molecules which are cyclic or branched. The information developed will significantly contribute to the selection of processes and refining techniques for future fuel production.

PYROLYSIS MECHANISMS

A large n-alkane breaks apart by a free radical mechanism to yield smaller hydrocarbons, both n-alkanes and 1-olefins. This process, as originally diagnosed by Rise (3), ultimately yields mostly small olefins with 2 to 4 carbon atoms. This behavior is encouraged by high temperatures and low pressures. At conditions

more typical of shale retorting and delayed coking, however, Fabuss-Smith-Satterfield (4) behavior occurs. In this situation, a single fragmentation step occurs and equal amounts of n-alkanes and olefins form. Further, the yield is about the same for hydrocarbons in the intermediate carbon range. Unbranched olefins formed in the pyrolysis reactions readily convert to n-alkanes by hydrogenation.

Thus, formation of n-alkanes in the jet fuel distillation range can be explained if large n-alkanes are present in the crude oil source. Quantities of large n-alkanes are insuffienct, however, to explain the amounts found - up to 37% n-alkanes in the jet fuel range (1). Other possible precursors to small straight chain molecules are substituted cyclic compounds. Attack in the side chain obviously affords a path to an n-alkane. Aromatic hydrocarbons, esters, acids, amines, and ethers also have the potential to form n-alkanes if an unbranched alkyl chain is present in the molecule.

EXPERIMENTAL STUDIES

Carbon-13 nmr studies indicate that oil shale rock contains many long unbranched straight chain hydrocarbon groups (5). The shale oil derived from the rock also gives indication of considerable straight chain material with large peaks at 14, 23, 30, and 32 ppm in the C-13 nmr spectrum.

Separation - A residue from Paraho shale oil was obtained by vacuum distillation at 40 torr to an end point of 300°. The residue was then separated on activated silicagel into a saturate fraction, an aromatic fraction, and a polar fraction. The saturate fraction was removed from the silica with n-pentane solvent, then the aromatic fraction was removed with a 25:75 benzene: n-pentane solvent. The polar fraction was desorbed with 25:75 benzene: methanol solvent. Although the polar fraction required methanol for desorption, it was only slightly soluble in methanol. It dissolved readily in benzene, however. The nitrogen content of various eluates was determined by Drushel's method (6) as an indication of the separation efficiency. The pentane eluant contained no nitrogen and the polar fraction (benzene:methanol) contained 97% of the recovered nitrogen. If 100% benzene was used to desorb the aromatic fraction, up to 20% of the nitrogen was found in the aromatic fraction. The nitrogen concentration in the separated fractions was 2.5% in the polar, 0.13% in the aromatic and less than 0.01 wt% in the saturate fraction. The input N concentration in the residue was 2.2 wt%.

The distillation residue comprises 48% of the shale crude oil. On a chemical basis, the polar compounds comprise 71%, the saturates 13% and the aromatics 16% of the recovered residue. Mass recovery from the separation was 85% but nitrogen recovery was much less, 70%. The material retained on the silicagel, consequently, appears to be highly polar and high in nitrogen.

Carbon-13 nmr Analysis - Samples of the various fractions were submitted to analysis by C-13 nmr. The C-13 spectrum affords a distinct separation of the aromatic and aliphatic absorption regions plus a good resolution of many peaks due to specific molecular structure. Thus, a good amount of useful information can be obtained even for a complex mixture such as a fuel fraction. With respect to

the present study, the aliphatic region of the spectrum is of particular importance.

Quantitative analysis of the aliphatic region was attained by including a known amount of methanol in the sample as an internal standard. A long unbranched fragment will exhibit peaks at several positions in the aliphatic region of the spectrum. The peak corresponding to the methyl end group (α-carbon) appears at 14 ppm with reference to tetramethlysilane at zero ppm. The CH_2 group adjacent to the methyl group (β-carbon) absorbs at 23 ppm and subsequent absorptions appear at 32 and 29.5 ppm for the γ- and δ- carbons. Beyond this, all other CH_2 groups in a long unbranched chain absorb at 30 ppm. Therefore, this latter peak would be quite large for a long chain. In fact, the ratio of the area of this peak to the α- β- or γ-peak can afford information on the average chain length of the unbranched fragment.

A spectrum for the aliphatic region of the polar fraction from the shale residue is shown in Figure 1. The distinctive peaks at 14, 23, 32, and 30 ppm demonstrate the presence of significant amounts of long unbranched groups in this fuel fraction. The 29.5 peak appears as a shoulder on the 30 peak and these two peaks were integrated together. Quantitation of the spectral information using the methanol internal standard gives the data listed in Table I. As expected, the content of long unbranched alkyl groups is greatest for the saturate fractions. Further, the straight chain alkyl groups in the saturate fraction are longer on the average than those in the aromatic and polar fractions. We conclude that there is a definite potential for making n-alkanes and 1-olefins in the jet fuel distillation range by cracking compounds found in the heavier shale oil cuts.

Pyrolysis - The residue fractions have been stressed at conditions corresponding to the petroleum refining process known as delayed coking (7). These conditions are about 450°C and 90 psi pressure. Each thermal stress was conducted in a 1/4 inch o.d. 316 s.s. tube fitted with a stainless steel valve via a Swagelok connection. The tube, with a weighed amount of sample (approximately 0.1 g), was attached to a vacuum system, cooled to -78°C, and pumped to remove air. The tube was then thawed and the cooling/pumping process repeated. The tubes were heated by inserting them into 9/32 inch holes in a six inch diameter aluminum block fitted with a temperature controller.

At the close of the heating period, the tubes were cooled to -78°C and the valve removed. A mixed solvent of n-pentane and benzene (50:50) was added to the tube which was then capped and warmed to room temperature. The solution and a subsequent rinse were transferred to a screw cap vial which was then stored in a freezer until analysis. A weighed amount of toluene was added as an internal standard prior to analysis.

The strssed samples were analyzed by two techniques, both based on gas chromatography. In the first, the solution with internal standard was injected into a 10 ft, 1/8 inch o.d., 5% OV-101 column which was programmed to 260°C at 12°/min after a 5.0 min initial hold at 60°C. The JP-5 cut was integrated as a single sum and compared to

the internal standard to determine the yield of JP-5 from the pyrolysis experiment. The initial gc cut point for the JP-5 was set midway between n-octane and n-nonane and the final point midway between n-hexadecane and n-heptadecane. The gc baseline did not rise during this portion of the analysis, hence reliable integration was obtained.

The second gc technique determined the individual n-alkanes and 1-alkenes in the pyrolyzed sample. A 100 m wall coated glass capillary gave the required resolution and the n-alkanes and 1-alkenes stood out as distinct, well resolved peaks. OV-101 or OV-17 wall coatings provide adequate separation. A carrier gas flow of one cc/min was combined with an inlet split ratio of 50:1 and a 310°C injector temperature. The column temperature was raised to 250°C at 4°/min after an 8.0 min initial hold at 80°C. Peak identification was based on retention time matching with n-alkane and 1-alkene standards.

Pyrolysis of the saturate fraction for 30 min at 450°C gave the n-alkane and 1-alkene yields shown in Fig. 2. The n-alkanes predominate over the 1-alkenes at all carbon numbers for this sample. This was generally true for all fractions and all stress times. The 1-alkenes were less stable than the n-alkanes and the larger alkenes were very minor products for stress times 60 min and longer. Fig. 2 indicates that the product exhibits a plateau in the 10-14 carbon number range, an integral part of the JP-5 distillation range.

The effect of stress time on yield is illustrated in Fig. 3. The n-alkane + 1-alkene sum for each carbon number is plotted. For a 16 min stress the yield for carbon numbers 10 through 14 are almost identical. Consequently, one-step Fabuss-Smith-Satterfield pyrolysis (4) is controlling. The total yield increases at 30 min but the shift to a maxima at C-10 indicates product is forming and undergoing secondary decomposition. This trend is extended significantly at longer times such as shown by the 60 min data. Here the maximum is outside the JP-5 range and the yield of molecules with 16 or more carbons is quite low.

For the polar fraction, the combined n-alkane + 1-alkene yield increased up to 60 min stress time, then reversed (Fig. 4). The yield of the larger molecules - 15 carbons and above - was drastically reduced at 180 min. Even at 16 min the products obtained in largest yield were on the low end of the JP-5 distillation range. This is consistent with the lower value found by nmr for the average unbranched alkyl chain length. The aromatic yield pattern fell between that for the saturate and polar fractions.

A summary of the yield data for all fractions stressed for various times at 450°C is presented in Table II. The saturate fraction affords the highest yield of JP-5 but the other fractions give yields in excess of 20% at intermediate stress times. The polar fraction requires a longer stress time to attain its maximum yield of JP-5.

The potential n-alkane yields in the JP-5 cut are also listed in Table II. These values were obtained by summing the capillary gc yields of n-alkanes and 1-alkenes for carbon numbers 9 through 16. This total was divided by the JP-5 yield in the left portion of Table II to give the potential n-alkane yield. The saturate fraction

attained the highest potential n-alkane yield, 22.7% at 16 min stress. The aromatic and polar fractions also gave about 20% yields but these came with longer stresses. The potential n-alkane yields for all fractions fell off at longer stress times.

DISCUSSION AND CONCLUSIONS

The best yield of the JP-5 cut comes at different times for the various fractions, but a time in the 60 to 120 min range would appear to be the optimum time for good yield at 450°C. The longer time would be preferred with respect to lower potential n-alkane yield.

None of the fractions gave n-alkane yields approaching the 37% amount found in the Shale-I JP-5 (1). A temperature different than the 450°C used here might affect the conversion percentage. Further the combined saturate, aromatic, and polar fractions may interact under pyrolysis conditions to give higher potential n-alkane yields than the fractions stressed independently.

ACKNOWLEDGMENT

The authors thank Dr. Hyman Rosenwasser of the Naval Air Systems Command for funding support.

REFERENCES

1. J. Solash, R. N. Hazlett, J. M. Hall, and C. J. Nowack, "Relation between Fuel Properties and Chemical Composition I. Jet Fuels from Coal, Oil Shale, and Tar Sands," Fuel, 57, 521 (1978).

2. E. Dimitroff, J. T. Gray, Jr., N. T. Meckel and R. D. Quillian, Jr., Seventh World Petroleum Congress, Individual Paper No. 47, Mexico City, Mexico, Apr. 2 - 9, 1967.

3. F. O. Rice, J. Am. Chem. Soc., 55, 3035 (1933).

4. B. M. Fabuss, J. O. Smith and C. N. Satterfield, Adv. Pet. Chem. Refin., 9, 157 (1964).

5. H. A. Resing, A. N. Garroway, and R. N. Hazlett, "Determination of Aromatic Hydrocarbon Fraction in Oil Shale by C-13 nmr with Magic-angle Spinning," Fuel, 57, 450 (1978).

6. H. F. Drushel, Anal. Chem., 49, 932 (1977).

7. J. H. Gary and G. E. Hardwerk, Petroleum Refining, Ch. 5, Marcel Dekker, Inc., New York, N. Y., 1975.

TABLE I. Carbon-13 nmr Examination of Shale Oil Residual Fractions

Fraction	Wt. % Carbon in Aliphatic Region	Wt. % Unbranched Alkyl Groups*	Average Chain Length**
Saturate	100	40	43
Aromatic	60	21	14-22
Polar	56	30	20

* Sum of areas of absorption peaks at 14, 23, 30, and 32 ppm.

** For unbranched alkyl groups: based on ratio of 30 ppm peak area to average of 14, 23, and 32 peak areas.

Precision: ± 10%

TABLE II. Product Yield*

Pyrolysis Time (min)	JP-5 Yield			Potential n-alkane Yield		
	SAT.	AROM.	POLAR	SAT.	AROM.	POLAR
16	20.4	18.8	5.7	22.7	14.4	14.7
30	28.0	24.4	11.9	20.8	19.4	20.8
60	27.3	-	20.0	15.5	-	21.3
120	-	12.0	22.5	-	15.1	12.8
180	-	-	16.3	-	-	15.5

* Yield in %, potential n-alkane yield is for JP-5 cut; pyrolysis temperature - 450°C.

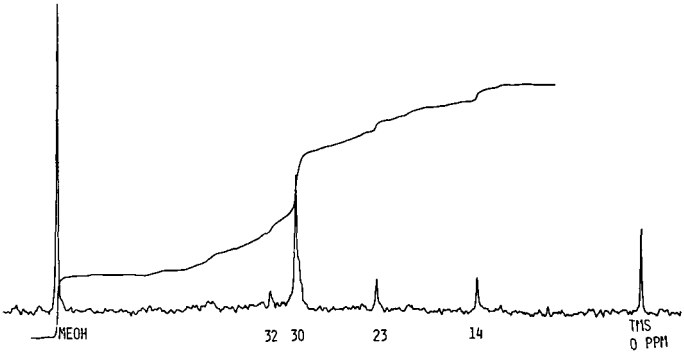

FIG. 1. C-13 NMR SPECTRUM OF SHALE OIL RESIDUA POLAR FRACTION, ALIPHATIC REGION, TMS REFERENCE, METHANOL INTERNAL STANDARD.

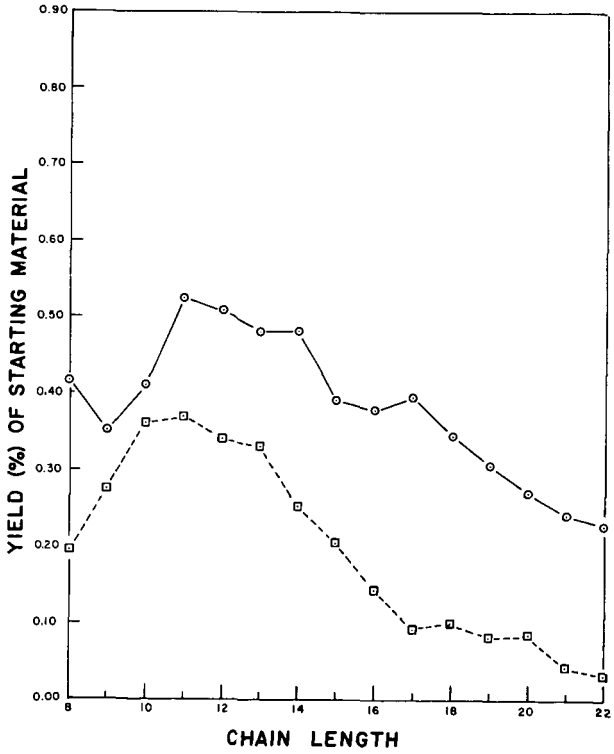

FIG. 2. PYROLYSIS OF SHALE RESIDUA SATURATE FRACTION AT 450°C FOR 30 MINUTES; UPPER CURVE -- N-ALKANES, LOWER CURVE -- 1-ALKENES.

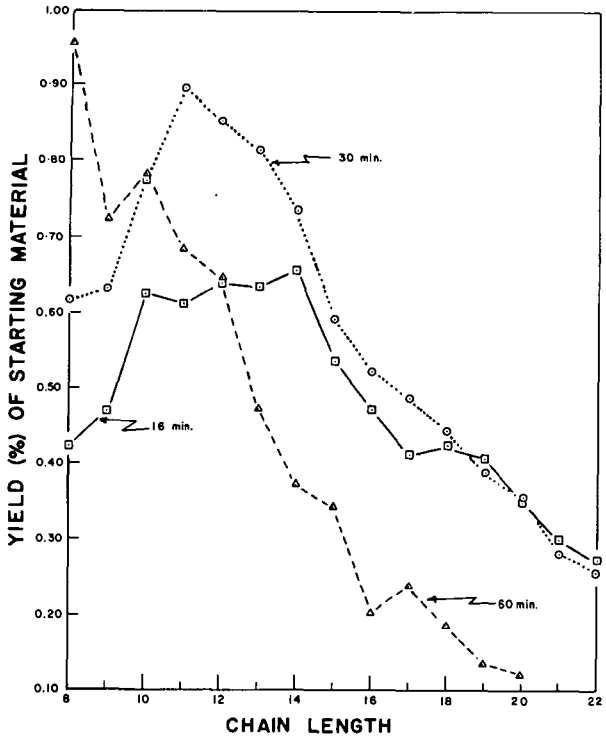

FIG. 3. PYROLYSIS OF SHALE RESIDUA SATURATE FRACTION AT 450°C; YIELD IS SUM OF N-ALKANE PLUS 1-ALKENE FOR INDICATED CHAIN LENGTH.

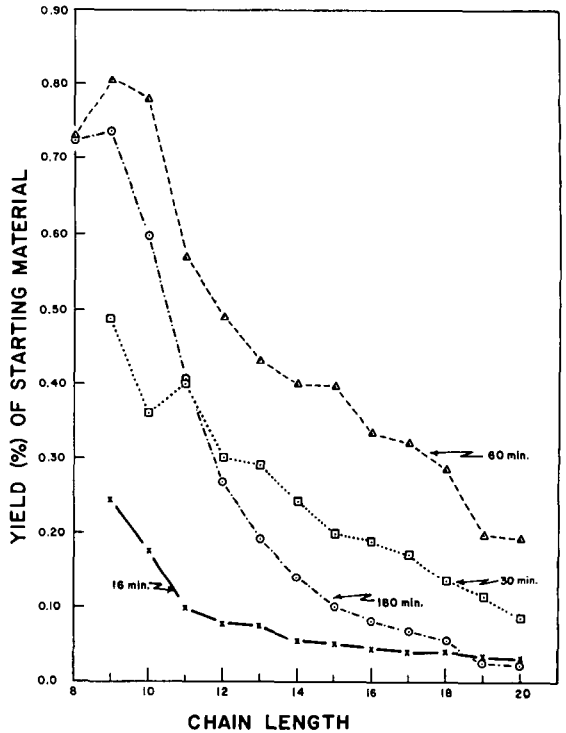

FIG. 4. PYROLYSIS OF SHALE RESIDUA POLAR FRACTION AT 450°C; YIELD IS SUM OF N-ALKANE PLUS 1-ALKENE FOR INDICATED CHAIN LENGTH.

SHELL PELLET HEAT EXCHANGE RETORTING - SPHER - AN ENERGY INTENSIVE, ENERGY EFFICIENT PROCESS FOR RETORTING OIL SHALE

J.E. Gwyn
S.C. Roberts
D.E. Hardesty
G.L. Johnson
G.P. Hinds, Jr.

Shell Development Company
P.O. Box 1380
Houston, Texas 77001

INTRODUCTION

Oil shales of primary interest for surface processing occur mainly in the Piceance Basin of western Colorado. These shales contain, typically, ten to 20 percent weight of hydrocarbons recoverable by simple pyrolysis.

Process research and development in shale oil production has gone on for decades, but the once plentiful supply of low cost petroleum crudes made the economics of such processes very unfavorable. The recent shortages and cost escalation of petroleum crudes have renewed interests in "unconventional" raw material sources such as coal and oil shale.

Several processes for above ground retorting of oil shale, which have been under development for some time, include the TOSCO-II, PARAHO, and Union technologies.[1] Shell had particular interests in the first two. The TOSCO (The Oil Shale Company) process uses hot balls to heat preheated shale in a rotary kiln to retorting temperatures. The shale is preheated during staged, pneumatic transport using flue gas from the retort ball heater. The PARAHO retort is a vertical kiln employing a downward moving rock bed with upflowing recycle gas and combustion products which sweep retorted hydrocarbons from the vessel. The Union process is similar but utilizes an upward flow of crushed shale. Shale is introduced at the bottom of the kiln and pushed upward by an air lock, mechanical "rock pump". Fluidized bed retorting of oil shale was proposed in the early fifties but was never developed to a commercial state.

The TOSCO-II process is capital intensive because it requires a large volume of heating gases and mechanically complex equipment; the PARAHO and Union processes are also capital intensive because they have long residence time requirements that entail massive hardware. The PARAHO process is, however, heat efficient as a result of countercurrent shale and gas flows. But the TOSCO process, although having some degree of heat recovery, uses heat relatively inefficiently.

The purpose of this work was to develop a new retorting process of relatively low capital cost that is mechanically simple, highly reliable, and uses heat efficiently. The process, [2] termed SPHER for Shell Pellet Heat Exchange Retorting, is a fluidization bed process conceived for the retorting of oil shale. The fluidization mode referred to in this discussion applies to a range of superficial gas velocities between those used for riser transport and dense bed operation in processes such as catalytic cracking. By this mode, shale can be made to flow upward, countercurrently to larger heat-carrier pellets that fall through the fluidized mixture. This counterflow of heat-carrier pellets and relatively coarse shale particles is the basic idea around which novel, small sized, thermally efficient and economically viable processes have been conceived. Other feedstocks to which SPHER may have potential applicability include numerous coals, lignite, wood and bark waste, agricultural residues, biotreater sludges, and industrial and municipal solid

wastes. Some specific process descriptions, with some variations, are discussed below.

Brief Description of Process Applied to Oil Shale

The SPHER process as originally conceived is shown schematically in Figure 1. This conceptual design produces 55,000 bbl/day (7575 t/d)* of raw shale oil from 66,000 ton/day (60,000 t/d) of 35 gal/ton (13.6%w) oil shale. It can be seen that there are two loops for circulation of heat carrying balls. The cool ball loop carries heat from the heat recovery column to the preheater. The hot ball loop carries heat from the ball heater to the retort.

Shale is crushed or ground to a fluidizable size; preferably as large as is compatible with heat transfer requirements and ready separation from heat-carrying balls. Initial work indicates that 1/16-inch (1.6 mm) minus shale and 1/4 (6 mm) or 5/16 (8 mm) inch balls are desirable.

The shale is preheated in a fast-fluidized (entraining) bed by outer loop, heat-carrying balls that rain through the bed in countercurrent fashion (Figure 2). With air as the fluidizing medium, preheating is limited to about 600°F (315°C) because there is danger from auto-ignition, which is time, temperature, and oxygen dependent.[3] With other nonoxidizing gases, preheating is limited to about 650°F (343°C) by the onset of kerogen pyrolysis.

In a dense-phase fluidized bed the preheated shale is further heated to and held at the retorting temperature for sufficient time to complete the pyrolysis reactions (Figure 3). The total inventory of shale in the retorting vessel is determined by the required residence time for complete kerogen conversion and the shale throughput. The retort heat requirements are supplied by ceramic balls which circulate in the inner loop. They are reheated in a separate vessel which may operate as a moving bed, raining pellet bed, or entrained flow heater.

The spent shale is cooled in a fast-fluidized bed by the recirculated cool pellets from the preheater. In this manner, countercurrent flow of heat carriers and the shale assures efficient energy utilization. This characteristic is a prime advantage of the process.

Most conditions and features of the conceptual process are chosen to assure high throughputs (small equipment) and hence relatively low capital and fixed costs. These include the choice of flow regimes, heat carriers (density and heat capacity) and the solids-to-gas weight ratios. Attendant features of the process, such as baffle design and gas routing, are chosen to achieve operability and optimum operation.

Segregation of the two ball loops permits the tailoring of the ball material, shape and size to each specific task. Circulation of balls in the outer loop is a relatively low temperature operation and is dedicated to heat transfer. Therefore, desired ball properties include high heat capacity, small size or large heat transfer surface, erosion resistance, and low cost. Hence, a pea gravel may be suitable. Corrosion resistance may not be needed unless condensation occurs in the heat recovery section. The use of the smallest balls separable from the shale increases heat transfer and reduces the size of the exchange vessel required.

In contrast, circulation of balls in the inner loop involves the ball heater and retort where high temperatures and longer residence times are required. Reaction rate rather than heat transfer is expected to be the controlling factor in the retort design. In order to achieve the residence time needed for high conversion

*ton=2000 pounds, t=metric ton= 1000kg.

a pseudo plug-flow device such as a rotary kiln or a staged, dense-phase fluidized bed may be desirable. Since heat transfer is not controlling, the balls can be larger for easier separation from shale but they must still be small enough to permit pneumatic transport. These inner loop balls must also be resistant to thermal shock, chemical attack by the hot gases and spent shale and exposure to high temperatures. Thus, the choice of the inner loop balls is limited to materials such as ceramics.

Detailed Process Description

A more process oriented schematic of the process is shown in Figure 4.

Shale Feed Preparation

Shale preparation for SPHER requires more energy than it does for processes such as TOSCO-II in that the larger crushed shale used in TOSCO-II, e.g., 1/2-inch (13mm) minus, must be reduced to a readily fluidizable size, e.g. 1/16-inch (1.6mm) minus, for use in SPHER. Grinding by separating and recycling coarse shale is expected to produce a better size range with less fines than once-through grinding is for the same maximum particle size. Separation of shale with the desired size from oversized material may be accomplished by elutriation with gas or by screening. The recovered coarse shale is conveyed back to the grinder. Shale with the desired top size may then be pneumatically transported to a feed hopper or standpipe.

Preheater

Figure 2 is a schematic of the preheat section.

Ground raw shale is allowed to slide into or is pneumatically transported (a minimal volume flow) into the lower part of the preheater. A standpipe of shale serves as a resistance seal to purging gas and allows the preheater to be pressurized by transporting gas. Although a slide valve near the bottom of the standpipe should provide adequate flow control for the shale, a flapper valve, screw feeder, or rotary lock may be considered as options.

The shale is carried up, countercurrent to the raining pellets, as a fast-fluidized bed by compressed gas (air or mixtures of air and flue gas or recycle process gas). The preheated shale is then recovered at the top of the preheater in high-efficiency, high-load cyclones. Extremely fine dust may be carried by elutriation to the ball heater when air or air containing mixtures are used for conveying. Thus, the energy content of even the finest shale dust can be recovered without requiring expensive dust-control equipment during the preparation of shale for retorting. As conceived, the use of standpipes and proper routing gas streams reduces the necessary number of air and gas compressors and also aids in heat recovery. In this fashion, pressure balance across the whole system is achieved with sufficient extra pressure differential available for process control.

Warm (∿625°F, ∿330°C) balls, pneumatically transported from the heat recovery section, are recovered at the top of the preheater by a cyclonic separator into a surge hopper. From the hopper they are admitted in controlled flow to the upper part of the preheater through an appropriate control valve and steam purge system. A conical (or other shaped) deflector is desirable to disperse the ball stream uniformly. Balls fall under the influence of gravity against the rising stream of fast-fluidized shale. The range of conditions under which countercurrent flow will exist is being studied. The smallest balls, i.e., those with the highest surface-to-volume ratio, that will fall sufficiently fast through the preheater at an economical shale mass flux are desirable for effective heat exchange.

Balls collecting at the bottom of the preheater in an appropriately dimensioned boot are stripped of shale particles by elutriating gas. Under ideal

conditions, the largest shale particles that can be readily elutriated from between the pellets are about half the size of the pellets. In practice the separation is more efficient when the ball/shale size ratio is 4-5. Balls drop by controlled flow into a transport line where they are pneumatically conveyed to the shale heat recovery section.

The countercurrent raining-ball/fast-fluidized flow regime must be operated so that staging is effected, i.e., backmixing must be effectively retarded. Temperature approaches were initially assumed to be 75°F (42°C) at the top and 50°F (28°C) at the bottom of the preheat vessel. Any increase in holdup of the balls in contact with shale will reduce the height of vessel required. Increased staging and holdup of balls are both accomplished by a system of baffles and/or grid plates. With such designs it is important to avoid dead hot spots where shale might accumulate because spontaneous ignition of shale might occur if air is used as the transporting gas.

Due to vaporization of water in the preheater it may be desirable to increase the diameter of the preheater with increasing height to maintain relatively constant flow conditions. At proposed preheater temperatures, the short residence time in the preheater should allow air to be used as a transporting gas without spontaneous ignition and with little shale degradation and yield loss. Dilution of transport air with flue gas may be used to permit a higher preheating temperature without ignition. The use of air as the entraining gas in the preheater permits the finest oil shale dust and any prematurely evolved hydrocarbons to be economically burned in the ball heater. Thus, combustion air is also preheated in the shale preheater. By operating the preheater in counterflow with a temperature approach of $\leq$100°F (55°C), overheating of small particles is avoided.

Retort

Figure 3 depicts the retort section of the raining pellet process.

Shale entrained from the preheater is fed to the lower portion of the retort through a high-load, high-efficiency separator and surge hopper (with aeration). The shale feed rate to the retort is controlled in the same way as it is to the preheater.

Steam or gas injection is required at the bottom of the retort to start the fluidization. However, some or all of this gas may be first used in the ball stripping section. Vapor emitted by retorting adds greatly to the volumetric flow of fluidizing gas as it rises up through the retort. The vessel cross-section is increased accordingly to maintain constant conditions for the dense fluidized bed.

Hot heat carrying balls (at about 1400°F, 760°C) are added to the top of the retort in the same manner as they are to the preheater, but in separate streams to different levels in the retort. This avoids overheating (and cracking) at the top of the retort. The ball diameters should be about 1/4-inch (6mm) to assure a reasonable fall velocity (0.25 fps, 0.08m/s) through the dense-phase fluidized bed of shale.

The balls collect in a boot at the bottom of the retort and are stripped of shale fines in an elutriating section. Superheated steam (1200°F, 650°C) provides both the stripping action and the feed shale fluidizing action. The cooled balls (900°F, 480°C) are then recirculated pneumatically to the ball heater for reheating. Air for the ball lift is combined with air from the preheater cyclones and with a third air/fuel-gas stream to provide the desired fuel mixture for the ball heater.

Processed shale is removed at the top of the retort. A circumferential weir is provided to maintain a constant bed height in the upper stage. Entrained shale particles are removed from the product vapor by high-efficiency cyclones

located in the vapor disengagement section. The dimensions of this top section are, in fact, determined by the cyclone configuration. Superheated steam (1200°F, 650°C) is injected in an effort to eliminate condensation coking in the vapor section.

Adsorbed and entrained vapors are removed from the retorted shale by steam in the spent shale stripper. Stripped shale is sent to the heat recovery section. The overhead products from the spent shale stripper are combined with the retort vapors and are further superheated with steam to reduce condensation coking and quenched with fractionator bottoms in a quench tower.

Staging of the retort can reduce the average residence time required for a given hydrocarbon yield. This staging could be achieved by adding restrictive horizontal grids spaced, for example, at ten-foot intervals of height. However, since staging may also introduce an unwanted temperature gradient across the retort, a single-stage design may be favored.

Pyrolysis data indicate that a relatively long (several minutes) residence time is required for the retorting reaction[4]. Hence, heat transfer is not limiting in the retort and larger balls with a lower surface-to-volume ratio may be used. Larger balls are desirable because, inter alia, their manufacturing cost is less. The maximum ball diameter is limited by the ability to transport them pneumatically and by their settling velocity through the fluidized bed of shale. Thermal shock could also be a factor that limits ball size, About 1/4-inch (6mm) diameter balls may be a good compromise on size, as mentioned above.

Ball Heater

The ball heater can be a moving bed, a raining pellet or an entrained flow design. Preheated air from the ball lift pipe plus air from the preheater and supplemental air and fuel form the combustion mixture used to heat the balls. Ball heater flue gas is routed partly to a waste heat boiler to recover energy in the form of high-pressure steam and partly to other vessels in the process to serve as a transport gas. Cooled gases are then scrubbed to remove both particulates and any sulfur oxides. The particulate shale dust naturally absorbs sulfur oxides in the wet scrubber. Exiting hot balls return to the retort through several feed standpipes.

Heat Recovery

The heat recovery section is similar to the preheat sections.

Fast-fluidized retorted shale is cooled from 990°F (482°C) to about 175°F (79°C) by contacting it countercurrently with balls from the preheat section. Since the conveying (flue) gas is cooled and contracts as it rises, it may be desirable to reduce the vessel size accordingly in the upper portion to maintain the desired flow rate of gas.

Elutriated cooled shale is separated in a high-efficiency separator and routed to a moisturizer in preparation for disposal. Gas from the heat recovery unit is water washed in a venturi scrubber and excess water from the scrubber is used in the moisturizer. Little water vapor is generated in scrubbing the gas and wetting the spent shale because the outlet temperature of the heat recovery unit is low (175°F, 79°C). Water usage in the SPHER process is, therefore, desirably low.

Problem Areas

Since SPHER represents the application of new regimes of fluidization to shale retorting, there are a number of questions that must be answered and factors that must be quantified. Some have been answered by simple experiments, the results of which would indicate either a "go" or a "no go" on future work, and some factors

will eventually require demonstration plant operation under design conditions to prove the process. Factors of primary concern are discussed below.

Heat Transfer Rates

Process evaluations have used a rate coefficient of 90 Btu/sq ft/hr °F (0.51 kw/m^2/°C), based upon the surface area of the balls. Literature data on transfer from fluidized beds to submerged objects indicate that even higher rates have been achieved, but these high rates are functions of bed density and the size of the fluidized particles. Data directly applicable to the SPHER system are required for final evaluations and designs.

Flow Regimes

The countercurrent flow of pellets relative to the fast-fluidized shale and its fluidizing gas suggests the existence of limiting or flooding velocities. The impingement of shale particles upon pellets (knockback effect) retards the upward flow of shale as well as the fall of the pellets. The size of the effect is different in dense-bed and fast-fluidized regimes. In dense beds, the falling velocity of pellets will be about 1/4 fps (0.08 m/s) while in the fast-fluidized bed the falling velocity is expected to be larger. Operational windows and pressure drop/holdup equations must be defined. These phenomena have been investigated on the 7-1/2-inch (19 cm) diameter cold-flow unit. Shale flux rates of 10 lb/sec/ft^2 (49 kg/sec/m^2) and ball flux rate of 15 lb/sec/ft^2 (73 kg/sec/m^2) were achieved at superficial gas velocities of 15 to 20 ft/sec (4.6 to 6.1 m/s).

Staging

Efficient use of heat and, to a lesser extent retorting yield, require some countercurrent staging to achieve the ecomonic advantages expected for the SPHER process. About six stages are desired for the preheater, four in the heat recovery section and two or three stages may be desired in the retort.

Gas-fluidized beds are basically unstable and they tend to have a high degree of backmixing due to circulation patterns caused by rising gas bubbles. Beds with a large height-to-diameter ratio (L/D) tend to restrict this circulation and increase the staging of fluidized solids. For example, the Shell's Anacortes CCU regenerator (L/D $\cong$ 2.5) performs with about four solids mixing stages.

Pneumatic lift pipes (risers) for solids do not exhibit large eddy mixing currents but they do have radial velocity profiles that peak toward the center of the pipe. It is even possible (at lower velocities) for solids in risers to flow down along the wall. Catalytic cracking feed risers (L/D $\cong$ 20) exhibit 4 to 6 solids mixing stages. The velocity profile flattens (approaches plug flow) with increasing pipe diameter but becomes more peaked with increased solids loading and decreased velocity.

Determination of staging and mixing of solids in the raining pellet system may require large test facilities.

Agglomeration and Defluidization

Two possible problems arise: (1) ground shale containing a sizeable fraction of 1/16-inch-or-less (1.6mm) particles will segregate into coarse and fine layers, even under moderate fluidization conditions, and (2) the ground shale might become tacky, due to the presence of liquids on the shale surface under retort conditions, and defluidize by agglomeration.

The question of agglomeration needs further resolution. Small scale experiments indicated direct vaporization of shale oil occurred during retorting and no

agglomeration tendencies were noted. However, agglomeration could take place in cold spots where hydrocarbon condensation might occur. Two requirements of retort design are to avoid cold spots and to provide sufficient mixing of fresh shale with inerts (i.e., with spent shale) to prevent agglomeration.

Overheating and Ignition

Air was originally conceived as the preheater gas for transporting shale but use of an inert gas may be preferred. If shale is heated in air to a temperature where retorting proceeds, then a combustible mixture is formed and ignition can occur. At atmospheric pressure this occurs at about 630°F, 332°C. Local stagnation zones of shale near the ball inlet should be avoided because they might lead to such a condition. Dilution with an inert gas or use of another gas as a carrier may be preferred because both will permit a broader range of operation without the possibility of shale ignition.

Pressure Balance - Operability

Overall operation, as in catalytic cracking, depends on use of standpipes to generate the pressure differentials necessary to cause shale and balls to flow into the process vessels. Excess pressures are taken out by slide valve control which also dampens the transfer of pressure surges between vessels.

The high permeability of the standpipe material, especially of the spheres or pellets, will allow appreciable gas leakage. Adequate purge gases in the standpipe will, therefore, be required.

Ball Separation and Recovery

The raining balls must be stripped free of shale before being removed from a vessel. This can be most readily done by use of a stripping gas at relatively high velocity (≥ 10 fps, 3 m/s) in a ball-collection boot. This might be a large fraction of the fluidizing gas in a vessel and reduces the quantity of gas available for transferring shale into the vessel above the boot.

Generation of Fines and Entrainment of Shale

Although retorting of shale does not, in itself, generate fines it does weaken the particles so that they are more readily attritable. Particle size distribution reported for a fluidized bed process is listed in Table 1. This potential generation of fines may not be serious for SPHER since operation will be once through for the shale and residence time in vessels with fluidized beds is only a few minutes.

Entrainment of shale in gas in the preheat and heat recovery sections is the basic mode of transport for shale. In the retort, excessive entrainment reduce the residence time below that needed for retorting and extra steps may be required for returning shale fines to the retort.

In all cases, high-load and high-efficiency (cyclone) separators will be required to prevent excessive carryover of shale in gas streams to other portions of the process. These recovered fines may need to be recycled to the appropriate vessels in order to insure the proper concentration of fines for smooth fluidization.

Choice of Ball Material

The purpose of the balls is to provide a means of conveying and exchanging highly concentrated heat energy. Thus, they should have a high external surface area (i.e., a small diameter) and a high heat capacity. However, they must be large enough to be readily separable from the shale. For ease of separation they should have a high density. Table 2 lists some properties of candidate materials. Other factors

to consider include cost and resistance to corrosion, abration and thermal shock. The quality of a material such as alumina is highly dependent upon its method of manufacture and the suitability of specific aluminas must be defined.

Erosion/Attrition/Thermal Shock

The high velocities of balls in lift pipes and the turbulent nature of the fluidized beds lead to the possibility of erosion of the equipment and attrition or fracturing of the balls. Erosion can be reduced by using abrasion resistant refractory linings in pipes. Attrition and fracturing of balls can be reduced by proper design to reduce the effect of impaction at elbows and on deflection plates.

Breakage by thermal shock is reduced by countercurrent operation, which allows reduced temperature gradients, and by a small ball size, which reduces thermal stresses.

Conclusions

As with most newly conceived processes there is considerable development work to be done before SPHER is a mature process. This report serves to present the basic features of SPHER and to point up some areas requiring development work.

References

1. Hendrickson, T. A., Quarterly of Colorado School of Mines 69(2):45 (1974).
2. U. S. Patent No. 4,110,193, dated August 29, 1978.
3. Allred, V. B., Quarterly of Colorado School of Mines 59(3):56 (1964).
4. Hinds, G. P. Jr., AIChE Annual Mtg., Miami, Nov. 1978.
5. U. S. Patent No. 2,717,869, dated September 13, 1955.

TABLE 1. PARTICLE SIZE DISTRIBUTIONS OF SHALE RETORTED BY TOSCO AND FLUIDIZED BED TECHNIQUES

Fluidized Spent Shale[a)]	
Size Range, μ	Percent
0-20	<25
20-60	5-15
60-200	20-50
200-400	20-30
<400	<5

a) See Reference No. 5

TABLE 2. PROPERTIES AND CIRCULATION RATES OF CANDIDATE MATERIALS FOR OUTER BALL LOOP

Material	Density		Heat Capacity		
	lb/ft^3	t/m^3	Btu/Lb°F	Btu/Ft^3°F	$Kcal/m^3$°C
High Density Alumina (ceramic balls used by Tosco)	231	3.70	0.22	50.8	814
Aluminum	168	2.69	0.23	38.8	622
Steel	487	7.80	0.12	58.4	935
Lead	686	10.99	0.03	20.6	330
Gravel	156	2.50	0.2	31.2	500

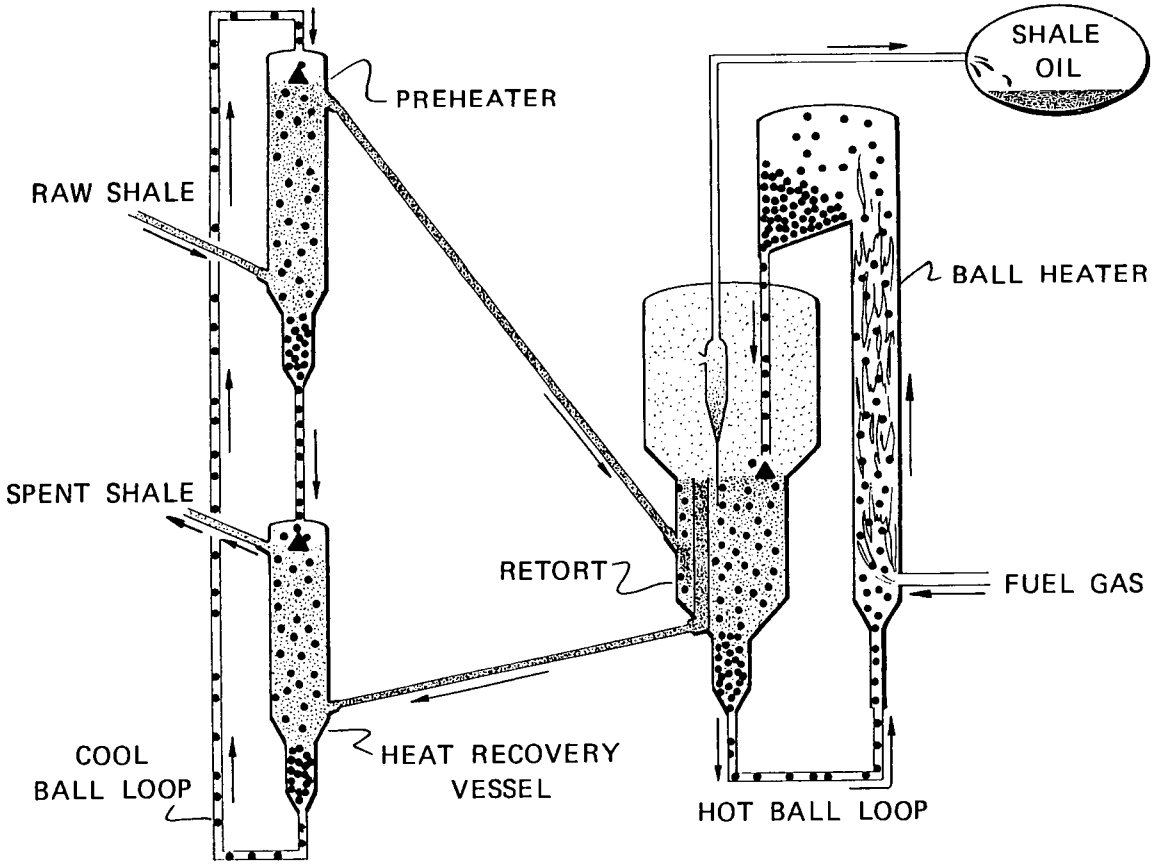

Figure 1. Spher Oil Shale Process

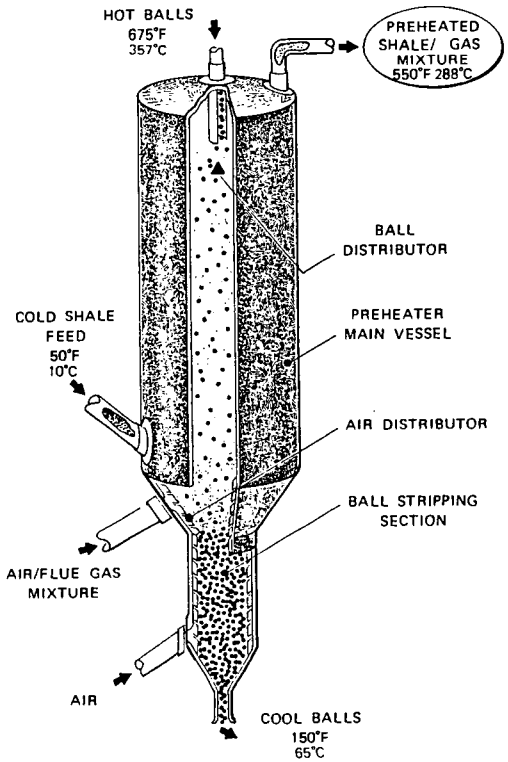

Figure 2. Spher Preheater

03784

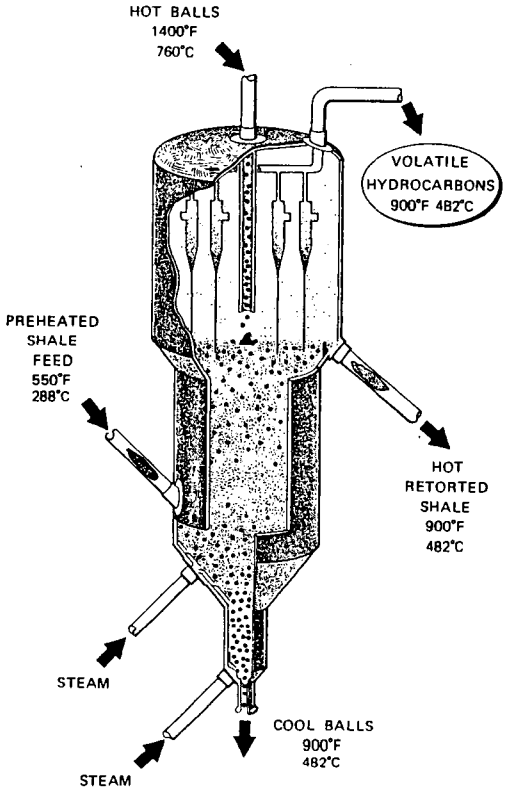

Figure 3. Spher Retort

03784

OIL SHALE RETORTING KINETICS

P. H. Wallman, P. W. Tamm, B. G. Spars

Chevron Research Company
576 Standard Avenue
Richmond, California 94802

Several aboveground oil shale retorting processes are characterized by rapid heating followed by retorting at essentially isothermal conditions. The objective of this study is to investigate the retorting kinetics applicable to processes characterized both by rapid heating of relatively small particles and by rapid sweeping of the produced hydrocarbon vapors out of the retort. Rather surprisingly, accurate kinetics for these conditions are not available in the literature.

Several previous investigators have taken an isothermal approach but have failed to eliminate significant heatup effects in the measured kinetics. The important investigation by Hubbard and Robinson (1) is in this category. Attempts were made to correct the Hubbard and Robinson data for the heatup effects by Braun and Rothman (2) and Johnson et al. (3). Allred (4) took new isothermal data with increased accuracy, but his results also suffered from interfering heat-transfer dynamics. Weitkamp and Gutberlet (5) used both isothermal and nonisothermal techniques but covered only low temperatures and presented no kinetic model.

A frequent characteristic of past investigations is excessive complexity of the proposed kinetic models. The works of Fausett et al. (6) and Johnson et al. (3) belong in this category. A goal of the present investigation is to keep the model as simple as possible.

One previous investigation that deserves special attention is that by the Lawrence Livermore Laboratory (LLL) described in Campbell et al. (7) and Campbell et al. (8). The LLL group determined retorting kinetics by both isothermal and nonisothermal experiments with reasonable agreement between the two approaches. However, the LLL work was directed toward in-situ retorting where heating rates are inherently low. Low heating rates were found to decrease the oil yield below Fischer Assay levels by increasing coke formation. For small particles, the detrimental effect of slow heating could be eliminated by sweeping the sample with an inert gas implying that the coking was associated with holdup in a liquid state. Such coking is not of importance in the present investigation where the sample is well swept, and heatup rates are three orders of magnitude higher than typical in-situ rates.

The LLL kinetic model predicts that the maximum achievable oil yield is that of Fischer Assay and that the coke associated with Fischer Assay is stoichiometrically related to the kerogen. This assumption may be appropriate for in-situ retorting, but it is not applicable to the present conditions where oil yields higher than Fischer Assay are measured. Consequently, another objective of this work is to extend the kinetics of oil production beyond the Fischer Assay limit.

Experimental Technique - A bench-scale fluidized bed reactor shown in Figure 1 was used to retort small samples of oil shale particles. The glass reactor held a bed of inert solids such as glass beads or sand that was continuously fluidized by a controlled flow of helium or any other gas. A weighed sample of shale in an amount no greater than 2% of the bed was dropped into the preheated reactor, producing a negligible drop in bed temperature. Heat transfer in the fluidized bed was very rapid, and the volatile products were rapidly swept out by the fluidizing gas. The vapor residence time in the reactor was typically 3 seconds. A small sample stream was diverted to a flame ionization detector (FID in Figure 1). The FID produced a signal proportional to the concentration of total hydrocarbon. Heteroatom content of evolved products was assumed constant with time. Since the hydrocarbon concentration dropped to very low levels at the end of the retorting reaction, the sensitivity of the detector had to be increased by at least a factor of ten as the retorting progressed. This increased sensitivity made it possible to record the full product-evolution curve including the long "tail" which contains information on the kinetics at high conversion levels. Attempts were made to use the FID for quantitative determination of volatile hydrocarbon yields, but the results were of insufficient accuracy. The area under the curve did, however, give an approximate yield which was used as an experimental check.

Oil and gas yields were obtained from another branch of the apparatus shown in Figure 1. The oil was condensed in a cold trap, and the gases were collected in a gas cylinder by liquid displacement. The amount of oil was determined gravimetrically, and the amount of hydrocarbon gas was determined from the total volume of gas collected and the gas composition. The oil was recovered by CS_2 extraction and subjected to GC analysis, standardized against n-paraffins. Finally, to close the hydrocarbon balance, the entire bed consisting of inert particles and retorted shale was recovered and its hydrocarbon content determined.

The oil collection trap shown in Figure 1 proved to be a critical part of the apparatus. The product oil tends to form a stable aerosol making it difficult to collect. This problem can be overcome by a trap design where the condensation occurs under a steep thermal gradient. The inside wall of the cold trap was kept at 300°F while the opposite wall was in contact with a bath at 5°F. A thermally induced outward radial flow promoted film condensation on the cold wall. Interestingly, this design eliminated aerosol formations when using helium as the fluidizing gas; but with heavier gases such as argon, nitrogen, and even methane, aerosol formation still occurred. The cause of this effect was not investigated, but it could be related to differences in conductivity between the gases. The selected bath temperature of 5°F proved practical because no butanes condensed, and only a small portion of light oil (C_5-C_7) was lost to the gas. This light oil was accounted for by use of the gas analysis.

Another area of experimental difficulty was gas analysis. At low temperatures requiring long reaction times, large amounts of helium were necessary; and the hydrocarbon products were in very low concentration. This difficulty was overcome by recycling the gas back into the fluidized bed and thereby allowing the hydrocarbon concentration

to build up. Some oil vapor was undoubtedly recycled increasing the possibility of thermal cracking.

The shale samples used in this work were obtained by screening from a single bulk sample of Colorado oil shale (Anvil Point Mine, courtesy of Development Engineering Incorporated and the U.S. Department of Energy). The Fischer Assay oil yield was 10.5% (27.5 gallons/ton) for the larger particles and somewhat lower for the finer size cuts, for example, 10.15% for 100 μm particles. These and all subsequent percentages reported in this paper are on a weight basis.

Yield Results - Experiments were conducted to determine the effect of oil shale particle size on product yields at 930°F. The yields obtained for particles of six different sizes are compared with Fischer Assay yields in Figure 2. It is apparent that oil yields higher than Fischer Assay are obtained for small particles; whereas large particles produce Fischer Assay yield. The incremental oil produced from small particles is balanced by a decreased coke make while the gas make remains constant. The oil yield appears to have a limit at about 110% Fischer Assay, but this may be entirely due to the limited range of particle sizes investigated. It is possible that the oil yield would increase further for, say, 10-μ or 1-μ particles. However, particles of this size could not be studied in the apparatus of this work.

Not only do smaller particles produce more oil, but there is also a change in the oil composition. The concentration of C_{29}+ in the product oil is shown in Figure 3. Increased oil yields are accompanied by increased heavy ends. Hence, the conclusion is that the incremental oil obtained from small particles is of higher molecular weight.

The effect of retorting temperature on the yields obtained from 0.4-mm particles and the accompanying change in oil composition are shown in Figures 4 and 5. The important findings here are that coke yield is unaffected by retorting temperature and that oil yield is increased due to decreased gas make at the lower temperatures. This second finding suggests decreased cracking since Figure 5 shows that a lighter oil product is obtained at the higher temperatures. It will also be noted that the data set shown in Figure 4 has some "extra" cracking in comparison with the data of Figure 2. This is due to the fact that the results of Figure 4 were obtained in the recycle gas mode where recycling of a small portion of the oil occurred. In general, the gas make was found to be very sensitive to equipment conditions such as the temperature of the product line leading to the condenser.

Kinetic Results - The kinetic complement to the yield results discussed above was obtained from the FID response curve. Integration of this curve gave the fractional conversion. Figure 6 shows the results of the particle-size effect experiments plotted as the logarithm of the fraction unconverted hydrocarbon versus time (the term hydrocarbon is used here to denote organic matter). It appears that the results can be described by a pair of first-order processes since the curves can be approximated by two straight-line segments. By comparing the slopes of the two segments, the rates of the two

processes are found to differ by a factor of ten. This is an important finding with consequences for the retorting model to be proposed in a subsequent section.

The small differences between the initial segments of the kinetic curves is due to differences in heatup time for the different particle sizes. However, heatup time is relatively unimportant even for the 3-mm particles because the straight-line segment extrapolates to only 15 seconds on the time axis. This "experimental" heatup time is about what one would calculate using a heat transfer coefficient of 500 W/m^2 °C.

An important feature of the results shown in Figure 6 is that the slope of the latter segment of the curve changes for particles of different size. The process corresponding to this segment appears to be slower for the small particles than for the large ones. This unexpected characteristic is at first surprising. It is, however, a consequence of the different yields for different particle sizes shown in Figure 2. The yield differences do not enter the kinetic results of Figure 6 because the ordinate is normalized by the total hydrocarbon evolved (this type of plot is required for determination of the rate constants).

The kinetic and yield data are combined in Figure 7 for the 0.4-mm and 3-mm particles. This figure shows that the hydrocarbon evolution is essentially independent of particle size up to 100% Fisher Asay oil yield. At this level the oil production stops for large particles, whereas it continues for small particles at a reduced rate.

The effect of temperature on the retorting kinetics is shown in Figure 8 for the 1-mm particles. Both processes respond to temperature but the fast one more so than the slow one.

Table I

Retorting Rate Expressions

Light Hydrocarbon Production:

$$\text{Rate} = f_1 \cdot k_1 \cdot C_o \cdot e^{-k_1 t}$$

$$\text{Amount} = f_1 \cdot k_1 \cdot C_o \cdot (1 - e^{-k_1 t})$$

Primary Heavy Oil Production:

$$\text{Rate} = f_2 \cdot k_2 \cdot C_o \cdot e^{-(k_2 + k_c) t}$$

$$\text{Amount} = f_2 \frac{k_2}{k_2 + k_c} C_o \cdot [1 - e^{-(k_2 + k_c) t}]$$

Intraparticle Coke Production:

$$\text{Rate} = f_2 \cdot f_c \cdot k_c \cdot C_o \cdot e^{-(k_2 + k_c) t}$$

$$\text{Amount} = f_2 \cdot f_c \frac{k_c}{k_2 + k_c} C_o \cdot [1 - e^{-(k_2 + k_c) t}]$$

Retorting Model - The combined kinetic and yield data can be correlated with the retorting model shown in Figure 9. Here kerogen decomposes into a "light" hydrocarbon product and a heavy intermediate product, "bitumen." The light product is largely a vapor at retorting conditions and is, therefore, produced rapidly without significant secondary reactions. The bitumen, on the other hand, is of high boiling range and remains in the particle for significant periods of time. It becomes subject to two competing processes: (1) heavy oil production and (2) intraparticle (liquid-phase) coking. The released heavy oil is further subjected to thermal cracking in the vapor phase surrounding the particles.

First-order rate expressions are proposed in Table I for the three principal steps: light hydrocarbon production (equals kerogen decomposition), primary heavy oil production, and coking.

The model accounts for the dramatic change in oil production rate which is observed. The fast initial rate is governed by the rate constant k_1 (first order in kerogen concentration). The latter slow rate is governed by the sum of the two bitumen reactions, which are assumed first order in the intraparticle bitumen concentration and have rate constants k_2 and k_c. At the temperatures of interest, k_1 is much greater than $k_2 + k_c$ so that the first step of the reaction goes virtually to completion before there is any appreciable conversion of the bitumen.

Table II

Light Hydrocarbon Fraction, f_1

Particle Size, mm	Light Hydrocarbon Total Volatile-Hydrocarbon Yield, % of Kerogen	Yield, % of Total Volatile Hydrocarbon	Light Hydrocarbon Yield, % of Kerogen
3	68.8	90	61.9
2	70.0	87	60.9
1	71.1	87	61.9
0.4	74.4	83	61.8
		Avg = 61.6	

The "stoichiometry" of the kerogen decomposition reaction is given by the product fractions f_1, f_2, and f_w in Figure 9. The (H_2O, CO, CO_2) fraction was set equal to that of Fischer Assay because the fraction of water in the liquid product could not be easily determined in the yield experiments. The light hydrocarbon fraction, f_1, was determined by a combination of the yield and the kinetic data. The light hydrocarbon yield as a fraction of total volatile hydrocarbon was obtained by extrapolating the slow reaction segments of Figure 6 to zero time and reading the fractions off the ordinate. The results are shown in Table II. The values of f_1 obtained for the four particle sizes are sufficiently constant to justify an average value of

61.6%. The stoichiometry is independent of temperature as shown in Figure 8 where all the slow reactor segments extrapolate back to approximately the same point on the ordinate, namely 87% light hydrocarbon. The bitumen fraction, f_2, in Figure 9 is obtained by difference and equals 24%. Hence, f_2 is constant with both particle size and temperature at least in the range of 900-1000°F. Finally, a ratio between coke and gas in the coking reaction of 80:20 was set on the assumption that the gas yield at 800°F in Figure 4 is the result of coking alone. Campbell et al. (8) used essentially the same coke-gas ratio for a similar reaction in their reaction sequence.

A second source of gas is vapor-phase cracking of the heavy oil released from the particle. Cracking of the light hydrocarbon fraction is also possible; but because it occurs to a lesser extent, it has been assumed to be zero. The kinetics of the cracking reaction lie outside the scope of the present investigation, but this important reaction has been studied by Burnham and Taylor (9).

A third source of gas is the initial decomposition of kerogen itself. The contribution of each step cannot be determined with the FID detector because it cannot distinguish between gas and oil.

The kerogen decomposition rate constant, k_1, and the bitumen disappearance rate constant ($k_2 + k_c$) are obtained directly as the slopes of the two straight-line segments of Figures 6 and 8 (and similar graphs for the other particle sizes). Figure 10 shows the temperature dependence of these rate constants. It is also seen that k_1 is independent of particle size. This implies that there is no significant resistance to the transport of light hydrocarbons from the interior of the particle into the bulk of the carrier gas. This condition is a consequence of the high vapor pressure of the light hydrocarbon fraction. Because of the rapid transport out of the particle, this fraction has no possibility to coke. The bitumen, on the other hand, is viewed as a high boiling liquid which can undergo intraparticle coking. The particle size dependence of ($k_2 + k_c$) in Figure 10 suggests that a diffusional resistance may be important in the heavy oil production step. Also, the activation energy for the reactions governing bitumen disappearance is only 22.6 kcal/mole as compared to 43.6 kcal/mole for the kerogen decomposition reaction.

In order to determine k_2 and k_c individually, the kinetically determined values for the sum ($k_2 + k_c$) must be used in consort with the expression for the coke yield $0.8 \cdot f_2 \cdot k_c/(k_2+k_c)$. The calculated values of the ratio $k_c/(k_2+k_c)$ together with the kinetically obtained values of ($k_2 + k_c$) are given in the Appendix. The resulting k_2 and k_c values show some interesting characteristics: k_2 is independent of particle size whereas k_c is proportional to particle size. Both have the same temperature dependence because the coke yield is constant with temperature. The temperature dependence and the particle size dependence of k_c are shown explicitly in Table III.

Table III

Rate Constants (Min.$^{-1}$)

Kerogen Decomposition:

$$k_1 = 5.78 \cdot 10^{12} \exp\left(-\frac{43.6 \text{ kcal/mole}}{R \cdot T}\right)$$

Heavy Oil Production:

$$k_2 = 1.8 \cdot 10^{5} \exp\left(-\frac{22.6 \text{ kcal/mole}}{R \cdot T}\right)$$

Coking:

$$k_c = A_c \cdot \exp\left(-\frac{22.6 \text{ kcal/mole}}{R \cdot T}\right)$$

where A_c	Particle Size, mm
$18 \cdot 10^5$	3
$9 \cdot 10^5$	2
$5 \cdot 10^5$	1
$3 \cdot 10^5$	0.4

Discussion - As part of this investigation, models different from the one proposed here were considered. One such model of particular appeal is similar in structure to the one given in Figure 9 but with a pure diffusion process for the heavy oil production. However, this alternative model is incompatible with some experimental findings: It predicts lower coke concentrations on the surface of the particle than in the interior, whereas microprobe results indicate a uniform coke distribution. Further, this diffusion model predicts zero coke yield for infinitely small particles, whereas the limited amount of data available for small particle sizes suggest a leveling-off of the coke yield below a particle size of 0.4 mm.

The approach to Fischer Assay yield structure with increasing particle size is accounted for in the proposed model by complete coking of the bitumen fraction. The model predicts a coke yield of 19% of the kerogen when the bitumen is completely coked well within Fischer Assay range. Therefore, fluid bed and Fischer Assay retorting give different yields for small particles only. The interpretation of this is that in a Fischer Assay retort small particles produce the same amount of coke as large particles because there is no sweep gas to facilitate oil removal from the small particles. The fluid bed retorting experiments have shown that additional oil can indeed be produced from small particles.

The proposed model can be compared with both the model of Allred (4) and that of Campbell et al. (8). Allred's model does not have the feature of competing parallel reactions that is essential to the retorting model proposed here. It does, however, have the intermediate product bitumen which reaches a maximum level almost identical to the one in this work. Allred postulates that all kerogen decomposes into bitumen, whereas bitumen in the present work is the remainder of the kerogen after the light hydrocarbon fraction has been stripped off.

There are some interesting similarities and contrasts between the present model and the Lawrence Livermore Laboratory (LLL) model of Campbell et al.(8) The activation energy of the initial decomposition

is similar in both models, 48-54 kcal/mole in the case of LLL and 44 kcal/mole here. Bitumen is treated merely as an intermediate in the kerogen decomposition by LLL; whereas, here it is one of several decomposition products. Coking steps are included in both models, but the material involved is different. The coking kinetics accounted for by LLL only apply to the light hydrocarbon of the present model, and this coking reaction does not occur here because of the high heating rate and the sweep gas. The coking considered in the present model involves the intermediate bitumen product and the coking rate depends on particle size. Small particles produce less coking and; consequently, oil yields higher than Fischer Assay.

Both Allred (4) and Weithamp and Gutberlet (5) observed the slow oil production regime. Calculating a rate constant for this slow production regime at 856°F from the results of the latter investigators gives a value of 0.12 min.$^{-1}$ identical to ($k_2 + k_c$) of this work.

A practical implication of the results of this work is that Fischer Assay yield is probably a practical upper limit for any retorting process. This work has shown that a very small particle size increases oil yield and decreases coke yield, but long reaction times are necessary. Low coke yields may not be desirable from overall heat balance considerations if the coke is to be used as an energy source for the process. Lowering the temperature also increases oil yield but at the expense of the gas yield and with the requirement of long reaction times. Very small particle sizes are uneconomical because of high grinding costs, and low processing temperatures are uneconomical because of the large reactor volumes required.

This work has added to the understanding of the very complex phenomena occurring during oil shale retorting. The simple retorting model will be useful in modeling product yields from retorting processes handling small size particles at high retorting rates.

References

1. Hubbard, A. B., and Robinson, W. E., "A Thermal Decomposition Study of Colorado Oil Shale," Report of Investigation 4744, Bureau of Mines, Washington, D.C., 1950.

2. Braun, R. L., and Rothman, A. J., Fuel, 54, 129 (1975).

3. Johnson, W. F.; Walton, D. K.; Keller, H. H.; and Couch, E. J., "Quarterly of the Colorado School of Mines," 70, No. 3, 237 (1975).

4. Allred, V. D., Chem. Eng. Progr., 62, No. 8, 55 (1966).

5. Weitkamp, A. W., and Gutberlet, L. C., Ind. Eng. Chem. Process Des. Develop., 9, No. 3, 386 (1970).

6. Fausett, D. W.; George, J. H.; and Carpenter, H. C., "Second-Order Effects in the Kinetics of Oil Shale Pyrolysis," Report of Investigation 7889, Bureau of Mines, Washington, D.C., 1974.

7. Campbell, J. H.; Koskinas, G. H.; and Stout, N. D., "The Kinetics of Decomposition of Colorado Oil Shale: I. Oil Generation," Report UCRL-52089 Prepared for the U.S. Energy Research and Development Administration, Lawrence Livermore Laboratory, June 1976.

8. Campbell, J. H.; Koskinas, G. H.; Coburn, T. T.; and Stout, N. D., "Oil Shale Retorting: The Effects of Particle Size and Heating Rate on Oil Evolution and Intraparticle Oil Degradation," Report UCRL-52256 Prepared for the U.S. Energy Research and Development Administration, Lawrence Livermore Laboratory, April 1977.

9. Burnham, A. K., and Taylor, J. R., "Shale Oil Cracking. 1. Kinetics," Report UCID-18284 Prepared for the U.S. Energy Research and Development Administration, Lawrence Livermore Laboratory, October 1979.

APPENDIX

HEAVY OIL PRODUCTION AND COKING RATE CONSTANTS, k_2 AND k_c (RATE CONSTANTS IN MIN.$^{-1}$, COKE YIELDS IN % KEROGEN)

Particle Size, mm		900°F	930°F	950°F	980°F	1000°F
3	$k_2 + k_c$		0.887		1.04	
	Coke Yield	16.8	→	→	→	→
	$k_c/(k_2 + k_c)$	0.875	→	→	→	→
	k_c		0.776		0.908	
	k_2		0.111		0.130	
2	$k_2 + k_c$		0.442		0.545	
	Coke Yield	15.6	→	→	→	→
	$k_c/(k_2 + k_c)$	0.813	→	→	→	→
	k_c		0.359		0.443	
	k_2		0.083		0.102	
1	$k_2 + k_c$	0.186	0.292	0.367	0.378	0.587
	Coke Yield	14.5	→	→	→	→
	$k_c/(k_2 + k_c)$	0.755	→	→	→	→
	k_c	0.140	0.220	0.277	0.285	0.443
	k_2	0.046	0.072	0.090	0.093	0.144
0.4	$k_2 + k_c$		0.197		0.296	
	Coke Yield	11.2	→	→	→	→
	$k_c/(k_2 + k_c)$	0.583	→	→	→	→
	k_c		0.115		0.173	
	k_2		0.082		0.123	

:vlh,kab

FIGURE 1

FLUID-BED REACTOR SYSTEM FOR OIL SHALE RETORTING

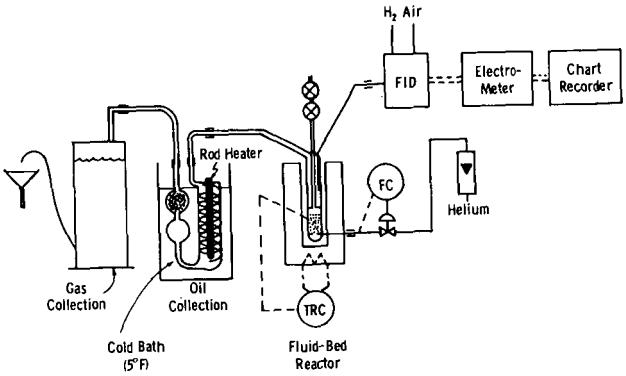

FIGURE 2

PARTICLE SIZE EFFECT ON HYDROCARBON YIELDS AT 930°F

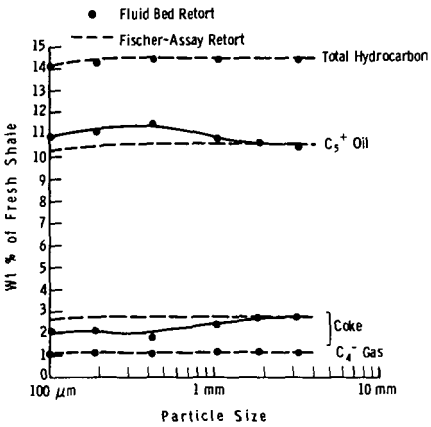

FIGURE 3

CORRELATION BETWEEN OIL YIELD AND OIL COMPOSITION

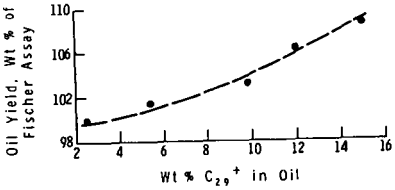

FIGURE 4

TEMPERATURE EFFECT ON HYDROCARBON YIELDS FOR 0.4 mm PARTICLES

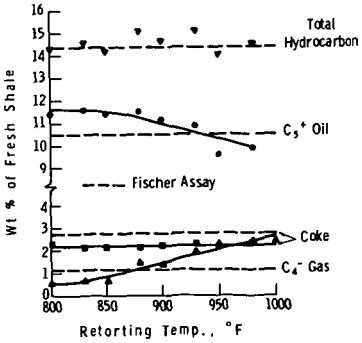

FIGURE 5

OIL COMPOSITION AS A FUNCTION OF RETORTING TEMPERATURE

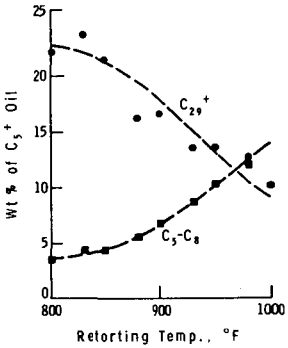

FIGURE 6

PARTICLE SIZE EFFECT ON RETORTING KINETICS AT 930°F

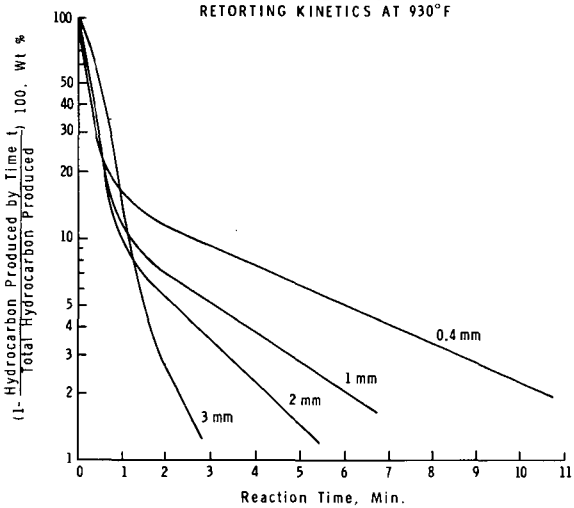

FIGURE 7

OIL PRODUCTION KINETICS AT 930°F

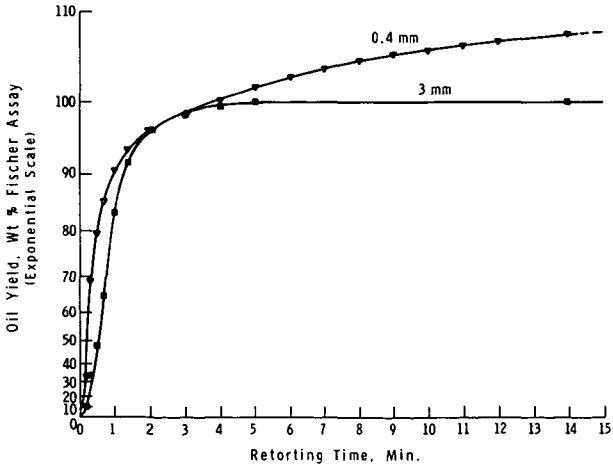

FIGURE 9

PROPOSED RETORTING MODEL

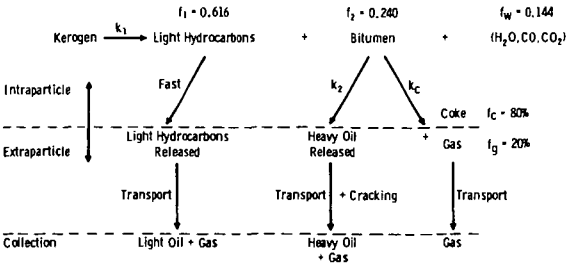

FIGURE 8

TEMPERATURE EFFECT ON RETORTING KINETICS FOR 1 mm PARTICLES

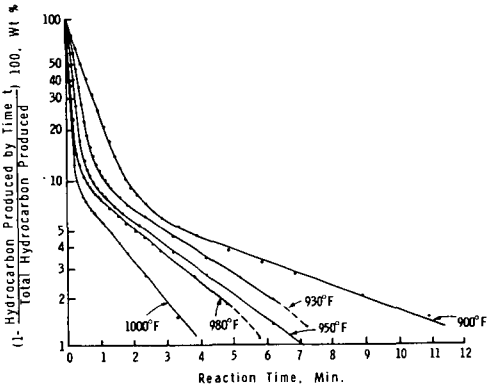

FIGURE 10

RETORTING RATE CONSTANTS

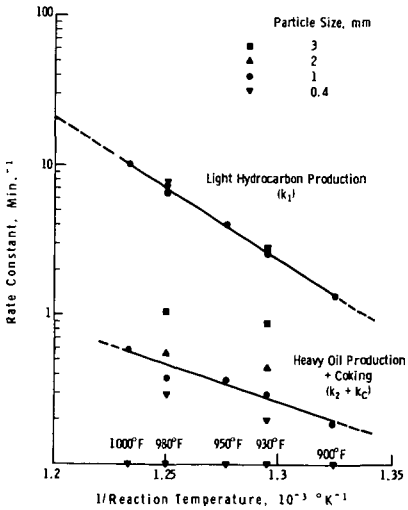

A POSSIBLE MECHANISM OF ALKENE/ALKANE PRODUCTION IN OIL SHALE RETORTING

A. K. Burnham and R. L. Ward

Lawrence Livermore Laboratory, University of California
Livermore, California 94550

INTRODUCTION

Alkene/alkane ratios have been used extensively as indicators of oil-shale retorting conditions. Jacobson, Decora and Cook (1) developed a "retorting index" which relates the ethene/ethane ratio to the retorting temperature. Campbell and coworkers developed relationships between ethene/ethane and propene/propane ratios (2), C_7 to C_{12} 1-alkene/n-alkane ratios (3), and total 1-alkene/alkane ratios (4) and the logarithm of the heating rate during retorting. Raley (5) developed a relationship between the ethene/ethane and propene/propane ratios and the yield loss in the Livermore combustion retorts. Uden and co-workers (6) demonstrated the dependence of the C_2 to C_5 alkene/alkane ratios on the presence of oxygen during retorting. Finally, Burnham (7) related the ethene/ethane ratio to the temperature at which shale oil cracking occurs.

The purpose of the work reported here is to clarify the reaction mechanisms which determine the observed alkene/alkane ratios under various conditions. When oil shale is pyrolyzed either isothermally or nonisothermally, the hydrocarbon and hydrogen concentrations are all time-dependent. To determine if the alkene-alkane-hydrogen system is in equilibrium, we have measured the C_1 to C_3 hydrocarbons and hydrogen as a function of time for oil shale heated at a constant rate. We have also determined the effect of an inert sweep gas on the time-dependent ethene/ethane and propene/propane ratios and the integral 1-alkene/n-alkane ratios in the oil. We demonstrate that the C_2H_4-C_2H_6-H_2 system is not in thermal equilibrium. We interpret our results in terms of a nonequilibrium free radical mechanism proposed by Raley (8).

Pyrolysis of both kerogen and shale oil is basically a process of breaking larger molecules into smaller molecules. For the alkene-alkane-hydrogen system to be in equilibrium, the reactions which lead to equilibrium must be faster than those which produce the smaller molecular fragments. For equilibrium to be satisfied, the ethene/ethane ratio must satisfy the condition

$$\frac{\left[P_{C_2H_6}\right]}{\left[P_{C_2H_4}\right]\left[P_{H_2}\right]} = K_{eq}$$

The enthalpy change of 34 kcal/mole (9) for the C_2H_4 plus H_2 reaction requires that the ethene/ethane ratio be a function of temperature with other conditions constant. Since the equilibrium expression has units of reciprocal pressure, the ethene/ethane ratio should be proportional to the amount of inert diluent if the system is at or near equilibrium.

From a more general viewpoint, an alkene/alkane ratio is determined by the relative rates of production of the alkene and alkane. In the pyrolysis of alkane moieties via a free-radical cracking mechanism, alkenes are formed by unimolecular decomposition of free radicals, and alkanes are formed by the free radical abstracting a hydrogen from another source. For example, ethene is formed from the decomposition of primary radicals (including ethyl), i.e.,

* Work performed under the auspices of the U.S. Department of Energy by the Lawrence Livermore Laboratory under contract number W-7405-ENG-48.

$$R\text{-}C\text{-}C\cdot \rightarrow R\cdot + C{=}C$$

and

$$C\text{-}C\cdot \rightarrow H\cdot + C{=}C$$

Ethane forms from ethyl by hydrogen abstraction, i.e.,

$$C\text{-}C\cdot + R \rightarrow C\text{-}C + R\cdot$$

Similarly, propene forms from decomposition of secondary free radicals and propyl while propane forms from propyl by hydrogen abstraction.

The free radical hypothesis leads to two interesting predictions:

(a) The alkene/alkane ratios should depend on total organic concentration since alkene formation is a unimolecular reaction and alkane formation is a bimolecular reaction.

(b) The alkene/alkane ratios should depend on retorting temperature because the activation energies for alkene formation are greater than the activation energies for alkane formation.

Therefore, both the equilibrium and free-radical hypotheses predict that the ethene/ethane ratio should depend on pyrolysis temperature and inert diluent. However, the predictions are quantitatively different and can be tested.

EXPERIMENTAL

The oil shale used in these experiments was a 22 gal/ton sample of Anvil Points shale which was ground and sieved to <0.84 mm. Aliquots from 14 to 40 g were held in a stainless steel can which had a porous frit in the bottom to allow gas and oil to escape. The sample was heated at a constant rate of 1.0 or 1.5°C/min in a programmable furnace. A constant flow of N_2 or Ar entered the system either near the bottom of the sample can or through the top of the sample can. The former configuration caused the retorting to occur under autogenous conditions (a self-generated atmosphere). The latter configuration caused the sweep gas to pass directly through the sample. Hydrocarbons were detected by a flame ionization gas chromatograph. H_2, N_2, and CO were detected by a thermal conductivity gas chromatograph. Ice water and dry ice-isopropanol traps preceded the chromatographs.

RESULTS

The rate of ethene and ethane evolution, ethene/ethane ratio and hydrogen partial pressure (relative evolution rate of hydrogen to total gas) are shown in Figure 1 for oil shale heated at 1.5°C/min under an autogenous atmosphere. The ethene/ethane ratio reaches a first minimum before the peak C_2 evolution rate. It then increases slightly before reaching a second minimum about 540°C. More pronounced results for the propene/propane ratio at 1°C/min are shown in Figure 2. We are able to combine the ethene/ethane ratios with the hydrogen partial pressures to demonstrate that the ethene-H_2-ethane system is far from thermal equilibrium under these conditions (typically 100 times too much ethene). Therefore a nonequilibrium explanation of the observed alkene/alkane ratios is required.

To form an alkane by the free-radical mechanism, there must be a source of reactive hydrogen. If this source is constant, the ethene/ethane ratio would increase continuously with temperature. However, the compositions of the gas and the solid are continuously changing which makes the problem more difficult. The first minimum in the ethene/ethane ratio occurs prior to the maximum in oil

evolution but near the temperature of a maximum in H_2S evolution (10). H_2S is a good donor of hydrogen to free radicals (11). Perhaps the second ethene/ethane minimum occurs because of a new source of reactive hydrogen in the char. The maximum rate of H_2 evolution from secondary char pyrolysis (2) occurs at about the same temperature as the second minimum observed in the alkene/alkane ratios.

The free-radical mechanism also predicts that the ethene/ethane ratio should be increased by the addition of inert diluent. This effect is demonstrated in Figure 3. The addition of an inert sweep causes both the instantaneous values above 450°C and the integral values of the ethene/ethane ratio to increase. The integral value of the ethene/ethane ratio increased from 0.21 under autogenous conditions to 0.29 in the slow sweep experiment and to 0.33 in the fast sweep experiment. A value of 0.34 for the ethene/ethane ratio is obtained by extrapolating the ethene/ethane ratios of the two sweep experiments to zero sample size/sweep rate.

The 1-alkene/n-alkane ratios in the oil as measured by capillary column GC/MS also increase with the addition of inert diluent as shown in Figure 4. This effect as well as the previously demonstrated dependence on heating rate is consistent with a free-radical mechanism. However, the alkene/alkane ratio in the presence of a sweep seems to show an even-odd dependence for reasons which we do not presently understand.

DISCUSSION

The general observation that temperature and inert diluent affect the ethene/ethane ratio is useful for correlating various data in the literature. An Arrhenius plot demonstrating the dependence of the ethene/ethane ratio on both temperature and sweep gas is given in Figure 5. In making this plot we used the temperature of maximum evolution rate as the effective temperature of retorting for the nonisothermal experiments (7). The ratio from all retorting and cracking experiments under autogenous conditions (or nearly so) can be described to within 20% by a single Arrhenius expression with an activation energy of 11 kcal/mole. This energy is substantially lower than the ethalpy of the ethane-H_2-ethene reaction (34 kcal/mole).

The ethene/ethane ratio from the Bureau of Mines entrained solids retort (12) lies substantially (2 to 3 times) above this line. We do not agree with the original interpretation of Jacobson et al (1) that residence time and extent of secondary cracking causes this effect. We have previously shown (7) that the ethene/ethane ratio during cracking is not a strong function of residence time at constant temperature. Instead, the effect is most likely caused by the steam diluent as outlined in prediction (a) above. To confirm our explanation, we show the ethene/ethane ratio from the infinite dilution extrapolation of our N_2 sweep experiments. This point shown as a black circle in Figure 5 is roughly consistent with an extrapolation of the entrained solids data to low temperature.

These findings have certain implications for the use of ethene/ethane ratios as an indicator of retorting conditions. The retorting index of Jacobson et al (1) should work well for retorting under autogenous conditions as in a Tosco or Lurgi process. It does not work in a retorting process where inert diluent is added. The case of a combustion retort is more complicated. For particle sizes greater than about 2 or 3 centimeters, retorting occurs under autogenous conditions, regardless of sweep, because of diffusion limitations. When oil combustion occurs, shale oil cracking also occurs at the interface of the combustion and kerogen pyrolysis zones. This produces locally high ethene/ethane ratios due to high temperatures, inert diluent and perhaps oxidative dehydrogenation. The ethene/ethane ratio at the exit depends on the amounts of C_2's produced by both kerogen pyrolysis and shale oil cracking at the combustion-oil generation interface and the conditions existing at both locations. Low ethene/ethane ratios produced at low heating rates when intraparticle coking occurs can be negated by high ratios produced during oil cracking in the gas stream. Therefore, any empirical relationship between oil destruction in a combustion retort and the ethene/ethane ratio must be used with caution when both coking and cracking occur.

ACKNOWLEDGEMENT

We thank J. H. Raley for his many helpful discussions concerning this work and R. W. Crawford for the GC/MS results.

REFERENCES

1. I. A. Jacobson, Jr., A. W. Decora, and G. L. Cook, "Retorting Indexes for Oil Shale Pyrolysis from Ethene/Ethane Ratios of Product Gases," published in Science and Technology of Oil Shale, Ed. T. F. Yen, Ann Arbor Science Publishers, Ann Arbor, p. 103 (1976).

2. J. H. Campbell, G. H. Koskinas, G. Gallegos, and M. Gregg, "Gas Evolution During Oil Shale Pyrolysis I. Non-Isothermal Rate Measurements," Lawrence Livermore Laboratory Preprint UCRL-82032-1 (1978).

3. T. T. Coburn, R. E. Bozak, J. E. Clarkson, and J. H. Campbell, "Correlation of Shale Oil 1-Alkene/n-Alkane Ratios with Process Yield," Anal. Chem 50, 958-62 (1978).

4. R. A. Evans and J. H. Campbell, "Oil Shale Retorting: A Correlation of Selected Absorbance Bands with Process Heating Rates and Oil Yield," In-Situ 3, 33-51 (1979).

5. J. H. Raley, "Evaluation of Retort Performance from Gas Data," 12th Oil Shale Symposium Proceedings, Ed. J. H. Gary, Colorado School of Mines Press, Golden, p. 342 (1979).

6. M. V. Robillard, S. Siggia, and P. C. Uden, "Effect of Oxygen on Composition of Light Hydrocarbons Evolved in Oil Shale Pyrolysis," Anal. Chem. 51, 435 (1979).

7. A. K. Burnham and J. R. Taylor, "Shale Oil Cracking. I. Kinetics," Lawrence Livermore Laboratory Report UCID-18284 (1979).

8. J. H. Raley, "Monitoring Oil Shale Retorts by Off-Gas Alkene/Alkane Ratios," Lawrence Livermore Laboratory Preprint UCRL-82457 (1979), to be published in FUEL.

9. American Petroleum Institute Research Project 44, Carnegie Institute of Technology, Pittsburgh, Pennsylvania.

10. N. Kirkman Bey and A. K. Burnham, unpublished results (1980).

11. A. F. Trotman-Dickenson and G. S. Milne, Tables of Bimolecular Gas Reactions, NSRDS-NBS 9 (1967).

12. H. W. Sohns, E. E. Jukkola, and W. I. R. Murphy, Bureau of Mines, R. I. 5522 (1959).

NOTICE

This report was prepared as an account of work sponsored by the United States Government. Neither the United States nor the United States Department of Energy, nor any of their employees, nor any of their contractors, subcontractors, or their employees, makes any warranty, express or implied, or assumes any legal liability or responsibility for the accuracy, completeness or usefulness of any information, apparatus, product or process disclosed, or represents that its use would not infringe privately-owned rights.

Reference to a company or product name does not imply approval or recommendation of the product by the University of California or the U.S. Department of Energy to the exclusion of others that may be suitable.

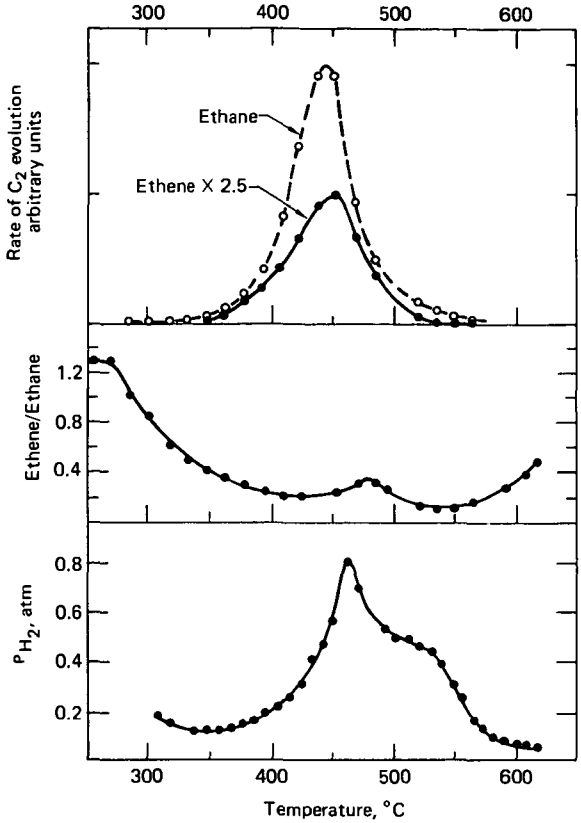

Figure 1. C_2 evolution rates, ethene/ethane ratio, and hydrogen partial pressure for oil shale heated at 1.5°C/min under an autogenous atmosphere.

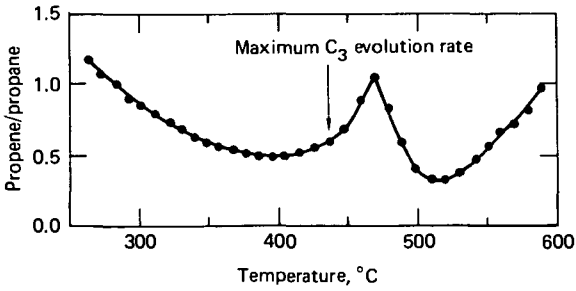

Figure 2. Propene/propane ratio from oil shale heated at 1°C/min under an autogenous atmosphere.

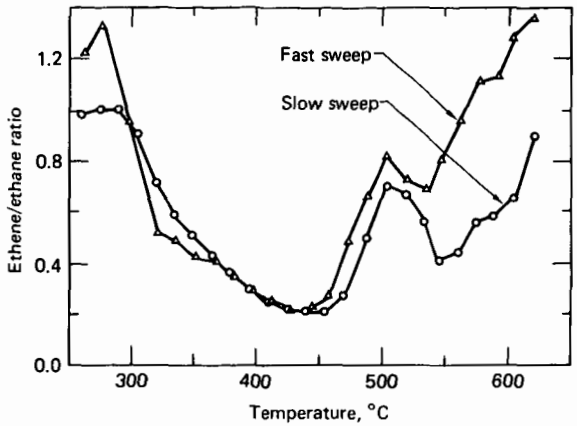

Figure 3. Effect of inert sweep gas on the time-dependent ethene/ethane ratio for oil shale heated at 1.5°C/min. The sample size and N_2 flow rate for the slow sweep experiment were 28 g and 50 cm^3/min. The sample size and flow rate for the fast sweep experiment were 14 g and 100 cm^3/min. Nearly all of the ethene and ethane is evolved between 400 and 500°C (see Fig. 1).

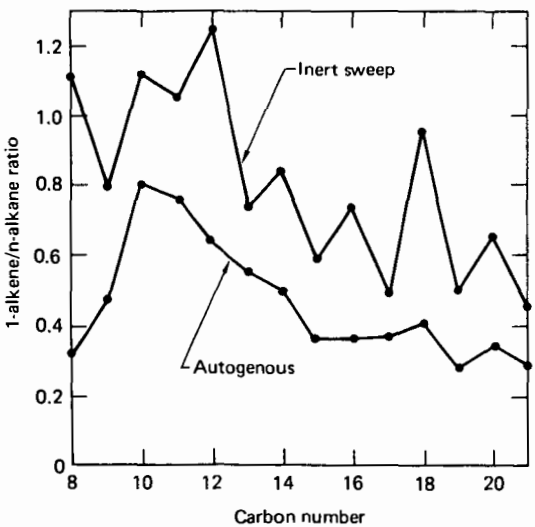

Figure 4. Effect of inert sweep gas on the 1-alkene/n-alkane ratios in shale oil. Peak height ratios were determined from capillary-column GC/MS total-ion chromatograms.

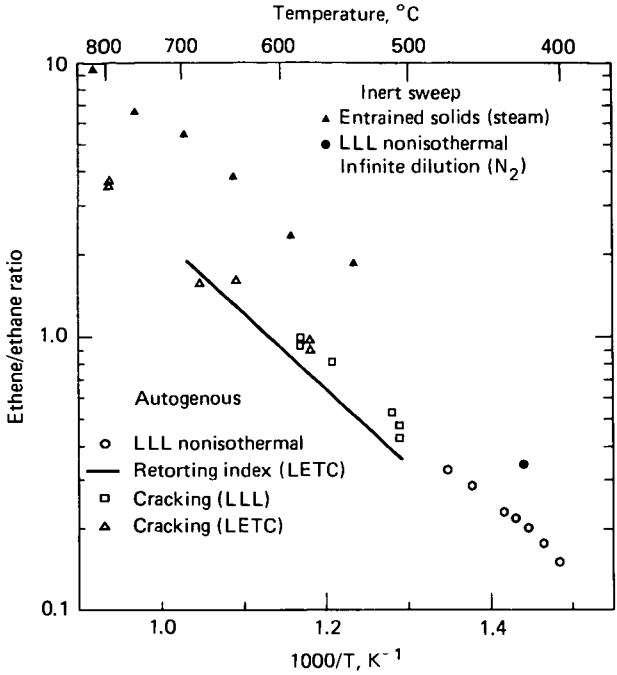

Figure 5. Demonstration of the effect of temperature and inert sweep gas on the ethene/ethane ratio from oil shale retorting. The temperature dependence of the ethene/ethane ratio can be described by an activation energy of about 11 kcal/mole.

A COMPARISON OF NATURALLY OCCURRING SHALE BITUMEN ASPHALTENE AND RETORTED SHALE OIL ASPHALTENE

Feng Fang Shue and Teh Fu Yen

Environmental and Chemical Engineering
University of Southern California
Los Angeles, CA 90007

INTRODUCTION

Asphaltene is usually defined as the pentane soluble and benzene insoluble fraction of crude oil. The molecular structure of this material has not yet been fully understood. Since asphaltene is generally recognized as the transitional stage from fossil fuel source to oil products (1,2), knowledge of the molecular structure of asphaltene is essential to the understanding of its occurrence and transition.

The majority of the organic material in oil shale is known as kerogen (organic solvent insoluble fraction). Bitumen (organic solvent soluble fraction) generally comprises only a small part of the total organic matter in oil shale. During retorting (thermal cracking), kerogen and bitumen undergo thermal decomposition to oil, gas and carbon residue. According to a number of investigators (3-5), the mechanism for thermal cracking of the oil shale is by decomposition of the kerogen to bitumen, gas and carbon residue and subsequently decomposition of the bitumen to oil, gas and coke. Asphaltene is ubiquitously present in both the natural occurring bitumen and the retorted shale oil. Very few cases for the comparison of asphaltene properties are available in the literature (6-8). In this research, a comparison of the shale bitumen asphaltene and the retorted shale oil asphaltene has been undertaken to investigate structural changes during thermal cracking.

It is anticipated that information obtained from this type of research will be helpful for the production and refining of shale oil. The role of asphaltene and its structure may be an useful indicator toward the severity of temperature effect during retorting or treatment.

EXPERIMENTS

A Green River oil shale from Anvil Points, Colorado was crushed to 8-20 mesh size prior to solvent extraction or retorting.

A. Solvent Extraction

The shale (130 g) was Soxhlet extracted with 90% benzene: 10% methanol (300 ml) for 72 hrs. Six sets of Soxhlet extraction were carried out to afford a total yield of shale bitumen 14.5 g.

B. Shale Retorting

The retort chamber is a cylindrical quartz column which is 47 mm in diammeter and 300 mm in length with a screen of 20 mesh size welded in the bottom. Heat is transferred to the shale through the quartz wall wrapped with two heating wires connected to a transformer. A stainless steel sheathed chromel-alumel(type K) thermocouple is inserted through the side arm and is assembled such that the

tip is roughly in the middle of the retort. The temperature was raised rapidly to 425°C in one experiment and to 500°C in another experiment over half an hour and maintained these for three hours. Air enters through the top of the chamber at a flow rate of 1 ml/sec and moves downward together with the product oil through the cooling column. The product oil was collected at the bottom of the retort into a receiver. The product gas was passed through acid and base traps but was not collected. The collected oil was separated from the water phase by extraction with benzene in a separatory funnel.

C. Isolation of Asphaltene

The asphaltenes were isolated according to the modified procedure (9,10). A sample of the shale bitumen or retorted shale oil was precipitated with 20-fold volume of n-pentane. The oil/resin (pentane soluble) fraction was separated from the precipitate by filtration and soxhlet extraction with n-pentane. The asphaltene (pentane insoluble, benzene soluble) fraction was obtained by soxhlet extraction of the residue with benzene. In the following text, these asphaltenes will be abbreviated as Bitu, R_{425}, and R_{500} representing bitumen asphaltene and asphaltenes derived from shale oil retorted at 425°C and 500°C respectively.

D. Physical and Chemical Analysis

The elemental analyses were done by Elek Microanalytical Laboratories, Torrance, California. A Mechrolab Model 301A Vapor Pressure Osmometer was used to determine molecular weight. IR spectra were recorded at a concentration of 25 mg/ml in CH_2Cl_2 using 0.5 mm NaCl cells on a Beckman Acculab 6 instrument. ^1H NMR spectra were obtained from a Varian XL-100 spectrometer with CD_2Cl_2 as solvent and internal reference (residue peak at 5.3 ppm). ^{13}C NMR spectra were obtained from a Varian XL-100 unit, with built-in minicomputer, operated at 25.2MHz. For all samples $CDCl_3$ is used as solvent and internal reference (central peak at 77.2 ppm). A sample of asphaltene (0.5 g) was dissolved in 2.5 ml of $CDCl_3$ with 35 mg of $Cr(acac)_3$ addedto it. To obtain reliable quantitative results, a delay time of 4 sec after each 35° pulse and 0.68 sec acquisition time was used in the gated decoupling sequence.

RESULTS

Fractionation of the three samples afforded the asphaltene fraction consituting 7.3%, 0.39%, and 0.74% by weight for the shale bitumen, shale oils retorted at 425°C and 500°C respectively.

A. Elemental Composition

Elemental Analysis data for the three asphaltene samples - Bitu, R_{425}, and R_{500} are presented in Table I.

B. Infrared Spectra

Infrared spectra of the three asphaltene samples are presented in Figure 1 for comparison. A number of well defined bands appear in all three spectra. These bands are centered at 3600 cm^{-1} attributed to phenolic O-H absorption, 3460 cm^{-1} attributed to pyrrolic N-H absorption, 3180 cm^{-1} attributed to hydrogen-bonded O-H or N-H absorption, 2925 cm^{-1} and 2860 cm^{-1} due to asymmetric and symmetric C-H stretching, 1800 cm^{-1} to 1600 cm^{-1} attributed to carbonyl C=O stretching, 1400 cm^{-1} to 1480 cm^{-1} attributed to C-H bending and 1375 cm^{-1} attributed to symmetric bending of the methyl groups. Differences in the absorption intensities of these peaks among the three asphaltene samples are shown in Talbe II.

C. ^1H NMR Spectra

The proton nmr spectra of Bitu, R_{425} and R_{500} are shown in Figures 2-4. If contributions from protons associated with hetero-atoms can be discounted, proton

types in the nmr spectra can be divided into four groups: aromatic protons (H_A), alpha alkyl protons (H_α), methyl protons in the gamma position or farther from the aromatic ring (H_γ) and other alkyl protons representing primarily the methylene protons which are beta or farther from the aromatic ring (H_β) (11). Fractional proton distribution were calculated directly from the integration curves. The separation point was chosen semi-empirically for the H_α and H_β bands at 1.9 ppm and for the H_β and H_γ bands at 1.0 ppm from the determination of the band shapes and areas. Fractional proton distribution of the three asphaltene samples are presented in Table III.

D. ^{13}C NMR Spectroscopy

Carbon-13 nmr spectra of the Bitu and R_{500} samples are presented in Figures 5,6. For the carbon group assignments, we have used the scheme developed by Ladner and coworkers (12). Carbon distributions derived from the ^{13}C nmr spectra are presented in Table V. Aromaticities determined directly by ^{13}C NMR are 0.24, 0.51, and 0.60 for Bitu, R_{425}, and R_{500} respectively.

DISCUSSION

The results of the elemental analysis indicate that asphaltenes derived from retorted shale oils have smaller H/C ratio and smaller oxygen and sulfur contents, but greater nitrogen content than that derived from shale bitumen. It seems that some of the oxygen and sulfur are eliminated as water and hydrogen sulfide during the retorting process. It remains unclear (13) whether the greater nitrogen content arises from incorporation of nitrogen gas from the air or from temperature effect as suggested by Hill (14) - "Nitrogen in the kerogen is present in molecules of very high molecular weight which tend to remain in the shale at temperatures below 800°F."

The retorted shale oil asphaltenes have greater pyrrolic N-H and hydrogen bonded O-H or N-H absorption than the shale bitumen asphaltene as revealed in the IR spectra. Band shapes for the carbonyl stretching region of the three samples also show remarkable differences. Since it is well known that either hydrogen bonding or conjugation with an olefinic or phenyl group causes a shift of the carbonyl absorption at lower frequencies, the result seems to indicate a relatively greater proportion of hydrogen bonded and/or conjugated carbonyl groups for R_{425} and R_{500} than for Bitu. The CH_3/CH_2 ratio is also increased for R_{425} and R_{500} than for Bitu as measured by absorbance at 1375 cm^{-1}.

In combination with average molecular weight and elemental compositions, the ^1H nmr data can be used to derive some average structural parameters: aromaticity (f_a), degree of substitution of the aromatic sheet (σ), number of carbon atoms per alkyl sustituent (n), ratio of peripheral carbon atoms per aromatic sheet to total aromatic carbons (H_{aru}/C_{aru}), and number of aromatic ring per molecule (R_A) can be calculated by the modified Brown-Ladner (15) method as described in Eq. (1)-(5).

$$f_a = \frac{C/H - H_\alpha/2 - H_\beta/2 - H_\gamma/3}{C/H} \quad (1) \qquad \sigma = \frac{H_\alpha/2}{H_A + H_\alpha/2} \quad (2)$$

$$n = \frac{H_\alpha/2 + H_\beta/2 + H_\gamma/3}{H_\alpha/2} \quad (3) \qquad \frac{H_{aru}}{C_{ar}} = \frac{H_A + H_\alpha/2}{C/H - H_\alpha/2 - H_\beta/2 - H_\gamma/3} \quad (4)$$

$$R_A = C_A \frac{1 - \frac{H_{aru}}{C_{ar}}}{2} + 1 \quad (5) \qquad C_A = \text{total number of aromatic carbons}$$

In these calculations, it is assumed that each carbon atom alpha to an aromatic ring carries two protons. The atomic ratio of proton to carbon in the H_β fraction is also assumed to be 2. The calculated average properties are shown in Table IV. On the basis of these calculated average properties, the retorted shale oil asphaltenes have relatively higher aromaticity, lower degree of substitution of the aromatic sheet and shorter alkyl substitutents. Based on these structural properties, the main reactions occurred in the retorting process are carbon-carbon bond fission and intramolecular aromatization.

The ^{13}C chemical shift range 168-210 ppm contains carbonyl resonance which was observed in Bitu but not in R_{500}, suggesting that carbonyl groups are very likely labile thermally. In the retorting process, the carbonyl groups may be involved in ring closure by intramolecular Friedel-Crafts acylation and subsequently reduced by hydrogen generated by aromatization within the system. The absence of the carbonyl resonance in the ^{13}C nmr spectrum of R_{500} does not prove the absence of the carbonyl group in this sample, since carbonyl carbons generally have very long relaxation times and are undetectable by ^{13}C nmr.

The chemical shift ranging from 148-168 ppm contains mainly resonances from aromatic carbons joined to hydroxylic or etheric oxygen. Both Bitu and R_{500} have the bulk of resonance occurred between 148 and 159 ppm indicating that there are much more phenols than aromatic ethers since the latter should resonate predominantly between 159 and 168 ppm. The percentage of phenolic carbon is greater for R_{500} ($\sim$2.8% of total carbons) than for Bitu ($\sim$1.1% of total carbons), which may account for the greater hydrogen bonding tendency of R_{500} as detected by IR.

In the aliphatic carbon region, the most prominent signal for Bitu is a sharp peak at 29.6 - 29.8 ppm attributed to nethylene carbons γ or further from an aromatic ring and δ or further from the terminal CH_3 group in n-alkyl chains of at least 7 carbon long. The area under this peak is 6% of the total aliphatic carbons. The total intensity of the 9-22.5 ppm range attributed to methyl carbons accounts for 40.6% and 16.7% of the total aliphatic carbons for R_{500} and Bitu respectively. The result is consistent with a longer average alkyl chain length for Bitu as calculated by proton nmr.

A comparison of the aromaticity determined by ^{13}C and ^{1}H nmr reveals that although the agreement is rather good for R_{500}, the aromaticity determined by ^{1}H nmr is smaller than that determined by ^{13}C nmr for Bitu. It is likely that since the aromatic proton (H_A) of Bitu constitutes only a very small percentage of the total proton, the effect of phenol OH and amide NH to the content of H_A is accentuated. For Bitu, the aromaticity determined by ^{1}H nmr is too large because contribution from phenol OH nad amide NH to the H_A content is neglected in the above calculation. For R_{425} and R_{500}, the effect of phenol OH and amide NH is perhaps compensated by the greater number of methyl substituents and therefore a good agreement in aromaticity is obtained. For Bitu, some of the average parameters would be in error as a result of the relatively greater contribution of phenol OH and amide NH to the value of H_A. For instance, f_a would be too high, H_{aru}/C_{ar} too low and R_A too large.

ACKNOWLEDGEMENT

This work was supported by U.S. Department of Energy, Office of Environment under Contract No. 79EV10017,000.

REFERENCES

1. I. Schwager and T. F. Yen, "Separation of Coal Liquids from Major Liquefaction Processes to Meaningful Fractions," in Liquid Fuel from Coal, (R.T. Ellington, ed.), Academic Press, 1977, pp. 233-248.

2. T. F. Yen, "The Role of Asphaltene in Heavy Crudes and Tar Sands," Proceedings of the First International Conference on the Future of Heavy Crude and Tar Sands, paper 54, UNITAR, 1979.

3. V. D. Allred, Quart. Colorado School Mines, 62, (3), 1967.

4. A. B. Hubbard and W. E. Robinson, "A Thermal Decomposition Study of Colorado Oil Shale," U.S. Bureau of Mines, R.I. 4744 (1950).

5. C. S. Wen and T. F. Yen, Chem. Eng. Sci., 32, 346 (1977).

6. T. F. Yen, Ext. Abstr. Program - Bienn. Conf. Carbon, 13, 322 (1977).

7. T. F. Yen, C. S. Wen, J. T. Kwan, and E. Chow, ACS Div. Fuel Chem., Preprints, 22 (3), 118 (1977).

8. T. F. Yen, ACS Div. Petrol. Chem., Preprints, 24 (4), 901 (1979).

9. I. Schwager and T. F. Yen, Fuel, 57, 100 (1978).

10. I. Schwager and T. F. Yen, Fuel, 58, 219 (1979).

11. R. B. Williams, Sym. on Composition of Petroleum Oils, Determination and Evaluation, ASTM Spec. Tech. Publ., 224, 168 (1958).

12. C. E. Snape, W. R. Ladner, and K. D. Bartle, Anal. Chem., 51, 2189 (1979).

13. H. B. Jensen, R. E. Poulson, and G. L. Cooks, ACS Div. Fuel Chem., Preprints, 15 (1), 113 (1971).

14. G. R. Hill and P. Dougan, Auart. Colorado School Mines, 62, (3), 75 (1967).

15. J. K. Brown and W. R. Ladner, Fuel, 39, 87 (1960).

Table I. Elemental Compositions of Shale Oil Asphaltenes

	Bitu	R_{425}	R_{500}
C[a]	74.53	76.50	78.22
H[a]	8.86	7.97	7.02
N[a]	2.71	4.49	5.03
S[a]	1.80	1.37	1.08
O[a,c]	10.32	8.01	7.71
Ash[a]	1.78	1.59	0.94
H/C	1.42	1.25	1.08
N/C	0.031	0.050	0.055
S/C	0.009	0.0067	0.0052
O/C	0.104	0.079	0.074
Molecular Weight[b]	1101	461	662
Empirical Formula	$C_{69.6}H_{98.5}N_{2.2}S_{0.6}O_{7.2}$	$C_{40.6}H_{43.9}N_{2.2}S_{0.2}O_{3.0}$	$C_{29.8}H_{37.3}N_{0.5}S_{0.2}O_{2.4}$

[a] percent by weight.
[b] by VPO in benzene
[c] by difference

Table II. IR Absorbance of Shale Oil Asphaltenes

Wavenumber (cm^{-1})	Bitu	R_{425}	R_{500}
3600	0.06	0.10	0.07
3460	0.08	0.20	0.24
3180	0.10	0.15	0.18
2925	1.76	1.19	0.91
2860	0.88	0.64	0.54
1700	0.61	0.59	0.38
1650	0.34	0.54	0.61
1600	0.30	0.52	0.63
1440	0.53	0.54	0.54
1375	0.35	0.42	0.53

Table III. Fractional Proton Distribution of Shale Oil Asphaltenes

Proton Type	Bitu	R_{425}	R_{500}
H_A	0.046	0.145	0.179
H_α	0.204	0.337	0.402
H_β	0.525	0.389	0.330
H_γ	0.225	0.129	0.089

Table IV. Average Structural Parameters of Shale Oil Asphaltenes

	Bitu	R_{425}	R_{500}
f_a	0.38	0.49	0.57
$f_a(C)$[a]	0.24	0.51	0.60
σ	0.69	0.54	0.53
n	4.31	2.41	1.97
$\frac{H_{aru}}{C_{ar}}$	0.56	0.80	0.71
R_A	6.8	2.5	4.4
$R_A(C)$[a]	4.7	2.5	4.5

[a] Calculated according to the aromaticity determined by ^{13}C NMR.

Table V. Fractional Carbon Disbribution of Shale Oil Asphaltenes

Assignments	Chemical Shift	Bitu		R_{500}	
		% of total carbon	% of aliphatic carbon	% of total carbon	% of aliphatic carbon
Carbonyl	168-210	1.3		--	
Aromatic C-O	148-168	1.1		2.8	
Mainly aromatic C-C	129.5-148	10.3		20.8	
Mainly aromatic C-H	100-129.5	12.7		36.0	
CH in alkyl groups (except iso-alkyls) and naphthenic rings. Ring joining CH_2. CH_2 in alkyl groups adjacent to CH.	37-60	17.3	23.2	6.7	16.6
CH_2 in alkyl groups not adjacent to CH (except some α CH_2 and CH_2 adjacent to terminal CH_3 in alkyl groups $>C_4$). CH_2 in ring joining ethylene groups α CH_2 and CH. β CH in hydro-aromatic rings. Naphthenic CH_2.	27.5-37	33.9	45.4	12.8	31.6
Naphthenic CH_2. Shielded α CH_2. β CH_2 in indan and propyl group β CH_3 in iso-propyl.	24-27.5	8.0	10.7	3.3	8.1
CH_2 adjacent to terminal CH_3 in alkyl groups $> C_4$. β CH_2 in unsubstituted tetralin structures. CH_3 on hydroaromatic and naphthenic rings.	22.5-24	2.9	3.9	1.3	3.1
α CH_3 not shielded by any adjacent rings or groups.	20.5-22.5	4.5	6.0	3.2	7.8
α CH_3 shielded by 1 adjacent ring or group.	18-20.5	4.0	5.4	3.7	9.1
β CH_3 in ethyl groups.	15-18	2.7	3.6	3.3	8.1
α CH_3 shielded by 2 adjacent rings or groups CH_3 γ or further from an aromatic ring.	9-15	1.3	1.7	6.3	15.6

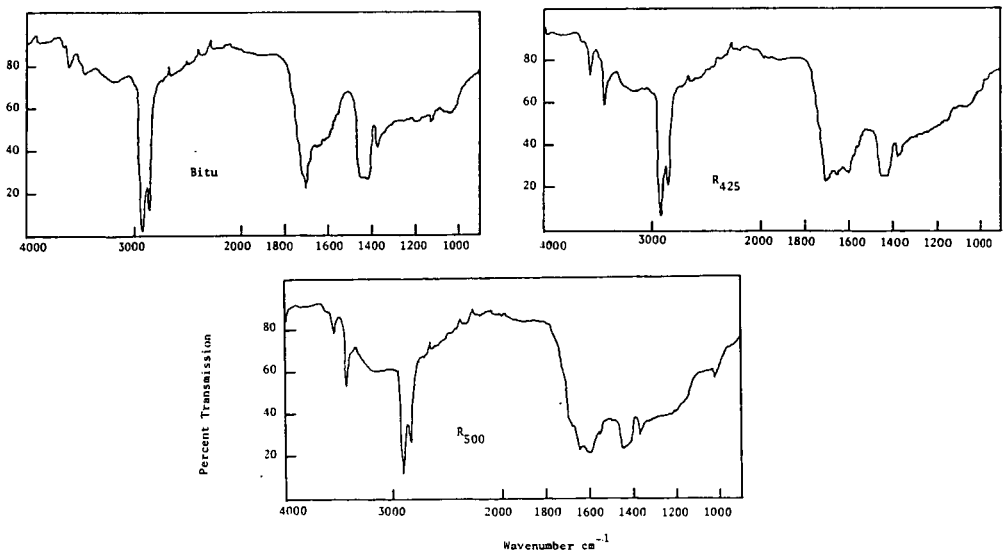

Figure 1. IR Spectra of Shale Oil Asphaltenes

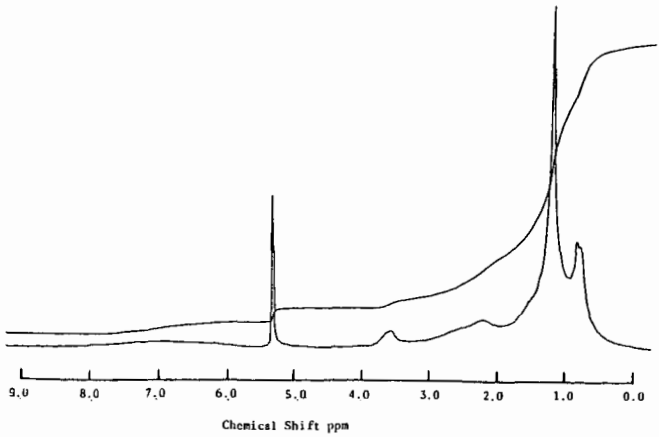

Figure 2. ^{1}H NMR Spectrum of Asphaltene From Shale Bitumen(Bitu).

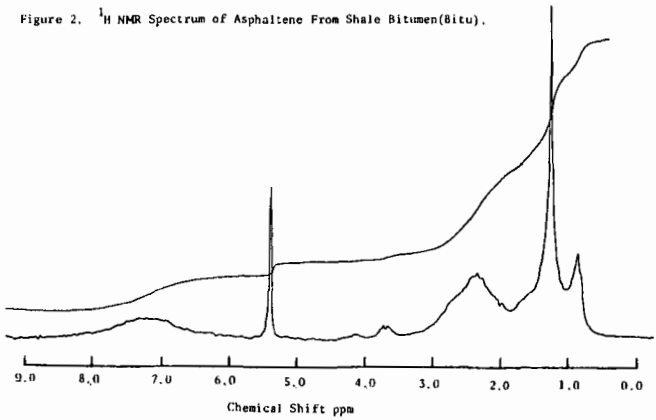

Figure 3. ^{1}H NMR Spectrum of Asphaltene From Shale Oil Retorted at 425° C(R_{425}).

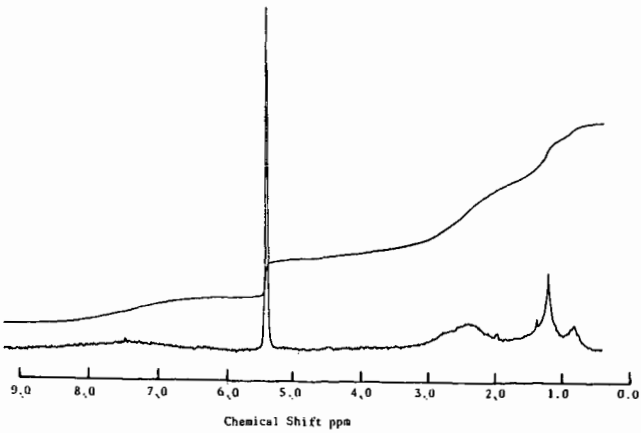

Figure 4. ^{1}H NMR Spectrum of Asphaltene From Shale Oil Retorted at 500° C(R_{500}).

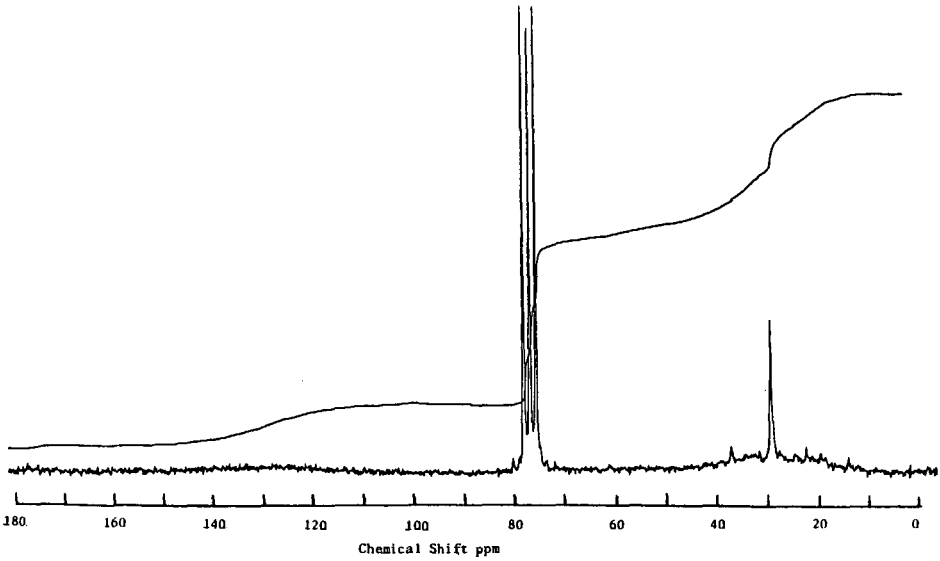

Figure 5. ^{13}C NMR Spectrum of Asphaltene From Shale Bitumen(Bitu].

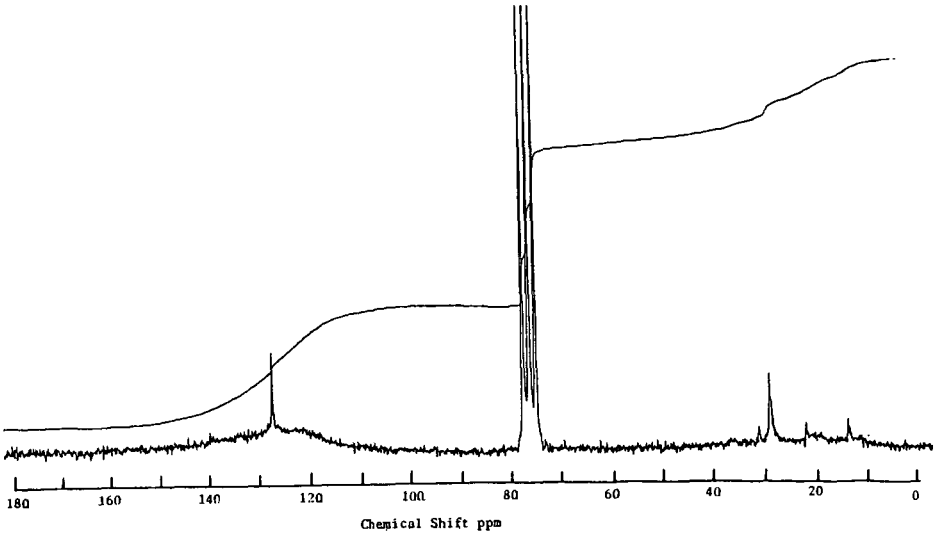

Figure 6. ^{13}C NMR Spectrum of Asphaltene From Shale Oil Retorted at 500° C(R_{500}).

THE KINETICS OF OIL SHALE CHAR GASIFICATION

W. J. Thomson, M. A. Gerber, M. M. Hatter, D. G. Oakes

University of Idaho, Moscow, Idaho 83843

INTRODUCTION

During oil shale retorting, whether it be by in-situ or surface techniques, a certain fraction of the organic carbon is left behind on the retorted shale. This "char" contains a significant fraction of the available energy in the raw shale and can actually supply all the energy for the retorting process for shales assayed at 20 gallons/ton or greater (1). To recover this energy, the char can be burned in air or gasified in O_2-steam environments; the latter in order to produce a low to medium BTU gas which can be burned elsewhere in the plant. Consequently we have been conducting kinetic studies of the reactions of oil shale char in an on-going research program under the sponsorship of DOE. Earlier we reported on the results of our oxidation experiments (2) and here we will report on our work with CO_2 and steam gasification of the char.

EXPERIMENTAL

All of the gasification experiments were conducted with the same apparatus employed in the earlier oxidation work and has been described in detail elsewhere (2). As before, powdered shale samples (200 mesh) of previously retorted oil shale from the Parachute Creek member in Colorado were suspended from an electrobalance and placed in a furnace. In this way continuous gravimetric readings were available to monitor the consumption of the char. The off-gases were analyzed on a Carle gas chromatograph equipped with a Carbosieve B column. The retorted raw shale assayed at 50 GPT and was exposed to CO_2 pressures as high as 100 KPa and H_2O pressures as high as 75 KP_a. Because there was evidence of the water gas shift reaction during steam gasification, separate experiments were also conducted in order to determine the rate of this reaction as a function of temperature and concentration of the reactant gases.

Since the char reactions can be accompanied by mineral decomposition reactions, every attempt was made to isolate the pertinent reactions. When studying CO_2 gasification the shale was first raised to 900 K in a helium environment in order to allow irreversible dolomite decomposition to take place. The predetermined CO_2-He mix was then fed to the reactor and the temperature was raised to the desired value. Since steam gasification takes place at elevated temperatures (>975K) it was necessary to first decompose the calcite present in the shale to CaO. If this was not done, then calcite decomposition would have occurred simultaneously with steam gasification. This was accomplished in a helium environment at 950K, a temperature high enough for calcite decomposition but low enough to minimize char consumption via CO_2 gasification. A few experiments were also conducted on acid leached shale. Here the shale was first soaked in either HCl or H_2SO_4 which removed Ca, Fe and Mg in the former case or converted these elements to their sulfates in the latter. Studies of the water gas shift reaction were conducted after reacting the calcite with the silica present in the shale to form inert silicates. For these experiments the shale was first decharred in 10% O_2 at 700K and then heated to 1150K in one atmosphere of CO_2 for 12 hours. The presence of CO_2 prevented decomposition of calcite to CaO during this procedure. The shale was then cooled to the desired temperature and various $CO/H_2O/CO_2/H_2$ mixtures were admitted to the reactor.

RESULTS

<u>CO_2 Gasification</u>. The rate expression given in Equation 2) was found to give a good correlation of the data, where r_{cc} is the CO_2-char reaction rate in moles/min.,

C is the unconverted char in moles, the partial pressures are in kilopascals and the activation energy is in kcal/mole. Although there was indisputable evidence of the

$$CO_2 + C \rightarrow 2CO \qquad 1)$$

$$\frac{r_{cc}}{C} = \frac{k_1 P_{CO_2}}{1 + K_1 P_{CO_2} + K_2 P_{CO}} \qquad 2)$$

$$k_1 = 4.7 \times 10^6 \exp[-44.3/RT]$$

$$K_1 = 0.05, \; K_2 \sim 0.4$$

inhibiting effect of CO, the value of K_2 is, at this time, only an approximation. The form of Equation 1) explains, to some degree, the results obtained by Burnham (3) who reported a reaction order with respect to CO_2 of 0.2 ± .2. However, the rates predicted by Equation 1) are about a factor of three less than those measured by Burnham.

Steam Gasification. Steam gasification of the char was found to produce a preponderance of H_2 and CO_2 with only a few percent CO. This is apparently due to significant water gas shift reaction rates so that steam gasification proceeds according to Equations 3) and 4). A separate determination of the rate of Equation 3) was

$$C + H_2O \rightarrow CO + H_2 \qquad 3)$$

$$CO + H_2O \rightarrow CO_2 + H_2 \qquad 4)$$

accomplished by initial rate measurements with the result that

$$\frac{r_{cc}}{C} = k_2 P_{H_2O}^{.5} \qquad 5)$$

$$k_2 = 210 \exp[-20.6/RT]$$

As expected, the spent shale prepared by the procedure described above was found to catalyze the water gas shift reaction and a reaction rate expression is given in Equation 6).

$$r_{wg} = \frac{k_3 (P_{CO} P_{H_2O} - 1/K_E \; P_{H_2} P_{CO_2})}{1 + K_3 P_{CO_2} + K_4 P_{H_2O}} \qquad 6)$$

where $k_3 = 0.25 \exp[-19.6/RT]$

$K_3 = 0.028, \; K_4 = 0.05$

and K_E is the thermodynamic equilibrium constant.

Equation 6) was found to be valid only for $P_{CO_2} > 10$KPa. At pressures between zero and 10KPa, the reaction rate *increased* with increasing P_{CO_2}. It is hypothesized that the sweep gas effects partial oxidation/reduction of the iron present in the shale and that iron is catalyzing the shift reaction. To test this, oxidation/reduction experiments of the spent shale were also carried out. The weight changes were found to approximate those expected from the quantity of iron present and the rates appeared to be first order with respect to unreacted iron and reactant gas concentration. At 1040K the rate constants for oxidation in CO_2 and reduction in CO or H_2 were all comparable at about 30 $(\text{KPa-min})^{-1}$.

The steam gasification rates for acid leached shale were found to be as much as a factor of five lower than those measured with thermally decarbonated shale. This is similar to our earlier measurements with char oxidation(1).

Mixed Gasification. A series of experiments were also conducted using various mixtures of CO_2 and H_2O in the sweep gas. The overall reaction rate expressions previously derived at Lawrence Livermore Laboratories (3,4) as well as those given here

were numerically integrated in order to provide a basis of comparison between the two laboratories and to see if isolated kinetic experiments could be used to predict mixed gasification results.

In general the Livermore results predicted char consumption rates which were much higher than those observed for mixed gasification runs with P_{CO_2} > 10KPa. The kinetic results from this work gave reasonable matches to the data at P_{CO_2} < 15 KPa but also predicted much higher rates at CO_2 pressures greater than 20 KPa. An example of these results is shown in Figure 1 for a 50-50 mix of CO_2 and H_2O at 980K. In this case the dashed curve corresponds to the predictions of both laboratories and the experimental results are shown as data points. The data clearly exhibit a much lower char consumption rate than predicted. Also shown in this figure are the predictions assuming that only CO_2 gasification takes place. Surprisingly the assumption provides a reasonable match to the experimental data and suggests that the presence of CO_2 is somehow inhibiting steam gasification. If, as suggested by our char oxidation studies (1), CaO acts as a steam gasification catalyst, an explanation for these results can be given. That is, the mixed gasification experiments were conducted on shale which had only been subjected to dolomite decomposition. Thus, at the initiation of mixed gasification the calcite was still present in the shale and would not decompose at these temperatures if P_{CO_2} > 10KPa. Since this would prevent formation of CaO, there would be no catalytic activity and steam gasification rates could be anywhere from a factor of 3-10 lower than those measured in the presence of CaO and given by Equation 4).

REFERENCES

1. Dockter, L., paper presented at 68th Annual AIChE Meeting, Los Angeles, November 20, 1975.
2. Soni, Y. and W. J. Thomson, I&EC Proc. Des. & Dev., 18, p. 661, 1979.
3. Burnham, A. K., FUEL, 58, p. 713, 1979.
4. Burnham, A. K., FUEL, 58, p. 719, 1979.

ACKNOWLEDGEMENT

The authors would like to acknowledge the financial support of DOE under contract number DE-AS07-77ET12099 and the assistance of Mr. Holt Quinn who helped with much of the experimental work.

CHAR CONSUMPTION FOR EXPERIMENT T-8
PCO_2 = .5 ATM, PH_2O = .5 ATM

T = 980°K

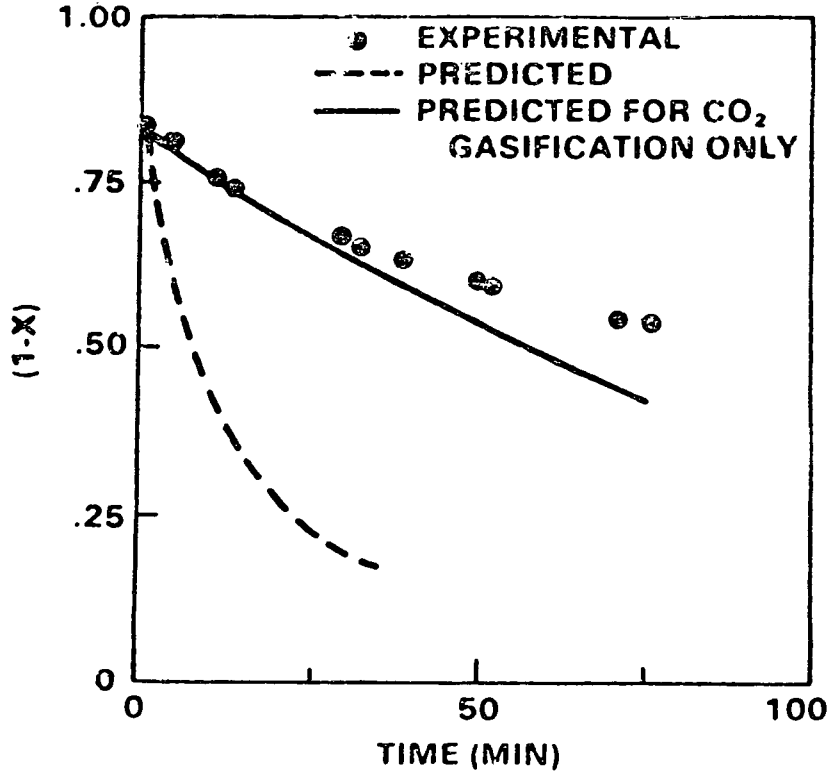

The Chemistry of Shale Oil and Its Refined Products

Donald M. Fenton, Harvey Hennig and Ryden L. Richardson

Union Oil Company of California, Science & Technology Division
P.O. Box 76, Brea, California 92621

"Oil Shale" is a term used to cover a wide range of materials which are found in many parts of the United States. The Green River oil shales are particularly high grade and are the only U.S. deposits having adequate size and availability for potential commercial value with present technology. The Green River formation contains the equivalent of 1.8 trillion barrels of shale oil. Assuming that only 600 billion barrels or one third of this oil is ultimately recoverable, this would still be 20 times the U.S. proved crude oil reserves.

The Green River oil shale is a marlstone (calcareous mudstone) that was formed in shallow lakes about 45 million years ago (1). The climate at this time probably varied from subtropical to arid. During wet periods these lakes may have been as large as 75 to 100 miles in diameter.

Sediment, mineral salts, minor plant debris and wind-transported pollen were carried into the lakes by small local streams, but the majority of the organic material that is in the oil shale came from colonies of algae that thrived in the lakes.

The organic matter found in the Green River shales formed in the deeper, central part of the lake. Rocks formed under these conditions are characterized by thin, alternating layers of carbonate and organic matter. The layers vary in thickness from 0.01 to 10 millimeters.

The layers are believed to have been formed by the precipitation of calcium carbonate in early summer, when the surface water temperature rises, followed by the seasonal high productivity of algae which occurs in late summer. The heavy carbonate minerals were deposited quickly; the organic matter settled more slowly--which gave an alternation of light and dark laminations.

The typical composition of Green River oil shale is shown in Table 1. The organic portion of the Green River oil shale is composed of around 0-5% bitumen, extractable organics, and 95-100% kerogen, unextractable organics. The kerogen is an organic matrix of high molecular weight, containing on the average several saturated rings with hydrocarbon chains having an occasional isolated carbon-carbon double bond and also containing, in addition to small amounts of nitrogen and sulfur, approximately 6% oxygen. There is also the possiblility that considerable amounts of non-crosslinked, long-chain compounds are trapped in the matrix.

If the nitrogen and sulfur are formally replaced by oxygen, for example by hydrolysis, then a simple formula weight is $C_{20}H_{32}O_2$, and the weight ratio of C/H is 7.5. This is about what would be expected for algae derived organics, since algae produce fatty acids in the C_{18} range as well as other hydrocarbons such as cartenoids at C_{40}. It has been shown that the extractable hydrocarbons from oil shale have a bimodal distribution at C_{17} and C_{29} supporting this contention (2). Strong evidence for the biogenesis of kerogen was shown when it was found that the ratio of odd to even number of carbon atoms in the extracted hydrocarbons was as high as four to one. A ratio of one to one would be expected from a nonbiological source. The higher proportion of the odd number hydrocarbons would be anticipated if their source was the decarboxylation of algal fatty acids, since these acids are predominantly even number acids.

An interesting question is: how did these predominantly algal acids become crosslinked to form kerogen? It can be seen from the kerogen formula that there are on the average four units of unsaturation, while it is known that under some conditions algae form fatty acids that are 95% unsaturated, and with some acids, such as arachidonic, an essential fatty acid, there are four olefinic linkages. It has also been shown that these polyunsaturated algal acids, under mild heating,

become crosslinked. It is clear that the unsaturated acids on diagenesis in the oil shale react to form naphthenes, the cyclic compounds found in kerogen. One reaction of this type is the Diels-Alder reaction which can occur at mild temperatures (3).

One big advantage of shale oil as compared to coal is the more favorable atomic composition of kerogen noted in Table 2. The hydrogen content of kerogen is almost twice that of many coals, and the oxygen content is lower. The sulfur content of kerogen is similar to that of coal. The nitrogen is higher in kerogen. Consequently, less hydrogen is required to remove the unwanted oxygen, nitrogen and sulfur, and less hydrogen is needed to bring the carbon/hydrogen ratio down to values required in liquid fuels such as gasoline, turbine and diesel fuels or heating oils.

Because of the impervious nature of the oil shale and the chemical nature of the kerogen, it is necessary to heat the shale to around 250°C (900°F) to thermally break up the kerogen. Under these conditions, kerogen decomposes to give oil (65-70%), gas (10-15%), coke (15-20%) and water (2-7%).

Also, during the retorting operation, there is significant loss of oxygen. About two-thirds is lost as carbon dioxide and about one-third as water. Because of the loss of carbon dioxide, the C/H ratio has beneficially decreased from 7.8 in kerogen to 7.3 in shale oil.

Some insight into the utility of shale oil can be gained by comparing its composition with coal-derived liquids and petroleum crude oil. See Table 3. Two representative liquid products from coal are shown: COED product, produced by carbonization or coking, which, like retorting of shale, is a thermal step (4), and a liquid from the H-Coal process by coal hydrogenation (5). Arabian Light crude oil is also shown.

Of the two thermally produced liquids, shale oil has a better (lower) carbon-to-hydrogen ratio, and a lower specific gravity which indicates the absence of high boiling aromatic tars. Both have high pour points; shale oil because of paraffins, COED liquid because of heavy polyaromatics. The liquid yields per ton of raw material mined are in the same order of magnitude. The solid residue of shale retorting is largely mineral matter, while the solid residue from coal carbonization, called a char, is a usable fuel containing more energy than the oil fraction. Conversion of the COED liquid product to transportation fuels, however, is a more difficult task because of its high tar, lower hydrogen and higher hetero atom contents.

The hydrogenated product from coal, H-Coal liquid, is more aromatic than shale oil but somewhat comparable in hetero atom content even though a considerable amount of hydrogen has already been added to the product.

Arabian Light crude is a wider boiling material than crude shale oil and is lower in all hetero atoms except sulfur. It has a more favorable carbon/hydrogen ratio because it contains fewer aromatics and no olefins.

In the upgrading of crude shale oil, solids removal is first achieved by optimal centrifuging, settling and filtering. Next, arsenic removal is achieved with a catalyst-absorbent.

In the third step, the hydrotreating step, the sulfur, nitrogen, and oxygen containing compounds are hydrogenated over metallic sulfide catalysts to hydrogen sulfide, ammonia, water and hydrocarbons. Olefins present in the raw shale oil are also hydrogenated.

The hydrotreated shale oil (or syncrude) now, save for pour point, resembles crude oil more closely. The amount of hydrogen consumed is listed in Table 4 either as the volume of hydrogen per barrel of product or the number of hydrogen atoms absorbed per hetero atom, that is, nitrogen plus sulfur plus oxygen atoms. The ratio of 10.8 exceeds the theoretical hydrogen consumption because double bonds are saturated and hetero as well as other compounds are hydrocracked.

The specific gravity and composition of hydrotreated shale oil are compared to a syncrude from coal. Note that we have converted crude shale oil to syncrude with much less hydrogen than would be required for a similar product from coal: 1,350 SCF per barrel compared with 6,000 SCF per barrel or more, and made a higher quality product, as indicated by the composition and carbon/hydrogen ratio.

The high pour points, and also high viscosities of the raw shale oil and of the hydrotreated shale oil, are a cause for concern. It appears that both the raw shale oil with its high nitrogen content, its high pour point and high viscosity and the hydrotreated shale oil with its high pour point may not be suitable for undedicated (to such oils) pipelines. In the absence of dedicated pipelines, conversion to pipelineable products (gasoline, diesel fuel, jet fuel, etc.) at or near the retorting site is one alternative. Another is to subject the raw shale to a coking operation which lowers the pour point and, when followed by hydrotreating, gives a low-sulfur, low-nitrogen oil of about 45°F pour point. The hydrotreated shale oil can be doped with a pour point depressant to give a 35 to 40°F pour point oil acceptable in common carrier pipelines.

If the thermal coking has to be used to make a product suitable for common carrier pipelining, an overall liquid yield loss of 15% to 20% will be incurred.

Shale oil from the retort contains on the order of 10% heavy naphtha, a precursor to gasoline. When hydrotreating the shale oil to reduce the nitrogen content to 1,000 ppm, some additional naphtha is formed. The syncrude will have close to 14% naphtha which is somewhat similar in quality to naphtha from Light Arabian crude. See Table 5. The octane number of the naphtha is low and will have to be improved by catalytic reforming. Reforming primarily dehydrogenates naphthenic rings to form high-octane aromatics, and also cyclizes or isomerizes low-octane straight-chain paraffins and hydrocracks some of the high-boiling paraffins. Reforming was developed to upgrade petroleum naphthas and will also be required for comparable liquid stocks from coal. The relatively high naphthene content of shale oil naphtha permits reforming to high-octane gasoline with only moderate yield loss, compared with Light Arabian naphtha. Naphthas from coal generally contain aromatic rings as well and so would give slightly better yields; but, because of the higher number of hetero compounds, lose some advantage.

The Department of Defense is interested in alternative sources of turbine fuels for military aircraft. JP-4 is the large-volume fuel they require. See Table 6. Shale oil is well suited for yielding turbine fuels because of its relatively low aromaticity. All specifications for JP-4 are met by separating the JP-4 boiling range material from crude shale oil by distillation and hydrotreating that fraction.

Refining of jet fuels from coal syncrude poses more of a problem because of the high aromatic content.

The diesel fuel fraction from the raw shale oil is too high in sulfur and olefins and too low in cetane number and storage stability to meet specifications. Product which meets all specifications can be made, however, by hydrotreating crude shale oil followed by distillation, refer to Table 7. An increasing number of petroleum crudes also require hydrotreating of the diesel fraction to reduce sulfur content.

The portion of shale syncrude boiling above the diesel fuel fraction can be used as a premium low-sulfur fuel oil or cracked to produce more valuable lower-boiling transportation fuels such as gasoline, jet and diesel fuels. This fraction is a better material than the corresponding fraction from crude (such as Arabian Light), because the shale oil has been upgraded by prior processing: retorting, which thermally cracked the highest boiling fractions and reduced its carbon residue, and hydrotreating which reduced the sulfur content. The corresponding crude oil fraction (from Light Arabian crude) still contains 32% (14% of crude) as a nondistillable asphalt. It is difficult to use as boiler fuel because of its 2.75% sulfur content. It is often utilized by blending it in bunker fuel or by converting it to acceptable distillate fuels by coking followed by hydrotreating.

REFERENCES

1. Cane, R. F., "Developments in Petroleum Science 5," Chapter 3 (Teh Fu Yen and G. V. Chilingarian, ed.), Elsevier, N. Y. 1976, p. 27.

2. Ibid, p. 66.

3. Ibid, p. 51.

4. Synthetic Fuels Data Handbook, Cameron Engineers, Inc., 2nd Edition, 1978, p. 193.

5. Ibid, pp. 238-42. H Shaw et al., (Exxon) Evaluation of Methods to Produce Aviation Turbine Fuels from Synthetic Crude Oils, Phase 1, For Air Force Aero Propulsion Laboratory, March 1975.

TABLE 1

TYPICAL COMPOSITION OF
GREEN RIVER OIL SHALE

		(25 Gal/Ton Shale Oil) Wt%
Kerogen Content	15 Wt%	
Kerogen Composition:		
Carbon		80.5
Hydrogen		10.3
Nitrogen		2.4
Sulfur		1.0
Oxygen		5.8
		100.0
Simple Chemical Formula (Sulfur & Nitrogen Replaced by Oxygen)		$C_{20}H_{32}O_2$
Mineral Content	85 Wt%	
Carbonates		48.0
Feldspars		21.0
Quartz		15.0
Clays		13.0
Analcite & Pyrite		3.0
		100.0

TABLE 2

KEROGEN VS COAL

	Weight Percent			
	Kerogen	Coal		
		Bit	Subb	Lignite
Moisture and Ash Free				
Carbon	80.5	78.8	73.5	72.5
Hydrogen	10.3	5.7	5.3	4.9
Oxygen	5.8	8.9	19.7	20.8
Nitrogen	2.4	1.4	1.0	1.1
Sulfur	1.0	5.2	0.5	0.7
C/H Ratio	7.8	13.8	13.9	14.8

TABLE 3

CRUDE SHALE OIL,
COAL LIQUIDS, CRUDE OIL

	Crude Shale Oil	Coal Liquids		Arabian Light Crude
		COED*	H-Coal	
Gravity, Specific	0.92	1.13	0.92	0.85
°API	22.2	-4	23.0	34.7
Boiling Range, °C	60-540	-	30-525	5-575+
Composition, Wt%				
Nitrogen	1.8	1.1	0.1	0.08
Sulfur	0.9	2.8	0.2	1.7
Oxygen	0.8	8.5	0.6	-
C/H Ratio	7.3	11.2	8.1	6.2
Pour Point, °F	60	100	<5	-15
Viscosity, 100°F, SUS	98	133	-	44
Hydrogen Added				
Scf/Bbl Product	0	0	6000	0
Wt%	0	0	10	-
Yield, Gallons/Ton	25-35	30-48	60-90	-

*COED: Char Oil Energy Development

TABLE 4

HYDROGEN REQUIREMENT TO
HYDROTREAT SHALE OIL

	Hydrotreated Shale Oil	H-Coal
Hydrogen Consumption		
Scf/Bbl Product	1350	6000
Atoms/Atom Hetero	10.8	---
Wt% Product	2.4	10
Gravity,		
°API	34	23
Specific	0.86	0.92
Pour Point, °F	+80	<5
Viscosity, 100°F, SUS	55	---
Composition, Wt%		
Nitrogen	0.08	0.01
Sulfur	0.002	0.2
Oxygen	-	0.6
C/H Ratio	6.5	8.1

TABLE 5

SHALE OIL PRODUCTS VS PETROLEUM PRODUCTS

NAPHTHA (GASOLINE PRECURSOR)

Naptha From:	Shale Oil*	Light Arabian Crude	Exxon Donor Solvent
Boiling Range, °C	70-205	25-190	70-205
50% Point, °C	154	123	177
Yield, Vol% Crude	13.6	26.7	10
Gravity, °API	51.6	63.0	30
Specific	0.77	0.73	0.88
Sulfur, ppm	9	320	4700
Nitrogen, ppm	34	---	2100
C/H Ratio	5.9	5.7	7.8
Octane Number			
Research, Clear	32.5	38.3	-
+ 3 ml TEL	61.9	63.6	-
Composition, wt%			
Paraffins	45	75	22
Naphthenes	44	14	42
Aromatics	11	11	36

*From shale oil which has been hydrotreated to reduce sulfur to 530 ppm. 1350 scf H_2 consumed per barrel of crude shale oil.

TABLE 6

SHALE OIL PRODUCTS VS PETROLEUM PRODUCTS

TURBINE FUEL

Source	JP-4 From Shale Oil	Typical JP-4
Boiling Range, °C	100-240	60-240
50% Point, °C	182	143
Gravity, °API	51.9	54
Specific	0.77	0.76
Sulfur, ppm	5	350
Freeze Point, °C	<-60	-62
Aromatics, Vol%	3.0	12.3
Smoke Point, mm	40	27.5
Thermal Stability, JFTOT at 260°C		
Pressure Drop, mm Hg	0	0.2
Preheater Deposit Code	0	1

TABLE 7

SHALE OIL PRODUCTS VS PETROLEUM PRODUCTS

DIESEL FUEL

Source	Diesel Fuel From Shale Oil	Typical
Boiling Range, °C	200-360	188-327
Yield, Vol%	42.3	--
Gravity, °API	37.2	36
Specific	0.84	0.84
Sulfur, ppm	19	2500
Nitrogen, Wt%	0.022	--
Pour Point, °F	-23	-4 to -48
Cetane Number	50	46
Viscosity, SUS @ 38°C	37.2	34.5

SYNFUEL STABILITY: DEGRADATION MECHANISMS AND ACTUAL FINDINGS

by

Dennis W. Brinkman
U.S. Department of Energy
Bartlesville Energy Technology Center
P. O. Box 1398, Bartlesville, OK 74003

John N. Bowden
Southwest Research Institute
8500 Culebra Rd., San Antonio, TX 78285

John Frankenfeld and Bill Taylor
Exxon Research and Engineering
Box 8, Linden, NJ 07036

Introduction

While substantial quantities of only a few experimental synfuels have been generated, those which are available have demonstrated the degradation problems that were predicted from work with petroleum. The high heteroatom and unsaturate content of syncrudes derived from shale and coal will necessitate closer attention to processing parameters required to produce a commercially viable product. This paper presents basic and applied data which should aid in the tradeoff decisions between further costly processing and product stability.

Degradation Mechanisms

Considerable work has been published on degradation mechanisms for compounds found in petroleum (1-4). Much of the previously reported research involved pure compounds in pure hydrocarbon solvents. The work reported here was performed with additive-free #2 diesel fuel or JP-8, both of which are middle distillate fuels in increasing demand.

Relative results for a variety of nitrogen compounds are displayed in Figure 1 according to sediment formation during accelerated storage stability tests. Alkyl substitution on the α-carbon has an obvious deleterious affect, with the most severe occurring with five-membered ring compounds.

While the reactivities of single compounds are of interest, a more realistic test would include several compounds in order to study interactive effects. As an example, Table 1 presents results from a binary mixture in diesel fuel in which an obvious interaction has occurred after 56 days at 110°F. If trioctylamine had been tested only by itself in #2 diesel fuel, it would have been labeled innocuous. However, in combination with dimethylpyrrole there is evidence for a synergistic effect. Additional studies currently underway also include sulfur and oxygen compounds.

The effects of storage temperature on sediment formation were studied using 2,5-dimethylpyrrole as the model compound. Arrhenius plots for both #2 diesel and JP-8 are shown in Figures 2 and 3. The fairly linear plots permit estimation of apparent reaction activation energies of 10.7 kcal/mole in #2 diesel and 14.4 kcal/mole in JP-8. These are rather low and suggest some catalytic effects are involved.

Synfuel Test Results

When reviewing the test results from actual synfuel samples, one must consider the source and history of the samples. For example, Table 2 shows typical properties for the same shale oil jet fuel before and after additional hydrotreating. Much of this difference in stability can be traced directly to heteroatom contents. Table 3 compares the elemental composition of two synfuels and of the gum produced after aging. The tendency for nitrogen, oxygen, and sulfur compounds to preferentially participate in the degradation reactions is obvious.

In some applications, thermal degradation can be more of a concern than storage stability. Table 4 presents data on several middle distillate synfuels as compared to a petroleum-based fuel. The tube deposits from the Jet Fuel Thermal Oxidation Test (ASTM D3241) are significantly higher for the synfuels, but the pressure build-up is normal except for one case. This indicates either rapid reactions at the hot surface or slow agglomeration. In either case, the deposit level demands further study.

Conclusion

All information published to date implies that the production of stable synfuels is possible but will require refining processes altered from those now required for petroleum. Stability research is currently focussing on both basic and applied considerations, and the results are encouraging. By continuing these efforts, it is hoped that stability will not be the limiting factor in providing adequate future fuel supplies.

REFERENCES

(1) Whisman, M. L., J. W. Goetzinger, and C. C. Ward, "Storage Stability of Aviation Turbine Fuels," BOM RI 7325, 1969, 23 pp.

(2) Whisman, M. L., F. O. Cotton, J. W. Goetzinger, and C. C. Ward, "Radiotracer Study of Turbine Aircraft Fuel Stability," BOM RI 7493, 1971, 30 pp.

(3) Frankenfeld, J. W. and W. F. Taylor, "Alternate Fuels Nitrogen Chemistry," EXXON/GRUS.1KWC.77, November 1977, 54 pp.

(4) Frankenfeld, J. W. and W. F. Taylor, "Continuation Study of Alternate Fuels Nitrogen Chemistry," EXXON/GRU.2KWC.79, February 1979, 50 pp.

Table 1. Interaction Between 2,5-Dimethylpyrrole (A, 150 ppm) and Trioctylamine (B, 1350 ppm) in #2 Diesel[1]

Presence of Compound B	Presence of Compound A: No	Presence of Compound A: Yes
Yes	0.5	61.8
No	0.5	131.8

56 Days at 110°F

[1] Sediment given as mg/100 ml fuel.

Table 2. Upgrading Effect on Composition and Stability of Jet Fuel From Shale Oil

Properties	Original	Upgraded
Sulfur, total, wt-pct	0.015	0.005
Carbon, wt-pct	86.2	85.43
Hydrogen, wt-pct	13.32	14.42
Oxygen, wt-pct	0.28	0.05
Nitrogen, ppm	1500	3.2
Total gum after 32 weeks at 110° F, mg/100 ml	6.4	1.8

Table 3. Elemental Analyses of Gums and Fuels

(wt-pct)

Gum Composition	Middle Distillate, SRC II Soluble Gum	Middle Distillate, SRC II Insoluble Gum	Kerosene, Tar Sands Soluble Gum
C	75.60	73.10	83.52
H	6.65	6.57	8.41
N	5.46	6.12	Trace
O	10.99	14.12	7.34
S	0.67	<0.01	<0.01
Original Fuel			
C	86.28		87.05
H	9.05		12.42
N	0.98		0.0004
O	3.36		0.30
S	0.32		0

Table 4. JFTOT Evaluations by ASTM Test Method D3241 Conducted for 2.5 Hours at 260°C Control Temperature

Description	JFTOT Ratings: Visual	Spun Tube	Spot Deposit	ΔP, mm Hg/Time, Minutes		
Paraho shale oil, JP-5	4	24.5	34.5	1/30	1/90	1.5/150
Tar sands, JP-5	4	15	17	0/30	0.5/90	0.5/150
COED coal liquid, JP-5	4	12	24	2/30	76/90	197/150
Paraho shale oil, Jet A(#4)	3	15	18	1/30	1/90	1/150
Paraho shale oil, Jet A(#23)	4	17	19	0.5/30	0.5/90	0.5/150
Paraho shale oil, Jet A(#10)	4	30	35	1/30	1/90	1/150
Petroleum based, JP-5	1	4	6	1/30	1/90	2/150
Paraho shale oil, DFM	3	11.5	19	0/30	0/90	0/150

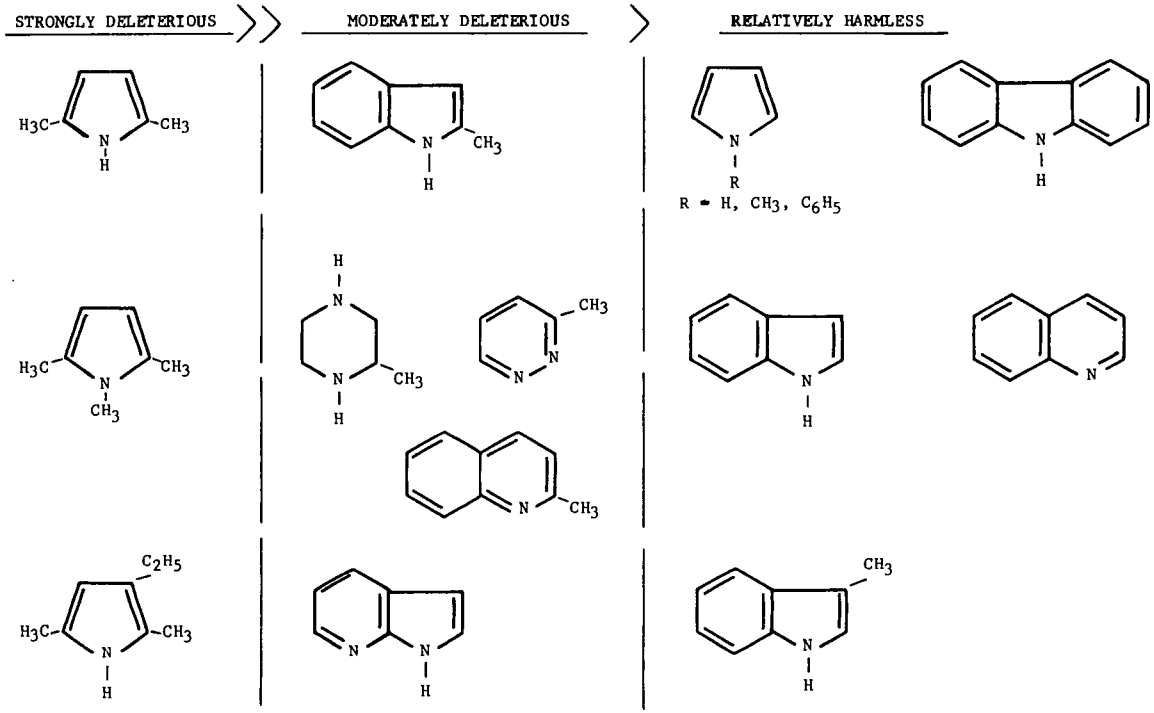

Figure 1. Structural Effects on Sediment Formation

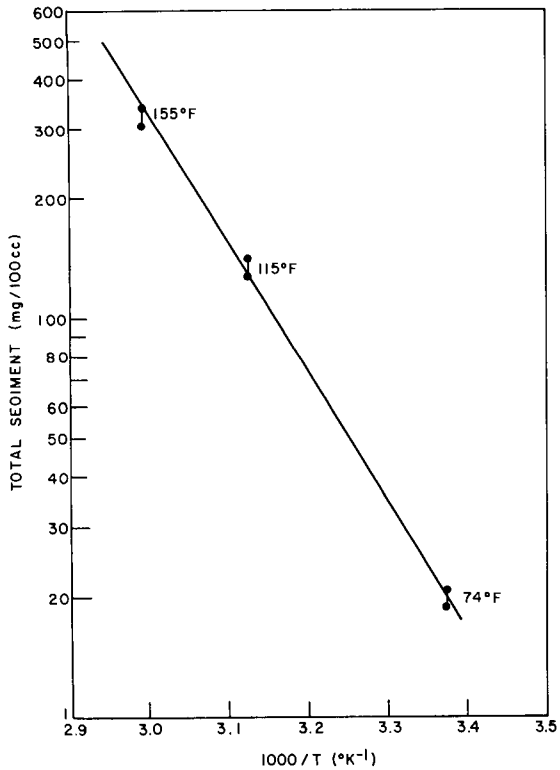

Figure 2. Arrhenius Plot of Dimethylpyrrole in #2 Diesel Fuel

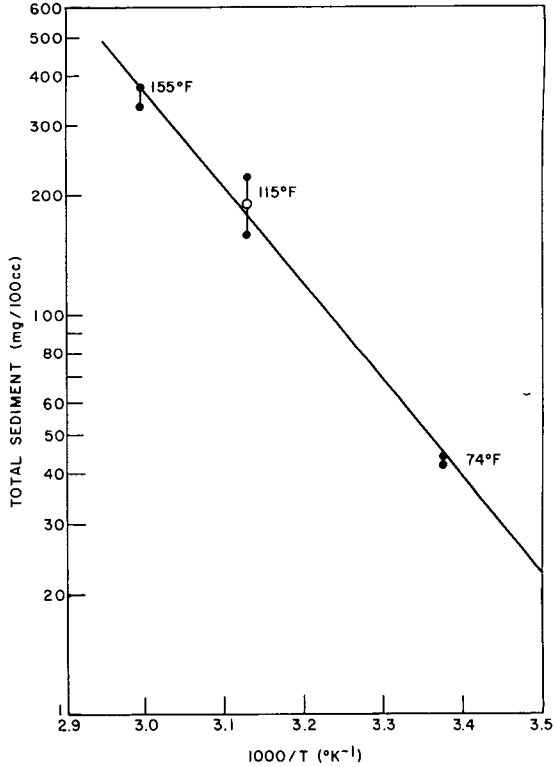

Figure 3. Arrhenius Plot of Dimethylpyrrole in JP-8

THE BENEFICIATION OF GREEN RIVER OIL SHALE BY PELLETIZATION

J. Reisberg

Shell Development Company, P. O. Box 481, Houston, TX 77001

BACKGROUND

Green River shale is a sedimentary, highly laminated, fine textured rock composed mainly of the minerals dolomite, calcite, quartz, feldspar, clay and frequently, pyrite. A minor portion, less than 50 percent by weight and averaging about 10 percent, consists of kerogen, a solid organic, highly cross-linked polymeric substance, polycyclic in nature, with an appreciable hetero-atom content. Oil shale, unlike tar sands and gilsonite, is largely insoluble in organic solvents. However, it exhibits a striking tendency to imbibe and swell in the presence of organic liquids. Kerogen can be converted by pyrolysis to liquid and gaseous fuels and to a carbonaceous residue.

The high mineral content of oil shale imposes a huge heat demand upon a thermal upgrading process and calls for very large processing facilities. A reduction in the mineral content of the feed by an ore beneficiation step can strongly influence the process economics and may also afford the ancillary advantage of a decreased volume of contaminated, possibly biologically harmful retort tailings. A process for the beneficiation of Green River shale was investigated which yields kerogen-enriched oleophilic pellets and a dispersion in water of most of the mineral matter. The study was restricted to two shale samples, one consisting of core material from the Marathon lease and another from the Dow-Colony surface lease.

There exist a number of familiar procedures for effecting mineral separations, including sink-float methods based on density differences and froth flotation based on wettability. Because of the tendency of kerogen to swell and soften in the presence of organic liquids and thus possibly to mobilize trapped mineral particles, and because most minerals are water-wetted and thus extractable with water, we investigated a liquid-liquid (oil-water) pelletization method.

Several related procedures for upgrading shales have been described in the literature. Generally these were developed as an adjunct to chemical analysis of kerogen - to reduce interference by minerals and to avoid the risk of oxidation of the organic matter by severe chemical deashing.

A South African shale, Torbanite,[1] was ground with water in a porcelain ball mill. Oil (unspecified) was added in sufficient quantity to form a paste with the organic-rich fraction and grinding was continued. Mineral matter became suspended in the aqueous phase and this was discarded. The oily paste was solvent washed, dried and analyzed. The ash content was reduced from an original value of less than 40 percent to a value of about 10 percent.

A new Brunswick oil shale containing 58 percent mineral matter[2] was processed in a similar way except that it was preground in a heavy gas-oil prior to the introduction of water. Following a 16-hour grinding period, the dried, enriched material had a mineral content of 34 percent.

Green River oil shale[3] was treated with 5 percent acetic acid to remove carbonate minerals prior to grinding in a water, n-octane system. The aqueous mineral suspension was removed and replaced repeatedly with fresh water until no mineral matter was observable in the water. Analysis of the residue indicated that the mineral content was reduced from an initial 75 percent to 16 percent.

These procedures resemble the process for coal purification described in 1922 by W. E. Trent.[4] It comprised fine grinding of coal to a 100/200 mesh size, sufficient to detach the mineral particles from the coal, then agitating with an organic, water insoluble liquid possessing a "selective affinity" for the coal. The process produced an "amalgam" of coal and organic liquid and rejected the inorganic gangue as aqueous slurry.

Recently, similar methods have been applied to the separation of tar from Alberta tar sands.[5]

EXPERIMENTAL

Procedure

The laboratory work described here was performed with two shale samples; one consisted of material from cores taken at a depth of 1830-1860 feet from the Marathon lease and the second in the form of rock fragments from the Colony mine (Dow property).

For the beneficiation we used a porcelain ball mill, the 5.5 gallon size with a 1.5-inch type grinding medium (Burundum of cylindrical form). The mill was charged with 10 pounds of grinding medium, 400-800 ml of water, 100-200 grams of shale (pulverized earlier to pass through a 100 mesh screen) and 50-100 cc of organic liquid binding agent (heptane). The mill was rotated for an hour. Typically, after about 10 minutes of operation, a kerogen-enriched fraction in the form of discrete flakes or pellets began to separate. Depending on the density of the binding agent and the degree of beneficiation, these would either float or sink in the aqueous suspension of gangue. After a one-hour milling cycle, the aqueous gangue dispersion was removed and replaced with fresh water. A small sample, 0.2-0.3 grams, of the enriched pellets was recovered for analysis and the milling operation repeated for as many cycles as deemed necessary. Both gangue and kerogen-enriched pellets were dried under vacuum at 70-80°C (see Plate I). The size of the enriched pellets is a function of the quantity of added organic binding agent. An insufficient quantity of binding agent yields pellets too small for easy separation from the gangue suspension by means of coarse sieves. An excess of binder results in the formation of a voluminous, soft kerogen paste which entrains gangue. The optimum condition described above yields pellets roughly 1 cm in diameter. The kerogen content was determined as weight loss by plasma ashing. (We used two plasma ashing devices: International Plasma Corporation, Model 1003B-248AN and LFE Corporation, Low Temperatures Asher, No. LTA-600.) Since the plasma combustion temperature does not exceed 50°C we avoid the mineral decomposition (especially carbonates) encountered during high temperature combustion.

Results

The results of a typical beneficiation experiment with Marathon lease material is shown in Figure 1. This entailed four one-hour milling cycles, the aqueous mineral dispersion being removed and replaced with fresh water after each cycle. Kerogen contents for both the organic-rich pellets (oleophilic) and the water dispersible mineral gangue (hydrophilic) are shown. The Figure also shows the results of two single cycle experiments.

The Marathon sample was obtained from a depth of more than 1800 feet. Since an ore beneficiation step would be more appropriate for a minable, shallow formation, we also tested samples from the Dow-Colony (Parachute Creek) mine. Starting with particles in the 8 to 10 sieve size range, the material was milled in water until 90 percent passed through a 100 mesh screen. Organic binder was added to the aqueous slurry and the process was continued as described above. Results of duplicate experiments are shown in Figure 2. The beneficiation obtained with this Dow-Colony shale is less favorable than that with Marathon lease material.

Particle Size of Shale Minerals

Analysis of oil shale surfaces by the scanning electron microscope prior to and following low temperature ashing reveals that the mineral matter occurs in the form of fine, discrete particles within a continuous kerogen matrix.

Figure 3 shows size distributions of inorganic mineral particles obtained by low temperature ashing of unprocessed oil shales. These minerals have mean particle diameters (50 percent frequency level) of 5-6 microns.

Minerals Distribution and Beneficiation

X-ray diffraction analysis of the products of the beneficiation of Dow-Colony shale is shown in Table 1. It is clear that the oleophilic extract (pellets) retains or concentrates the carbonates (dolomite, calcite, aragonite), particularly the dolomite. The hydrophilic gangue consists mainly of feldspar and quartz. Since silica, silicates and carbonates, in a clean condition, are water wetted the above results would indicate that the beneficiation procedure renders at least a portion of the carbonates oil-wet. The mechanism for the wettability reversal of the carbonate may reside in the adsorption, by the carbonate minerals, of certain carboxylic constituents of the shale - the bitumens. Bitumens are a solvent-extractable high molecular weight component of oil shale. They are rich in carboxylic functional groups - containing about 35 percent of fatty acids, resinous acids, polymer acids and benzenoid acids[6] (see below). Their dissolution in the added organic binder would make them accessible to the carbonates. Carboxylic acids are the most commonly utilized "collectors" for carbonate minerals in froth flotation processes. They adsorb strongly and decrease the water wettability of calcium carbonate thus facilitating its separation from a hydrophilic gangue with the gas phase. Similarly, in the pelletization process, the action of the adsorbed bitumen constituents on the carbonate mineral particles renders them largely inseparable from the oleophilic kerogen. Where pyrite is present, one would expect that, due to its inherent oil wettability, it too would accumulate in the oleophilic pellets.

Determination of Bitumens

Samples of pulverized Dow-Colony oil shale were extracted both at room temperature and by Soxhlet refluxing with n-heptane and with toluene. Solvent was stripped from the extract under vacuum and the acid numbers of the tar-like residual bitumens were determined. Results for duplicate samples are shown in Table 2. We note that significant quantities of carboxylic acids are indeed extracted.

Table 1

MINERAL DISTRIBUTION FOLLOWING BENEFICIATION STEPS
DOW-COLONY SAMPLE
(Estimated Weight Percent in Crystalline Portion - X-ray Diffraction)

	Untreated	Kerogen Extract (Oleophilic Pellets)	Gangue (Hydrophilic)
Calcite	10	10	5
Dolomite	65	83	20
Aragonite	5	5	-
Quartz	10	1	20
Feldspar	10	1	52
Dawsonite	-	-	3

Table 2

EXTRACTION OF BITUMEN FROM DOW-COLONY SHALE

Solvent	Bitumen Recovered % of Shale	Acid Number, MgKOH/gram
Toluene, Room Temp.	0.7	9.2, 9.5
Heptane, Room Temp.	0.9	3.6, 2.6
Toluene, Soxhlet	1.5	12.7, 18.8
Heptane, Soxhlet	1.6	19.2, 13.1

Mineral Contents of Marathon and Dow-Colony Lease Shales

In view of the above, one would anticipate difficulty in upgrading by this method, shales containing large quantities of carbonate mineral (dolomite, calcite, aragonite) and/or pyrite (FeS_2). In Table 3 we show the mineral distributions, determined by X-ray diffraction, for samples from the Marathon and Dow-Colony leases. The sums of the weights percent of the carbonates and pyrites in the Marathon samples lie between 30 and 35 percent whereas in the Dow-Colony samples, they lie between 47 and 80 percent. This supports the finding that superior upgrading is accomplished with the Marathon lease shale.

Table 3

MINERAL CONSTITUENTS OF MARATHON LEASE
AND DOW-COLONY MINE SHALE SAMPLES
(Estimated Weight Percent in Crystalline Portion)

	Marathon Lease		Dow-Colony		
Calcite	-	-	10	10	10
Dolomite	35	30	27	40	65
Aragonite	-	-	-	-	5
Pyrite	-	-	10	10	-
Quartz	15	20	12	10	10
Feldspar	15	20	25	15	10
Analcite	-	-	3	10	-
Dawsonite	20	15	5	-	-
Nahcolite	10	10	-	-	-
Clay	-	-	5	-	-
Unidentified	5	5	3	5	-

THE MECHANISM OF BENEFICIATION

Kerogen, as noted earlier, is a polymeric substance that can imbibe large quantities of organic liquids. This is accompanied by swelling and a slight softening of the matrix. Such gross swelling, as well as exfoliation, under the influence of various organic liquids can be observed visually with raw oil shale. We suggest that this swelling and softening of the kerogen is a key element in the beneficiation scheme described here. During the milling process the inorganic mineral particles are not ejected via a comminution of a brittle matrix (chopped out of the

kerogen, so to speak) but are instead worked out of the softened kerogen mass by a deforming and kneading process. The kerogen particles introduced initially become fused rather than bridged by pendular rings of binding agent as in coal pelletization. After drying, the gangue disintegrates into its component small particles but the kerogen pellets dry to a hard brittle mass exhibiting no evidence of the presence of discrete small particles.

Chemical Additives

In an effort to improve the ore upgrading process - to increase the level of carbonate minerals rejection - we studied the effect of chemical additives.

1. Flotation depressants: It was indicated earlier that the release of oil soluble carboxylic acids may be responsible for the retention of carbonates by the kerogen-organic binder pellets. Chemical flotation depressants are sometimes applied to overcome the collecting tendency of fatty acids and thus to increase the water wettability of the carbonate particles.(7) The introduction of such flotation depressants, including sodium oxalate, chromium nitrate, copper nitrate, ferric sulfate and aluminum nitrate failed to improve the beneficiation process described here.

2. Sodium bicarbonate: Marathon lease samples which exhibit high levels of beneficiation also contain nahcolite ($NaHCO_3$). The beneficiation process thus operates at an elevated pH. To investigate the effect of high pH on Dow-Colony shale, experiments were performed with added sodium bicarbonate and sodium hydroxide. No improvement in kerogen enrichment was obtained.

3. Surfactants and dispersants: A selection of typical commercial surface active agents, both anionic and nonionic, were tested to determine whether beneficial interfacial or wetting conditions could be obtained. These agents included:

Triton X-100 (nonionic, ethoxylated octyl phenol)
Phuronic F68 (nonionic, ethylene oxide - propylene oxide condensation product)
NEODOL® 25-7, 25-9, 25-30, 25-45 (nonionic, linear primary alcohol ethoxylates)
NEODOL® 25-3S (anionic, sulfated form of NEODOL® 25-3).

Several dispersants too were checked, including:

Marasperse N22 and CB (lignosulfonates)
Guartec (industrial grade guar gum)

This approach also was unrewarding.

Product Assay

Fischer Assays were performed with samples of Marathon lease material, with both raw shale and with the beneficiated pellets. Spent shale (char) from the assay was subjected to heat value analysis (Btu content). Results are shown in Table 5.

Table 5

FISCHER ASSAYS
MARATHON LEASE SHALE

	Raw Shale	Beneficiated Product
Oil, gal/ton	44.3	154.2
Oil, % by weight	16.6	57.4
Water, gal/ton	6.4	2.5
Water, % by weight	2.7	1.0
Spent Shale (char), % by weight	74.4	33.0
Gas + Loss, % by weight	6.3	8.6
Btu/lb of char	693	5,352

DISCUSSION

Two shale samples were studied - one from the Marathon lease (cores) and the other from the Dow-Colony mine. Clearly, the latter is the more relevant to an ore beneficiation process. The result obtained with this material is less favorable than that achieved with the Marathon cores. Still the increase in kerogen content from a value of 21 percent for the raw material to 62 percent for the upgraded pellets represents a rejection of 83 percent of the mineral matter (neglecting a small loss of kerogen to the gangue). This can mean a sizable decrease in the heat demand of a retorting process. There may also be an ancillary environmental benefit. The rejected inorganic gangue contains only a small residue of kerogen, in unmodified form. This is no more damaging chemically than the original oil shale. The residue, char, from the retorting of the enriched pellets has a sufficiently high Btu content (Table 5) and low minerals content to be useful as a process fuel. Its ash would be free of organic matter and low in silica dust. Thus the returns to the environment from a process involving ore beneficiation, retorting of the kerogen-enriched pellets and char burning would be free of organic pyrolysis products.

The laboratory experiments were performed batchwise in small ball mills. A larger scale operation would call for continuous processing, probably in a rod mill. At present the procedure does not appear to be economically feasible. A major cost is that of the initial comminution of the shale. Because the material possesses a very unfavorable grindability work index, this step requires an excessive power outlay. Furthermore, the process calls for a large quantity of organic binding agent, the recovery of which too is very costly. Whether means can be devised for improving the economics must await further investigation.

References

1. Quass, F. W. (1939), The Analysis of the Kerogen of Oil Shales, Inst. Pet. J., v. 25, 813.

2. Himus, G. W. and Basak, G. C. (1949), Analysis of Coals and Carbonaceous Materials Containing High Percentages of Inherent Mineral Matter, Fuel, v. 28, 57.

3. Smith, J. W. and Higby, L. W. (1960), Preparation of Organic Concentrate from Green River Oil Shale, Anal. Chem., v. 32, 1718.

4. Trent, W. E. (1922), Process of Purifying Materials, U. S. Patent No. 1,420,164.

5. Puddington, I. E. and Farnard, J. R. (1968), Oil Phase Separation, U. S. Patent No. 3,999,765.

6. Investigation of Colorado Oil Shale (1966), First Annual Report, Denver Research Institute, pp. 19-20.

7. Sutherland, K. L. and Wark, I. W. (1955), Principles of Flotation, Australasian Institute of Mining and Metallurgy, pp. 320-321.

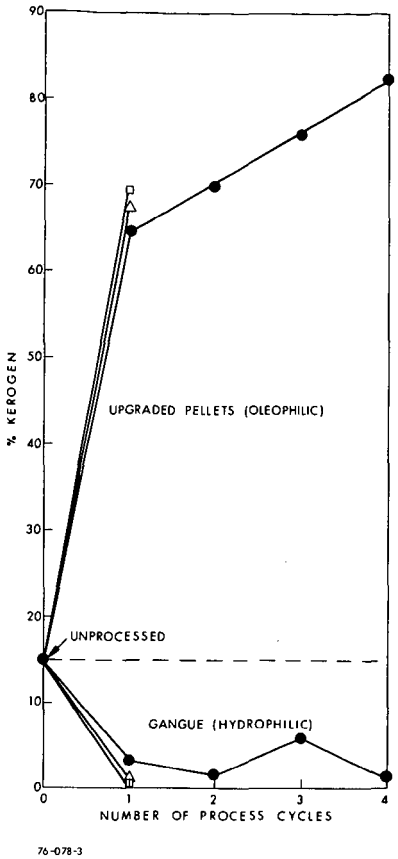

Fig. 1 The recovery of Marathon Lease kerogen as a function of number of beneficiation cycles. (Kerogen determined as weight loss on low temperature ashing)

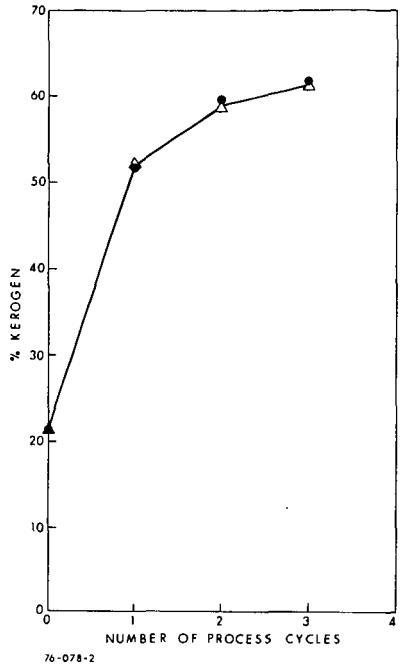

Fig. 2 The beneficiation of Dow-Colony shale.

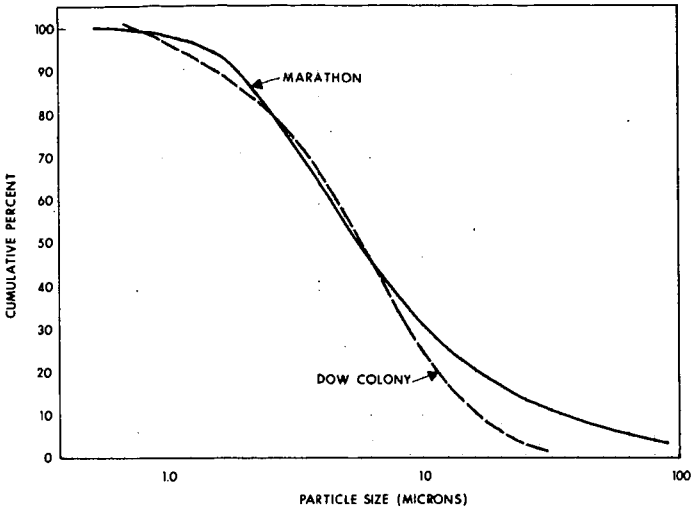

Fig. 3 Cumulative particle size distribution of the mineral constituents of oil shales (from low temperature ashing). Particle size by Coulter counter.

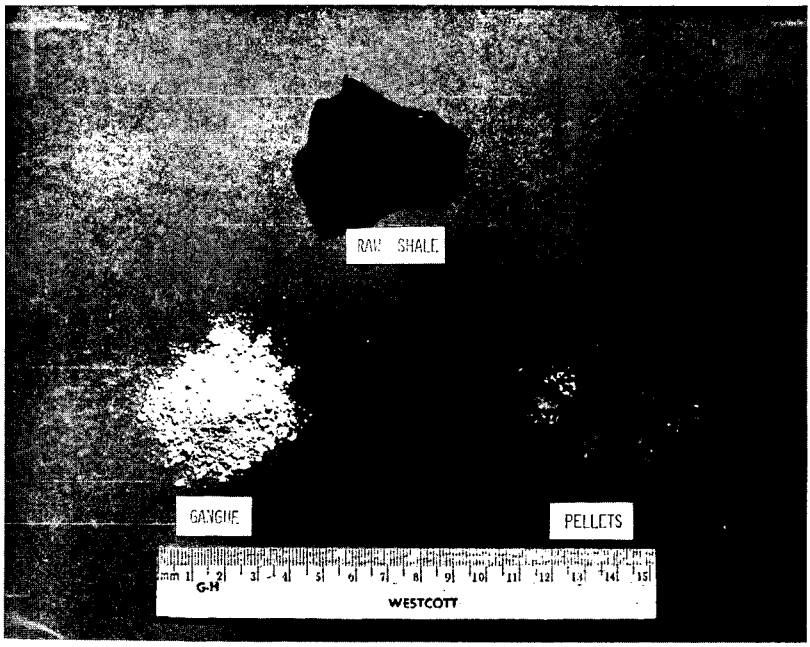

PLATE 1

The Beneficiation Products of Green River Oil Shale

RETORTED OIL SHALE DISPOSAL RESEARCH

R. N. Heistand
Paraho Development Corporation
Box A, Anvil Points
Rifle, Colorado 81650

SUMMARY

Although the retorted, or processed, shale represents the largest by-product from oil shale retorting operations, results from detailed studies indicate that it can be managed in an environmentally acceptable manner. Laboratory and field tests have demonstrated the following properties: compaction to 1600 kg/m^3, using normal vehicular traffic; cementation strength to 1480 kPa, using only retorted shale and optimum water; permeabilities as low as 1×10^{-7} cm/s, using proper handling techniques. In addition, tests have shown that dusting, auto-ignition, and leaching pose no special problems. These research results indicate that properly managed retorted shale exhibits the properties of a low-grade cement. Thermal reactions occurring during retorting and the chemical composition of retorted shale are related to the cement-like physical properties.

INTRODUCTION

In the quest for alternate energy sources, oil shale appears particularly attractive because of the large domestic deposits and because the retorting process produces liquid and gaseous fuels directly. However, the retorting process also produces large quantities of retorted shale which could pose a potentially adverse environmental impact if not disposed of properly. A mature, million-barrel-per-day oil shale industry would produce over 125 million Mg of retorted shale during each day of operation.

During the Paraho operations at the U. S. Department of Energy Anvil Points Oil Shale Research Facility, the potential problem of retorted shale disposal was recognized. A seven-stage retorted shale research program, jointly supported by the U. S. Bureau of Mines, was carried out using both laboratory and field studies (Holtz, 1976). Highlights of this retorted shale research program showed that retorted oil shale, produced by the Paraho process, can be effectively compacted and handled to produce strong and water impervious structures (Heistand and Holtz, 1980). These desirable properties of Paraho retorted shale are believed due to the formation of a low-grade cement by thermal reactions which occur during retorting.

In this paper, the chemistry of Paraho retorted shale, the nature of the thermo-chemical reactions that can contribute to its cement-like properties, and the chemistry of the leachates obtained from permeability studies will be presented. Although civil engineering information now exists which permits the disposal of retorted shale in an environmentally acceptable manner, a better understanding of the thermal reactions of retorting and the chemical composition of retorted shale may suggest changes in retorting operations which would further lessen any possibly adverse environmental impact.

EXPERIMENT DESIGN

Because the disposal of retorted shale is, ultimately, a field exercise, this paper will discuss the experimental design (and data) from field studies which have been carried out. Laboratory experimentation and data will be used to complement the results of field studies. Two field studies were carried out during the Paraho research operations. These retorted shale field studies included compaction studies and permeability, or infiltration, studies.

The field compaction studies were carried out in a relatively flat area, 2-3 km from the retorting operations (see Fig. 1). The compaction site, measuring 55 m wide by 120 m long, was divided into two sections. In one section the retorted shale was placed dry; in the other, optimum water was added before placement. The material was hauled directly from the retorted shale disposal system and spread as soon as possible. No problems with dusting or auto-ignition were noted. The material was spread in 20-30 cm layers and subjected to various compactive efforts. Approximately 12000 m^3 (15000 Mg) of retorted shale was used in these field compaction studies.

The field infiltration studies were carried out near the retorting operations. Two shallow ponds were constructed using techniques developed during the earlier field compaction studies (see Fig. 2). Both ponds were constructed out of Paraho retorted shale placed in layers to an overall thickness about 1 m. Both ponds had sloping sidewalls to obviate wall effects and to eliminate any wall-bottom interface. One pond was constructed with dry retorted shale using light compaction. The other pond was constructed of retorted shale, mixed with optimum water, and placed using heavy compaction. After construction, both ponds were filled with water and the infiltration rates were measured using staff gauges and flows through the drain lines.

RESULTS AND DISCUSSION

Compaction. The field compaction studies confirmed earlier laboratory studies regarding the effect of compactive effort, moisture addition, and aging on density and strength. Shown in Figure 3 is the relationship of compactive effort and added moisture on the densities of retorted shale. At least three in-place density measurements were made in each layer. Results show that densities averaging 1500 kg/m^3 can be achieved. The strength of the compacted retorted shale was measured using

unconfined compression (ASTM 1976). The relationship between this strength data and added moisture at various seasoning times are shown in Figure 4. The remarkable strength increase obtained with the addition of optimum water indicates the occurrence of some sort of cementing reaction. Further evidence of this cementing reaction is apparent where the compressive strength gains with aging. Aging 60 days after the addition of optimum water produced compressive strengths of nearly 1500 kPa.

Infiltration. Infiltration data for the two ponds are listed in Table 1. Also listed are in-place and core densities, moisture contents, and compressive strengths. These data show that Pond I (high compaction, optimum water) was well-constructed. Densities matched those achieved in earlier laboratory and field compaction tests. The strength, measured in a core sample (1480 kPa), exceeded those achieved during those earlier tests. The field permeability, as measured by staff gauge, (4×10^{-6} cm/s), when corrected for initial absorption and normal evaporation, approaches the value obtained from analysis of the core (6×10^{-7} cm/s). Actual infiltration from the highly compacted pond shows the permeation rate to be 3×10^{-7} cm/s.

Pond II, receiving only light compaction and no added water, showed a permeability rate of 2×10^{-4} cm/s. Although the permeability of this material is quite high, effluents could be contained in a disposal area using properly-placed, well-constructed material such as used in Pond I. Even though the loosely compacted Pond I exhibited a high permeability rate, an additional field experiment indicated that permeability may not pose a serious problem. After Pond II (light compaction) had dried thoroughly for several months following the field infiltration test, a special test was conducted. The surface was sprayed with 17,400 ℓ of water to represent a rainfall of 5 cm in 30 minutes. No effluent occurred for nearly one full day. A small seepage began the second day and continued for two days. Only 7 ℓ

were collected from the drain pipe. Essentially all of the simulated rainfall was lost to absorption and subsequent evaporation. This indicates that leaching and permeability may not be a problem for Paraho retorted shale, even when lightly compacted, because even heavy rainfall will not penetrate the pile to significant depths.

Chemical and Physical Properties. Paraho retorted shale is described according to standard soils classification as a silty-gravelly material (Holt, 1976). A size distribution diagram is presented in Figure 5. Some of the favorable properties of the retorted shale is attributed to this size distribution - like a good aggregate mix, this material has the proper ratio of fines to larger sized pieces so that the voids between the larger pieces are filled with fines. This relationship increases density, promotes strength, and reduces dusting and erosion. The chemical composition of retorted shale depends on the composition of the raw shale and the retorting process. The mineral composition of the Green River shale used in the Paraho operations consists of a complex mixture of minerals. These include: carbonates (50%), clays (40%), quartz (8%), and sulfides and others (2%). The principal carbonate mineral undergoing thermal reactions during the normal retort conditions are dolomite ($CaCO_3 \cdot MgCO_3$), or more properly ferroan ($CaCO_3 \cdot Fe_x$, $Mg_{1-x}CO_3$) where a portion of the magnesium is replaced by iron. It is believed that ferroan undergoes the following chemical reaction during normal retorting conditions:

(1) Ferroan + Heat $\rightarrow$ Calcite ($CaCO_3$) + Magnesia (MgO) + FeO + CO_2

The mean chemical analysis of Paraho retorted shale is presented in Table 2. Although it is important to know this chemical composition, it is not helpful in assessing the components responsible for the cement-like properties. Much emphasis has been placed upon the formation of reactive oxides, such as

free lime and magnesia, from carbonate decomposition. Although free lime can be formed under laboratory conditions (Heistand, Jones, Morriss, 1978), it has not been detected in the retorted shale used in the field studies. Although free lime was not detected, magnesia (MgO) has been found in Paraho retorted shale. Sulfur minerals, known to exhibit cement-like properties, have been found in Paraho retorted shale (Holt 1976). These include: anhydrite ($CaSO_4$), bassanite ($CaSO_4 \cdot 0.5H_2O$), gypsum ($CaSO_4 \cdot 2H_2O$). These sulfur minerals present in the retorted shale may be there as a result of the raw shale composition or as a result of absorption of hydrogen sulfide by the retorted shale. It is believed that the magnesia and sulfur minerals are responsible for the cement-like properties of the Paraho retorted shale.

Many studies have been carried out concerning the analysis of leachates from retorted shale. Results from these studies are highly dependent upon the procedure that is employed. Listed in Table 3 are some of the leachate data obtained during the retorted shale studies. The data show the variations obtained from various test procedures. For the most part, the leachate consists of the major components in retorted shale (see Table 2). As the compaction is increased, the column experiments show that the leachate concentration is increased, but the total amount leached is decreased. Also, the leaching diminishes as the leachate is recirculated which would indicate that leaching should not proceed to great depths in a retorted shale disposal area. Batch experiments indicate that about 1 wt% of material is extracted from the retorted shale; this meets established engineering standards (Holtz, 1976). Data shown in Table 3 consists of materials which can contribute to salinity, toxic elements had not been considered. More recently, the U. S. Environmental Protection Agency has proposed an extraction procedure to determine hazardous wastes (EPA, 1979). Results obtained using the proposed EPA extraction procedure are shown in Table 4 for both Paraho raw and retorted shales. The low

concentrations shown in Table 4 indicate that these materials are not hazardous wastes as indicated by the U. S. EPA. These low concentrations of toxic materials found in leachates from Paraho retorted shale using the proposed U. S. EPA extraction procedure would not be increased to hazardous levels if all of these materials present in the retorted shale (see Table 2) were solubilized.

CONCLUSIONS

Detailed laboratory and field studies have shown that Paraho retorted shale can be compacted easily; is not subject to dusting, erosion, or auto-ignition; and can be handled to create structures of very low permeability. A basis for these beneficial properties can be found, in part, by an examination of the chemical and physical properties of the retorted shale. However, more studies are needed to further define these chemical and physical properties. Results from these additional studies can further reduce the possibility of any potentially adverse impact from retorted shale disposal.

ACKNOWLEDGEMENT

The retorted shale research studies discussed in this paper were carried out at the U. S. Department of Energy Anvil Points Research Facility located on the Naval Oil Shale Reserves Nos. 1 and 3 near Rifle, Colorado.

REFERENCES

American Society for Testing and Materials, "ASTM Standards, Parts 10 and 19", Phila., PA, 1974.

Heistand, R. N. and W. G. Holtz, "Retorted Shale Research", 13th Oil Shale Symposium, Golden, CO, April 1980.

Heistand, R. N., D. B. Jones, and L. L. Morriss, "Free Lime in Retorted Oil Shale", Energy Sources, 4, 195-202 (1978).

Holtz, W. G., "Disposal of Retorted Shale from the Paraho Oil Shale Project", (J0255004, U. S. Department of Interior, Bureau of Mines), Dec. 1, 1976.

U.S. EPA, "Hazardous Waste Guidelines and Regulations", Federal Register, 43, 58956-7 (1978).

TABLE 1

FIELD INFILTRATION ANALYSIS

	Pond 1		Pond 2
	Initial	Cores	Initial
Moisture, wt%	22.1	18.5	0.0
Density, Bottom kg/m^3	1488	1697	1466
Side kg/m^3	1395		
Strength, kPa		1482	
Permeability, cm/sec x 10^{-6}	0.3	0.6	2000

TABLE 2

RETORTED SHALE COMPOSITION

A. Major Elements

Element	Wt%	Element	Wt%
Al	4.6	Mg	4.3
Ca	12.6	Na	2.0
Fe	2.3	Si	17.3
K	1.4	Ti	0.2

B. Trace Elements

Element	ppm	Element	ppm
As	62	Mo	35
B	140	Ni	35
Ba	530	Pb	33
Cd	1	Sb	3
Cr	38	Se	2
Cu	51	Sn	< 2
Hg	0.02	V	108
		Zn	83

TABLE 3

FIELD LEACHATES

Material	Loose Fill	Compacted
Leachate Volume, ℓ	250,000	1500
pH	10.4	11.4
	mg/ℓ	mg/ℓ
Calcium	480	55
Magnesium	2.6	1.4
Sodium	1,740	3510
Potassium	161	91
Silicon	3	3.3
Sulfate	1,112	1314
Chloride	651	112
Alkalinity (as $CaCO_3$)	1.9	454
Arsenic	5.8	3.9
Boron	1.7	1.7
Cadmium	< 0.005	< 0.005
Lead	0.07	0.07
Mercury	0.012	0.010
Molybdenum	1.7	4.3

TABLE 4

LEACHATE DATA
EPA EP TEST (RCRA)

Arsenic	< 0.1	ppm
Barium	< 10	ppm
Cadmium	< 0.05	ppm
Chromium	< 1	ppm
Mercury	14	ppb
Lead	220	ppb
Selenium	23	ppb
Silver	30	ppb

FIGURE 1

FIELD COMPACTION SITE

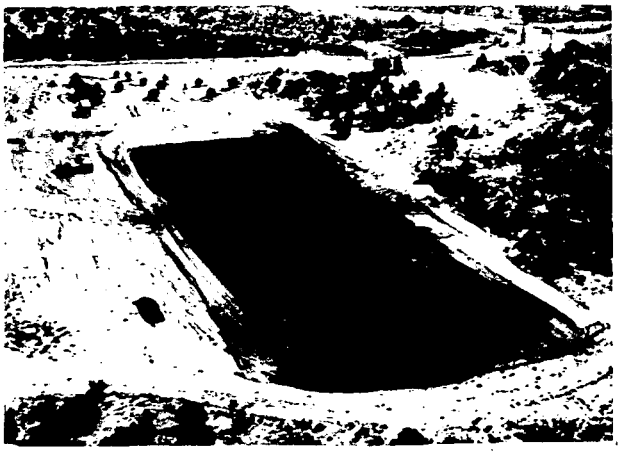

FIGURE 2

FIELD INFILTRATION SITE

POND 2 POND 1

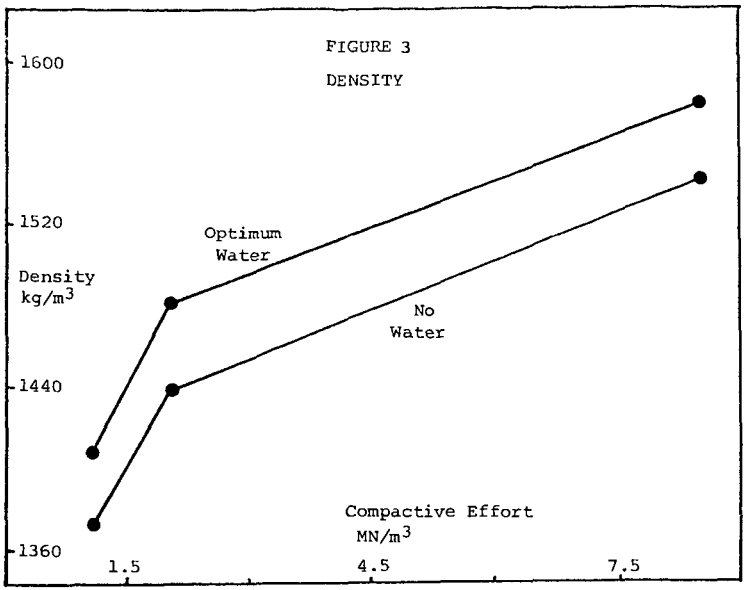
FIGURE 3
DENSITY
1600
1520
1440
1360
Density
kg/m3
Optimum
Water
No
Water
Compactive Effort
MN/m3
1.5
4.5
7.5

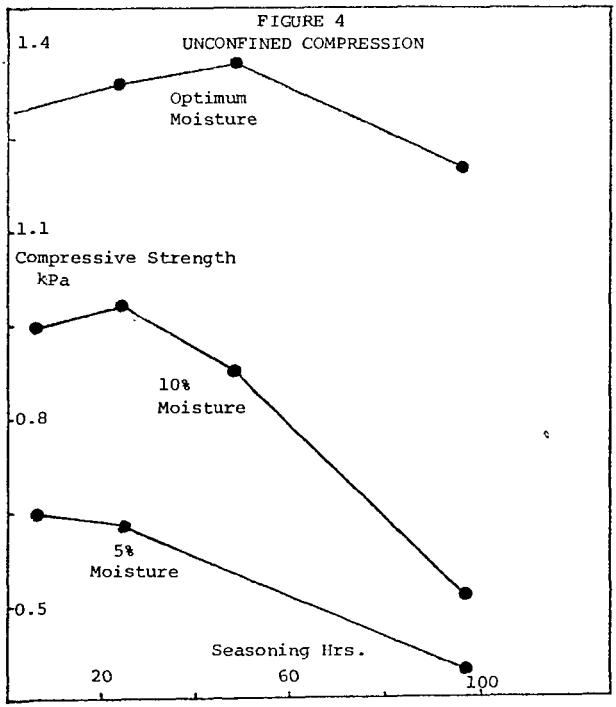
FIGURE 4
UNCONFINED COMPRESSION
1.4
Optimum
Moisture
1.1
Compressive Strength
kPa
10%
Moisture
0.8
5%
Moisture
0.5
Seasoning Hrs.
20
60
100

FIGURE 5
GRADATION RESULTS

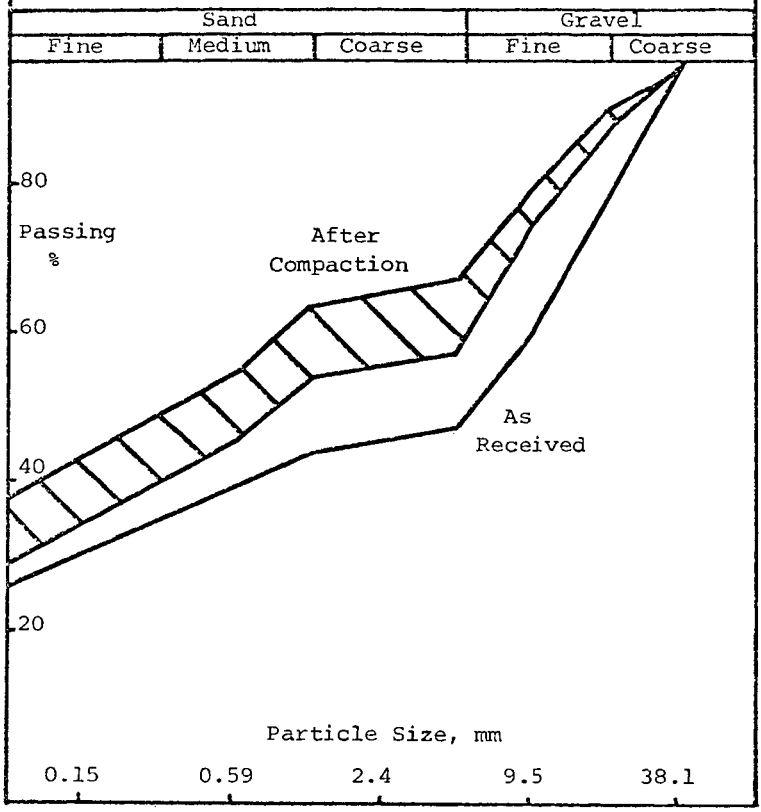

Effect of Thermal Processing on the Properties of Cold Lake Asphaltenes

Kenneth A. Gould and Martin L. Gorbaty

Corporate Research Science Laboratories
Exxon Research and Engineering Company
P. O. Box 45, Linden, New Jersey 07036

Introduction

A better understanding of the composition and properties of heavy feeds such as Cold Lake and Arabian Heavy oils is central to the development of improved upgrading technology. An important question which must be answered is to what extent these materials are thermally altered during refinery distillation. These heavy oils already contain large percentages of refractory materials such as asphaltenes, and it would be highly undesirable to increase the amount or degrade the quality of these components. We have, therefore, investigated the effect of heat treatment during distillation on the quantity and physical and chemical properties of asphaltenes. Cold Lake crude was chosen for this study since it is known to be a thermally sensitive material. Any changes caused by thermal treatment should, therefore, be more obvious than with a more stable feed. We report here the results of a variety of measurements made on the asphaltenes isolated from Cold Lake crude oil and from its vacuum distillation residue. It should be borne in mind that Cold Lake crude is subjected to the high temperatures of pressurized steam used in the production process and may conceivably have already undergone some thermal alteration. The present study, however, is designed primarily to learn if any further changes might occur during refining.

Background

The question of whether and to what extent asphaltenes are formed or altered during crude oil handling and processing has remained unresolved. In one investigation, samples of a Tartar mineral oil distillation residue were heated for five hours to 163°C and then for another five hours to 400°C to simulate conditions during distillation.[1] Both an increase in asphaltene content and a decrease in asphaltene H/C ratio were observed. In addition, distillation residues from various other crudes were heated to various temperatures for three hours and then pentane deasphaltened. It was observed that asphaltene H/C ratios decreased rapidly above 300°C from 1.1 to 0.6.

Table 1[1] shows the asphaltene yields obtained by these investigators after heating maltenes in sealed vials to various temperatures. Although the conversions were approximately first order at the lower temperatures, they changed significantly at 450°, the region of technical interest for many refining operations. Significant formation of new asphaltenes was seen to occur. Deasphaltened maltenes were also separated by alumina chromatography into a non-aromatic "gasoline" eluate, a strongly aromatic benzene eluate, and a resinous benzene-methanol eluate. Pentane insolubles were obtained from all three fractions upon heating at relatively low temperatures, although the rates were quite different. Resins gave the highest yields at the fastest rates while the aromatic oils showed about the same yield, but at a much slower rate. The yield and rate were lowest for the non-aromatic oils, and their pentane insolubles were mostly toluene insolubles and pyridine insolubles rather than asphaltenes. The report also claimed that asphaltenes were formed even at 20° in the absence of air at relatively slow rates.

A study of the effect of heat on asphaltene decomposition at 350-380°C in a helium flow system[2] resulted in the following observations:

1. decomposition was found to be first order in asphaltenes

2. the percent coke make expressed as a percent of asphaltenes decomposed did not vary with the extent of cracking implying that the mechanism is independent of the percent cracking
3. a "20,000 fold increase in surface area" of the asphaltenes via introduction of carbon black (manner not specified) did not change the reaction rate
4. toluene insolubles were formed in amounts that decreased with increasing reaction time, implying that these products are intermediates in pyridine insoluble formation.

These observations led to the proposal of a free radical, chain reaction mechanism. Aspects of the mechanism include: (1) formation of small radical fragments which could abstract hydrogen and leave as light products, (2) reaction of stabilized free radicals (formed by hydrogen abstraction) which could interact with asphaltenes to form larger and larger condensation products, and (3) formation of toluene insolubles, i.e. linear condensation products, and pyridine insolubles, i.e. cross-linked products. These chain reactions could be terminated by formation of very stable radicals that could not react further.[2] This mechanism is in accord with the conclusions of Speight, who has stated that formation of paraffins during pyrolysis of Athabasca asphaltenes probably occurs via interaction of alkyl radicals with hydrogen produced during aromatization and condensation of polycyclic structures.[3] Carbon-carbon bond breaking in these asphaltenes was found to occur primarily β to aromatic rings.

In other work[4], x-ray analysis led to the conclusion that not only did asphaltene melting point increase with increasing fractional aromaticity, f_a, but thermal sensitivity increased in the same direction. Thus, asphaltenes with f_a >0.32 were more sensitive and were transformed to a large extent to toluene insolubles after one hour at 375°C. When f_a was 0.17 and 0.24, only 18-32% conversion to toluene insolubles was observed.

Experimental

Preparation of Asphaltenes - Asphaltenes were obtained by n-heptane precipitation from either Cold Lake crude or vacuum residuum using typical deasphaltening procedures. (i.e. One part of residuum was refluxed for one hour with 10 parts of heptane. The mixture was then filtered and the insoluble asphaltenes washed several times with heptane and pentane and dried in vacuo at 80°.)

Pyrolysis of Asphaltenes - Pyrolyses were performed using the apparatus shown in Figure 1.[5] The appropriate material was placed in a quartz tube with 24/40 ground joints and a dry ice condenser was attached. After alternately evacuating and flushing with nitrogen several times, the material was pyrolyzed at the appropriate temperature for 10 min. Char and liquid yields were calculated from the weights of the pyrolysis tubes and condensers before and after reaction.

Analytical Data - Instrumental analyses and spectra were made on the following equipment: infrared spectroscopy, Digilab FTS-14 Fourier transform spectrophotometer; vapor pressure osmometry, Hitachi-Perkin Elmer 115; gel permeation chromatography, Waters Assoc. 200; nuclear magnetic resonance spectrometery, Varian Assoc. A60 and XL100; thermogravimetric analysis, modified Stanton thermobalance; differential scanning calorimetry, Perkin Elmer DSC 2; and electron spin resonance spectrometer, Varian Assoc. Century spectrometer with E102 X band microwave bridge operating at 9.5 GHz.

Results and Discussion

The findings discussed above[1-4] indicate that changes in asphaltene quality and quantity during thermal treatment depend strongly on both the origin of the oil and the severity of the treatment. This means that specific questions concerning stability can only be answered via studies on the particular oil at the particular conditions of interest.

To provide raw material for this comparative study of untreated and heat-treated oils, asphaltenes from Cold Lake crude (crude asphaltenes) and from Cold Lake vacuum residuum (residuum asphaltenes) were prepared by n-heptane precipitation as described in the Experimental Section. The Cold Lake residuum fraction was prepared by Imperial Oil Enterprises, Ltd. at Sarnia, Ontario, Canada. The distillation history of this bottoms fraction indicates that the pot material was subjected to temperatures as high as 314-318° during atmospheric and vacuum distillation. The length of time at 300°C or higher was about two hours. This is well in excess of what would be experienced in a pipestill and should have provided ample time for any decomposition. It should be noted, however, that since it was possible to maintain the system vacuum at 0.35 mm, the maximum temperature experienced by the residuum was not quite as high as it might be during refinery distillation (e.g. ca 370°C).

Table II shows the yields of asphaltenes obtained from several deasphaltening operations on crude oil and bottoms. The yields on bottoms were normalized to yields on crude by correcting for the quantity of distillates in the crude.

The average percentage of asphaltenes in the bottoms is 10.8% on crude and is thus slightly higher than the average value of 10.2% for the crude oil. The 0.6% difference is, however, within the observed experimental variation of 1.0% and is therefore not considered significant.

The average elemental compositions for several preparations of crude and residuum asphaltenes are shown in Table III. As can be seen, the two asphaltenes are quite similar with the differences between them being less than the typical errors from analysis to analysis. The H/C ratios are almost identical.

Both the number average molecular weights as determined by vapor pressure osmometry and extrapolated to zero concentration and the gel permeation chromatographic molecular weight distributions indicate that the crude and residuum asphaltenes do differ in molecular weight. The VPO results are summarized in Table IV and comparative GPC traces are shown in Figure 2. As can be seen from these data, both techniques indicate that the crude asphaltenes have a significantly higher molecular weight than the residuum asphaltenes. This result is somewhat surprising since one would not a priori expect thermal cracking at such low temperatures, ∿320°C, even with a thermally sensitive crude such as Cold Lake. This explanation, however, cannot be ruled out. Another possibility which could account for lower molecular weights in the residuum asphaltenes, side chain dealkylation, can be eliminated on the basis of nuclear magnetic resonance results (vide infra). Another possible cause of the molecular weight reduction is thermally induced dissociation of π-π complexes which may help to hold the asphaltenes macrostructure together.*

The two asphaltenes were also examined spectrometrically by infrared, nuclear magnetic resonance, and electron spin resonance techniques. Figures 3, 4 and 5 show the results of the IR analysis. It is immediately apparent that the two asphaltene spectra (Figures 3 and 4) are quite similar, showing no obvious qualitative differences. To learn if more subtle differences existed, a difference spectrum (Figure 5) was generated by computer using the data accumulated for Figures 3 and 4. This demonstrates that virtually complete cancellation can be obtained. The only residual absorption of any significance in this highly magnified spectrum is the small peak at 2950 cm^{-1}. This may result from traces of residual solvent or it may represent a very minor difference between the two asphaltenes.

*Deasphaltening done at higher solvent to oil ratios, i.e. from 20:1 to 40:1, show similar molecular weight differences between crude and residuum asphaltenes, implying that the ratio used here, 10:1, did not cause the observed differences. (6)

In the case of the magnetic resonance characterization, both ^{13}C NMR and proton NMR were employed to obtain the percentages of aromatic carbon and hydrogen. The results are shown in Table V. Although the measured levels of aromatic hydrogen are within experimental uncertainty of each other, the difference in aromatic carbon is probably significant. Nevertheless, this difference is small and indicates that the aromatic carbon contents are quite similar. In addition, attempts to discern qualitative differences in the ^{13}C NMR were in vain. These results imply that very little, if any, dealkylation or aromatization has occurred during the crude distillation procedure.

Petroleum asphaltenes exhibit two general types of signals when examined by electron spin resonance techniques. One is the 16-line, anisotropic, vanadyl ($V=O^{+2}$) resonance of the solid state while the other arises from unpaired electrons which are present in the form of relatively stable free radicals. The crude and residuum asphaltenes were examined by ESR, and the relevant data are summarized in Table VI.

It is apparent from the chemical shifts (g-values), the hyperfine coupling constants (A-values) and the linewidths that the free radicals and vanadyl species are in very similar environments in both samples. It was not possible to obtain meaningful values for the absolute numbers of spins per gram for either species, but estimates of the relative concentrations obtained by measuring peak heights indicate that the vanadyl and free-radical concentrations do not differ significantly between the two asphaltenes. It thus appears that heat treatment of Cold Lake asphaltenes to 320° does not alter the nature or abundance of paramagnetic centers.

Since most of the physical properties of the asphaltenes did now show any major differences, thermal reactivity was investigated in an effort to discern any differences which might exist in chemical reactivity. Differential scanning calorimetry and thermogravimetric analysis as well as rapid pyrolysis were employed. The only notable features of the DSC analyses were what appeared to be glass transitions occurring at 175° and 172° for the crude and residuum asphaltenes, respectively. The TGA curves for the two materials were also virtually identical, differing by less than one percent volatile matter at any temperature. Both of these techniques thus indicate essentially no discernable differences in the two asphaltenes.

Similarly, when the pyrolysis behavior was studied in a rapid heating unit with a heatup time of one to two minutes, virtually identical residue yields were obtained.

Summary and Conclusions

The characteristics of Cold Lake crude and residuum asphaltenes have been compared by a number of instrumental and physical techniques. They were essentially identical in quality and quantity except that the crude asphaltenes exhibited higher average molecular weights as well as molecular weight distributions peaking at higher molecular weights than did the residuum asphaltenes.

The thermal history of these particular residuum asphaltenes is much more severe in terms of heating time than would ordinarily be the case for a refinery product from a pipestill since, in the present instance, a pot distillation was used. It therefore seems likely that refinery asphaltenes should be even less different from their respective crude asphaltenes than in this investigation, assuming that pipestill temperatues would be kept below the decomposition temperatures for the asphaltenes. Furthermore, any differences should be further diminished in the event that a crude which is less thermally sensitive than Cold Lake is involved.

Since the Cold Lake crude used in this investigation has been exposed to the temperature of the pressurized steam used in the oil production, one cannot be certain that some thermal changes had not already occurred in the crude oil. To study this possibility the properties of cold bailed (i.e. recovered without steam injection) Cold Lake crude asphaltenes are being investigated by many of these same techniques and will be described in a future report.

Acknowledgments

We would like to thank R. B. Long for his assistance in the preparation of this manuscript, R. Rif for help with the experimental work, and the following individuals for their assistance in the various analytical measurements: L. Ebert, J. Elliott, B. Hager, B. Hudson, M. Melchior, E. Prestridge, W. Schulz and B. Silbernagel.

REFERENCES

1. Hrapia, H., Meyer, D., and Prause, M., Chem. Tech., 1964, 16, (12), 733-737.

2. Magaril, R. Z., and Aksenova, E. J., Khim. Technol. Top. Masel, 1970, 15, (7), 22-24.

3. Speight, J. G., Am. Chem. Soc., Div. Fuel Chem. Prepr., 1971, 15, (1), 57-61.

4. Bestougeff, M. A., and Genderel, P., Am. Chem. Soc., Div. Petrol. Chem. Prepr., 1964, 9, (2), B51-B68.

5. Design supplied by R. J. Lang, Exxon Res. and Eng. Co., Baytown, Texas.

6. R. C. Schucker, private communication from these laboratories.

Table I[1]

Asphaltene Yields from Heat Treating of Maltenes

T (°C)	Maximum % Asphaltenes	$t^{1/2}$ (hr.)
350	18	70
400	32	8
450	36	1

Table II

Asphaltene Yields from Cold Lake Crude and Residuum

Source	% Asphaltenes (On Crude)
Residuum	10.6
Residuum	10.9
Crude	9.9
Crude	9.8
Crude	10.8

Table III

Average Elemental Analyses for Crude and Residuum Asphaltenes

Asphaltene Source	% C	% H	% N	% S	Ni (ppm)	V (ppm)	H/C
Residuum	81.81	7.75	1.42	8.01	329	893	1.14
Crude	82.14	7.65	1.28	7.78	345	935	1.12

Table IV

Number Average Molecular Weights
(M_N) for Crude and Residuum Asphaltenes

Asphaltene Source	M_N	Average M_N
Residuum	5120	
	4400	
	5850	5305
	5850	
Crude	8250	
	6120	6955
	6850	
	6600	

Table V

Aromatic Carbon and Hydrogen
Contents of Cold Lake Asphaltenes

Asphaltene Source	% C_A	% H_A
Crude	52.0 ± 1	13.7 ± 0.5
Residuum	50.4 ± 1	14.2 ± 0.5

Table VI

ESR Parameters for Cold Lake Asphaltenes

Parameter	Crude Asphaltenes	Residuum Asphaltenes
Vanadyl:		
$A_{\parallel}$ (G)	174.0	174.4
$A_{\perp}$ (G)	56.3	56.7
$g_{\parallel}$	1.9632	1.9629
$g_{\perp}$	1.9837	1.9813
Free Radical:		
g	2.00308	2.00307
linewidth (G)	6.4	6.6

FIGURE 1[5]

RAPID HEATUP PYROLYSIS UNIT

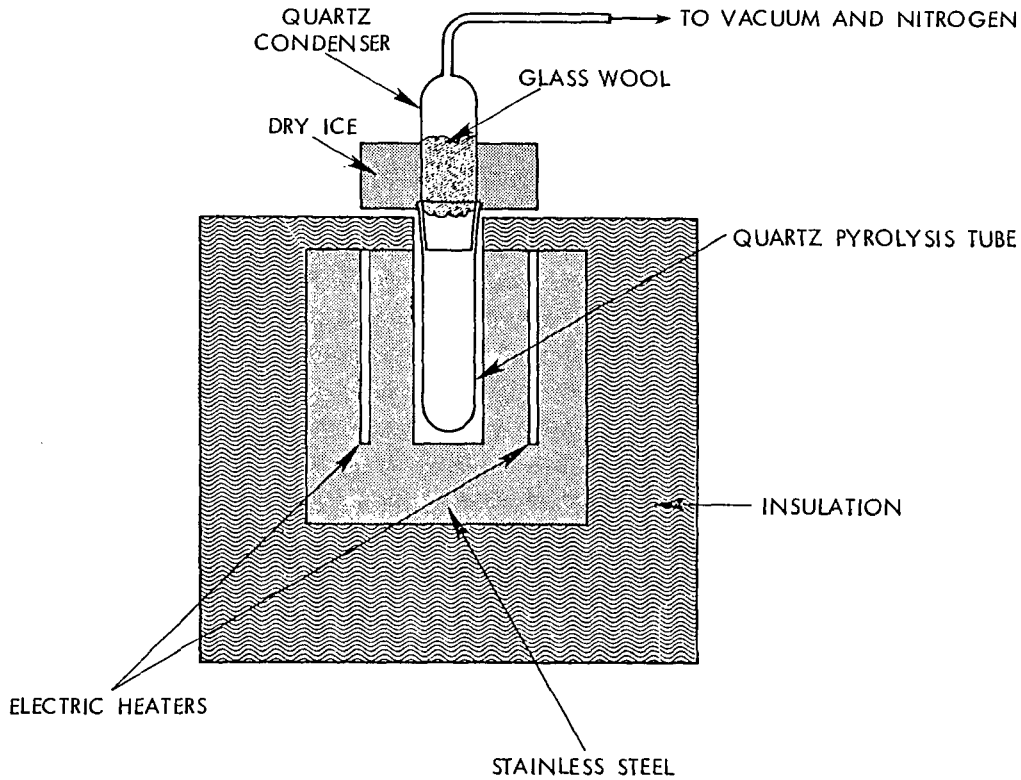

FIGURE 2

MOLECULAR WEIGHT DISTRIBUTIONS OF COLD LAKE CRUDE AND RESID ASPHALTENES

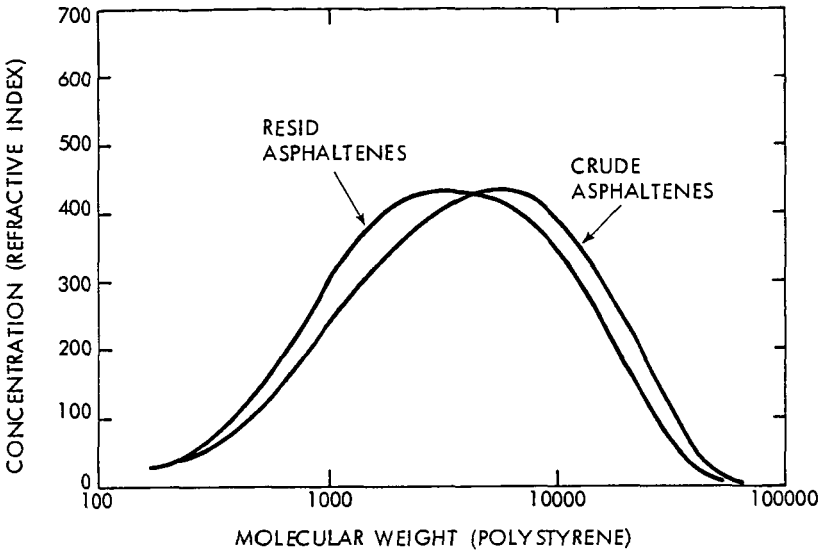

FIGURE 3

IR SPECTRUM OF COLD LAKE CRUDE ASPHALTENES (1% KBr)

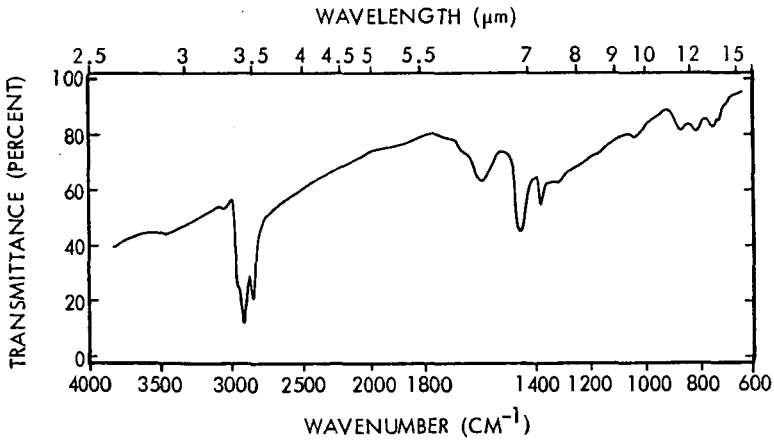

FIGURE 4

IR SPECTRUM OF COLD LAKE RESID ASPHALTENES (1% KBr)

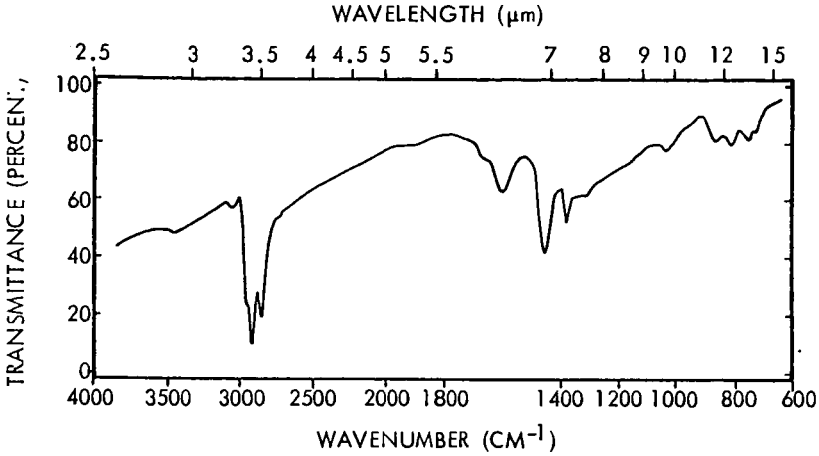

FIGURE 5

DIFFERENTIAL IR SPECTRUM OF CRUDE AND RESID ASPHALTENES

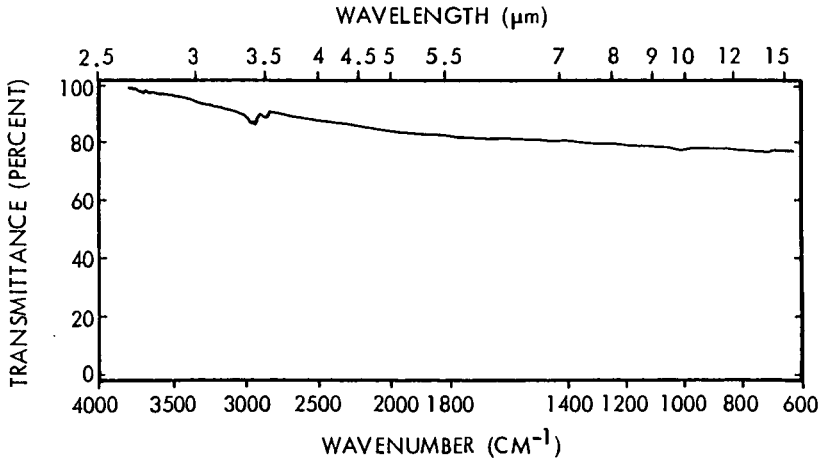

THERMAL RECOVERY OF OIL FROM TAR SANDS BY AN ENERGY-EFFICIENT PROCESS

K. M. Jayakar, J. D. Seader, A. G. Oblad, and K. C. Hanks

Departments of Chemical Engineering and Fuels Engineering
University of Utah, Salt Lake City, Utah 84112

Oil-impregnated rock deposits, more commonly referred to as tar sands, are found on every continent except Australia and Antarctica [1]. The largest known deposits occur in northern Alberta, Canada, where two full-scale commercial plants for producing synthetic crude oil are in operation and two more plants have been approved for construction. Of the 24 states that contain tar sands in the United States, Ritzma [2] estimates that about 90-95 percent of these tar sands lie in Utah. Although the Utah deposits contain only about 25 billion barrels of in-place bitumen, compared to 900 billion barrels in Canada, as discussed by Oblad et al. [3], the Utah deposits represent an important potential domestic source of synthetic petroleum.

Operating plants in Canada employ a hot-water process for recovering bitumen from tar sands. Although Utah tar sands can be considerably different from Canadian tar sands with respect to physical and chemical properties [4], Sepulveda and Miller [5] have successfully processed tar sands from high-grade Utah deposits with a modified hot-water process that uses high-shear conditions to overcome the higher viscosity of Utah tar-sand bitumens. More recent work by Misra and Miller [6] has been successful in processing medium-grade Utah deposits. Other methods for processing tar sands that have been studied extensively [1] include various in-situ techniques and mining followed by direct coking, solvent extraction, or cold-water separation. Of the other methods that use mined material as the feed stock, direct coking processes, generally referred to as thermal recovery methods, appear to exhibit the most promise as alternatives to hot-water processing because thermal recovery methods avoid handling of viscous bitumen, recovery of sediment from solutions, and recovery and recycle of water and/or solvents. In the work presented here, a new energy-efficient thermal process was developed and applied to tar sands from three Utah deposits.

THERMAL RECOVERY PROCESSES

The concept of recovering liquid and/or gaseous hydrocarbons from solid hydrocarbon-bearing materials by thermal treatment has been known for several centuries [7]. Thermal treatment essentially entails processing at high temperature. In most thermal processes, the feed material is heated in an inert or non-oxidizing atmosphere. The mode of heating and the operating temperature largely determine the type of changes occurring to the feed, which can include: 1) volatilization of any low-molecular-weight components in the feed, 2) generation of vapors by cracking reactions, and 3) conversion of part of the material into coke, by reactions such as polymerization. In the case of feed materials such as tar sand, which contain a significant amount of silica sand or other inorganic inert matter that remains substantially unchanged through the thermal treatment, coke is obtained as a deposit on the inorganic matter.

Thermal processing can require a substantial input of energy to provide the necessary sensible, latent, and reaction heats. However, as discussed by Oblad et al. [3], coke, when produced as above and subsequently combusted, can generally provide much or all of this energy requirement. Combustion, referred to by some authors as decoking or burning, is therefore an important aspect of thermal-recovery methods.

Moore et al. [8] classify thermal processes into two general groups, direct heated and indirect heated, depending on whether pyrolysis and combustion steps are carried out in one or two reaction vessels. The processes further differ from each other with respect to fluidized-bed or moving-bed

state of solids in each of the two steps. Table I shows a general process classification scheme that fits most known thermal processes. References are included in that table. Regardless of the thermal process used, as discussed in detail by Bunger [4], the synthetic crude oil product obtained cannot, in general, be used as a substitute for crude petroleum but must be upgraded to reduce sulfur and nitrogen contents, average molecular weight, and C/H ratio.

In all thermal recovery processes, tar sand is subjected to high processing temperatures, about 450-550°C for pyrolysis, and the residual coked sand is further heated to about 550-600°C during the combustion step. At these conditions, an acceptable thermal efficiency can only be obtained if a significant portion of the sensible heat in the spent sand is recovered and introduced back into the process. Almost all the processes in Table I provide for heat recovery from spent sand before it is discarded.

Perhaps the best known fluidized-bed process is the one developed by Gishler and Peterson [17, 24, 25] in Canada. The process scheme resembles that of catalytic cracking as used in the petroleum industry. Tar sand is fed to the pyrolysis or coker bed, where the oil vapor produced is carried by the fluidizing gas to the product collection system. Coked sand is withdrawn from the coker and blown by preheated air into the burner where the coke is burned. A portion of the hot sand is recycled to the coker to supply heat for the pyrolysis step, with the remainder discarded through an overflow pipe in the burner bed. Two serious drawbacks of this process, as noted by Camp [1], are the large recycle of hot sand required and the high energy content of the net spent sand. Rammler [23] has described the application of the Lurgi-Ruhrgas process to tar sands. Like the Gishler and Peterson process, it uses sand as the heat carrier.

DEVELOPMENT OF AN ENERGY-EFFICIENT THERMAL PROCESS

The particulate nature of the mineral matter in most tar sands permits fluidized processing with several advantages: 1) disintegration of lumps of tar sand to individual particles upon the pyrolysis of the bitumen; hence such feeds do not have to be reduced to a small size prior to entry into the pyrolysis reactor; 2) relative ease of handling solids because fluidized solids flow through pipes like liquid; 3) high heat-transfer rates between fluidizing medium and solid particles; 4) nearly isothermal operation, which permits close control of the temperature of pyrolysis, a variable affecting product yields, quality, and energy requirements; 5) high rates for mass transfer between particle surface and fluidizing medium, which is important for a high rate of feed per unit area without forming agglomerates; 6) accommodation of variations in bitumen content of feed by regulating the flow of fluidizing gas; and 7) ease of immersion of heat transfer tubes or heat exchangers in the fluidized beds with accompanying high heat-transfer coefficients. The last factor is particularly important for the type of process developed in this study and constitutes the primary reason for the choice here of fluidized pyrolysis. A fluidized bed recommends itself for burning coke for essentially the same reasons as for pyrolysis and was used, therefore, for the process developed here.

Previously developed processes employ various features to accomplish heat transfer for preheat and pyrolysis. These include 1) preheating the tar-sand feed, separately from the pyrolysis step, generally to recover heat from outgoing hot gaseous streams; 2) preheating the incoming process gas streams, generally to recover heat from spent sand or solids residue leaving the process; 3) transfer of heat from the burner to the pyrolysis reactor in the form of sensible heat of gases leaving the burner, generally by direct heat exchange with the contents of the pyrolysis zone; and 4) internal combustion of coke in the pyrolysis reactor itself with a controlled amount of oxidizing gas so that only a portion of the hydrocarbons in the pyrolysis zone,

preferably coke, is combusted; 5) transfer of heat from the burner to the pyrolysis step by recycle of hot, spent sand as a heat carrier.

Feature 1 has not been shown to be practical because, when preheated, tar sand becomes soft and sticky, making it impossible to feed by common feeding devices such as a screw conveyor. Feature 2 can be and generally is incorporated into most thermal processes. However, a maximum of only about 25 percent of the energy in the hot, spent sand can be recovered by preheating the oxidizing gas for coke combustion. In Feature 3, the amount of energy that can be carried by gases from the combustion zone to the pyrolysis zone is relatively small. Feature 4 requires a means for direct heat transfer between the two zones by conduction, convection, and/or radiation. Unless this can be accomplished on a large scale with little or no combustion of bitumen, Feature 4 is not practical. Feature 5 is practical, but excessive recycle of hot, spent sand is required, thus greatly increasing the required sizes of pyrolysis and combustion reactors and necessitating large devices to convey the sand.

Another possible means of transferring heat from the coke-combustion stage to the pyrolysis stage is by the use of indirect heat exchange not involving sand or gas. In the process developed in this work, this means was implemented by incorporating heat pipes to transfer the bulk of the energy required for solid preheat and pyrolysis from the coke-combustion stage. A heat pipe, for the purpose here, may be defined simply as a completely enclosed tubular device with very high effective thermal conductance, which transfers heat by two-phase circulation of a working fluid [28].

In operation, heat is transferred to one end of the heat pipe, causing the working fluid to vaporize. The vapor flows to the other, cooler end due to the pressure gradient set up inside the central vapor core of the heat pipe. There, the vapor condenses on the tube wall and inside a wick, transferring heat to the surroundings. The condensate then returns to the warmer end, thus completing the cyclic flow of the fluid. Because a large amount of heat can be transferred by a heat pipe, its so-called effective thermal conductivity can be extremely high. For application to thermal processing of tar sands, potassium was selected as the working fluid.

The essential features of the reactor system for the new thermal process developed in the work reported here are illustrated in the simplified process scheme of Figure 1. Freshly mined and sized tar sand is dropped into the upper bed of a multi-staged fluidized-bed column. The upper bed is a pyrolysis reactor, which is maintained at a temperature of generally between 400 and 550°C. Here, bitumen in the feed is cracked and/or volatilized, leaving a coke deposit on the sand particles. The oil vapors and light hydrocarbon gases produced are carried off by the inert fluidizing gas to fines-separation and product-recovery sections, while coked sand flows down by gravity through a control valve to the burner section of the column where the coke is burned to generate heat. The burner is maintained at a temperature of generally between 550 and 650°C. Preheated air is used to fluidize the solids in the combustion bed and to provide oxygen for combustion. Gaseous products of combustion, mostly nitrogen and carbon dioxide, then flow upwards to fluidize solids in the upper bed as noted above.

A number of heat pipes, as required by the heat-transfer load, are placed vertically in the fluidized-bed column such that they extend into the pyrolysis and combustion beds as depicted in Figure 1. The heat pipes transfer excess heat generated in the burner to the pyrolysis reactor, thus maintaining the reactor and burner at proper temperatures.

Hot, spent sand leaving the burner flows down through a control valve to a heat-recovery section, where process air recovers heat from the spent sand. Additional energy can be recovered from the sand by heat exchange to produce steam. A more detailed description of the process is given by Seader and Jayakar [26].

The new process retains most of the simplicity of direct-heated processes. Solids move only downwards by gravity, the equipment is essentially a single vessel, and there is no recycle of solids. Most importantly, the heat-transfer features used--heat pipes, heat recovery from spent sand to preheat process air, transfer of some heat by combustion gases, and some radiative heat transfer from coke-combustion stage to the pyrolysis reactor--permit efficient management of the energy that is within tar sand itself to help achieve high energy efficiency. The heat pipes effectively link the pyrolysis reactor and the coke-combustion stage thermally without necessarily imposing any other constraints on the process such as flow patterns, reactor configuration, or dimensions of the column (except for the volume of heat pipes, which is a small fraction of bed volumes).

The basic process as outlined above is very flexible, and modifications and variations can be easily incorporated into it to further improve the overall efficiency and/or to make it more suitable for specific types of feeds. Thus, external fuel, recycle gas, or liquid fuels can be easily introduced into the burner in the case of lean tar sands. By providing for a purge gas stream off the top of the combustion bed, one can adjust the flow rate of fluidizing gas to the pyrolysis bed. If desired, after recovery, gas produced in the pyrolysis bed can be recycled back to that bed and used instead of combustion gases to fluidize it. This is very important for lean tar sands which would otherwise have very low product concentration in the combined exit gas stream, making product recovery difficult.

LABORATORY TESTING OF NEW PROCESS

A laboratory apparatus was used to demonstrate the new thermal process. It consisted of a 10-foot-high by nominal 2-inch diameter, two-staged, fluidized-bed column, a screw feeder for feeding tar sand, a hot cyclone and filter system for separation of fines from the products, and a product-recovery section consisting of condensers, phase separators, cyclones, and an electrostatic precipitator. A single 0.75-inch-diameter by 7-foot-long heat pipe extended into the pyrolysis and coke-combustion beds. The apparatus was completely insulated and instrumented with thermocouples, pressure taps, flow meters, and sampling taps. Electrical heaters and a propane burner were used to provide heat during startup conditions. The equipment was designed to handle a nominal feed rate of 5 lb/hr of tar sands containing up to 14 weight percent bitumen. Further details of the apparatus are given by Jayakar [27].

Several problems in solids handling were encountered in operating the laboratory apparatus. Originally solids were transferred from the pyrolysis bed to the combustion bed by means of a weir and dip leg. Because gas tended to flow up through the dip leg, this system was abandoned in favor of a simple solids downcomer with a specially designed solids flow-control valve. Although this valve permitted proper operation of the bed, it was a recurrent source of operating difficulty as it tended to stick after a few runs and had to be dismantled and cleaned every two to four runs. Flow of solids from the combustion bed was controlled by a similar valve, which presented no operating problems.

Tar-sand feed materials were ground to particles or pieces no larger than about 1/4-inch in size. Materials tending to be sticky were dusted with fines or coal dust prior to feeding. The screw feeder did not plug as long as it was kept at a near-ambient temperature. Run durations were typically one hour after spending several hours to reach essentially steady-state conditions.

The experimental work was divided into three parts: fluidization studies at elevated temperatures, processing of tar sands in the pyrolysis section without use of the heat pipe, and operation of the complete heat-piped apparatus. Only typical results of some of the latter tests are reported here.

A total of 75 runs was made under thermal processing conditions at near-ambient pressure with tar sands from three different deposits: Tar Sand Triangle, Sunnyside, and Asphalt Ridge. Data from representative runs for feed materials from each of the three deposits are given in Table II. A complete accounting of all the bitumen in the feed material was generally not achieved mainly because of difficulties in removing oil product from the product recovery equipment. Thus, values reported for oil yield are believed to be low. Based on the best runs, it is estimated that for Sunnyside and Asphalt Ridge materials, a typical yield structure for near-optimal operating conditions would be: 70 wt% oil, 10 wt% gas, and 20 wt% coke.

CONCLUSIONS

1. The basic concept of a thermal process using pyrolysis and combustion stages coupled by heat pipes is workable and eliminates the need to recycle large amounts of sand.

2. Tar sands containing as low as 8 percent bitumen can be thermally processed without external energy input to get satisfactory yields of oil. Tar sand with even lower bitumen content can be processed with good oil yield if a portion of the gas or oil products or some cheaper external fuel, such as coal, can be added to the combustion stage to provide energy.

3. Modifications of the process, such as introducing recycle of gas and oil, allowing for purge of some combustion gas, etc., can improve the energy efficiency of the process and the yields of oil and gas.

4. The process developed during the course of this work is simple, direct, and efficient. It is capable of wide application to processing of tar sands in Utah, Canada, and perhaps other deposits. Moreover, the concept of using heat pipes is of even broader applicability in the process industries in general and in energy-related industries in particular. For example, the basic processing concepts investigated here may have potential for application in the processing of oil shale and coal.

REFERENCES

1. Camp, F. W., "Tar Sands" in *Kirk-Othmer Encyclopedia of Chemical Technology*, 2nd Edition, Vol. 19, John Wiley and Sons, New York, pp. 682-732 (1969).
2. Ritzma, H. R., *AIChE Symposium Series No. 155, 72*, 47 (1976).
3. Oblad, A. G., J. D. Seader, J. D. Miller, and J. W. Bunger, *AIChE Symposium Series No. 155, 72*, 69 (1976).
4. Bunger, J. W., K. P. Thomas, S. M. Dorrance, *Fuel, 58*, 183 (1979).
5. Sepulveda, J. E., and J. D. Miller, *Mining Engineering, 30*, 1311 (1978).
6. Misra, M., and J. D. Miller, *Mining Engineering, 32*, 302 (1980).
7. Gustafson, R. E., "Shale Oil" in *Kirk-Othmer Encyclopedia of Chemical Technology*, 2nd Edition, Vol. 18, John Wiley and Sons, New York, pp 1-20 (1969).
8. Moore, R. G., D. W. Bennion, J. K. Donnelly, "Anhydrous Extraction of Hydrocarbons from Tar Sands." Paper presented at local ISA Meeting, Calgary Section, April 1975.
9. Cheney, P. E., R. W. Ince, and C. M. Mason, U. S. Patent 3,487,002, December 30, 1969.
10. Dannanberg, R. O., and A. Matzick, "Bureau of Mines Gas-Combustion Retort for Oil Shale." U. S. Bureau of Mines Report of Investigation 5545 (1960).
11. Saunders, F. J., U. S. Patent 3,130,132, April 21, 1964.
12. Bennett, J. D., U. S. Patent 3,623,972, November 1971.
13. Berg, C. H. O., U. S. Patent 3,905,595, September 22, 1959.
14. Fitch, C. M., U. S. Patent 3,267,019, August 16, 1966.
15. Gifford, P. H., II. U. S. Patent 4,094,767, June 1978.
16. Peck, E. B., E. Tomkins, and D. G. Tomkins, U. S. Patent 2,471,119, May 1949.
17. Gishler, P. E., and W. S. Peterson, *Treatment of Bituminous Sand*. Canadian Patent 530,920, September 25, 1956.

18. Nathan, M. F., G. T. Skaperdas and G. C. Grubb, U. S. Patent 3,320,152, May 16, 1967.
19. Roetheli, B. E., U. S. Patent 2,579,398, December 18, 1951.
20. Murphree, E. V., U. S. Patent 2,980,617, October 13, 1959.
21. Alleman, C. E., U. S. Patent 2,647,077, July 28, 1953.
22. Donnelly, J. K., R. G. Moore, D. W. Bennion, and A. E. Trenkwalkder, "A Fluidized Bed Retort for Oil Sands." Paper presented at the AIChE Meeting, Florida, 1978.
23. Rammler, R. W., "The Production of Synthetic Crude Oil from Oil Sand by Application of the Lurgi-Luhrgas Process," *Canadian Journal of Chemical Engineering, 48* (October 1970):552-560.
24. Peterson, W. S., and P. E. Gishler, "A Small Fluidized Solids Pilot Plant for the Direct Distillation of Oil from Alberta Bituminous Sands," *Canadian Journal of Research, 28* (January 1950):62-70.
25. Peterson, W. S., and P. E. Gishler, "Oil from Alberta Bituminous Sand," *Petroleum Engineer, 23* (April 1951):553-561.
26. Seader, J. D., and K. M. Jayakar, *Process and Apparatus to Produce Synthetic Crude Oil from Tar Sands*, U. S. Patent 4,160,720, July 10, 1979.
27. Jayakar, K. M., "Thermal Recovery of Oil from Tar Sands," Ph.D. Thesis in Chemical Engineering, University of Utah (1979).
28. Dunn, P., and D. A. Reay, *Heat Pipes*, 2nd Edition, Pergamon Press, 1978.

TABLE I. CLASSIFICATION OF AND REFERENCES FOR THERMAL RECOVERY PROCESSES

	Direct Heated	Indirect Heated
Moving-bed pyrolysis and combustion	Cheney et al. [9] Dannanberg and Matzick [10] Saunders [11]	Bennett [12] Berg [13] Fitch [14]
Fluidized-bed pyrolysis and combustion	Gifford [15] Peck et al. [16]	Gishler and Peterson [17] Nathan et al. [18] Roetheli [19] Murphree [20] Alleman [21]
Fluidized-bed pyrolysis and moving-bed combustion	Donnelly et al. [22]	No examples known
Moving-bed pyrolysis and fluidized-bed combustion	No examples known	Rammler [23]

TABLE II. LABORATORY RESULTS FOR PROCESSING OF UTAH TAR SANDS

	Deposit		
	Tar Sand Triangle	Asphalt Ridge	Sunnyside
Run No.	58	67	74
Bitumen Content of Feed, wt%	4.70	11.67	10.56
Tar-Sand Feed Rate, lb/hr	3.85	3.90	4.41
Pyrolysis Bed Temperature, °C	475	482	449
Combustion Bed Temperature, °C	603	649	604
Oil Yield, wt%	49.5	52.7	45.4
Gas Yield, wt%	20.6	15.7	6.2
Coke Yield, wt%	22.0	7.8	17.2
Total Yield, wt%	92.1	76.2	68.8
API Gravity of Oil, 20°C	13.1	15.2	18.2
Viscosity of Oil, cps, 25°C	142	102	291

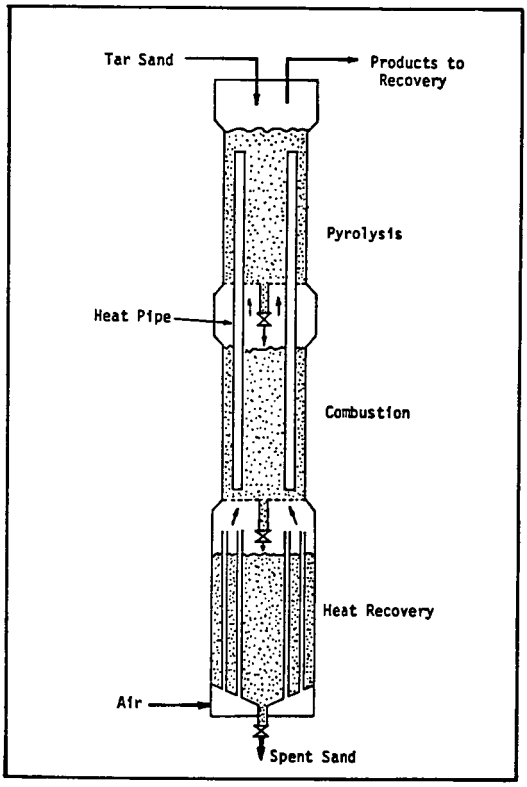

Figure 1. University of Utah Process

THE REACTIVITY OF COLD LAKE ASPHALTENES

R. C. Schucker and C. F. Keweshan
Corporate Research Science Laboratories
Exxon Research and Engineering Company
P.O. Box 45
Linden, New Jersey 07036

INTRODUCTION

As known reserves of light crudes become depleted, the conversion of heavy crudes and residua to distillate fuels is becoming increasingly important. While reserves of Canadian and Venezuelan bitumen and Arabian heavy oils represent vast, largely untapped resources, their usefulness to a large extent depends on our ability to chemically convert macromolecules such as asphaltenes and polar aromatics to smaller molecules boiling typically in the mid-distillate/naphtha range. To optimize the utilization of these feedstocks, we need a much better understanding of the structure and reactivity of petroleum macromolecules, particularly asphaltenes.

While there has been a significant amount of research done to date to elucidate structural characteristics of asphaltenes, there apppears to be no consensus of opinion even on major issues such as the average size of asphaltene aromatic units. For example, proposed structures for Athabasca pentane asphaltenes vary from the twelve-ring naphtho-ovalene structure of Speight[1] to the two-ring sulfur polymer structure of Ignasiak et al.[2]. With this kind of disagreement regarding crude asphaltene structures, it is easy to see why little progress has been made in the area of asphaltene reactivity.

Recently it has been reported by Bearden and Aldridge[3] that certain molybdenum catalysts can substantially reduce coke formation in the hydroconversion of asphaltene - containing feeds under thermal cracking conditions. We have now applied this method to obtain asphaltene fragments in high yields for characterization of the structure of asphaltenes from Cold Lake crude. The goal of our work has been to define the major building blocks in Cold Lake asphaltenes in order to begin to bring together the concepts of structure and reactivity. We have approached the problem by carrying out mild, thermal hydroconversion reactions on neat asphaltenes and characterizing both reactant and reaction products in detail. While previous research has concentrated on crude asphaltenes, we have focused on reacted asphaltenes. By combining structural and kinetic information obtained in this study, we have been able to postulate a global asphaltene reaction mechanism which is consistent with all of our observations.

EXPERIMENTAL

Cold Lake asphaltenes for this study were prepared by precipitation with n-heptane using a solvent to crude ratio of 20:1. The precipitated asphaltenes were separated from the maltenes (n-heptane solubles) by filtration, then washed with an equal volume of n-heptane and dried at 100°C *in vacuo*. Total yield of asphaltenes on crude was 12.6% (by weight). Elemental composition was measured by routine analytical techniques. Oxygen was measured directly by neutron activation analysis and not obtained by difference. Number average molecular weights were obtained by vapor pressure osmometry (VPO)

in toluene at 50°C. Nickel and vanadium concentrations were measured by atomic absorption spectrophotometry. Mole fractions aromatic carbon and hydrogen were determined directly by pulsed Fourier transform nmr techniques. A summary of analytical data for the reactant asphaltenes is given in Table 1.

All reactions were carried out as batch experiments in tubing bomb reactors using either Cold Lake asphaltenes as precipitated or Cold Lake asphaltenes impregnated with a molybdenum catalyst which had been previously shown to reduce coke formation in the hydroconversion of heavy hydrocarbons.[3] In a typical experiment the reactor was charged with five grams of asphaltenes and pressurized to 6 MPa with hydrogen. It was then plunged into a preheated, fluidized sandbath, held for the desired reaction time while agitating, removed from the bath and quenched in cold water. The temperature of the reaction mixture was monitored at all times using a thermocouple located in the bomb. Typical heatup time from ambient temperatures to 95% of reaction temperature was three minutes. At the end of a run gases were vented through an H_2S scrubber into a gas bag. Hydrocarbon gases (C_1-C_4) were analyzed by gas chromatography using flame ionization detection and 1,1-difluoroethane as an internal standard. Toluene was used to remove the liquid and solid products from the bomb and the toluene solution was filtered to determine the coke (toluene insolubles) yield. After removing toluene from the filtrate by vacuum, n-heptane was added to separate asphaltenes (toluene soluble, n-heptane insoluble) from maltenes (n-heptane soluble). Coke and asphaltene fractions were dried overnight at 100°C in vacuo. An overall material balance was obtained by summing the coke, asphaltene, maltene and gas fractions and for lower severity runs averaged between 97-101%. Further separation of maltenes into resins (polar aromatics) and oils was achieved in selected cases by adsorption onto Attapulgus clay using a modification of ASTM D2007 (clay-gel separation).

RESULTS AND DISCUSSION

The thermal hydroconversion of Cold Lake asphaltenes was studied initially to provide a basis for evaluation of catalytic effectiveness in subsequent work. Series of thermal runs were made at 335°C, 365°C and 400°C and the reaction products were separated as described previously. Several kinetic models were tried, but after examining the variability of our data, we decided on the simple first-order asphaltene decomposition model shown below:

$$A \rightarrow aA^* + bM \qquad (1)$$

where A = weight fraction reactant asphaltenes

A* = weight fraction reacted asphaltenes

M = weight fraction maltenes

a,b = stoichiometric coefficients (based on weight)

Rate expressions for total asphaltenes and maltenes were integrated to yield Equations (2) and (3).

$$A_t = a + (1-a)e^{-kt} \quad (2)$$

$$M = b(1-e^{-kt}) \quad (3)$$

Equations (2) and (3) were fit to experimental data using non-linear regression to obtain values of the first-order reaction rate constants and the stoichiometric coefficients at each temperature. The conversion data from the 400°C thermal run and the best fit of the kinetic model are shown in Figure 1. It is interesting to note that at the time of incipient coke formation (~60 minutes) the asphaltene and maltene data deviate from predicted first-order behavior. From this we concluded that both asphaltenes and maltenes were participating in secondary coke-forming reactions. Further separation of the maltenes into resins (polar aromatics) and oils confirmed this to be true and showed that it was the resin fraction that was involved in coke formation.

The same experiments were run using asphaltenes impregnated with molybdenum. The conversions and best fit of the kinetic model at 400°C are shown in Figure 2. Previous work[4] had suggested that the molybdenum would sulfide and thus be able to activate hydrogen resulting in improved hydrogen transfer to radical fragmentation products. Increased hydrogen transfer above the thermal base case would explain the stabilization of resin fragments shown in Figure 2 and the lower olefin/paraffin ratio in the gas illustrated in Table 2 for the C_3 gases.

The temperature dependence of the reaction rate constants obtained for the thermal and catalytic runs was assumed to follow the Arrhenius relationship and the resulting plot of these data is shown as Figure 3. As we can see, the catalyst had no real effect on the activation energy. It did, however, increase the rate of reaction at all temperatures. Interpretation of these data, though, is at best somewhat subjective. In complex reaction systems like these, the measured rate is generally considered to be that of the slowest or rate-limiting step in the reaction sequence. The low values of the activation energies obtained strongly suggest that primary bond breaking is not the rate-limiting step and that some other step such as hydrogen transfer might be. This is supported by the fact that the observed rate increased under improved hydrogen transfer conditions.

The unique behavior of the asphaltenes in the presence of molybdenum provided us with an excellent opportunity to look closer at the structure of the reacted asphaltenes. Since these reactions were carried out neat, maltenes could be separated and analyzed directly. There were no maltenes initially so these molecules must at one time have been attached to the reactant asphaltene molecules. Furthermore, the reacted asphaltenes could also be analyzed to determine what chemical changes were taking place during reaction.

Elemental analysis showed some interesting results with regard to H/C, sulfur and nitrogen levels. Figure 4 shows a plot of the (H/C) values in the reacted asphaltenes and the product maltenes. As can be seen, the (H/C) ratio in the reacted asphaltenes drops continuously while that of the product maltenes rises continuously. The weighted average of the measured asphaltene and maltene fractions rises slightly indicating the addition of some hydrogen to the system. This is the kind of behavior that might be expected of an asphaltene structure containing a large, hydrogen deficient core to which are attached smaller, hydrogen-rich molecules. It is not consistent with the

smaller asphaltene structure proposed by Ignasiak et al.[2] for Athabasca asphaltenes.

Next the question of sulfur distribution was addressed. Sulfur in the asphaltene and maltene fractions was measured directly and that in the gas was obtained by difference. The result for this same series of runs is shown in Figure 5. What we found was is that approximately 50% of the sulfur remained in the reacted asphaltene, 28% was found in the maltenes while 22% wound up in the gas (presumably as H_2S). Studies with model sulfur compounds under the same reaction conditions led us to conclude that the majority of the sulfur in both the asphaltene and maltene products was either heterocyclic or an intermediate reaction product from the cleavage of diaryl or alkyl-aryl sulfide linkages. More easily cleaved bonds such as those in dialkyl sulfides or disulfides were found to be converted very quickly.

Nitrogen was also measured in the asphaltenes and maltenes and the results are shown in Table 3. What we found was that, unlike sulfur which is distributed pretty evenly between the asphaltene core and the peripheral groups, nitrogen is primarily in the core structure. In addition, during reaction very little if any of the nitrogen is removed from the system. This suggests that nitrogen is in predominantly condensed heterocyclic structures in the core with only about 12-14% existing as smaller condensed nitrogen structures on the periphery.

Oxygen was measured only in the asphaltenes due to sample size limitations. Combined results indicated that over 50% of the oxygen was liberated during these reactions as gaseous species and this is in good agreement with recently published work of Moscopedis et al.[5] suggesting the presence of carboxylic acid and aldehyde functionality.

In addition to elemental analyses, number average molecular weights ($\bar{M}_n$) were obtained on both asphaltene and maltene fractions from this series. The resulting curves are shown in Figure 6. The starting asphaltenes are observed to have a number average molecular weight of 6640 ± 120. This decreases monotonically to an apparent asymptote of 3400. At the same time, maltenes which are produced exhibit much lower molecular weights starting at 645 and decreasing to 415. It is not unreasonable at this point to postulate that the maltenes, once formed, continue to break down. Here again, the observed variation in average molecular weight is consistent with the concept that asphaltenes have a larger core structure to which are attached smaller ($\sim$1/10 the size of the core) groups. We are not saying that 3400 represents the molecular weight of the core structure. Experimental nmr and other VPO evidence points to the contrary. We are saying that at 400°C we have broken all bonds that can be thermally broken at a reasonable rate and are left with the core plus peripheral groups attached by much stronger bonds (i.e. biphenyl linkages, etc.) and some alkyl side chains.

One of the most powerful tools available to us for characterization of these fractions is nuclear magnetic resonance spectroscopy. Proton and ^{13}C Fourier transform nmr spectra were run in deuterochloroform on these same asphaltene and maltene samples and some of the spectra are shown in Figures 7 and 8. One of the first interesting points we find is that the asphaltenes with M_n = 3400 still have 40% aliphatic carbon. Both ^{13}C and ^{1}H spectra confirm these as predominantly paraffinic side chains although some naphthenic

character still remains. These side chains need not be connected to the asphaltene core since the smaller peripheral gorups are also known to be highly alkyl substituted. In general we can say that the increase in the fraction of aromatic carbon and hydrogen during reaction is consistent with (1) the loss of alkyl side chains, (2) loss of highly substituted aromatic and naphthenic groups, and (3) loss of naphthenic hydrogen. We believe that to a certain degree all of these are occurring but that (2) is the dominant reaction. We can also say based on subsequent experimental work using n-decyl benzene as a model alkyl aromatic that under these conditions (400°C, 120 min, 7 MPa H_2) β-scission of alkyl side chains is preferred 20:1 over α.

One maltene sample generated under somewhat milder conditions (3 hrs, 365°C, CoMo/γ-Al_2O_3) was analyzed by gas chromatogrpphy and the resulting chromatograph is shown in Figure 9. It is clear that while the vast majority of the area is contained in the lower envelope, a definite pattern of regularly-spaced peaks is observable above the base. These were identified by gas chromatography/mass spectrometry as n-paraffins ranging in length from C_{11} to C_{39}. The smaller peaks in between were identified as primarily iso-paraffins which may have been formed by isomerization during hydroconversion over the somewhat acidic CoMo/γ-Al_2O_3 or which may represent the natural distribution of isoparaffins in the alkyl side chains.

In summary, we have presented experimental evidence which supports the concept that Cold Lake asphaltenes have somewhat large, hydrogen-deficient core structures to which are attached alkyl side chains and highly substituted aromatic groups. We have shown that sulfur tends to be relatively evenly distributed between the core structure and the peripheral groups and that nitrogen is concentrated predominantly in the core. The overall picture of asphaltene reactivity that has emerged from this is shown schematically in Figure 10. During mild hydroconversion, weaker linkages are thermally broken resulting in the formation of maltenes having a higher (H/C) and reacted asphaltenes having a lower (H/C). Some alkyl side chains are also lost predominantly by β-scission. In the absence of effective hydrogen transfer, some of these reaction fragments can recombine to form coke. With improved hydrogen transfer the coking reactions can be significantly delayed. Total conversion of asphaltenes to maltenes would at this point seem to be an improbable goal; however, more research is needed in order to see how far the structural concepts developed here for Cold Lake asphaltenes can be generalized to others.

REFERENCES

1. Speight, J. G., "A Structural Investigation of the Constituents of Athabasca Bitumen by Proton Magnetic Resonance Spectroscopy", Fuel, 49, 76-90 (1970).

2. Ignasiak, T., Kemp-Jones, A. V. and Strausz, O. P., "The Molecular Structure of Athabasca Asphaltenes. Cleavage of the Carbon-Sulfur Bonds by Radical Ion Electron Transfer Reactions", J. Org. Chem. 42(2), 312-320 (1977).

3. Bearden, R., Jr. and C. L. Aldridge, U.S. 4,134,825 (1979).

4. Private communication.

5. Moscopedis, S. E., Parkash, S. and Speight, J. G., "Thermal Decomposition of Asphaltenes", Fuel 57, 431-434 (1978).

TABLE 1

ANALYSIS OF COLD LAKE CRUDE ASPHALTENES

C (WT.%)	80.64
H (WT.%)	7.64
O (WT.%)	1.84
N (WT.%)	1.60
S (WT.%)	7.95
Ni (PPM)	310
V (PPM)	815
Mn (VPO, TOLUENE, 50°C)	6640 ± 120
C_A (MOLE %)	47.3
H_A (MOLE %)	11.4
$(H/C)_{TOTAL}$	1.14
$(H/C)_A$	0.274
$(H/C)_S$	1.91
T_M (°C)	209

TABLE 2

EFFECT OF HYDROGEN TRANSFER ON OLEFIN/PARAFFIN RATIO IN GAS PRODUCTS

		$C_3^=/C_3$	
TEMP. (°C)	REACTION TIME (MIN.)	THERMAL	200 ppm MOLYBDENUM
365	42	0.18	0.08
	87	0.13	0.05
	177	0.07	0.03
	357	0.04	0.02
335	87	0.26	0.14
	177	0.15	0.06
	357	0.08	0.03
	747	0.04	0.02

TABLE 3

NITROGEN CONTENT OF REACTION PRODUCTS

REACTION TIME (MIN)	% ASPHALTENE CONVERSION	N/N_O ASPHALTENES	N/N_O MALTENES
0	0	1.0	0
27	26.0	0.83	0.12
57	38.3	0.83	0.12
117	42.7	0.76	0.14

400°C, 200 ppm Mo

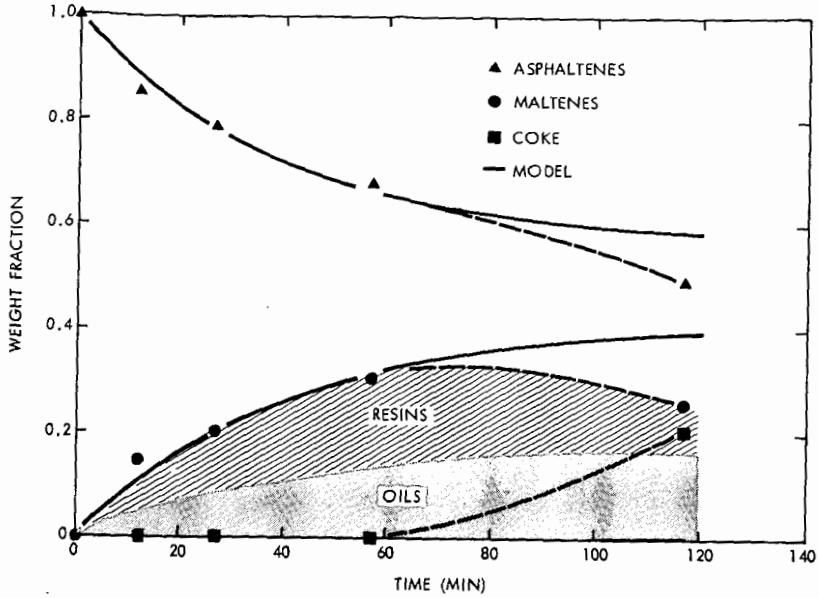

Figure 1 - Thermal Hydroconversion of Cold Lake Asphaltenes at 400°C and 6 MPa H_2.

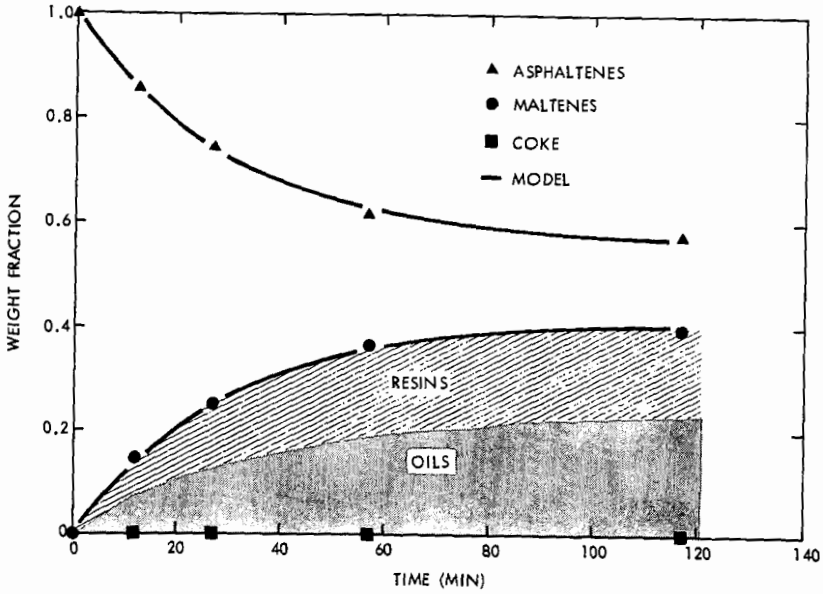

Figure 2 - Hydroconversion of Cold Lake Crude Asphaltenes with 200 ppm Molybdenum at 400°C and 6 MPa H_2.

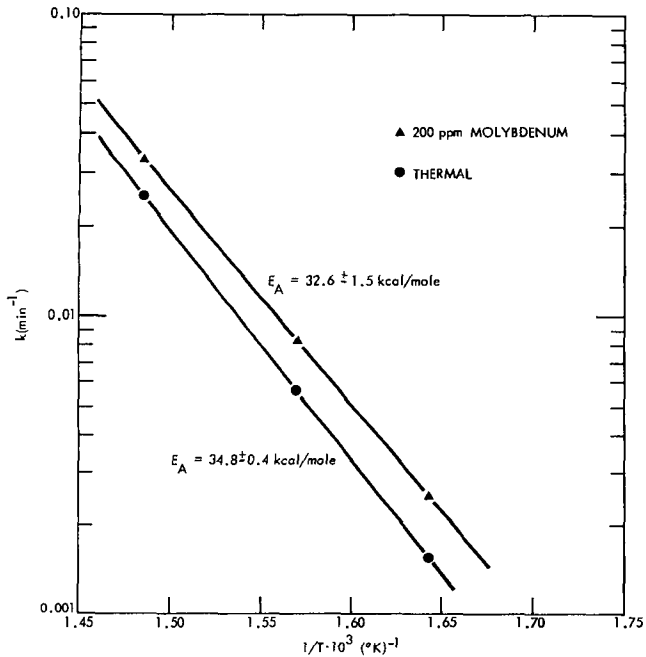

Figure 3 - Arrhenius Plot for Hydroconversion of Cold Lake Asphaltenes

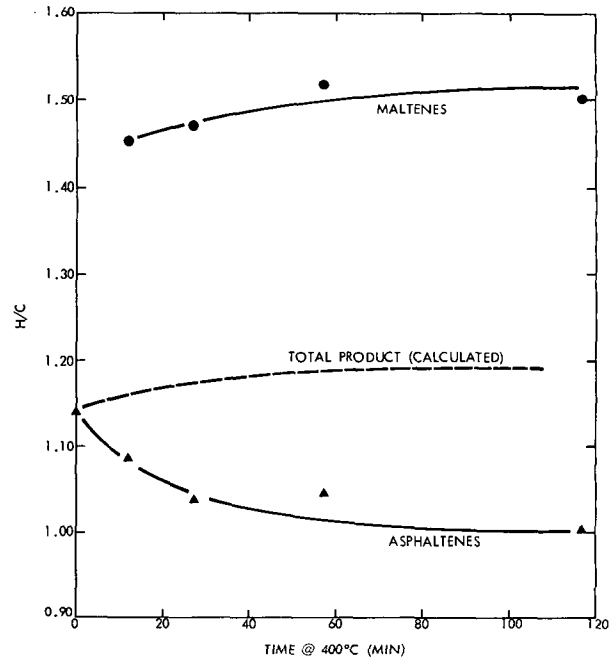

Figure 4 - Hydrogen to Carbon Ratios in Reaction Products

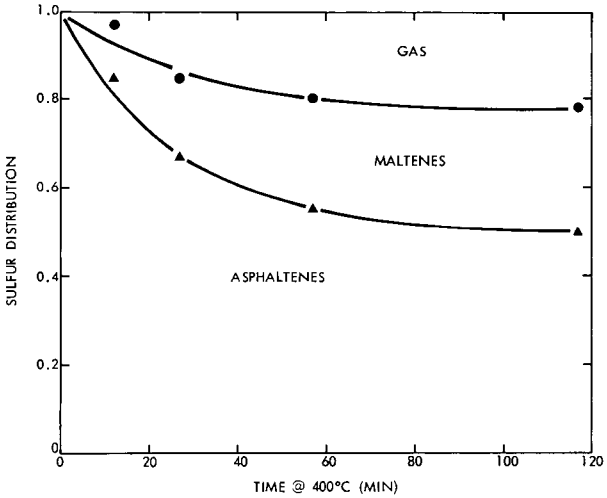

Figure 5 - Sulfur Distribution in Reaction Products

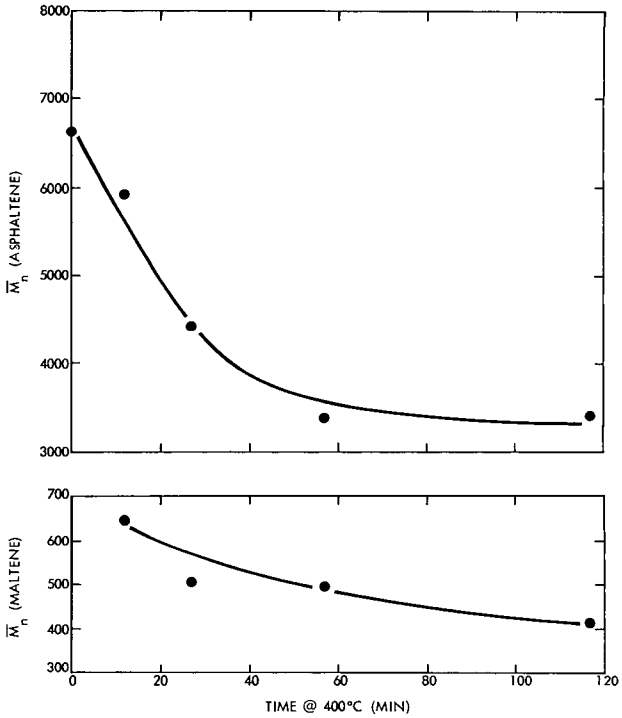

Figure 6 - Molecular Weights of Reaction Products

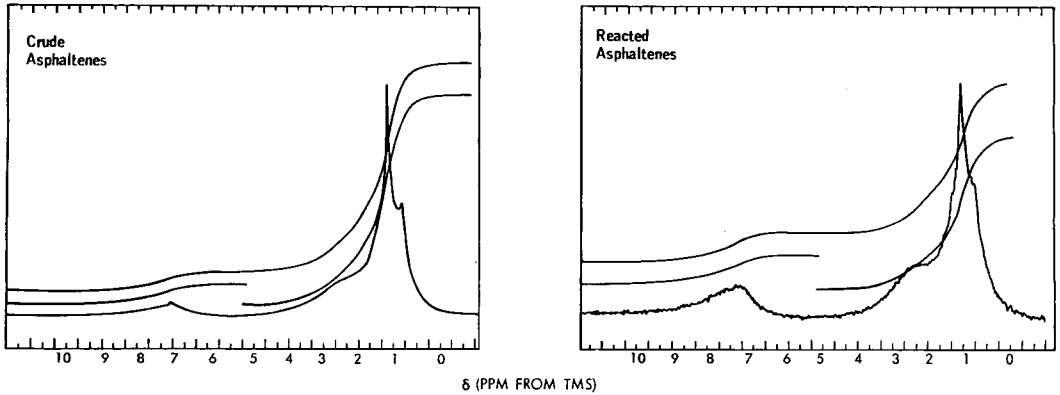

Figure 7 - ^{1}H NMR Spectra of Crude and Reacted (400°C, 2 hr) Asphaltenes.

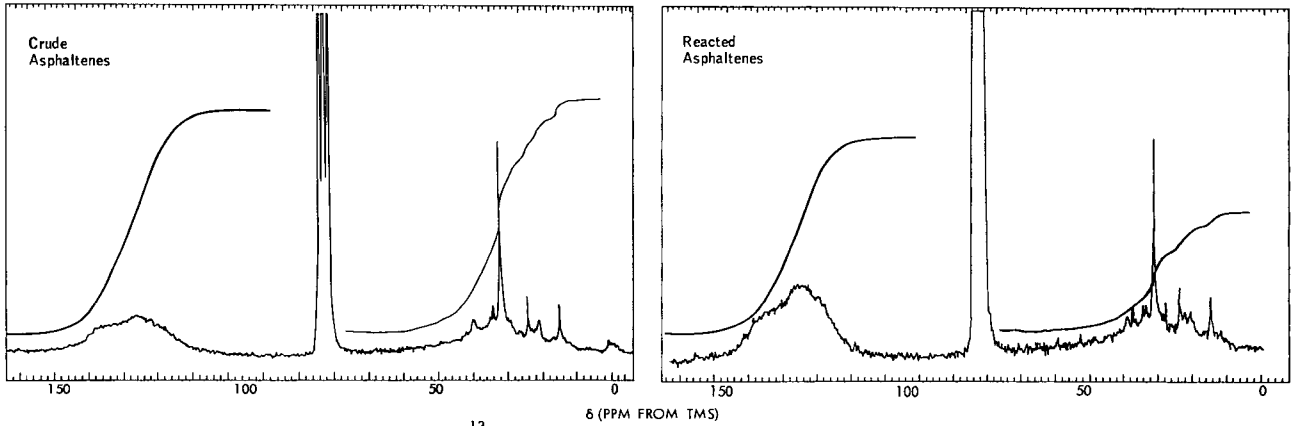

Figure 8 - ^{13}C NMR Spectra of Crude and Reacted (400°C, 2 hr) Asphaltenes

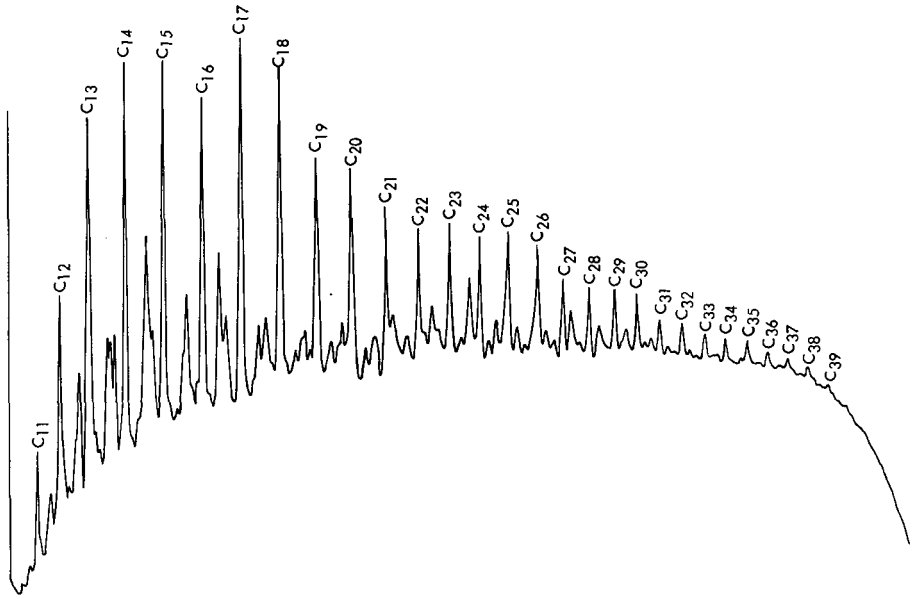

Figure 9 - Gas Chromatogram of Maltene Fraction from Run at 365°C, 6 MPa H_2, 3 hr.

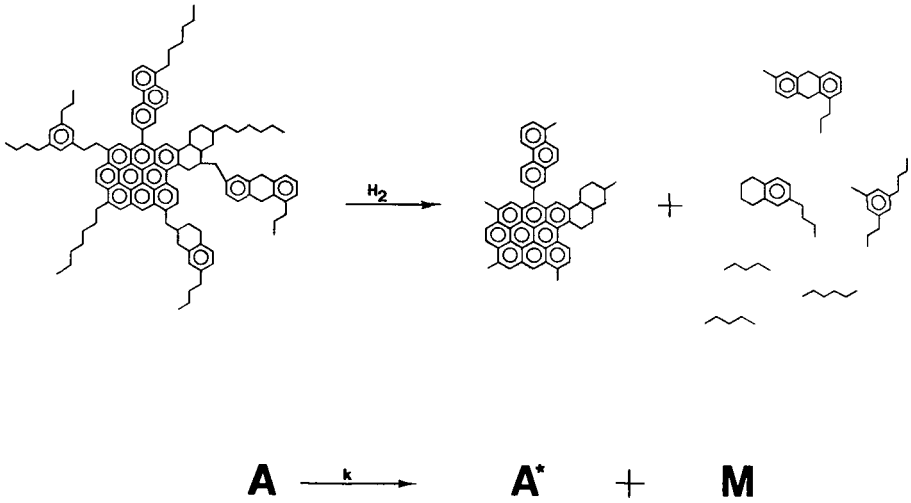

Figure 10 - Reaction Mechanism for Asphaltene Hydroconversion.

HYDROPYROLYSIS - POTENTIAL FOR PRIMARY UPGRADING OF TAR SAND BITUMEN

J. W. Bunger, D. E. Cogswell, R. E. Wood
and A. G. Oblad

Department of Mining and Fuels Engineering
320 WBB, University of Utah
Salt Lake City, Utah
84112

INTRODUCTION

Upgrading of high molecular weight, residual materials is becoming increasingly important as a result of scarcity of lighter feedstocks. Conversion processes for residual materials must contend with high heteroatom content, low volatility (high molecular weight), high aromaticity and high metals content not encountered to the same degree in lighter feedstocks. These characteristics result in higher process costs and typically lower conversion and yield of desired products. As yield and conversion efficiency become more important, conventional techniques, e.g. coking, may prove economically unacceptable, especially for primary upgrading of bitumens or black oils.

Hydropyrolysis is a process for thermal cracking in the presence of hydrogen. This process has been shown to dramatically improve the yields of liquid and gaseous products compared to coking.[1-4] It does not rely on heterogeneous catalysts but requires elevated pressures. Through model compound work[5] and characterization and processing of high molecular weight tar sand bitumen, an understanding of the chemistry of this reaction is beginning to emerge. This paper reports our latest results and hypothesis and the general reactions which may be occurring. The implication of the reaction pathways to the suitability of various feedstocks for hydropyrolysis is also discussed.

EXPERIMENTAL

Elemental Analysis and Physical Properties

Elemental analysis was accomplished by conventional microanalytical techniques in a commercial testing laboratory. Densities were measured on Mettler/Paar digital density meter, model D.M. 40. Average molecular weights were determined by VPO in benzene. Simulated distillation was accomplished using a 1/4" by 18" column of 3% dexsil 300 on chromosorb W, programmed from -30° to 350° C at 10°/minute

with a 4 minute hold at 350° C. The detector was a flame ionization detector maintained at 400° C. The percent nondistillable was determined by use of an internal standard, an equal volume mixture of C_9 to C_{16} n-alkylbenzenes. (See also references 6,7)

Hydropyrolysis Process

Two hydropyrolysis reactors were used in this study. Feeds A and B were processed on a reactor consisting of a coiled stainless steel tube 3/16" i.d. x 236" long. This reactor has been previously described by Ramakrishnan.[1] Feed C was processed in a reactor originally developed for short residence time coal liquifaction. This reactor also consists of coiled stainless steel tubes 3/16" i.d. The length of this tube system can be varied from 20 to 120 feet, and has been previously described by Wood, et. al.[8] Average residence times were calculated from the volumetric flow rates and the reactor volume at process conditions.

RESULTS

Feedstocks for hydropyrolysis processing were derived from Uinta Basin, Utah, tar sand deposits. Three differing feedstocks were used for which elemental analysis and physical properties are given in Table 1. While the carbon-type chemical structure of these feedstocks is probably similar, some important differences are noted. Feed B is of the highest molecular weight, carbon residue, and viscosity and lowest in API gravity and volatility. Elevated temperatures of 100-150° C are required to pump this material. Feed C is the lightest of the three with Feed A of intermediate quality. These feeds represent a range of properties among heavy oils.

These materials were processed by hydropyrolysis under varying conditions of space time, residence time, temperature, and pressure. The general effect of these variables on process results has been previously reported.[9] Higher temperatures and longer residency times contribute sensitively to higher gas production. Representative results attained at conditions determined to be operable for 1-2 hour run times are given in Table 2.

Results show virtually 100% conversion of feedstocks to liquids and gases. Ammonia, hydrogen sulfide and water were inferred from the material balance on the respective heteroatoms and direct analysis of these compounds were not conducted. The values shown in Table 2 were used to calculate the hydrogen consumption. Hydrogen consumption is not underestimated by the method of calculation[9] and is

TABLE 1

Elemental Analysis and Physical Properties of Feedstocks

PROPERTY	FEED A	FEED B	FEED C
Carbon (wt %)	86.2	86.3	86.7
Hydrogen	11.3	11.1	11.6
Nitrogen	1.1	0.8	0.7
Sulfur	0.4	0.35	0.5
Oxygen	0.9	1.4	<0.5
H/C atomic	1.56	1.53	1.59
Specific gravity 20/20	0.981	1.003	0.959
API gravity	12.7	9.5	16.0
Average M.W. (VPO)	713	778	410
Conradson Carbon Residue	9.1	14.1	6.8
% distillable below 530° C	44	34	69
Viscosity KP 77°F .05/sec	69	1500	3.9*

*shear = 200 sec^{-1}

modest considering the effect on yields. Calculations of hydrogen requirements reveal that a hydropyrolysis plant could easily operate in hydrogen balance by steam-reforming methane gas produced.

Characteristics of hydropyrolysis liquid products are given in Table 3. Only modest improvement has been made in the H/C ratios and heteroatom removal, but notable improvements have been made in physical properties compared to the feed material. Average molecular weights of A and B have been reduced in half and viscosities have been reduced by 4 to 5 orders of magnitude. The properties given in Table 3 suggest that a synthetic crude oil has been produced which is amenable to conventional refining. Based on the observation that olefin production is inhibited by hydropyrolysis, it is anticipated that hydropyrolysis liquids will be

TABLE 2

Representitive Results of Hydropyrolysis

Process Conditions

	Product A	Product B	Product C
Temperature °C	525	500	525
Pressure (psig)	1500	1800	1800
Average residence time (sec)	18	30	5
Space velocity (LHSV)	1	1	1

Yields

	Product A	Product B	Product C
Weight % gases	27.3	27.3	12.8
liquid	73.7	73.9	85.6
residue	*	*	2.1
NH_3	0.61	0.38	0.1
H_2S	0.21	0.13	0.3
H_2O	0.79	1.15	-
	102.6	102.9	100.9
Hydrogen consumption (wt %)	2.6	2.9	0.9
(scf/bbl)	1600	1800	600

* Residual material for those runs was counted as liquids.

more stable for storage, transportation, or distillation than coker distillates.

TABLE 3

Characteristics of Hydropyrolysis Liquid Products

	Product A	Product B	Product C
Carbon	86.8	86.9	86.2
Hydrogen	11.4	11.4	11.6
Nitrogen	0.8	0.7	0.7
Sulfur	0.3	0.3	0.2
Oxygen	0.3	0.50	1.20
H/C atomic	1.56	1.56	1.61
Specific gravity 20/20	0.903	0.967	0.920
API gravity	25.2	14.8	22.3
Average MW (VPO)	321	352	312
% distillable below 530°C	85	68	97
Viscosity 77°F cp,	8.1	7000	246

DISCUSSION

The general reaction mechanism for hydropyrolysis follows free radical chemistry. Free radical initiation most likely proceeds through unimolecular bond scission

$$RR' \rightleftarrows R\cdot + \cdot R'$$

or bimolecular single atom transfer reaction to an unsaturated bond

$$RH + C{=}X \rightleftarrows R\cdot + \cdot CXH$$

where X is most likely carbon or oxygen. (see reference 9 for arguments supporting this reaction)

Free radical propogation reactions proceed through transfer of hydrogen or other radical as:

$$RH + \cdot R' \rightleftarrows R\cdot + R'H$$

Perhaps the most important reaction occuring during hy-

dropyrolysis is participation of hydrogen in this propagation reaction as follows:

$$H_2 + \cdot R \rightleftarrows H\cdot + HR$$

Shabtai, et. al.[5] have postulated this reaction in the hydropyrolysis of n-decane. An activation energy of 14-15 kcal/mol is estimated on the basis of thermochemical data[10,11].

The significance of this reaction is to increase the relative effects of free radical saturation compared to β-scission.[5] Thus, a dramatic decrease in ratio of olefin to saturates is observed as a result of hydrogen participation. Also, the dilution of hydrocarbon species with hydrogen reduces the relative effect of second-order molecule-molecule reactions. As a result, dehydrogenation reaction. condensation reactions, and polymerization reactions are all inhibited by the high partial pressure of hydrogen, or indeed, light hydrocarbon gases.

Free radical termination may involve hydrogen radicals to a large extent as radical-radical recombination

$$R\cdot + \cdot R' \rightleftarrows RR'$$

is again inhibited by the presence of hydrogen-rich gases. The production of hydrogen radicals during hydropyrolysis raises the prospect of hydrogeneration or hydrogenolysis reactions. The contribution of these possible reactions (probably minor) can only be inferred from the results of hydropyrolysis where the average number of rings in the aromatic nucleii appears to be reduced.

The effects of hydrogen on pyrolysis of bitumen are obvious when compared with coking at 525° C which exhibits yields of 4% gas, 83% liquid and 13% coke for feedstock A. Clearly, the formation of coke has been severely inhibited while considerable quantities of gas are produced. Considering that the amount of gas produced is closely related to the amount of hydrogen consumed, optimum conditions will be those which can effect the greatest molecular weight reduction without attendent high gas production. Shorter residence times than those achievable on the present equipment may afford this objective.

Preliminary estimates of capital costs for hydropyrolysis reveal an investment of about $3000/daily bbl capacity will be required. This is considerably less than the investments of approximately $6000/daily bbl capacity required for coking/ hydrotreating necessary for the Syncrude plant in

Alberta, Canada. This advantage accrues partially from the fact that Uinta Basin bitumen is lower in total heteroatoms, especially sulfur, than Athabasca bitumen. Also, the hydropyrolysis oil is not as light as the synthetic crude produced by Syncrude. The economic projections never-the-less reveal that for low sulfur, highly naphthenic bitumen, that hydropyrolysis may be an attractive alternative to coking.

SUMMARY

Hydropyrolysis promises to be a process for reducing molecular weight of residual material without the formation of coke, the use of catalysts or an inordinantly high consumption of hydrogen. Estimations of capital costs appear to be competitive with a coking/hydrotreating sequence. Additionally, hydropyrolysis affords 10-15% improved yield over coking/hydrotreating and this factor will have a significant impact on the economics of the recovery steps.

Hydropyrolysis gains its attractiveness principally through the inhibition of second-order hydrocarbon-hydrocarbon reactions relative to first order cracking reactions. Hydropyrolysis is, therefore, predicted to be most useful for processing of very high molecular weight feedstocks of moderate aromatic character. Naphthenic feedstocks are particularly benefited from the inhibition of dehydrogenation reactions.

REFERENCES

1. Ramakrishnan, R: Ph.D. Dissertation, Dept. of Fuels Engineering, Univ. of Utah (1978), 143 pp.
2. Bunger, JW, et. al.: ACS Petr Div Prepr, 23(4):98-109, 1978.
3. Bunger, JW, et. al.: ACS Petr Div Prepr, 24(4):1017-1027, 1979.
4. Pruden, BB et. al.: Can Chem Proc, 61:37-38, 1977.
5. Shabtai, J, et. al.: Chap. 18 in Advances in Chemistry Series (183), Oblad, AG, et. al. (eds), ACS, pp. 297-328, 1979.
6. Poulson, RE, et. al.: Analysis Instrumentation, Instrument Society of America, 10:193-200, 1972.
7. Bunger, JW, et. al.: Fuel, 58(3):183, 1979.
8. Wood, RE, et. al.: Ind Eng Chem, Process Res Dev, Vol. 15, No. 1, 1976.
9. Bunger, JW: Ph.D. Dissertation, Dept. of Fuels Engineering, Univ. of Utah (1979), 217 pp.
10. Bensen, SW: "Thermochemical kinetics"; Wiley, NY, 1976.
11. Rosenstock, HM, et. al.: J Phys Chem Ref Data, 1977, 6 (suppl. 1), pp. I-774-I-783.

FRACTURING OF OIL SHALE BY TREATMENT WITH LIQUID SULFUR DIOXIDE

D. F. Burow and R. K. Sharma

Department of Chemistry, University of Toledo, Toledo, Ohio 43606

Introduction

Development of oil shale deposits as sources of fuels, lubricants, and chemical feedstocks is being considered as an alternative to present reliance on conventional petroleum reserves. Procedures, advantages, and disadvantages for mining/surface processing and for *in situ* retorting have been widely discussed.[1-3] In the former approach, crushing of the shale is essential for efficient oil recovery. As a result of tests with a variety of mechanical crushers,[4] it is apparent that the effectiveness of mechanical crushing is limited by the characteristics of the shale. A slab-forming tendency allows large pieces to pass through many conventional crushers. The resilience and slippery nature of the shale limits the effectiveness of mechanical impact; furthermore, the shale often adheres to crusher surfaces. *In situ* retorting is enhanced by fracturing with explosive charges or expansion of existing fractures with fluids such as water. Fracturing by explosive charges is frequently limited to the vicinity of the charge since the explosive shock is dissipated by shale resilience. Efficient fracturing by aqueous fluids is limited by a tendency for capillary adhesion of water in the fissures and by available water supplies in arid regions where oil shale deposits often occur.

Employment of chemical comminution techniques for fracturing oil shales could circumvent many of the limitations to mechanical crushing as well as reduce or eliminate capital and maintenance costs of crushers. Our recent success in comminuting and desulfurizing coal by treatment with liquid sulfur dioxide,[5] suggested that similar treatments might be successful in fracturing oil shales.

Liquid SO_2 is a remarkably subtle solvent with moderate Lewis acid properties, a substantial resistance to oxidation and reduction when pure, and a propensity to support a variety of ionic, free radical, and molecular reactions.[6] Since SO_2 has a boiling point of $-10^{o}C$, it is easily liquified and/or removed after reaction; it can be easily manipulated without the need for exotic construction materials. Furthermore, it is an inexpensive material which is readily available in large quantities from smelting and fossil fuel combustion; if not utilized, it must be disposed of in some stabilized form at considerable expense. Thus, the direct use of sulfur dioxide could provide an alternative means of cost recovery for pollution abatement technology.

Here we wish to report the results of preliminary experiments in which oil shales are treated with liquid sulfur dioxide to effect comminution. We are, presently, unaware of any previous reports of such experiments.

Experimental

Sulfur dioxide was dried and manipulated as described elsewhere.[6] Larger shale pieces (6-8 cm) were treated directly in a stainless steel autoclave reactor (Parr model 4641). Smaller shale pieces were sealed in fritted glass tubes with liquid SO_2 (ca. 2:1 or less SO_2/shale by weight) to facilitate recovery of any extract. Sulfur dioxide was distilled on to the shale at -78°C; the system was then sealed and brought up to processing temperature. Temperatures of 25, 70, and 170°C were used; the latter temperature corresponds to supercritical conditions for SO_2. No mechanical agitation was employed. Upon cooling, the SO_2, shale, and extract were recovered. The shales were inspected immediately upon recovery and at several intervals thereafter. Sulfur analyses and infrared spectra of the shales were performed on original, processed, and processed/heated samples to determine residual SO_2 content. Infrared spectra of the extracts were also obtained.

Results and Discussion

Results for samples of Green River, Antrim, and Moroccan oil shales were obtained in these preliminary experiments. Extensive fracturing, both along and across laminations, was observed with all three shales. Initial experiments were carried out at 170°C for 3 to 5 hours; subsequent experiments indicated that the degree of fracturing was almost as extensive when milder conditions (e. g. 25°C for 1 hour) are used. Some fracturing was even observed to occur by exposure to gaseous SO_2 alone. With the large lumps, laminations are frequently expanded to 1-2 cm; fractures across laminations are less pronounced but distinctly visible. Immediately upon recovery from the reactor, the samples are so brittle as to be easily broken with the fingers; after standing for a time, the samples become slightly less brittle but all fracturing is maintained. Although no quantitative tests of mechanical properties have been made, it appears that little of the resilience and slipperyness of the original shales is retained. Surfaces of the processed samples have a soft lusterous appearance.

At this stage, the mechanisms responsible for fracturing of these oil shales are not obvious. Among the mechanisms which should be considered, however, are the following: 1. partial conversion of carbonates to sulfites would disrupt microcrystalline lattices in carbonate rich shales, 2. displacement of hydroxyl groups on silica surfaces would disrupt hydrogen bonding in siliceous shales, and 3. extraction of physically and chemically bound water would break up interstitial forces in both types of shale.

The sulfur content of the shales was increased somewhat by processing in liquid SO_2; residual sulfur increases significantly with the temperature of the treatment, however. For example, at room temperature, residual sulfur increases by 1-2% but at 170°C, it increases by 5-10%. Such an increase in sulfur content suggests that processing at higher temperatures is detrimental to the shale.

Upon exposure of Green River and Antrim shales to liquid SO_2, a yellow color develops in the SO_2 solution which progressively deepens to a dark brown; a brown residue is isolated upon evaporation of the SO_2. Moroccan shale, on the other hand, produces an orange SO_2 solution and an orange residue. It appears that the quantity of extract can be increased somewhat by use of higher temperatures. Infrared spectra of these residues reveal that water, aliphatics, and carbonyls are the predominant species although a small amount of aromatics are also obtained. Cross polarization, magic angle spinning ^{13}C nmr results for the solids indicate that the carbon content in the shales themselves differs much more than do these extracts: Green River shale organic carbon is predominately aliphatic whereas Moroccan shale carbon is ca. 3:1 aliphatic/aromatic and Antrim shale carbon is ca. 1:1 aliphatic/aromatic. Thus, extraction by liquid SO_2 would appear to be selective for the aliphatic components of these shales. Since the organic part of these extracts constitutes ca. 2% of the original shales, it is presumed that they represent most of the bitumen portion of the shale and that the kerogen still remains in the shale itself. These observations would, therefore, be consistent with those for extraction by more conventional solvents.[8] Other materials are also extracted from the shales by liquid SO_2. These materials are found as colorless or light brown crystals deposited in the fissures and on the surfaces of the shale after the isolation procedures. At present, we have not identified these crystals.

The results of these experiments suggest that many of the limitations of conventional crushing and fracturing procedures are not encountered here; there are however other limitations to be dealt with. These observations are, nevertheless, sufficiently promising to warrant further detailed investigation into the utility of comminution with liquid SO_2 for both surface and in situ processing of oil shales. Experiments designed to establish the generality of the observations reported here, to develop an understanding of the mechanisms involved, and to devise means of reducing the impact of present limitations to practical use are underway.

Acknowledgements

The support of this research by the U. S. Department of Energy under Contract No. ET-78-G-01-3316 is gratefully acknowledged. Provision of oil shale samples and sample documentation by Dr. F. P. Miknis, Laramie Energy Technology Center, is also gratefully acknowledged.

References

1. E. M. Perrini, "Oil from Shale and Tar Sands," Chemical Tech. Rev. No. 51, Noyes Data Corp., Park Ridge, N. J., 1975.

2. T. F. Yen, "Shale Oil, Tar Sands, and Related Fuel Sources," Adv. Chem. Ser. No. 151, ACS, Washington, D. C., 1976.

3. T. F. Yen and G. V. Chilingarian, "Oil Shale," Dev. in Pet. Sci. No. 5, Elsevier, Amsterdam, 1976.

4. A. Matzick, R. O. Dannenberg, and B. Guthrie, "Experiments in Crushing Green River Oil Shale," Bureau of Mines Report No. 5563, 1958.

5. D. F. Burow and B. M. Glavincevski, "Removal of Organic Sulfur from Coal: The Use of Liquid Sulfur Dioxide," ACS Fuel Division Preprints, Vol. 25, No. 2, pp. 153-164, presented in Houston, March, 1980.

6. D. F. Burow,"Sulfur Dioxide," in Chemistry of Non-Aqueous Solvents, J. J. Lagowski, Ed., Vol. 3, p. 138, 1970.

7. F. P. Miknis, private communication.

8. See, for example, Ref. 3, Chapters 3,6,7.

ION PAIR LIQUID CHROMATOGRAPHY OF COAL-DERIVED LIGHT OILS

J. K. Olson and B. W. Farnum

Grand Forks Energy Technology Center, DOE
Box 8213 University Station
Grand Forks, ND 58202

INTRODUCTION

The growing emphasis on coal liquefaction technology has resulted in increased interest in the development of methods to determine the composition of liquids produced by the process. This information can facilitate understanding of the relationship of the occurrence of various chemical species to the structure and reactivity of the parent coal. This report describes an ion pair liquid chromatography study of the light oil fraction from the liquefaction of lignite with CO and H_2 at 460°C and 27.6 MPa.

The light oil is a gas condensate collected in a water-cooled receiver at atmospheric pressure. The sample studied was collected on the 30th recycle pass of a Beulah lignite liquefaction test using anthracene oil as start-up solvent. Based on MAF coal, the light oil represents about 19% of the yield. A detailed description of the GFETC continuous process unit has been published previously (1).

EXPERIMENTAL

Waters* M-6000 pumps, U6K injector, model 440 UV_{254nm} detector, and model 660 solvent programmer were used for the ion pair study. All separations were conducted using Whatman Partisil ODS2, a 10μm octadecyl-silica packing containing about 15% (w/w) carbon. The column was 250 mm long, 6.4 mm O.D. and 4.6 mm I.D. Column temperature was maintained by a Haake FK-2 circulating water bath. Infrared spectra were obtained on a Perkin-Elmer 283 spectrophotometer.

The mobile phase solvents used were Baker HPLC grade water and Waters HPLC grade methanol and acetonitrile. Buffers were prepared using Baker HPLC grade ammonium acetate, phosphoric and acetic acids, Regis potassium dihydrogen phosphate, potassium monohydrogen phosphate, both 99+% purity, and Waters tetrabutylammonium phosphate (PIC A) and sodium hexanesulfonate (PIC B-6) reagents.

The liquefaction light oil sample was extracted according to a scheme, shown in Figure 1, adapted from Fruchter et al. (2). The resulting four fractions will be designated basic, phenolic, HA(aromatic), and HC(hydrocarbon) throughout this paper.

RESULTS AND DISCUSSION

The light oil is a mixture of relatively low molecular weight, volatile hydrocarbons. The boiling point of 98% of the sample was in the 40-200°C range and the molecular weight range was 60-365 daltons. The nature of each fraction may be described drawing upon information from elemental analysis, shown in Table 1; infrared spectra, shown in Figure 2; and low voltage mass spectra (3).

* Reference to specific brand names or models is made to facilitate understanding and neither constitutes nor implies endorsement by the Department of Energy.

The oxygen-containing compounds found in the phenolic and basic fractions appear to be of the same compound class -- substituted phenols. Almost all of the nitrogen-containing compounds, primarily aryl amines, were isolated in the basic fraction. The HA fraction consists primarily of two- and three-ring aromatic compounds. The hydrogen/carbon mole ratio for the HA fraction is 1.0 as compared to 1.6 for the HC fraction. Although the HC fraction contains some of the same aromatic compounds found in the HA fraction, the principal components are saturated hydrocarbons as indicated by the infrared spectrum. To summarize, the phenolic fraction consisted of substituted phenols; the basic fraction contained substituted phenols and aryl amines; the HA fraction contained aromatic compounds; and the HC fraction contained primarily saturated hydrocarbons and some aromatic compounds.

TABLE 1. - Elemental Analysis of Light Oil Fractions

	%C	%H	%O	%N	%S
Basic	79.6	9.2	4.2	6.8	0.0
Phenolic	78.9	8.7	12.8	0.1	0.0
HA	89.4	7.7	1.8	0.6	0.7
HC	88.9	11.6	0.1	0.0	0.0

Favorable separations of ionizeable organic compounds such as those found in the basic and phenolic fractions may be obtained by ion pair liquid chromatography -- a technique originally proposed by Eksborg, Schill, and coworkers (4,5). The method involves adjusting the pH of the mobile phase to assure maximum ionization of the compounds of interest and adding a hydrophobic counter-ion capable of forming ion pairs with the ionized compound. The ion pair behaves as a neutral compound and retention by the nonpolar stationary phase is enhanced. For example,

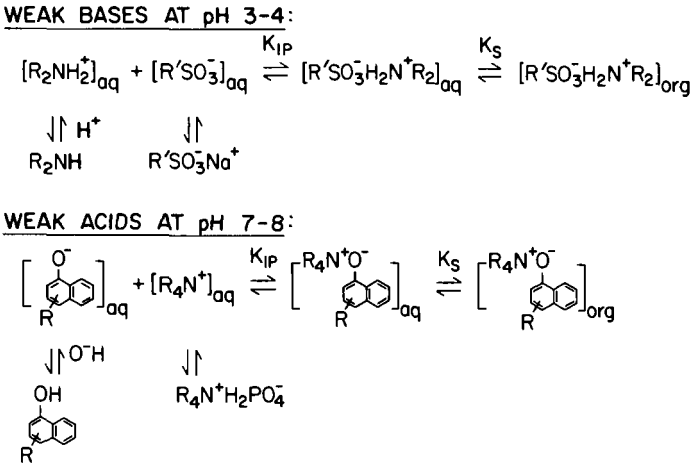

Criteria for selection of counter-ion, pH, and other considerations in the development of an ion pair separation has been addressed by Gloor and Johnson (6). Briefly, the major considerations are selecting a mobile phase pH that will insure

maximum ionization of the solutes and selecting a counter-ion that will produce the desired effect; for basic solutes, an alkyl sulfonate, and for acidic solutes, a quarternary amine. In general, an increase in the length of the alkyl chain of the counter-ion will result in increased retention of the ion pair.

Liquid chromatographic separations of each of the four light oil fractions were carried out with several ion pair and ion suppression systems, shown in Table 2, at 25°C, 45°C, and 65°C. Because solute-liquid phase solubility and the weak electrostatic ion pair equilibrium are affected by temperature, it was anticipated that an increase in temperature would facilitate the separation. However, all of the separations of the four fractions indicated a decrease in both the resolution and the number of peaks resolved. For example, Figure 3 shows decreased resolution for the phenolic fraction at 65°C as compared to 25°C using an ion suppression system.

TABLE 2. - Ion Pair and Ion Suppression Solvent Systems

ACETATE

0.05M	Ammonium acetate/acetic acid (pH 3.5) → Acetonitrile
0.05M	Ammonium acetate/acetic acid (pH 3.5) → Methanol
0.01M	Ammonium acetate/acetic acid (pH 3.5) → Acetonitrile
1.00M	Ammonium acetate/acetic acid (pH 3.5) → Acetonitrile

PHOSPHATE

0.005M	Potassium dihydrogen phosphate (pH 3.0) → Acetonitrile
0.05M	Potassium dihydrogen phosphate (pH 3.0) → Acetonitrile
0.05M	Potassium monohydrogen phosphate (pH 6.9) → Acetonitrile
0.05M	KH_2PO_4/50% Acetonitrile (pH 3.0) → 0.05M K_2HPO_4/50% Acetonitrile (pH 6.9)

SULFONATE

0.01M	Sodium n-hexane sulfonate (pH 3.5) → Acetonitrile
0.1M	Sodium n-hexane sulfonate (pH 3.5) → Acetonitrile
0.01M	Sodium n-hexane sulfonate (pH 3.5) → Methanol
0.1M	Sodium n-hexane sulfonate (pH 3.5) → Methanol

TETRABUTYLAMMONIUM PHOSPHATE

0.005M	Tetrabutylammonium phosphate (pH 7.5) → Acetonitrile
0.05M	Tetrabutylammonium phosphate (pH 7.5) → Acetonitrile

Since the extent to which the sample is ionized is influenced by the ionic strength of the mobile phase, an increase in buffer concentration should result in an increase in ion pair formation (7). Therefore, if ion pairing is the predominant mechanism in the separation, capacity factors, that is, elution times, of ion-paired components would increase with increasing buffer concentration. Separations of each of the four light oil fractions were carried out at pH 3.5 using two buffer concentrations, 0.01 M and 0.1 M hexane sulfonate. Except for slightly earlier overall elution times at higher concentrations, the phenolic, HA, and HC fractions displayed nearly identical peak pattern and resolution at both concen-

trations. This was expected since there should be no ion pair effect on the components in these fractions. In the separations of the basic fraction, there were distinct shifts in the positions of some of the component peaks at the higher buffer concentration. These peaks were presumed to be due to compounds capable of forming ion pairs at pH 3.5, such as aryl amines.

Three buffer systems were investigated at pH 3-3.5: 0.01 M hexane sulfonate, 0.005 M potassium dihydrogen phosphate, and 0.05 M ammonium acetate. At low pH, two predominant processes affect the separation: ion suppression of weak acids (for example, phenols), and ion pair formation of weak bases (for example, aniline). Compared to reverse phase separations, the buffer separations of the HC and HA fractions indicated no change other than slight overall reduction in retention times. The effect of ion suppression, that is, an increase in elution times of weak acids due to their undissociated state, was not evident in the phenolic fraction separations for any of the three systems. For compounds with small dissociation constants such as phenols and cresols, the distribution coefficients of the undissociated compounds are relatively unaffected by change in pH in the 2-6 pH range (8). Since separation by ion suppression is dependent on liquid/ liquid distribution, the addition of a buffer does not significantly alter the capacity ratios of these compounds. Assuming that the phenolics in the basic fraction are likewise unaffected in these systems, all changes in the separations of the basic fraction were attributed to nitrogen-containing components. All three separations of the basic fraction displayed increased resolution and decreased capacity ratios. The effectiveness of these systems is in the order 0.05 M ammonium acetate > 0.05 M potassium dihydrogen phosphate > 0.01 M hexane sulfonate. Figure 4 compares the separation of the basic fraction with reverse phase and 0.05 M ammonium acetate systems.

At pH 7.5, weak bases are present in the non-ionic form and weak acids in the ionic form. The counter-ion studied at this pH was 0.005 M tetrabutylammonium phosphate. In comparison to reverse phase separations, the phenolic fraction, as well as the basic fraction, displayed increased capacity ratios and improved resolution indicating that both ion suppression and ion pair formation were predominant factors in the separation. Overall, however, the hexane sulfonate separations were superior to the tetrabutylammonium phosphate separations. A comparison of the separations of the phenolic fraction with 0.005 M tetrabutylammonium phosphate and 0.01 M hexane sulfonate systems is shown in Figure 5. Again, the separations of the HC and HA fraction were generally unaffected by the buffer system.

CONCLUSION

It appears that several factors and different mechanisms contribute to the separation of eight oils by ion pair and ion suppression reverse phase liquid chromatography. An increase in column temperature affected the capacity factors reducing elution times, but the viscosity change and disruption of thermal equilibrium adversely affected the resolution.

Due to the variety of species found in the light oil, the separation behavior of certain constituents may be affected by ion pair formation or ion suppression. The relationship depends on the concentration of the counter-ion, its solubility in the bonded phase, and the degree of ionization of the solute which bears a direct relationship to the pH of the mobile phase.

The separation of heteroatom and phenolic compounds are generally enhanced by specific ion pair and ion suppression techniques; however, aromatic and hydrocarbon compounds show separations similar to traditional reverse phase techniques.

In applying these relationships to the separation of light oils, optimization of chromatographic conditions for each class of compounds must be considered. A summary of these parameters and their influence in the separation of light oils is shown in Table 3. Capacity ratios of certain components can be effectively altered by ion pair and ion suppression techniques so as to significantly improve the separation, resolution, and identification of components in the light oil.

REFERENCES

1. Willson, W.G., et al. Application of Liquefaction Processes to Low-Rank Coals. Ind. Eng. Chem. Prod. Res. Dev. 18: 297 (1979).

2. Fruchter, J.S., et al. High-Precision Trace Element and Organic Constituent Analysis of Oil Shale and Solvent-Refined Coal Materials. Analytical Chemistry of Liquid Fuel Sources, Adv. in Chem. Series 170. Amer. Chem. Soc., Washington, D.C., 1978, pp. 255-281.

3. Miller, D.J. Analysis of Light Oils from the Conversion of Low-Rank Coals by Capillary Gas Chromatography and Mass Spectrometry. Pres. at N.D. Acad. of Sci., April 1980.

4. Eksborg, S., et al, Ion-Pair Chromatography of Organic Compounds. J. Chromatogr. 83: 99 (1973).

5. Eksborg, S., and Schill, G. Ion Pair Partition Chromatography of Ammonium Compounds. Anal. Chem. 45: 2092 (1973).

6. Gloor, R., and Johnson, E.L. Practical Aspects of Reverse Phase Ion Pair Chromatography. J. Chromatogr. Sci. 15: 413 (1977).

7. Kraak, J.C., and Huber, J.F.K. Separation of Acidic Compounds by High-Pressure Liquid-Liquid Chromatography Involving Ion-Pair Formation. J. Chromatogr. 102: 333 (1974).

8. Kraak, J.C., and Huber, J.F.K. Separation of Acidic Compounds by High-Pressure Liquid-Liquid Chromatography Involving Ion-Pair Formation. J. Chromatogr. 102: 333 (1974).

TABLE 3. - Summary of Chromatographic Parameters and Their Influence on Light Oil Separations

PARAMETER	FACTOR(S) AFFECTED	OBSERVATIONS HC HA	Phenolic	Basic	EXPLANATION
Temperature	Liquid phase solubility Ion pair equilibrium	Decrease in resolution and number of peaks with increasing temperature.			Decreased mobile phase viscosity. Disruption of thermal equilibrium of ion pair and increased mobile phase solubility.
Ionic Strength	Ionization of sample ion pair formation	No effect		Some peaks shifted with increasing ionic strength	Should be no ion pair effect in HC, HA, or phenolic. Ion-pair formation occurs with aryl amines in basic fraction
Buffer addition at pH 3-3.5	Ion suppression of weak acids Ion pair formation of weak bases	No effect	No ion suppression effect	Increased resolution and decrease of capacity ratios	Phenols and cresols unaffected in this system.
Buffer addition at pH 7.5	Ion suppression of weak bases. Ion pair formation of weak acids.	No effect	Increased capacity ratios and improved resolution		Both ion suppression and ion pair formation occur
		HC HA	Phenolic	Basic	

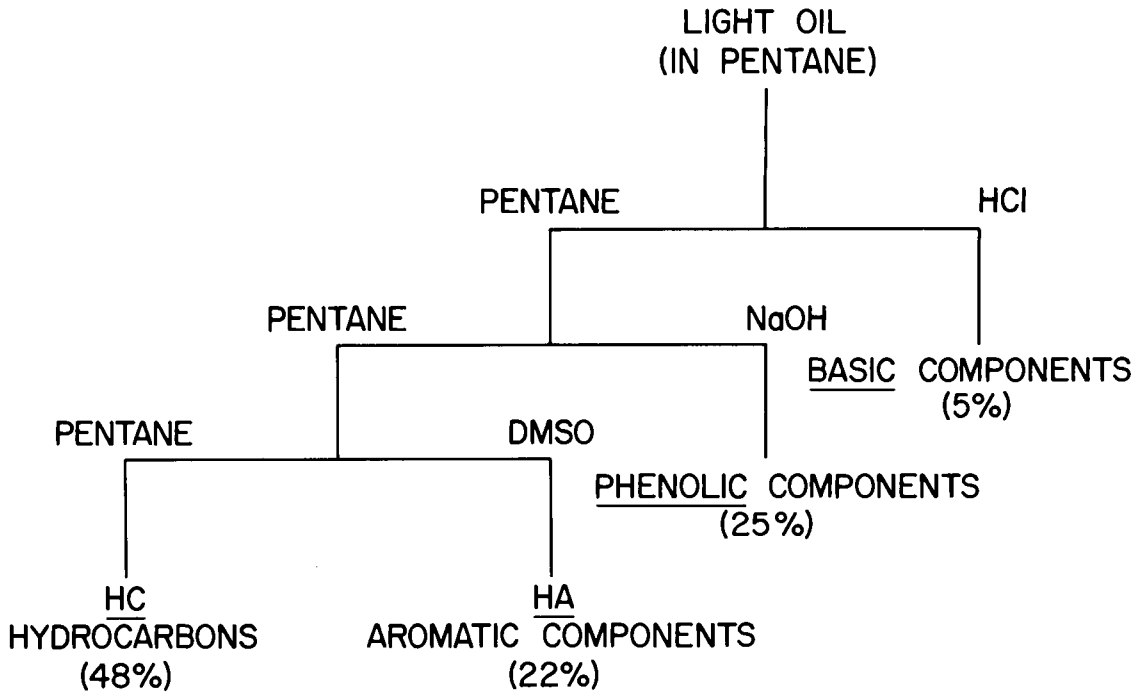

Figure 1. - Flow diagram of light oil separation procedure.

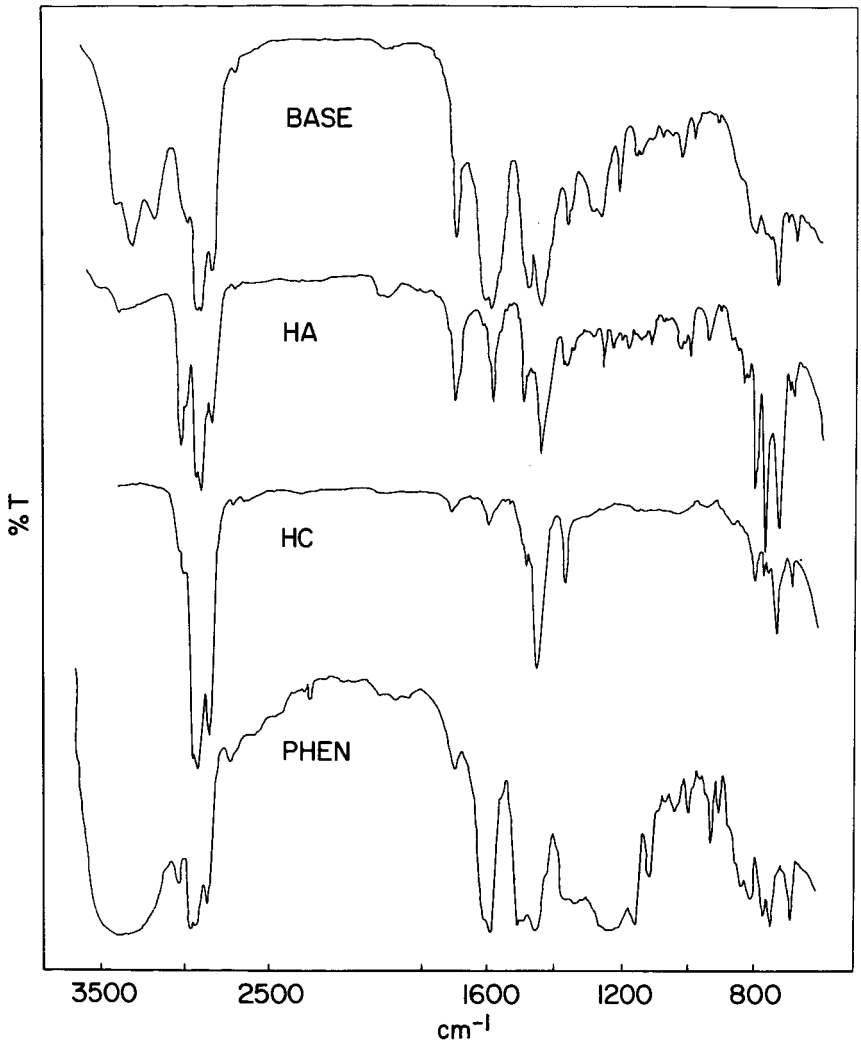

Figure 2. - Infrared spectra of light oil fractions. Capillary films.

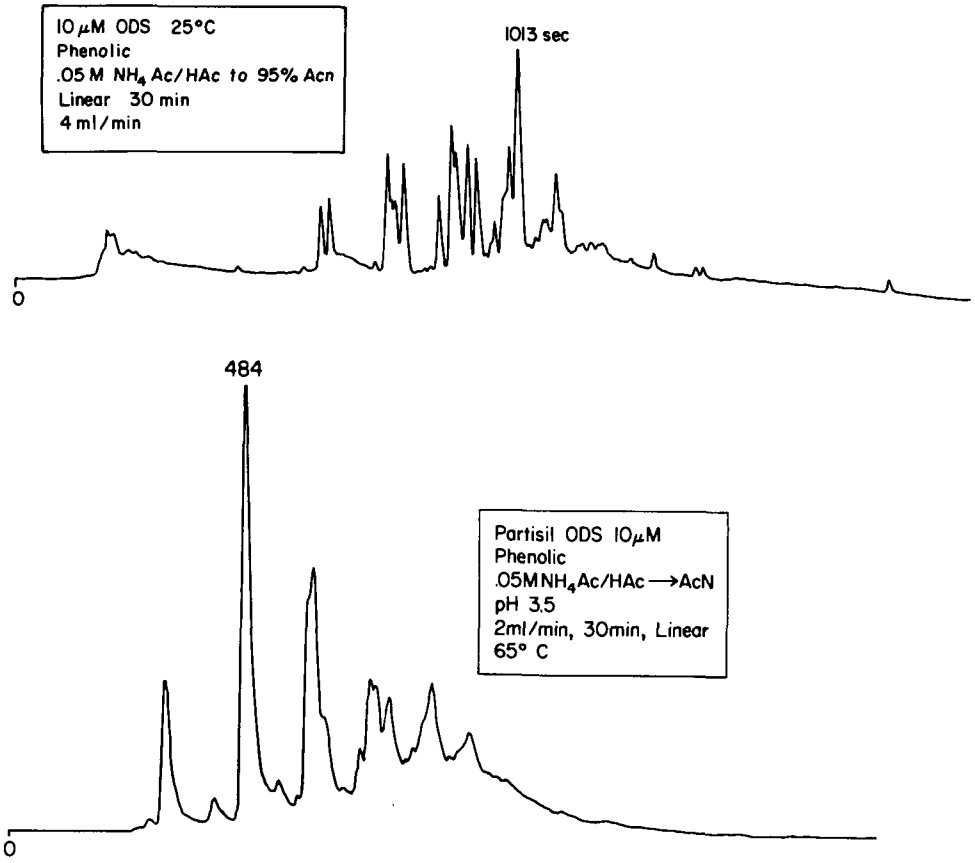

Figure 3. - Comparison of ion suppression LC separations at 25° and 65° of the phenolic fraction of light oil.

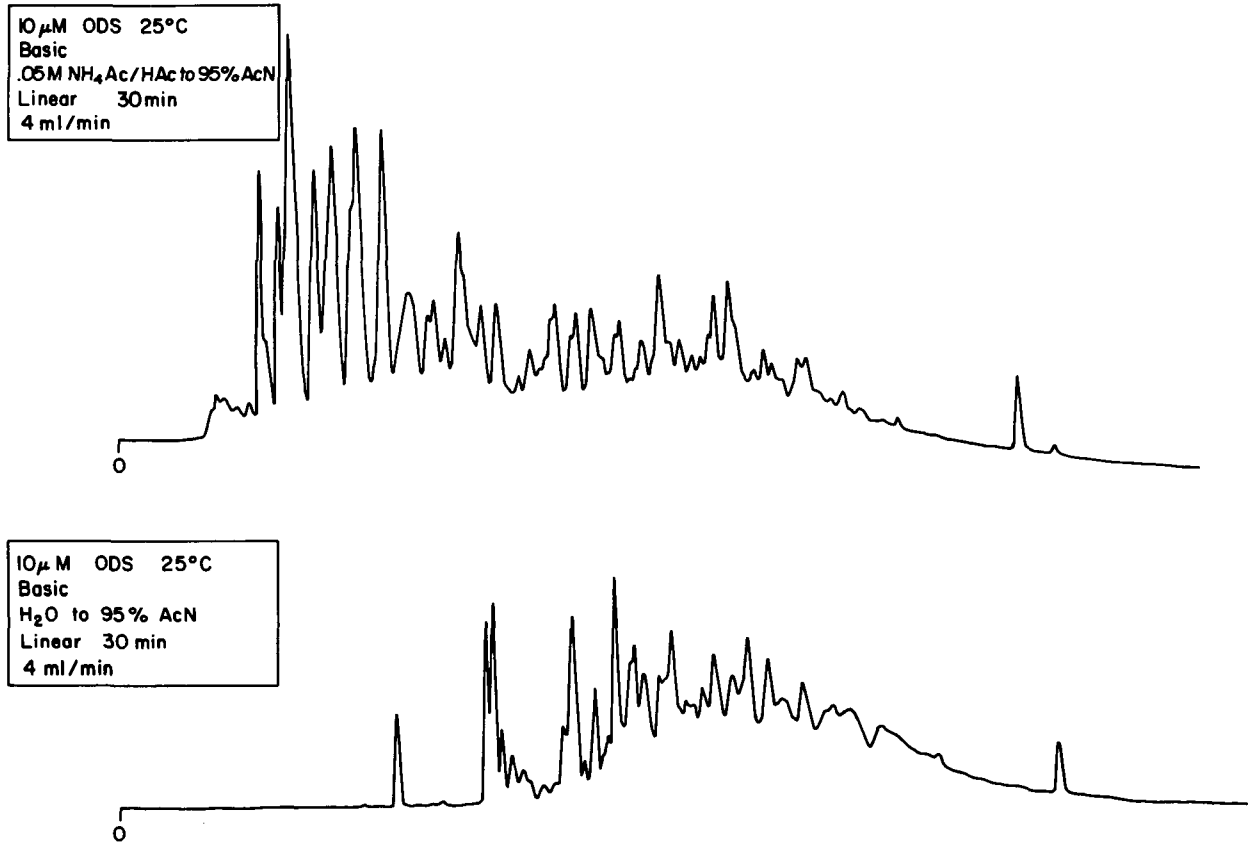

Figure 4. - Comparison of reverse phase and .05M acetate/acetic acid (pH 3.5) LC separations of the basic fraction of light oil.

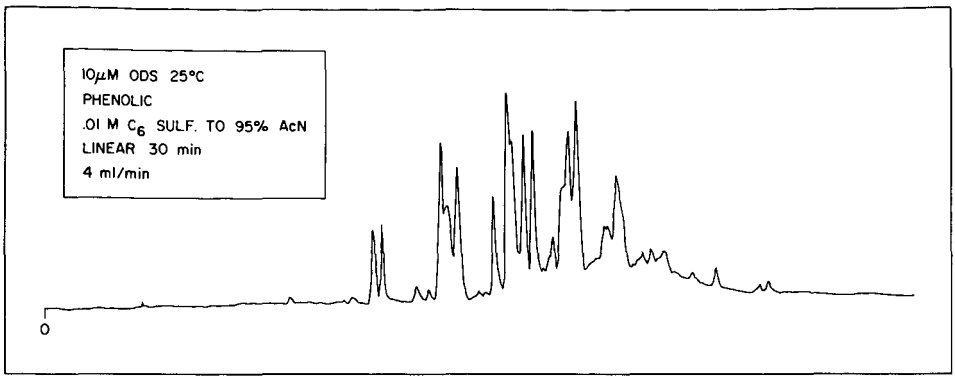

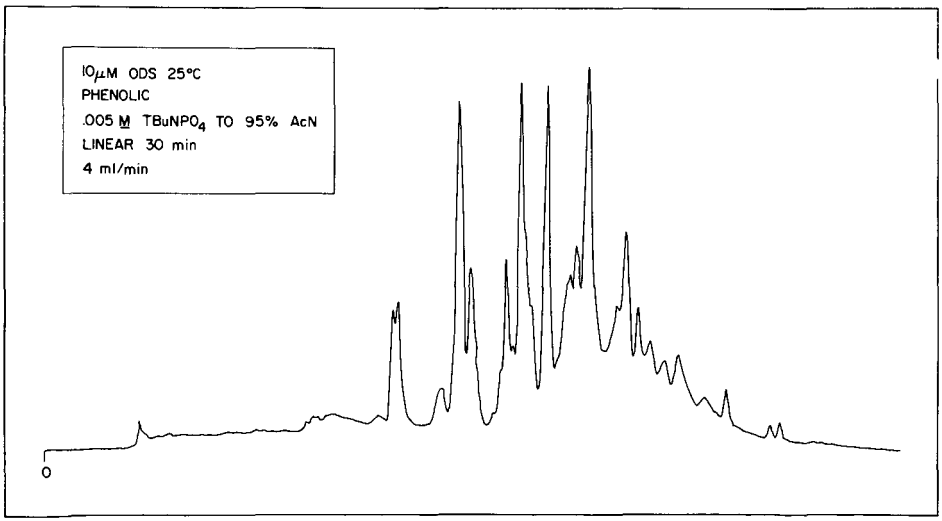

Figure 5. - Comparison of phenolic fraction separations with 0.05 M tetrabutylammonium phosphate (pH 7.5) and 0.01 M n-hexane sulfonate (pH 3.5)